

ORGANOID KIDNEY TUBULE CULTURE FOR  
DRUG TOXICITY SCREENING

by

Anna Astashkina

A dissertation submitted to the faculty of  
The University of Utah  
in partial fulfillment of the requirements for the degree of

Doctor of Philosophy

Department of Pharmaceutics and Pharmaceutical Chemistry

The University of Utah

May 2012

Copyright © Anna Astashkina 2012

All Rights Reserved



# The University of Utah Graduate School

## STATEMENT OF DISSERTATION APPROVAL

The dissertation of Anna Astashkina

has been approved by the following supervisory committee members:

|                             |          |                                    |
|-----------------------------|----------|------------------------------------|
| <u>David Grainger</u>       | , Chair  | <u>03/05/2012</u><br>Date Approved |
| <u>Brenda Mann</u>          | , Member | <u>03/05/2012</u><br>Date Approved |
| <u>Thomas Cheatham, III</u> | , Member | <u>03/05/2012</u><br>Date Approved |
| <u>Alfred Cheung</u>        | , Member | <u>03/05/2012</u><br>Date Approved |
| <u>John Mauger</u>          | , Member | <u>03/06/2012</u><br>Date Approved |

and by David Grainger, Chair of  
the Department of Pharmaceutics and Pharmaceutical Chemistry

and by Charles A. Wight, Dean of The Graduate School.

## ABSTRACT

Experimental models that faithfully reflect both normal physiological and pathological conditions represent an essential cornerstone of both the basic and applied sciences. However, the degrees to which these models represent actual *in vivo* conditions and environments greatly affect their ability to accurately produce clinically relevant responses to stimuli such as drug exposures. This dissertation introduces an *in vitro* kidney proximal tubule model that aims to retain tissue architecture, cell organization, cell-matrix and cell-cell interactions, and physiological cellular responses in long-term culture, and assess its ability to preserve differentially and functionally stable primary cells during exposure to drugs known to be nephrotoxic. These features are achieved by encapsulating suspended harvested viable proximal tubule fragments containing their epithelial cells in a three-dimensional hyaluronic acid (HA) hydrogel matrix. Proximal tubule fragment (i.e., “organoid”) encapsulation, and not their isolated cells suspensions, in the hydrogel endows the model with the capability to retain native cellular organization, extracellular matrix, and intra- and extra-cellular interactions, while limiting non-native cell-polymer interfaces. Data collected for these cultures indicate that proximal tubule epithelial cells sustain cellular gluconeogenic potential, differential markers, and functional ligands. Moreover, these kidney cells *in vitro* were capable of responding to exogenous agents (i.e., drug introductions) with induction of *in vivo*-relevant gene and protein biomarkers as well as accurate cytokine, cytochrome, and

metabolite expression patterns.

The utility of the model for assessing potential nephrotoxic agents was further validated by comparison to the “gold standard” of current *in vitro* toxicology: immortalized cell monolayers grown on plastic. Results demonstrate significant improvements in cell phenotypic fidelity for 3D organoid cultures over cells supported via standard *in vitro* culture techniques that produce most clinically measured biomarkers. The obtained results indicate that preservation of the cellular microenvironment is key to not only sustaining functional proximal tubule cells *in vitro* but also in preserving their natural responses to the same nephrotoxic indicators as expressed in animal toxicity models. The proposed 3D *in vitro* culture model bridges the gap between overly simplistic cellular and costly *in vivo* assessment, and opens possibilities for direct, reliable and predictive comparisons between *in vitro* and clinical data.

## TABLE OF CONTENTS

|   |      |
|---|------|
| ABSTRACT.....   | iii  |
| LIST OF TABLES.....   | vii  |
| ACKNOWLEDGEMENTS.....   | viii |
| Chapter   |      |
| 1 INTRODUCTION THE TO DISSERTATION.....   | 1    |
| 2 A CRITICAL EVALUATION OF IN VITRO CELL CULTURE MODELS FOR HIGH<br>THROUGHPUT DRUG SCREENING AND TOXICITY..... | 4    |
| Abstract.....   | 5    |
| Introduction.....   | 6    |
| In vivo-relevant cell responses: the role of microenvironment.....  | 11   |
| In vitro cell culture models: review, strengths, and limitations.....   | 17   |
| Conclusions.....  | 24   |
| Acknowledgments.....  | 25   |
| References.....   | 25   |
| 3 A 3-D ORGANOID KIDNEY CULTURE MODEL ENGINEERED FOR HIGH THROUGHPUT<br>NEPHROTOXICITY ASSAYS .....             | 30   |
| Abstract.....   | 30   |
| Introduction.....   | 31   |
| Methods.....  | 35   |
| Results.....  | 43   |
| Discussion.....   | 54   |
| Conclusions.....  | 63   |
| Acknowledgments.....  | 64   |
| References.....   | 64   |

|   |     |
|---|-----|
| 4 INFLUENCE OF DRUG HYDROPHOBICITY, CELL CONFLUENCE, AND ASSAY SELECTION ON TOXICITY ASSESSMENT IN VITRO IN PRIMARY AND TRANSFORMED KIDNEY CELL CULTURES..... | 76  |
| Abstract.....   | 76  |
| Introduction.....   | 77  |
| Methods.....  | 80  |
| Results.....  | 85  |
| Discussion.....   | 103 |
| Conclusions.....  | 111 |
| Acknowledgments.....  | 113 |
| References.....   | 113 |
| 5 COMPARING PREDICTIVE DRUG NEPHROTOXICITY BIOMARKERS IN KIDNEY 3-D PRIMARY ORGANOID CULTURE AND IMMORTALIZED CELL LINES.....                                 | 129 |
| Abstract.....   | 129 |
| Introduction.....   | 130 |
| Methods.....  | 132 |
| Results.....  | 141 |
| Discussion.....   | 150 |
| Conclusions.....  | 162 |
| Acknowledgments.....  | 163 |
| References.....   | 164 |
| 6 SUMMARY AND FUTURE WORK.....  | 173 |
| Summary.....  | 173 |
| Future Work.....  | 176 |
| References.....   | 186 |
| APPENDIX: STANDARD OPERATING PROTOCOLS.....   | 186 |

## LIST OF TABLES

| Table   | Page |
|---|------|
| 2.1 Drug product withdrawals from the market due to toxicity from 1974-20.....  | 6    |
| 2.2 Common <i>in vitro</i> assays used in drug toxicity assessments.....  | 8    |
| 3.1 (Supplemental) RT-PCR primers used .....  | 71   |
| 3.2 (Supplemental) Hydrogel formulations tested for use in proximal tubule encapsulation.....   | 72   |
| 4.1 (Supplemental) Lack of detectable drug aggregation in culture media solutions containing<br>4mM colchicine after 2 hours of incubation in different media.....  | 123  |
| 4.2 (Supplemental) General properties for drugs taken from the literature (parentheses<br>are references).....  | 124  |
| 5.1 Effective EC <sub>50</sub> values for nephrotoxic drugs in different kidney cell line (2-D HEK293,<br>LLC-PK1 monolayers) and primary PT 3-D hydrogel cell cultures. Data reflect<br>background subtraction of drug adsorption to HA gel matrix (see Materials<br>and Methods)..... | 138  |
| 6.1 Comparison of profused plate to the Transwell® 12-well Corning® plate.....  | 180  |

## ACKNOWLEDGEMENTS

This dissertation would not have been possible without the encouragement and guidance of several individuals who provided valuable assistance in preparation of this work.

First and foremost, I would like to thank my supervisor, Professor David W. Grainger, for the opportunity to work in his laboratory. His support was critical in enabling my understanding of the subject as well as development of my critical thinking and writing skills. Dr. Brenda Mann has provided unfailing moral and technical support as a committee member, manuscript co-author, and friend. Dr. Glenn Prestwich has offered valuable insight as a manuscript co-author, particularly during the editorial process as well as for graciously providing 3-D culture materials for this project. Finally, Dr. John Mauger, Dr. Thomas Cheatham, III, and Dr. Alfred Cheung have supplied invaluable support and guidance in completion of this work.

I also owe a debt of gratitude to the Grainger research group whose encouragement and sense of humor were of tremendous help during my doctoral work.

Last but not least, I am filled with gratitude for my family for their patience and unwavering reassurance during my entire graduate career.

## CHAPTER 1

### INTRODUCTION TO THE DISSERTATION

*In vitro*-sustained cellular cultures are the most promising and accessible toxicity and biomarker assessment tools used routinely during preclinical drug development. Unlike their *in vivo* or animal counterparts, *in vitro* systems can be easily propagated and scaled up in both academic and industrial settings, are relatively inexpensive, and currently are the only assessment models capable of high-throughput evaluation. Unfortunately, traditional cell culture approaches that utilize immortalized or genetically transformed cell lines on two dimensional (2-D) plastic cell culture surfaces are over-simplified and incapable of reproducing the complexity of whole tissue processes, namely cellular toxicity (as explained in Chapter 2). The goal of this research was to develop improved, more *in vivo*-relevant cell culture methods that would retain the benefits of current *in vitro* techniques while improving reliability and predictive capabilities for *in vivo* translation of the acquired data, particularly for preclinical studies on drug toxicity screening.

While current dogma recognizes that different variables present in the cellular microenvironment contribute to cellular changes, initiation of damage-specific pathways in cellular models relies both on differentiation and functional maintenance of cells as well as sustained signaling cross-talk within the cellular niche (also reviewed in Chapter 2). Reliable production of *in vivo*-like biomarkers of cell toxicity within cell cultures has proven difficult. Maintenance of



organotypic cellular interactions appears to be required for cell fidelity necessary to recapitulate cell toxicity responses representative of those *in vivo*. This reinforces the necessity to maintain cellular microenvironments during *in vitro* culture models of toxicity. Traditional 2-D monolayer cell cultures on plastic cannot provide these requirements.

These observations form the overarching hypothesis driving this dissertation: that cell-cell and cell-matrix interactions resembling structure and function of native tissue architectures are critical for guiding and maintaining cellular identities *in vitro* and producing clinically-relevant toxicity biomarkers in culture (reviewed in Chapter 2). To explore this hypothesis, an organoid kidney culture model that retains native cell-ECM interactions, intercellular communication, and 3-D organization has been developed, fully characterized (see Chapter 3) and validated (see Chapters 4 and 5). An *in vitro* organoid kidney proximal tubule culture model (Chapter 3) provides minimal perturbations to critical cell-cell and cell-matrix interactions in kidney proximal tubules, prolonging kidney cell functions and viability while concurrently eliminating unpredictable non-native cell-polymer interactions that often plague other 3-D tissue culture models. Extensive characterization of the kidney proximal tubule organoid culture model (Chapter 3) based on: 1) cellular histological and molecular markers, 2) cellular metabolic activity, 3) cellular polarization, and 4) gluconeogenic potential are all reported. Subsequent validation of the 3-D organoid tissue culture model (detailed in Chapters 4 and 5) against the 'gold standard' for *in vitro* toxicological evaluation -- kidney cell monolayers grown on 2-D surfaces -- compares production of known, validated clinical biomarkers of kidney toxicity in both traditional 2-D and 3-D organoid cell culture models in exposures to four clinical drugs known for nephrotoxicity. The study seeks to prove the

concept that preservation of *in vivo*-like organization within kidney organoid constructs will elicit more relevant and reliable pharmacological toxicity and toxicity marker up-regulation compared to 2-D cell cultures. Specifically, Chapter 3 describes how this 3-D culture methodology elicits toxicity markers for four clinically used drugs in 96-well plate assays over several weeks – a significant difference from drug responses from common immortalized cell lines HEK293 and LLC-PK1. The chapter analyzes the results and proposes broad reaching implications for *in vitro* toxicity assessments. This functional analysis is extended in Chapter 4 to further evaluate and quantitatively assess the ability of each *in vitro* culture system to predict kidney drug toxicity *in vivo* using clinically accepted biomarkers of *in vivo* kidney toxicity. Ultimately, the new *in vitro* 3-D organoid kidney tissue model confirms the hypothesis that endowing culture systems long-term with native cellular interactions instead of employing a minimalist's approach to *in vitro* cell culture better ensures that not only are biological requirements for creating and sustaining tissue replacement models met, but that the data obtained are relevant and impacting.

All of the advantages attributed to the proposed high-throughput 3-D organoid kidney culture systems support the value of the cell culture model that yields better-quality, more accurate, tissue-specific information to significantly improve the assay for nephrotoxicity, its predictive value, and more accurate translation between *in vitro*, animal, and clinical human studies. Moreover, such capabilities would open new avenues for application of analogous *in vitro* cell-based organoid models for other organ toxicities (e.g., liver) in addition to new research that integrates data utilization, improves drug screening results, and yields higher quality pharmacokinetic assessments. Further developments using 3-D models that focus on production and preservation

of fully native (and not minimalist equivalent) extracellular matrix, cell-cell interactions, relevant tissue architectures, and maintenance of both chemical and mechanical tissue-like stimulation using bioreactors are suggested to be critical for advancing *in vitro* cell-based experimental capabilities in high-throughput modes to obtain clinically relevant data in drug toxicity screening (Chapter 6).

## CHAPTER 2

### A CRITICAL EVALUATION OF IN VITRO CELL CULTURE MODELS FOR HIGH-THROUGHPUT DRUG SCREENING AND TOXICITY

Astashkina A, Mann B, Grainger DW

Journal of Pharmacology and Therapeutics 134:82-106, 2012

Reprinted with permission from Elsevier

License Number: 2855420225072

## ARTICLE IN PRESS

JPT-06420; No of Pages 25

Pharmacology &amp; Therapeutics xxx (2012) xxx–xxx



Contents lists available at SciVerse ScienceDirect

## Pharmacology &amp; Therapeutics

journal homepage: [www.elsevier.com/locate/pharmthera](http://www.elsevier.com/locate/pharmthera)

## A critical evaluation of in vitro cell culture models for high-throughput drug screening and toxicity

Anna Astashkina<sup>a</sup>, Brenda Mann<sup>b</sup>, David W. Grainger<sup>a,b,\*</sup><sup>a</sup> Department of Pharmaceutics and Pharmaceutical Chemistry, University of Utah, Salt Lake City, UT 84112-5820 USA<sup>b</sup> Department of Bioengineering, University of Utah, Salt Lake City, UT 84112-5820 USA

## ARTICLE INFO

## Keywords:

Toxicity  
Reasons for failure  
Cellular models  
HTS screens  
Role of microenvironment  
3-D and 2-D culture

## ABSTRACT

Drug candidate and toxicity screening processes currently rely on results from early-stage in vitro cell-based assays expected to faithfully represent essential aspects of in vivo pharmacology and toxicology. Several in vitro designs are optimized for high throughput to benefit screening efficiencies, allowing the entire libraries of potential pharmacologically relevant or possible toxin molecules to be screened for different types of cell signals relevant to tissue damage or to therapeutic goals. Creative approaches to multiplexed cell-based assay designs that select specific cell types, signaling pathways and reporters are routine. However, substantial percentages of new chemical and biological entities (NCEs/NBEs) that fail late-stage human drug testing, or receive regulatory “black box” warnings, or that are removed from the market for safety reasons after regulatory approvals all provide strong evidence that in vitro cell-based assays and subsequent preclinical in vivo studies do not yet provide sufficient pharmacological and toxicity data or reliable predictive capacity for understanding drug candidate performance in vivo. Without a reliable translational assay tool kit for pharmacology and toxicology, the drug development process is costly and inefficient in taking initial in vitro cell-based screens to in vivo testing and subsequent clinical approvals. Commonly employed methods of in vitro testing, including dissociated, organotypic, organ/explant, and 3-D cultures, are reviewed here with specific focus on retaining cell and molecular interactions and physiological parameters that determine cell phenotypes and their corresponding responses to bioactive agents. Distinct advantages and performance challenges for these models pertinent to cell-based assay and their predictive capabilities required for accurate correlations to in vivo mechanisms of drug toxicity are compared.

© 2012 Elsevier Inc. All rights reserved.

## Contents

|   |   |
|---|---|
| 1. Introduction   | 0 |
| 2. In vivo-relevant cell responses: the role of microenvironment    | 0 |
| 3. In vitro cell culture models: review, strengths, and limitations | 0 |
| 4. Conclusions  | 0 |
| Acknowledgments   | 0 |
| References  | 0 |

**Abbreviations:** NCE, new chemical entity; NBE, new biological entity; FDA, Food and Drug Administration; EU, European Union; CYP, cytochrome; GGT,  $\gamma$ -glutamyl transferase; MDR, multidrug-resistance; NABs, neutralizing antibodies; MDCK, Mandin–Darby Canine Kidney; ECM, extracellular matrix; HTS, high throughput screening; ICAMs, intracellular adhesion molecules; 2-D, two dimensional; 3-D, three dimensional; IL, interleukin; PBPK, physiologically based pharmacokinetics; PCTS, precision cut tissue slices; SV40, simian virus 40; HPV, human papillomavirus.

\* Corresponding author at: Department of Pharmaceutics and Pharmaceutical Chemistry, University of Utah, Salt Lake City, UT 84112-5820, USA. Tel.: 801 581 3715; fax: 801 581 3674. E-mail addresses: [anna.astashkina@utah.edu](mailto:anna.astashkina@utah.edu) (A. Astashkina), [brenda.mann@utah.edu](mailto:brenda.mann@utah.edu) (B. Mann), [david.grainger@utah.edu](mailto:david.grainger@utah.edu) (D.W. Grainger).

0163-7258/\$ – see front matter © 2012 Elsevier Inc. All rights reserved.

doi:[10.1016/j.pharmthera.2012.01.001](https://doi.org/10.1016/j.pharmthera.2012.01.001)

Please cite this article as: Astashkina, A., et al., A critical evaluation of in vitro cell culture models for high-throughput drug screening and toxicity, *Pharmacology & Therapeutics* (2012), doi:[10.1016/j.pharmthera.2012.01.001](https://doi.org/10.1016/j.pharmthera.2012.01.001)

## 1. Introduction

A key challenge in drug candidate screening and development of new chemical entity (NCE) or new biological entity (NBE) as therapeutic agents is accurate determination of their human toxicity (Dorato & Buckley, 2001; Li, 2004; Giezen et al., 2008). Recent critical reviews on drug development attrition rates from 1964 to 2000 estimated less than an 11% success rate in bringing a drug to market in the US and/or Europe (see Fig. 1) (Prentis et al., 1988; Lasser et al., 2002; Kola & Landis, 2004). Furthermore, nearly 3% of all drugs making it into the clinic were withdrawn later due to adverse side effects. Over 10% more acquired post-marketing U.S. Food and Drug Administration (FDA) “black box” warnings (Kola & Landis, 2004; Wang et al., 2010), the strongest caution that the FDA issues for marketed drug associations with serious or even lethal clinical or animal toxicity studies. Black box warnings are also correlated with post-marketing product withdrawals, accounting for about 30% of all removed NCEs (L. M. Wang et al., 2010). Unexpected drug toxicity encountered in the development pipeline is the second leading cause of drug attrition (see Table 1 for a list of drugs withdrawn from the market due to patient toxicity between 1974 and 2007), with overall withdrawal numbers doubling between 1991 and 2000 (Kola & Landis, 2004). With drug withdrawal costs estimated at \$804 million and considering that the most costly failures occur in late stages of drug development (Phases II and III), needs for greater reliability and predictability in identifying toxicity-free lead NCE/NBE compounds become very compelling (DiMasi et al., 2003; Kola & Landis, 2004).

### 1.1. Underlying causes of failure in assessing toxicity in preclinical studies

The lack of progress in improving predictive toxicity testing in humans is a result of both basic science and technical factors. Every NCE/NBE has unique mechanisms of toxicity; hence no single aspect of cell-based toxicity testing reviewed here can address this broad, complex spectrum. A critical analysis of current cell-based drug toxicity evaluation models is required to both understand their intrinsic deficiencies and identify limitations in their assessment mechanisms.

#### 1.1.1. Lack of mechanistic understanding and use of organ-specific toxicity mechanisms

In vivo drug toxicity is a multi-factorial, dynamic, and complex sequence of physiological events. Processes that lead to tissue damage as a result of pharmacological exposure may vary in significance or be specific to every organ, and involve interactions between cells

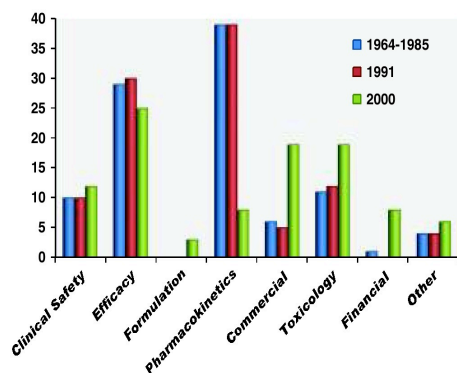


Fig. 1. Drug attrition rates from 1964 to 2000. Data from Prentis et al. (1988) and Kola and Landis (2004).

Table 1

Drug product withdrawals from the market due to toxicity from 1974 to 2011.

| Drug              | Indication  | Type of toxicity          | Year withdrawn                              |
|-------------------|---|---------------------------|---|
| Cylert            | Attention-deficit hyperactivity disorder and narcolepsy | Liver toxicity            | 2005  |
| Nefazodone        | Depression  | Liver toxicity            | 2003  |
| Rezulin           | Anti-inflammatory and anti-diabetic                     | Liver toxicity            | 2000  |
| Duract            | Non-steroidal anti-inflammatory drug                    | Liver toxicity            | 1998  |
| Ebrotidine        | Gastrointestinal lesions                                | Liver toxicity            | 1998  |
| Tolcapone         | Parkinson disease                                       | Liver toxicity            | 1998  |
| Tolrestat         | Diabetic neuropathy                                     | Liver toxicity            | 1996  |
| Chlormezanone     | Anxiety disorders                                       | Liver toxicity            | 1996  |
| Alpidem           | Anxiety disorders                                       | Liver toxicity            | 1994  |
| Bendazac          | Non-steroidal anti-inflammatory drug                    | Liver toxicity            | 1993  |
| Dilevalol         | Hypertension  | Liver toxicity            | 1990  |
| Fipexide          | Psychostimulation                                       | Liver toxicity            | 1990  |
| Tirynafen         | Diuretic and uricosuric                                 | Liver toxicity            | 1982  |
| Temafoxacin       | Bacterial infections                                    | Kidney toxicity           | 1992  |
| Nomifensine       | Antidepressant  | Kidney and liver toxicity | 1986  |
| Methoxyflurane    | Anesthetic  | Kidney and liver toxicity | 1974 in US but still used in Australia 1993 |
| Sorivudine        | Herpes simplex and varicella-zoster virus infection     | Gastric toxicity          | 2007  |
| Pergolide         | Parkinson's neurodegeneration                           | Cardiac toxicity          | 2005  |
| Adderall-XR       | Attention-deficit hyperactivity disorder                | Cardiac toxicity          | 2004  |
| Vioxx             | Acute and chronic pain                                  | Cardiac toxicity          | 2003  |
| Levacetylmethadol | Treatment of opioid addictions                          | Cardiac toxicity          | 2001  |
| Droperidol        | Premedication for anesthesia                            | Cardiac toxicity          | 2000  |
| Cisapride         | Gastrointestinal reflux                                 | Cardiac toxicity          | 1999  |
| Hismanal          | Antihistamine   | Cardiac toxicity          | 1999  |
| Encainide         | Antiarrhythmic  | Cardiac toxicity          | 1998  |
| Seldane           | Antihistamine   | Cardiac toxicity          | 1997–1999                                   |
| Terfenadine       | Allergies   | Cardiac toxicity          | 1997  |
| Fenfluramine      | Appetite suppressant                                    | Cardiac toxicity          | 1993  |
| Flosequinan       | Vasodilator   | Cardiac toxicity          | 1992  |
| Terodiline        | Urinary incontinence                                    | Cardiac toxicity          | 1990  |
| Grepafloxacin     | Bacterial infections                                    | Cardiac toxicity          |   |

and drugs, drug metabolites, and drug–protein conjugates. These events are seldom recapitulated in molecular detail, kinetics, dynamics or cellular metabolic processing in simplified in vitro models. Although much is written about general cellular mechanisms of apoptosis such as DNA fragmentation, caspase activation, and oxidative stress, very little is known about specific organ toxicities (Balis, 2002; Xu et al., 2004; P. O'Brien & Haskins, 2007). For example, both the kidneys and heart are cytochrome (CYP) P450-active organs with abundant  $\gamma$ -glutamyl transferase (GGT) activity. Although CYP and GGT have both been implicated in drug metabolism and conjugate adduct toxicity mechanisms in liver, little is known regarding their specific roles in renal or cardiovascular chemical-induced damage despite published anecdotes and empirical examples of their importance.

In addition, drug metabolites produced via these mechanisms may prove more toxic than the original drug. Cisplatin, a commonly used chemotherapeutic drug and also potent nephrotoxin, has been shown to be converted to at least seven kidney-specific metabolites more damaging than cisplatin itself (Daley-Yates & McBrien, 1984; Mistry et al., 1989). Similarly, terfenadine (Seldane®), an antihistamine drug, was pulled from the market in 1998 due to unexpected cardiotoxicity (see Table 1), possibly through inhibition of CYP2J2, an important enzyme regulating vascular tone and anti-apoptotic events (Lafite et al., 2006; Lafite et al., 2007; Zhou, 2008; Chaudhary et al., 2009). Current methods of cellular toxicity assessment are often most appropriate for identification of well-identified and specific, often molecular, routes of cellular damage, such as up-regulation of multidrug-resistance (MDR) proteins or utilization of specific drug transporters, by using cell lines specifically engineered to over-express these molecular features (further discussed in Section 3). Hence, current toxicity testing methodology is not ideal for assessing or identifying unknown modes of toxicity in vitro, leaving the burden of their identification to costly animal and clinical studies.

#### 1.1.2. Limited use of pre-lethal indicators

In addition to the lack of mechanism-specific cellular damage targets, current toxicity assessment is limited in testing for pre-lethal cell-stress indicators (Balis, 2002; Xu et al., 2004; P. O'Brien & Haskins, 2007). A growing volume of evidence suggests that cell-based toxicity in many cases is manifested by profound alterations in cell function in organs/cultures exposed to xenobiotics but without cellular death. For example, toxic substances were shown to interact with cell–cell and cell–matrix adhesion molecules in kidney proximal tubule cells and their corresponding intracellular scaffolding proteins. These proteins trigger signal cascades within the cell that alter cell polarization, permeability, gene expression, post-translational modifications, and the ability to initiate and sustain inflammatory processes. This disrupts the cytoskeleton and promotes cellular de-differentiation (Ackay et al., 2009). Likewise, drug-induced inhibition of the bile salt transport pump, and most likely also MDR1, MDR2, and MDR3 pumps, in hepatocytes leads to reduced bile formation, intra-hepatic cholestasis and jaundice (Geier et al., 2006). Thus, limited use of pre-lethal indicators of adverse effects on whole-animal tissues or cell cultures can result in inadequate toxicity assessment, as well as biased testing of NCEs/NBEs using super-physiological concentrations. Furthermore, the inability to assess early cell damage events leads to a greater need for extended time- and dose-response point toxicity assessment, as all NCEs/NBEs would likely have unique therapeutic windows and kinetics of toxicity induction.

#### 1.1.3. Lack of immune system validation

All exogenous agents interact with diverse host immune system components upon introduction into the human body. NBEs are the most susceptible to such encounter eliciting toxicity from immune processing as they directly contact the immune system surveillance and processing components. Protein-based drug candidates are known to elicit product-specific neutralizing antibodies (NABs) that recognize and clear NBE molecules from circulation, limiting drug bioavailability (Perini et al., 2001; Porter, 2001; J. W. Lee et al., 2011). Host immune response to NBEs depends on many factors, including patient health and immune competence, size and chemical structure of the protein, and manufacturing process (Cromwell et al., 2006; Rosenberg, 2006; Gupta et al., 2007). The effect of the NABs can vary from limiting drug efficacy to causing severe health problems, as in the case of recombinant human erythropoietin producing severe anemia caused by NABs that eliminated both endogenous and exogenous erythropoietin and normal red blood cell production (Casadevall et al., 2002; Sanchez et al., 2011). Currently, the FDA recommends evaluating the presence of NABs during preclinical research as part of the drug-development process (FDA, 2009). The only

established in vitro test of immunogenicity and immunotoxicity currently available is an acute lymphocyte test that examines freshly prepared blood samples for lymphocyte proliferation and cytokine induction (Portner & Giese, 2007). The test is limited to acute dose testing and is not capable of recognizing longer-term adverse effects of host antigen processing by antigen-presenting cells or T cells. Cell-based evaluation using histological equivalence to human immunological systems would need to be considered for appropriate evaluation in vitro (Portner & Giese, 2007).

While direct immune interactions with NCEs, are less problematic in drug development (with exceptions for rare allergic reactions), secondary interactions between the immune system and chemical-induced injury in the form of tissue inflammatory processes are quite common. Inflammation is an important host response to cellular damage and repair after drug-induced exposure. Cellular damage in the affected organs in vivo leads to cytokine and other inflammatory mediator secretion, and recruitment of inflammatory and immune system cells to the site of injury (Ackay et al., 2009). Inflammatory cells can in turn either sustain inflammatory processes, further damaging tissues, or initiate removal of apoptotic cells, aiding in tissue remodeling and restoration (Ackay et al., 2009). Selection of either path might be dose- or molecular pathway-dependent, but knowing this processing is requisite to properly understand adverse drug candidate processes in vivo. Lack of analogous immunological processing competence in most in vitro models is a major drawback, especially for NBE screening.

#### 1.1.4. Lack of validated in vitro–in vivo or interspecies toxicity correlations

The well-known “Paracelsus doctrine” states that the difference between a toxic and harmless compound is the dose. Unfortunately, the dose–toxicity relationship is not always linear and depends critically on absorption, distribution, metabolism, and elimination characteristics of the drug. The term “toxicokinetics” is used to describe methods for relating drug dose to exposure levels and correlating both to development of toxicity indicators (Dorato & Buckley, 2001). The goal of toxicokinetics in preclinical safety assessments is prediction of human toxicity profiles from in vitro and laboratory animal data (Dorato & Buckley, 2001). Lack of accurate mathematical approaches for this extrapolation remains a most basic limitation of current toxicity assessment. Existing toxicity measurements rely on statistically significant increases in histological or secondary biomarkers (for example, blood urea nitrogen and creatinine in functional kidney damage) in animal studies, and in apoptotic or necrotic indicators in cellular models over untreated controls (see Table 2). Unfortunately, even if certain doses (or concentrations) are found to be toxic, there is no way to know if the toxicity range overlaps with the effective dose in humans without established methods of relating in vitro and/or animal dose data to human in vivo doses.

Physiologically based pharmacokinetics (PBPK) remains a most powerful approach in predictive extrapolation methods from animal to human data (P. Zhao et al., 2011). Unlike conventional pharmacokinetics, PBPK does not simply mathematically fit existing data, but describes multi-compartment biological systems defined by individual tissue compartments. PBPK quantitatively accounts for relationships between tissue compartments by incorporating empirically obtained physiological data for each animal on biological processes important in absorption, distribution, metabolism, and elimination. These processes may include blood flow, breathing, excretion rates, blood/tissue partition coefficients, and metabolic variables (P. Zhao et al., 2011). Because each animal physiology is “self-adjusted” based on its unique physiological characteristics, commonly derived physiological parameters (i.e., biodistribution, half-life) can be compared between different animal species. PBPK can therefore produce the most reliable interspecies correlations, but requires substantial physiological and pharmacokinetic data inputs to condition the model (Kamgang et al., 2008; P. Zhao et al., 2011). Furthermore, PBPK models are built on the principle of adjusting physiological



**Table 2**  
Common in vitro assays used in drug toxicity assessments.

| Assay name  | Assay mechanism  | Type of assessment   | Evaluation end-point  | Advantages and limitations   |
|---|--|--|---|--|
| 3-(4,5-Dimethylthiazol-2-yl)-2,5-diphenyltetrazolium bromide (MTT), 2,3-bis-(2-methoxy-4-nitro-5-sulphophenyl)-2H-tetrazolium-5-carboxanilide (XTT), 3-(4,5-dimethylthiazol-2-yl)-5-(3-carboxymethoxyphenyl)-2-(4-sulphophenyl)-2H-tetrazolium (MTS) Alamar Blue, Cell Titer Blue | Reduction of MTT, XTT, and MTS (in the presence of phenazine methosulfate) to formazan derivatives                 | Measurement of anti-metabolic effects. Used in cell viability and proliferation assessment, cell activation                                      | Formazan derivatives absorb at 500–600 nm (MTT), 450–500 nm (XTT), 490–500 nm (MTS) | Advantages: easy to perform<br>Limitations: do not distinguish between apoptosis and necrosis; not very sensitive  |
| CellTiterGlow   | Reduction of resazurin to resorufin  | Measurement of anti-metabolic effects. Used in cell viability and proliferation assessment   | Resorufin fluoresces at ex: 560 nm, em: 590 nm and absorbs at 573 nm                | Advantages: easy to perform<br>Limitations: do not distinguish between apoptosis and necrosis; not very sensitive  |
| ToxiLight   | Adenosine-5'-triphosphate (ATP) quantification through mono-oxygenation of luciferin in the presence of luciferase | Measurement of energy depletion effects. Used in cell viability and proliferation assessment   | Luminescent assay   | Advantages: easy to perform; little interference with background<br>Limitations: does not distinguish between apoptosis and necrosis   |
|   | Adenylate kinase (AK) quantification through mono-oxygenation of luciferin   | Measurement of cytolysis. Used in cell death assessment. Most commonly attributed to cell necrosis, although cell leakage can occur in apoptosis | Luminescent assay   | Advantages: non-destructive; little interference with background<br>Limitations: necrosis in vitro occurs at higher drug doses than apoptosis; requires separate 100% death assessment |
| Lactate dehydrogenase (LDH) assay, CytoTox-ONE  | LDH quantification through lactate to pyruvate conversion coupled to formazan or resorufin (CytoTox) reduction     | Measurement of cytolysis. Used in cell death assessment. Most commonly attributed to cell necrosis, although cell leakage can occur in apoptosis | Formazan absorbs at 490–520 nm; resorufin fluoresces at ex: 560 nm, em: 590 nm      | Advantages: non-destructive<br>Limitations: necrosis in vitro occurs at higher drug doses than apoptosis; requires separate 100% death assessment                                      |



|  |   |   |  |   |
|--|---|---|--|---|
| Neutral red, TOX-4   | Dye uptake by lysosomes of live cells   | leakage can occur in apoptosis<br>Measurement of endocytic ability. Used is cell viability                          | Dyes absorb at 539–544 nm  | Advantages: easy to perform<br>Limitations: does not distinguish between apoptosis and necrosis   |
| Live/dead assays-Calcein AM/ethidium homodimer or Hoechst 33342, DAPI, and propidium iodide (PI) | Dye uptake or exclusion by live cells. Calcein AM is a live cell indicator, PI and ethidium homodimer are dead/necrotic indicators, DAPI and Hoechst are nuclear stains | Measurement of membrane integrity   | Calcein fluoresces at ex: 495 nm, em: 516 nm; ethidium homodimer fluoresces at ex: 528 nm, em: 617 nm                            | Advantages: easy to perform, Hoechst's can be used to trace nuclear fragmentation<br>Limitations: visual quantification; all dyes can be toxic at high concentrations |
| CyQuant  | DNA staining. CyQuant binds to nucleic acids for quantification.  | Measurement of DNA concentration and anti-proliferative events. Used in cell viability and proliferation assessment | CyQuant fluoresces at ex: 485 nm, em: 530 nm   | Advantages: very sensitive<br>Limitations: CyQuant cannot distinguish between apoptosis and necrosis  |
| 5-Bromo-2'-deoxyuridine (BrdU), radioactive incorporation  | DNA incorporation. Radiolabeled thymidine and BrdU (thymidine analog) incorporate into DNA during cell proliferation.   | Measurement of anti-proliferative events. Used in proliferation assessment  | BrdU is quantified using anti-BrdU antibody staining (immunohistochemistry). Radiolabeling is measured by scintillation counting | Advantages: proliferation specific assays<br>Limitations: toxicity visual quantification for BrdU; associated with radioactive materials                              |
| Trypan blue, methylene blue  | Dye incorporation by dead/necrotic cells  | Measurement of membrane integrity. Used for cell viability assessment   | Visual cell counting under light microscope  | Advantages: easy to perform<br>Limitations: visual quantification, only for small cell sample counts  |
| Caspase 3/7 assays — Apo-One, etc.   | Caspases are quantified using proluminescent (Caspase-Glo) or profluorescent substrates   | Apoptosis measurement   | Luminescent assay (Caspase-Glo); Caspase-3/7 fluoresces at ex: 495 nm, em: 521 nm  | Advantages: pathway specific apoptosis  |

## ARTICLE IN PRESS

6

A. Astashkina et al. / Pharmacology &amp; Therapeutics xxx (2012) xxx–xxx

variables (such as rates), but cannot account for intrinsic differences in animal physiologies (such as differences in liver detoxification pathways, anatomical differences, or different metabolic features).

One aspect of PBPK that has not yet been fully explored is correlation of in vivo and in vitro toxicities using drug exposure history. Provided with pharmacokinetic data sufficient to approximate drug dispositions in different organ structures (such as proximal epithelial cells in kidneys responsible for the majority of “kidney toxicity”), it should be possible to correlate PBPK-derived in vivo human or laboratory animal data to xenobiotic exposure in cell-based assays (Kamgang et al., 2008). Comparisons might be made either in terms of body weight correlations or scaled to affected tissue surface area. Both methods for estimating drug exposure are currently used for rough animal–human dose adjustments. Nonetheless, correlations based on surface area were shown to yield more accurate interspecies extrapolations and are the preferred method for preclinical safety assessment methods in the European Union (EU) (Dorato & Buckley, 2001).

#### 1.1.5. Animal models frequently do not reflect human toxicity

While animal research has played a pivotal and instrumental role in understanding most pathological and non-pathological processes in humans, significant differences in interspecies metabolic capacities, physiologies, and disease adaptation mechanisms are often ignored. For example, while all mammals use cytochrome P450 to detoxify and eliminate toxic compounds, specific CYP distribution and drug handling responsibilities, rates of phase I reactions, and pathway preference in phase II vary significantly between rodents, hares, canines, and humans (Smith, 1991). Functional differences in drug handling by the kidneys and drug absorption in the digestive tract due to different gut pHs among carnivores and herbivores are recognized (Smith, 1991). Plasma concentration and composition varies among species, thereby affecting drug–protein partitioning interactions and consequently half-life and bioavailability. Breathing and excretion rates also fluctuate significantly between small (rodents) and large mammals (monkeys and humans), causing discrepancies in drug distribution and tissue accumulation (Smith, 1991). Interspecies differences often mask toxicity signals of lead compounds in preclinical studies, resulting in costly withdrawals once moved into human clinical trials. Multiple species testing in combination with human cell line assays might more accurately predict toxicity profiles, and distinguish important inter-species disparities.

#### 1.1.6. High-throughput limitations

The pharmaceutical industry strives continuously to produce new, safer and more efficacious drugs for unmet needs, while also meeting commercial objectives. Evolving combinatorial small molecule chemical synthesis capabilities in parallel with rapid advances in protein selection, expression, amplification, and characterization have widely expanded numbers of leads for potential drug candidates. However, this abundance has also created a new set of challenges in efficient processing of drug libraries for target validation and toxicity assessment. Unfortunately, screening of thousands of compounds is not economically practical, nor ethically responsible, using whole animal models, restricting drug screening tools in initial testing to use of mammalian cell-based assays. High-throughput screening (HTS) is thought to be key in handling this flow of new potential therapeutics in a systematic and time-efficient manner. HTS methods with cells/cell lines in multi-well plates, robotic/automated processing and read-out, and flow cytometric assays have the capacity to test many drug concentrations and exposure times in a time-efficient manner. HTS requires coordinated, automated techniques for assays that are limited by: 1) tools and/or assays available for rapid, reliable micro-analytical assessments, and 2) the quality of existing cell culture models (see Section 3.3). Reliability and accuracy of both are key to obtaining relevant, reliable toxicity data.

Examination of primary causes of NCE and NBE toxicity (vida supra) is instructive in identifying strategies to maximize probabilities for successful progression of drug candidates from preclinical studies through the development pipeline. As previously discussed, several biological (limited animal-to-human correlations, see Section 1.1.5) and practical (testing large libraries of drug leads, see Section 1.1.6) reasons limit the applicability of animal testing in early drug development; hence, in vitro cytotoxicity testing using human cell lines or cells that exhibit appropriate cellular mechanisms is increasingly relied upon as an effective method of screening lead drug compounds. Furthermore, using cell-based assays in initial steps of drug discovery may have additional advantages in addressing concerns described in the previous section. First, given the complex nature of toxicity that characterizes drug exposure to human physiology (Section 1.1.1) and lack of precise correlations between in vitro and human doses discussed in Section 1.1.4, it is clear that cell-based assays that truly predict in vivo-relevant toxicity would require a multi-parametric type of assessment — one that is not easily exploited or even available using cell monocultures. Second, the need to address many end-points of possible cell toxicity mechanisms, both pre-lethal (see Section 1.1.2), apoptotic, and necrotic (see Table 2), may require panels of multiplexed assays run in parallel. Only HTS methods would allow for such assessment in a reasonable amount of time. Third, HTS methods may allow for multiple cell type and cell line testing simultaneously, incorporating cell targets from multiple organ sources (e.g., kidney, liver, heart, lung, nervous system), cell types (e.g., epithelial, endothelial, myoskeletal, neural, germ line, leukocyte, etc.) and different species (e.g., zebrafish, rodent, sheep, human, etc.). Fourth, even though it is not directly associated with cell toxicity, cell-based assays might be important in target validation as a stepping stone to further animal or human testing. Use of whole cell vs. simpler solution-binding assays better reflects the complexity of the protein-rich, diverse biological milieu that drugs interact with in vivo.

HTS assessment methods contribute regularly to the preclinical components of drug discovery and screening. Recent developments in biomarker identification and validation using toxicogenomics, proteomics, and metabolomics produce vast quantities of data. These data, while generated using wide ranges of state-of-the-art technologies with the best of intentions, are not utilized effectively towards the screening goals: the amounts and diverse types of data lack ready manipulation, processing and integration capabilities required for facile use in drug and toxicology screening (Amin et al., 2004; Gallagher et al., 2009). The few extensive biomarker studies conducted — the Innovative Medicines for Europe project, ILSI Health and Environmental Sciences Institute initiative, Predictive Safety Testing Consortium — were limited by their reliance on costly in vivo models due to limitations inherent in in vitro cell culture screens. Additionally, these efforts required consortia of pharmaceutical industry, academia, and regulatory agencies due to the excessive expenses and workload associated with the studies (Hoffmann et al., 2010). Hence, development of improved in vitro culture approaches better reflective of in vivo cell behaviors and reactions to drugs would significantly impact both the cost and accessibility of future HTS work.

Pathologies and toxicologies even with similar symptoms often result from very different origins at the genomic level. In some cases, drug targets can be identified using RNA and DNA microarrays. However, diagnostics that measure transcript and protein biomarkers often fail to predict or detect diseases or toxicities produced from genetic variations. New emerging efforts in toxicogenomics claim to better address these predictive deficiencies by assessing single nucleotide polymorphisms and chromosomal aberrations. As diseases and tissue toxicity sensitivities can originate in genomic variations, it is rational to proceed with in vitro assays correlating susceptibilities to genomic variations — a correlation more frequently observed in

clinical trials. Importantly, as witnessed in the Innovative Medicines for Europe study (see [www.innomed-predtox.org](http://www.innomed-predtox.org)), combinations of gene expression markers, copy number variants, epigenetic variations, non-coding DNA, single nucleotide polymorphisms, and post-transcriptional biomarkers – and not single markers – must be considered for accurate genomic predictions for drug efficacy and safety. However, this is not a simple undertaking conducted with microarray technology. Such correlation is currently a mammoth, coordinated team-based effort to produce and process data from many sources and technologies (e.g., as seen currently in follow-on large-team genomics initiatives at the Critical Path Institute, USA, and Toxicogenomics Project from the National Institute of Biomedical Innovations, Japan), producing translational bottlenecks unlikely to transcend beyond the efforts of large consortia without substantial progress in data integration and routine handling protocols (Hoefkens, 2011).

## 1.2. Current methods of toxicity assessment

Productive paths to drug discovery, lead compound validation and formulation vary widely among academic laboratories and pharmaceutical companies; academia relies primarily on hits discovered during a focused research process for a single mechanistic model, while industry tends to identify initial lead compounds from large target-binding screens. The main focus is on end-point assays that establish cell survival and proliferation and indications of target efficacy after exogenous agent exposure in cultures. Some popular screening bioassays as well as their advantages and limitations are outlined in Table 2 (Storer et al., 1996; Lisheng Wang et al., 1996; McKeague, Wilson, & Nelson, 2003; O'Brien et al., 2007; Kendigand & Tarloff, 2007; Abraham, Towne, Waring, Warrior, & Burns, 2008). As previously mentioned in Section 1.1.1, most toxicity assays measure general cell viability or cell proliferation endpoints, and are not specific to toxicity mechanisms. Moreover, very few assays are specific enough to distinguish between apoptosis and necrosis cell death mechanisms, which for in vitro toxicity assessment is often a function of drug concentration. Lack of multiple points of comparison can lead to misleading and in vivo-irrelevant data. Suggestions for improving mechanism-specific toxicity assays that go beyond conventional cytotoxicity measurement were extensively discussed in previously published reviews (Xu et al., 2004; P. O'Brien & Haskins, 2007; Donato et al., 2008).

While low-cost, high-speed, and multi-parametric assessment advantages of cell-based toxicity assays are undisputed, their use comes with a major assumption of cell phenotypic equivalence to their in vivo tissue-resident counterparts. As discussed in detail in Section 3, this might be misleading for cell-based models currently in practice. Firstly, many cell lines supplied from commercial sources are over-passaged, contaminated with other cells, or rarely validated for phenotype (Masters, 2002; P. Hughes et al., 2007; Nardone, 2007; Capes-Davis et al., 2010). Secondly, no in vitro model completely mimics all complexities of cell, tissue or organ toxicity in vivo. However, advancements in understanding molecular and biochemical pathways involved in drug-induced pathogenesis, in vitro bioreactor-based tissue engineering approaches for tissue regeneration, and existing model characterization should be better exploited to better assert and validate in vivo-relevant results. Thorough, systematic evaluation of in vitro models as well as factors critical in their limitations must be considered prior to model implementation for specific toxicity assessments (Fig. 2). This review focuses on the current understanding of the many variables required to incorporate physiologically relevant responses into in vitro culture and then further evaluate available cell model systems with these variables in mind.

## 2. In vivo-relevant cell responses: the role of microenvironment

Cellular microenvironment, and more specifically, cell–cell and cell–matrix interactions, tissue architectural organization, and proper

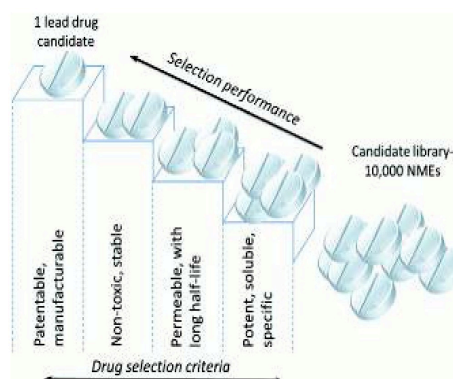


Fig. 2. Drug candidate identification steps in the preclinical development pipeline.

oxygen and nutrient supply have all been implicated as key factors in supporting cell native phenotype. In this regard, it is reasonable to assume that many, if not all of these factors, would need to be maintained in an in vitro culture to attain physiologically or pathologically relevant results from cells in culture (see Fig. 3). The specific in vivo context of cell function and survival is often not considered in cell cultures, leading to disconnects between drug dose–response cell culture results on plastic and in vivo pharmacology.

### 2.1. Cell–cell interactions in toxicity

Intercellular interactions are essential to normal physiological and pathological processes. Tissue injury associated with drug toxicity disrupts intercellular connections, initiating a cascade of cellular events that leads to loss of function, induction of inflammation, tissue necrosis, and apoptosis. Hence, recapitulation of these interactions similar to their in vivo counterparts is critical for creating in vitro models that respond to environmental assaults with clinically relevant biomarkers and physiological fidelity.

Cell–cell communication mechanisms are essential for cells to sense and respond to their environment, guiding critical processes in cell migration, differentiation, healing, and development (Cukierman et al., 2001, 2002; L. E. O'Brien et al., 2002; Yamada et al., 2003; Larsen et al., 2006). Furthermore, intercellular contacts facilitate groups of cells to interact as a functionally integrated tissue

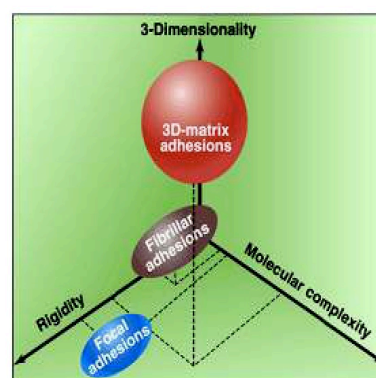


Fig. 3. Extracellular matrix factors affecting cell function in vivo. From Geiger (2001).



## ARTICLE IN PRESS

8

A. Astashkina et al. / Pharmacology &amp; Therapeutics xxx (2012) xxx–xxx

by “forwarding” signaling information and prompting synchronization, communal response to injury (Ichimura et al., 1998; Ichimura et al., 2008; Huo et al., 2010), changes in differentiation (Crosby & Waters, 2010), and initiation/down-regulation of pro-apoptotic or homeostatic responses (Saez et al., 1989; Lin et al., 1998; Peracchia et al., 2000; Brosnan et al., 2001). These “local” tissue responses are critical in establishing homeostasis and toxicity-injury circumvention processes, but commonly lost in vitro in cellular culture models. This results in cell-specific, uncoupled, and physiologically incomplete evaluation processes in culture. Several superfamilies of intercellular communication proteins, better known as cell-membrane adhesion molecules (CAMs), have been identified in vivo. These and other glycoproteins are implicated in chemical cell injury or cellular changes associated with in vitro models, such as cadherins, gap junctions, intercellular adhesion molecules (ICAMs), and selectins.

Cadherins constitute a family of  $\text{Ca}^{2+}$ -dependent type I signaling transmembrane proteins estimated to include over 350 members, further divided into classical cadherins, cadherin-related signaling proteins, protocadherins, desmosomal cadherins, and atypical cadherins (Angst et al., 2001; Pokutta & Weis, 2007; Hulpiau & van Roy, 2009). Classical cadherins form cadherin–catenin complexes by binding intracellular regions of cadherin glycoprotein with  $\beta$ -catenin already bound to either  $\alpha$ - or  $\gamma$ -catenin. This in turn interacts with the cell's cytoskeleton (Angst et al., 2001; Hulpiau & van Roy, 2009). The cadherin–catenin role in tissue homeostasis is two-fold: it acts as a structural part of adherens junctions – junctional complexes responsible for cell permeability and polarization – and is also a cell mechano-chemical transduction mechanism component, regulating cell-signaling pathways in the cell including wingless nuclear signaling gene expression-regulating pathway (Brown & Moon, 1998; Gumbiner, 1998; Bienz, 1999; Hulpiau & van Roy, 2009). Classical E (epithelial)- and N (neuronal)-cadherins are two members expressed in adult tissues and typically associated with drug toxicity induction in in vivo experiments (Parrish et al., 1999; Prozialeck et al., 2003). The mode of cellular damage depends on the organ: in liver, cadherins are disrupted by oxidative stress (Parrish et al., 1999); in kidney, they are thought to be disturbed in the process of cell shedding from the luminal space of the nephron (Sheridan & Bonventre, 2000); and in heart, certain toxins, including drugs (e.g., doxycycline and lenalidomide), affect the vascular endothelial lining, resulting in increased chances of hemorrhage and thromboembolism (Fainaru et al., 2008; Lu et al., 2009; Albini et al., 2010). Despite the mode of damage, cadherin complex impairment is thought to result in cell-cell disruption, and subsequent changes in fluid redistribution and/or alterations in function and integrity of cellular monolayers. For example, in kidney failure animal models and human clinical studies, disruption of cadherin complexes was a confounding factor in toxicity due to  $\text{HgCl}_2$  (Jiang et al., 2004), cisplatin (Imamdi et al., 2004), ochratoxin A (Mally et al., 2006), glycerol (Racusen et al., 1991),  $\text{Cd}^{2+}$  (Chakraborty et al., 2010), bismuth (Leussink et al., 2001), cyclosporine A (Zimmerhackl et al., 1997), yessotoxin (Ronzitti et al., 2004), diatrizonate and toxaglate (radiocontrast agents) (Schick & Haller, 1999). Specifically, damage to the epithelial lining of the proximal tubules was associated with shedding of viable cells into urine (Racusen et al., 1991) as well as “backleak” of glomerular ultrafiltrate into interstitium and the venous system (Myers et al., 1979; Moran & Myers, 1985; Kwon et al., 1998). Despite the differences in pathological outcomes, deregulation of many cell–cell interactions analogous to cadherin disruption results in abrogation of normal physiological processes and induction of pathological cellular changes. Hence, utilization of in vitro models that accurately predict such pathological changes would be of great interest to drug screening platforms.

Gap junctions are intercellular transmembrane channels comprising two hemi-channels located on adjacent cell membranes, spanning the extracellular space (Saez et al., 1989; Chipman et al., 2003). Each hemi-channel is formed by six oligomerized connexin proteins,

allowing passage of small (<1.2 kDa) molecules, such as  $\text{Ca}^{2+}$  or ATP (Saez et al., 1989; Chipman et al., 2003). Gap junctions are gated channels; hence, they are affected by intracellular pH, radicals, and  $\text{Ca}^{2+}$  ion concentrations (Chipman et al., 2003). They are commonly thought to be responsible for tissue homeostasis, signal propagation in nerve cells, synchronization of cardiomyocyte contraction, and differentiation and development in embryogenesis (Loewenstein, 1981). More recent studies also suggested that gap junctions might be important in cell proliferation and apoptosis (Dermietzel et al., 1987; Dufrot-Dancer et al., 1997; Moorby & Patel, 2001). Although not thought to be involved directly, gap junctions were shown to act as a “check point” during mitosis, allowing cell-cycle progression (Chipman et al., 2003). Disruption of these critical gap junction operations produces cell dysfunction, toxicity and death. Nonetheless, the relationship between functional gap junctions and apoptosis due to toxic injury is poorly understood; some gap junction disruptors induce cellular death, but this empirical rule does not seem to extend similarly to all tested compounds (Kolaja et al., 2000a, 2000b; Mally & Chipman, 2002). Gap junction signaling is thought to be important either in the early events leading to apoptosis and proliferation, or has an additive effect to a more powerful regulator (Chipman et al., 2003). Impairment of gap junctions, either by narrowing of channels due to changes in cellular membrane fluidity, decreased connexin production, or through physical obstruction is a well-documented form of cellular toxicity in vivo. For example, alcohols, such as octanol and heptanol, and anesthetics were previously shown to reduce membrane fluidity (Saez et al., 1989) and non-genotoxic carcinogens such as tetrachlorodibenzo-*p*-dioxin disrupts gap junction by down-regulating connexin 32 (Chipman et al., 2003). Furthermore, several carcinogens such as pesticides dichlorodiphenyl-trichloroethane, dichlorodiphenyldichloroethylene, lindane, heptachlor, and dieldrin, as well as tumor-promoting agents such as phenobarbitone, the phorbol ester 12-*O*-tetradecanoylphorbol 13-acetate, tetrachlorodibenzo-*p*-dioxin, and polychlorinated biphenyls showed deregulation of gap junctions as part of carcinogenesis and loss of tissue homeostasis after toxic exposure (Swierenga & Yamasaki, 1992). Additionally, because gap junctions are chemically gated channels, their conductance is extremely sensitive to toxin-induced changes in intracellular redox states (for example, through mechanisms involving  $\text{Ca}^{2+}$  gating) (Saez et al., 1989). Although the exact mechanism linking cellular damage, apoptosis, and gap junction deregulation remains to be elucidated, the vast toxicological literature record supports a strong correlation between gap junction dysfunction and tissue injury in kidney, liver, cardiovascular, and nervous system toxicology (Mehendale et al., 1994; Pluciennik et al., 1996; Fukumoto et al., 2001; Ozog et al., 2002; Chipman et al., 2003). Hepatic gap junctions are frequently impaired by numerous chemical and pharmaceutical insults, validating their function for use in drug screening and hepatotoxicity (Vinken et al., 2009).

Intercellular adhesion molecules (or ICAMs) are members of the immunoglobulin superfamily (Staunton et al., 1988; Albelda, 1991). They are  $\text{Ca}^{2+}$ -independent membrane proteins with a characteristic single trans-membrane domain, extracellular amino-terminated domain, and carboxy-terminated intracellular domain (Casasnovas et al., 1998). Many different types of ICAMs are expressed in different tissue linings, some of which are constitutively expressed (for example, ICAM-2, ICAM-3, and platelet endothelial cell adhesion molecules along vascular endothelial cells (Jaeschke, 1997)), and some are injury-inducible in toxic insult (e.g., ICAM-1 in liver and kidney toxicity from toxins, drugs and ethanol) (Essani et al., 1995; Farhood et al., 1995). Selectins are another major branch of adhesion molecules, characterized by lectin binding domains (McEver et al., 1995). The selectin family includes P (platelet)-, L (leukocyte), and E (endothelial)-selectins, where P-selectins are primarily found on platelets and endothelial cells, L-selectins on leukocytes and lymphocytes, and E-selectins on endothelial cells (Kishimoto et al., 1989; McEver et al., 1995).

ICAMs and selectins are primary regulators of inflammatory-induction processes associated with cell toxicity. Inflammation, either acute or chronic, commonly accompanies drug toxicity (Akçay et al., 2009). Initial injury by endogenous agents is proposed to trigger a cascade of events leading to morphological and functional cellular changes within the tissue as well as associated vascular endothelium. These changes, in turn, result in secretion of inflammatory mediators by the injured tissues, such as cytokines and chemokines, as well as induction of adhesion molecules, such as ICAMs and selectins. Soluble inflammatory molecules then facilitate recruitment of inflammatory cells (macrophages, neutrophils, natural killer cells, and lymphocytes), which adhere and extravasate into damaged tissues via interaction with adhesion molecules. Specifically, ICAMs and selectins are up-regulated on tissue and immuno-modulatory cells, respectively, providing leukocytes with localized signals for migration, attachment, activation and extravasation at the site of injury to initiate the inflammatory cascades (Akçay et al., 2009). The balance of pro- and anti-inflammatory molecules regulates down-stream healing and apoptotic responses in damaged tissue or promotes further injury. Both induction and duration of these inflammatory processes in vivo are thought to be critical contributors to drug-associated pathophysiology (Akçay et al., 2009). Hence, in vitro models that accurately respond to drug-induced injury by reproducing these key inflammatory modulators are critical for clinically relevant toxicity screening of drug candidates.

## 2.2. Cell–matrix interactions

Cell receptor-based interactions with extracellular matrix (ECM) direct many normal and pathological tissue processes in vivo (Cukierman et al., 2001, 2002; Larsen et al., 2006). Use of collagen only, or dilute serum, or combinations of single matrix protein-culture plastic materials in vitro is often insufficient to reliably preserve or promote cultured cell phenotypic fidelity in adhesion-dependent cell cultures (Cukierman et al., 2001). Hence, preservation of in vivo-like matrix composition is important for cell engagement that allows detection of pre-lethal as well as molecular and paracellular signaling changes associated with cell damage or toxicity. Cell–ECM interactions transmit haptic, stress-induced, mechanical, and soluble signals between cells, and mutually alter respective functions of both cells and ECM in bi-directional manners. On one hand, intracellular tensile forces resulting from both specific and non-specific cell interactions with adhesive matrix substrates are key factors determining cell migration, rearrangement, spreading, and tissue morphology (Hynes, 1999; Geiger et al., 2001). Cell mechanical coupling requirements for their ECM engagement and reliable signal processing both inter- and intra-cellularly is just now beginning to be explored. Together, biochemical and mechanical cues from cells modulate ECM remodeling through de novo protein synthesis, degradation, and cell contraction (Hynes, 1999). ECM remodeling in vivo is a critical step in development of pathological states such as tumor-associated stromatogenesis as well as normal processes of development and tissue repair (Bissell & Radisky, 2001; Sviridis et al., 2004; Paszek et al., 2005). Similarly, in vivo oxidation of ECM components is important for prompting macrophage infiltration into damaged tissue, initiating inflammatory toxicity-associated processes (Mattana et al., 1998). Furthermore, ECM may act as “immuno-vascular memory” for inflammatory processes associated with vascular damage (Loppnow et al., 2008). Hence, preservation of normal cell engagement processes with native ECM production, processing and cell binding, and not its minimalist substitution using adhesive protein adsorption to rigid plastic, is critical for preserving these native complex pathological and physiological intracellular mechanisms. Few cell toxicity assays provide, validate or preserve these critical cell–ECM features.

Diverse cell–ECM and cell–cell interactions produce mechanical integrity in tissues, as well as modulate communication between

the extracellular environment and cytoplasmic processes. Cells receive both mechanical (i.e., forces conveyed to/through the cytoskeleton) and chemical (signaling molecules, growth factors, ligands, and soluble inflammatory modulators) signals transmitted via cell–cell and cell–matrix cell membrane surface glycoproteins into the nucleus to adjust cellular functions in response to stimuli. Several cell receptor classes for these mechanochemical interactions have been identified in vivo, with cadherins and integrins receiving most attention.

Integrins are the best-studied cell–ECM adhesion receptor molecules, comprising transmembrane heterodimeric glycoproteins that connect cell membranes to specific ECM ligand sites, inducing subsequent formation of focal adhesions (Qin et al., 2004). Integrins are often proposed as the primary mediators of cell–matrix interactions, although at least one integrin,  $\alpha_3\beta_1$ , has been shown to be important for cell–cell interactions as well (Carter et al., 1990). At least 24  $\alpha$ – $\beta$  heterodimer combinations have been identified in vivo (Hynes, 2002; Humphries et al., 2004; Qin et al., 2004). Unlike other cell–matrix adhesion proteins, integrins can convey both “outside-in” and “inside-out” information trafficking (Qin et al., 2004). This bi-directional signaling allows rapid communication and continual adjustment of cellular processes in response to environmental changes. The best studied examples of “inside-out” regulation involve (1) inflammatory activation of integrins on leukocytes that bind ICAM molecules expressed in damaged tissues, and (2) platelet aggregation in response to fibrinogen binding at sites of vascular injury. “Outside-in” signaling is initiated by receptor binding to ECM proteins (e.g., collagens, fibronectins, laminins), producing recruitment of intracellular signaling molecules, such as talin,  $\alpha$ -actinin, focal adhesion kinase, and vinculin. Assembly of these signaling molecules into focal adhesions on the intracellular membrane surface then activates downstream pathways that regulate cell proliferation, survival, motility, control of gene transcription, and cytoskeletal reorganization processes (Legate et al., 2009). Therefore, it is not surprising that integrin disruption is a part of tissue injury mechanisms. For example, in the kidney,  $Hg^{2+}$  (Molina et al., 1994),  $Cd^{2+}$  (Bernard et al., 1984), and S-(1,2-dichlorovinyl)-L-cysteine (Nony & Schnellmann, 2003) are all implicated in nephrotoxic damage due to integrin disruption. Similarly, in the heart any drug that produces reactive oxygen species up-regulates a family of ectoproteases (Shizukuda & Buttrick, 2002) with structural similarity to snake venoms (Arndt et al., 2002), resulting in integrin–ECM disruption as part of cardiotoxicity.

Furthermore, the diversity of integrin functions is important in comparing in vitro cell responses in three-dimensional (3-D) and two-dimensional (2-D) culture methods. Although information has been collected for a limited number of attachment-dependent cell lines, it is clear that significant differences in integrin utilization and function are manifested between these models. These differences are important for understanding how cell culture design influences cell responses to drugs and toxins. For example, fibroblasts, mesenchymal, and neural crest cells in 3-D matrices rely for initial adhesion on their  $\alpha_5\beta_1$  integrins and lack  $\alpha_v\beta_3$  integrins, whereas traditionally cultured cells use the  $\alpha_5$  subunit only in fibrillar adhesions – structures involved in linear assembly in fibronectin polymers (Sastry & Burridge, 2000; Cukierman et al., 2001; Geiger et al., 2001; Geiger & Bershadsky, 2002). Similarly, cells in 3-D cultures exhibit reduced phosphorylation of focal adhesion kinases and enhanced phosphorylation of mitogen-activated protein kinases compared to cells grown on 2-D surfaces (Cukierman et al., 2001; Ishii et al., 2001). Additionally, mature focal adhesions in 3-D gels exhibit substrate-specific integrin utilization; collagen I matrices predominantly interact with  $\alpha_2\beta_1$  while fibronectin-based matrices prefer to bind  $\alpha_5\beta_1$  (Maaser et al., 1999; Cukierman et al., 2001). Cell integrin receptors also exhibit differential preferences for 2-D vs. 3-D cultures; for example, up to 88% of cellular responses were inhibited using anti- $\alpha_5$  blocking antibodies in fibronectin 3-D gels seeded with human fibroblasts vs. only 36% in 2-D coated cultures (Cukierman et al., 2001). Differences in integrin selection and downstream signaling have



## ARTICLE IN PRESS

10

A. Astashkina et al. / Pharmacology &amp; Therapeutics xxx (2012) xxx–xxx

been attributed to dissimilarities in cellular morphology, adhesion, migration, and proliferation rates in 3-D vs. 2-D environments, which further influences cellular identity, phenotypes and responses to in vitro cultures (Cukierman et al., 2001; Yamada et al., 2003).

Extracellular matrix mechanical properties are also known to play a role in determining the nature of integrin adhesions. For example, cells in 2-D culture exposed to a rigid adsorbed ECM that they could not remodel – in this case, a cross-linked protein – formed exaggerated focal adhesions with trapped  $\alpha_5$  integrins (Pelham & Wang, 1997, 1998). Because the integrin could no longer be translocated to form fibrillar adhesions, formation of fibronectin fibers was inhibited, resulting in limited matrix assembly. Similar cell responses to matrix stiffness were observed in 3-D cultures of highly cross-linked polymers; 3-D specific adhesions were replaced with structures resembling focal adhesions with immobilized  $\alpha_5$  transmembrane proteins (Pelham & Wang, 1997, 1998). Since integrins regulate downstream signaling pathways, differences in ECM rigidity predictably resulted in dissimilar molecular regulation; highly cross-linked polymer substrates produced stable and hyper-phosphorylated focal adhesions, whereas soft, low modulus substrates had more diffuse, dynamic, and poorly phosphorylated adhesion sites (Pelham & Wang, 1997, 1998). Mechanical properties of the cell culture matrix, therefore, are critical for cells' ability to form "normal" cell–matrix interactions in vitro. These data underscore the importance of extracellular matrix composition, mechanical properties, and architecture in physiologically relevant cell integrin engagement and chemo-mechanical coupling that determine cell fate and functionality. By the same token, the functional significance of integrins in cellular crosstalk with their environment makes these receptors essential molecular components for in vivo-relevant cell-based assessments, such as cellular and inflammatory processes that accompany chemical-induced toxicity.

Cell membrane-localized cadherins also transmit mechanical and chemical signals to the cell nucleus in response to stimuli. Much less is known about cadherin's dynamic regulatory influences in comparison to the better-studied integrins, but both types of adhesion molecules are believed to have similar "inside-out" regulation mechanisms (Hynes, 2002; Tadokoro et al., 2003; Gumbiner, 2005). Cellular contractile machinery linked to cadherins is of particular interest because it accounts for subtle cellular rearrangements important in morphogenesis, homeostasis, and tissue turnover (Gumbiner, 1996, 2005). Cadherin-mediated adhesions provide a direct link between the cytoskeleton of neighboring cells: adherens junctions formed by cadherins in the cytoplasmic space are directly connected to actin filaments comprising the cytoskeleton (Gumbiner, 2005). This arrangement results in production of cell forces that can reshape cell outlines, cause cell movement, or change cell polarization (Matsunaga et al., 1988; Kim et al., 2000; Geisbrecht & Montell, 2002; Tepass et al., 2002). Recent literature on the quantitative measurements of cadherin-mediated adhesion strengths highlights the force dependence produced at adherens junctions on the substrate stiffness (Young's modulus,  $E$ ) (Chen, 2008; Ladoux et al., 2010). Rigid surfaces such as glass (modulus  $E = 100$  GPa) or highly crosslinked polyacrylamide gels (modulus  $E = 95$  kPa) resulted in traditional in vitro 2-D culture "egg-shaped" cells with lamellipodia formation, whereas soft polymer gels ( $E < 10$  kPa) exhibit more extended lamellipodia-free cell morphologies. The increase in substrate rigidity positively correlates with forces transduced through cell–cell cadherin interactions, reorganizing and recruiting cadherin adhesions (Ladoux et al., 2010).

This relationship between mechanical coupling of cell receptors to culture supports and resulting cell behavior embraces the idea that environmental alterations influence cells through changes in physical forces transmitted via membrane receptors such as cadherins or integrins. Dysfunctions in cellular adhesions are known to result in loss of tissue homeostasis in vivo and restoration of the cellular microenvironment improves cellular functionality in vitro (Petersen et al., 1992; Dirix et al., 2006; Shen et al., 2006). Substantial data

support careful and consistent preservation of native inter- and extracellular interactions for maintaining expected, normal tissue responses to environmental stimuli. Cell responses to drugs in the context of cell-based screening assays are analogous: their responses to these stimuli rely upon their cell microenvironment. There is little evidence to date that cell–substrate adhesive and resulting mechano-coupling processes in cultured cells facilitates behavior in vitro yield cell responses to drug candidates that faithfully reproduce responses seen in vivo.

### 2.3. Tissue architectures as a cellular niche

Single isolated cell phenotypes, such as those studied in dissociation cultures or single-cell-type 3-D (mono)cultures, are capable of many physiologically relevant processes including cell division, adhesion, migration, differentiation, and apoptosis. However, these generic responses do not equate directly to sub-lethal toxicity markers characteristic of cells in tissues. Hence, to produce more complex responses present in tissues, cells must manage and synchronize responses across diverse cell types as a function of both space and time. Some of the first and most striking examples of how tissue architecture affects and maintains cell function come from the notion of "niche". This is particularly evident recently in understanding stem cell development. "Niche" loosely identifies the essential features of the stem cell microenvironment and includes collective interactions with adjacent stem cells and associated differentiated cells, matrix elasticity, ECM components and adhesion molecules, oxygen tension, growth factors and cytokines,  $Ca^{2+}$  and ATP concentrations, and local pH (Engler et al., 2006; Scadden, 2006). These factors together determine stem cell differentiation and maintenance (Kobel & Lutolf, 2010; Reilly & Engler, 2010). Importantly, this profound influence of local cellular microenvironment transcends the developmental stages of the cellular life cycle and is equally impacting during adult cell maintenance. For example, polarization, tissue-appropriate cell orientation, and function of mammary glands' epithelial cells in vivo are maintained by assembled laminin (L. E. O'Brien et al., 2001), secreted by surrounding myoepithelial cells (Gudjonsson et al., 2002). These examples demonstrate that 3-D organization, coordination, and integration of cell–cell interactions regulate cellular tissue-level functions, cellular assembly, and maintenance of cellular homeostasis. These controls for cell destiny are commonly missing in monocultures in vitro.

Other examples of 3-D local environment governance and determinants for controlling developing in vivo-relevant cell–tissue interactions come from development studies of epithelial architecture. Epithelial cells, unlike many other cells, commonly exist as a tight, organized cell monolayer lining hollow structures in tissues. Epithelial cells coating these lumen-enclosed structures exhibit three different types of cell membrane surfaces: basal (surface facing ECM), lateral (cell–cell interfaces), and free (apical surfaces facing the lumen) (L. E. O'Brien et al., 2002). Extensive studies using Mandin–Darby Canine Kidney (MDCK) cells, thyroid cells, and mammary cells showed spontaneous tissue formation of cysts and tubules in 3-D cultures and in suspension (MDCK and thyroid cells), but importantly not in 2-D cultures (Chambard et al., 1984; Wang et al., 1990a, 1990b). Specifically, these cells arrange into cyst-like formations that consistently polarize with apical surfaces facing the liquid and basement membrane facing the ECM (Fig. 4) (Chambard et al., 1984; A. Z. Wang et al., 1990a, 1990b). In 3-D gels, such organization would result in normal cysts while suspension cultures yield inverted cysts. When conditions were experimentally altered to reverse the ECM-liquid orientation, as in the case of taking inverted cysts and encapsulating them in ECM, these cells then create de novo lumens by degrading ECM in the center of the cyst (Chambard et al., 1984; A. Z. Wang et al., 1990a). Additionally, when the process of ECM degradation is pharmacologically impaired, cells create lumens within the cyst by separating adjacent cells (A. Z. Wang et al., 1994). O'Brien et al. hypothesized that epithelial morphogenesis is hard-wired to produce

## ARTICLE IN PRESS

A. Astashkina et al. / Pharmacology &amp; Therapeutics xxx (2012) xxx–xxx

11

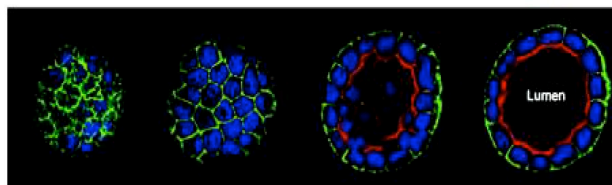


**Fig. 4.** MDCK cyst cultures shown as a series of 5  $\mu$ m sections. The free luminal surface with microvilli is stained in red (actin). The basal and lateral surfaces labeled in green (p58). Nuclei are stained in blue. (For interpretation of the references to color in this figure legend, the reader is referred to the web version of this article.)  
From L. E. O'Brien et al. (2002).

all three surfaces — free, basal, and lateral — in 3-D culture, and it does so through molecular cross-talk with ECM, adjacent cells, and luminal fluid (L. E. O'Brien et al., 2002). They also forwarded the idea based on current literature that cells' abilities to sense different surface types comes from the cell-membrane adhesion molecules present or their state of activation (L. E. O'Brien et al., 2002). For example, the  $\alpha 2$  integrin subunit was critical for MDCK cyst survival, presumably allowing cells to sense the ECM (Saelman et al., 1995). Further, the inactive form of  $\alpha 2\beta 1$  integrin on the apical surface is thought to be an indicator of the free surface, whereas the active form of the same integrin is a signature of both basal and lateral surfaces (Ojakian & Schwimmer, 1994; Schwimmer & Ojakian, 1995; Zuk & Matlin, 1996). These data further indicate that tissue architecture and 3-D geometry of the cellular scaffold is critical for physiologically relevant cellular organization, and that cells' ability to recognize its microenvironment is dependent on different types of surface adhesion molecules.

For other cases, the effect of tissue-level microenvironment is more subtle, but no less important. Many early studies using cultures and co-cultures on 2-D surfaces noted that cellular responses were distinct from their in vivo analogs (Chamberlain et al., 2009; Holt et al., 2010). The best supporting evidence to date on the importance of tissue architecture on cell functional maintenance comes from comparisons of traditional (2-D) culture to a variety of 3-D cultures. An extensive literature using cells of many origins shows significant functional and morphological differences between cells maintained in 2-D vs. 3-D cultures. Due to commercialization and on-going simplification of 3-D culture methods, 3-D cultures are now routine and extensively used; an exhaustive review of all the experimental findings is impossible here. However, data consistently indicate that tissue architecture modulates gene expression, cellular differentiation, polarization, morphology, and functional capability (Hartmann & Bissell, 1982; Cukierman et al., 2001; Bissell et al., 2002; Ghosh et al., 2005; Levenberg et al., 2005; Canton et al., 2010). It is also important to note that culture substrate topography on its own did not produce these effects; rather, 3-D culture organization elicited proper presentation of "natural" cues, such as protein composition and organization within extracellular matrix and its cellular engagement, providing a native-like regulatory microenvironment that controls cell physiology and function. Given the fundamental importance of specific cell–cell and cell–substrate interactions as well as cellular ability to dynamically respond to changes in their surroundings, this seems intuitive.

Traditional cell culture methods often utilize enzymatically digested or cation-depleted, dissociated cells grown on 2-D surfaces in contact-inhibited cell monolayers on rigid thermoplastics. Although convenient and routine, this strategy introduces a separate set of variables that can adversely affect cell-based data collection. Most cells in vivo maintain interactions with ECM along the dorsal (upper) and ventral (lower) surfaces of the cell. As described (vide infra), cell–matrix interactions regulate many physiological processes via bi-directional mechanochemical transduction. Lack of dorsal ECM interactions in 2-D cell culture is likely responsible for some of the

functional differences seen between 2-D and 3-D cultures, although the exact factors responsible for these differences remain to be elucidated. For example, fibroblasts have a well-spread morphology in 2-D and stellate morphology in 3-D, but their stellate shape can be induced in 2-D by physical engagement of the cells' dorsal integrins (Beningo 2004). Similarly, fibroblasts in 3-D actively remodel ECM and are capable of fibronectin matrix assembly. In 2-D, these cells could do the same only with exogenous stimulation (e.g., urokinase-type plasminogen activator, activating antibodies, manganese cation) that activated surface integrins (Mao 2005). These examples suggest that 3-D integrin receptor engagement plays an important role in tissue polarization and for producing and maintaining in vivo-relevant morphology and function.

Another factor contributing to native tissue architectural maintenance may be cadherins, suggested to play a role in basolateral polarization. However, cadherins are likely not solely responsible given that MDCK cells with mutant non-functional cadherins produce normal cysts in 3-D gels (Troxell et al., 2001). Forces generated by cell–matrix adhesion recognition and tensile stimuli may also contribute to cell differences observed between 2-D and 3-D cultures. Matrix tension from cytoskeletal organization after receptor engagement is hypothesized to affect how proteins are presented to cells or the 3-D conformation of proteins in ECM (Cukierman et al., 2002), effectively regulating downstream signaling cascades. Examples of how forces within the matrix, or ECM rigidity, affect in vivo physiology include changes in ECM as a consequence of stromatogenesis and pathological alteration in tumor-associated stroma. As part of desmoplastic changes in normal tissue, fibroblasts surrounding tumors increase production of collagen I and fibronectin (Bissell & Radisky, 2001; Sivridis et al., 2004), resulting in significant changes to tissue architecture and increased ECM rigidity in malignant breast tissue and underlying stroma as compared to healthy tissue (Paszek et al., 2005). Changes in ECM tension were also found to specifically affect conformation of at least one integrin (Katsumi et al., 2004),  $\alpha 4\beta 3$ , proposed as a breast cancer marker (Gasparini et al., 1998). The same integrin was reported to be activated by Rho GTPases (Tang et al., 2008; L. Wang et al., 2008) and ERK-dependent pathways (Tan et al., 2009) in cancers. Interestingly,  $\alpha 4\beta 3$  is also activated by altered tumor-associated stroma, resulting in Rho-mediated cytoskeleton strain and ERK-dependent growth (F. Wang et al., 1998; Wozniak et al., 2003). Furthermore, malignancy reversal was observed through disabling of both signaling pathways independently (Paszek et al., 2005).

These data collectively support the concept that bi-directional signaling between cells and ECM regulate both normal and pathogenic phenotypes and that integrin conformational changes might be a key to relaying that information. Furthermore, the data reflect the complexity of cross-talk between mechanotransducing integrins and growth factor-stimulated signaling in regulating tumor expansion, cellular malignant transformation, and stromatogenesis (Larsen et al., 2006). Specific mechanisms correlating adhesion molecules that modulate cell–cell and cell–matrix signaling, cell–matrix forces generated as a result of these interactions, cell phenotypes, and the



in vivo microenvironment remain to be determined. Nevertheless, appropriate adhesion molecule presence together with presentation of appropriate receptor–ligand conformations that generate cell–cell and cell–matrix engagement and traction forces are recognized as critical in eliciting clinically relevant signaling pathways and eventual functional cell behaviors.

This observation has far-reaching implications in terms of how 3-D cell culture substrates might be used to produce clinically relevant cellular results in response to drug candidates and disease. The idea that three-dimensional matrices alone might not be sufficient to generate in vivo-relevant data for drug screening in cell culture should resonate with both the tissue engineering/regenerative medicine as well as toxicological communities. Design parameters for producing functional in vitro tissue-like surrogates competent in physiological processing of matrix signals and drugs should be analogous. The general idea that any 3-D matrix is better for prompting more realistic cell physiology simply because it is 3-D, without extensive necessary validation against well-established in vivo markers and mechanisms, can lead to the generation of matrix-specific but not necessarily in vivo-relevant information. While differences between 2-D and 3-D culture supports are well-recognized and important to consider in understanding deficiencies in routine approaches to cell screening, creating tissue-specific 3-D culture models that respond to stimuli with reproducible and clinically significant outputs remains a critical goal for improving drug development HTS as well as basic toxicological science studies. Success in achieving this goal will require recapitulating native cell–microenvironment interactions in culture systems.

#### 2.4. Drug–protein and cell–protein interactions

Human blood and its plasma and serum components comprise approximately 6–8% protein or about 7 g/dL (Anderson & Anderson, 1977; Adkins et al., 2002; Jacobs et al., 2005). High protein content is responsible for several drug–protein interactions in drugs with low therapeutic index (i.e., a small ratio between toxic and therapeutic doses) that are critical for appropriate pharmaceutical characterization under in vitro conditions. Such drug exists in two states: protein-bound and free. The bound fraction of the drug (i.e., from drug partitioning into globular blood proteins, such as albumins and lipoproteins) is typically considered non-pharmacologically active, but increases the drug's circulating half-life and acts as a reservoir for longer-term release to the free state. Furthermore, multiple drugs with affinities for the same blood protein create a competitive environment that forces protein-bound drugs with lower affinity to re-partition into the blood stream, resulting in abnormally high drug concentrations that can induce toxicity or other unexpected side effects. The best studied example of competitive displacement is anticoagulant drug warfarin, which in vivo can be displaced from albumin by a series of drugs such as aspirin, simvastatin, mefenamic acid, and some non-steroidal anti-inflammatory drugs (Sudlow et al., 1976; Wells et al., 1994; Dasgupta & Timmerman, 1996; Zahran et al., 2006). Hence, in vitro testing conditions that reflect the high protein content of the blood is critical to account for drug–protein interactions expected in many parenterally administered dosage forms. Protein-rich culture media are also important for proper toxicity assessment from the point of cellular health and physiological processing functions. Commonly employed low protein or serum-free drug testing conditions both stress and damage cells, forcing them to increase endocytosis and pinocytosis rates in culture, resulting in abnormally high drug uptake and amplified toxicity indications (Fisher et al., 1988; Nagel et al., 1998; Lewinski et al., 2008; Jones & Grainger, 2009). Both arguments illustrate the importance of using the most in vivo-relevant conditions in pharmacological assessments.

#### 2.5. Tissue and cell oxygenation

Among cellular nutrients provided to cells in vitro, oxygen is the most readily depleted (Griffith & Swartz, 2006). Reasons for oxygen as a nutrient-limiting factor are two-fold; first, oxygen has a relatively poor solubility in cell culture media, and second, many 2-D and 3-D culture conditions do not consider oxygen diffusion limitations (Griffith & Swartz, 2006). Oxygen is often supplied artificially in the culture atmosphere, notably below atmospheric partial pressures (i.e., induced hypoxia). In common tissue culture systems, oxygen diffuses through the quiescent media surface, through at least several millimeters of media, to anchorage-dependent cells at the bottom of the culture container. This diffusion in an incubator requires ~24 h to reach steady-state concentrations with normal metabolically active plated cells. Cell metabolism in most growth modes rapidly depletes available oxygen at the cell surface, meaning that oxygen supply is diffusion-limited. By contrast, in living tissues in vivo, oxygen is delivered to cells via diffusion from a closely located vascular network. Distances between a blood vessel and a cell varies among tissues, but has been approximated to be a few cell diameters (~150–200 µm) (Kaully et al., 2009). In common culture conditions, cell-support constructs larger than 250 µm have significant oxygen gradients, resulting in variable cell viability, compromised metabolism, cell stress and locally variable degrees of hypoxia (Kellner et al., 2002). Most common 2-D cell cultures using adherent cell monolayers are frequently and mistakenly assumed to be immune to these oxygen transport, depletion and variability issues. However, dissolved oxygen concentration in media quickly drops from the media surface to the bottom of the tissue culture plastic where cells reside; specifically, as much as 50% of the dissolved oxygen at the air–liquid interface is lost at a depth of 2 mm (Guppy et al., 2002). Given that most cell culture equipment, such as plates and tissue culture flasks typically use 5–15 mm of media above cellular monolayers, it is easy to predict that currently used in vitro culture conditions result in less than optimal oxygenation levels, and certainly levels distinct from in vivo conditions. Media oxygenation, oxygen depletion gradients, and cell metabolism are linked as well to media protein content (Naciri et al., 2008); cell metabolic capacities also change with protein content (vide infra), also impacting oxygen utilization. While metabolic by-products (e.g., lactate) commonly result in media acidification, consequent oxygen stress effects on resultant cell phenotypes and responses to drug candidate exposure are not often measured or reported. Various culture responses include increased cell death, cell phenotype changes from media acidification or necrotic by-products in cultures, cell stress and quiescence from hypoxia, and cycling growth rates as cell death changes local oxygen demands. All of these factors influence cell phenotype and resultant drug processing and metabolic indicators for toxicity testing.

Seeded cell density in vitro in cultures influences local oxygen demand. Common 2-D planar plastic wells can be seeded with widely varying amounts of cells. Initially adherent at low density with abundant oxygen, seeded cells adhere and grow exuberantly until limited by contact inhibition, nutrients, and dissolved oxygen. Hence, local metabolic demands vary widely and transiently until steady state is produced at the plastic surface. Generally, 3-D culture constructs that use cell aggregates or matrices with high internal surface areas accommodate millions of cells, resulting in significant oxygen gradients throughout the constructs driven by increased consumption under high metabolic demand and poor mixing or transport. Although a general in vitro technology that results in active transport and high oxygen tension for most cells could be engineered, such a model should reflect the specific cell type or tissue being reproduced. For example, meniscal and stromal tissue have significantly lower cell density than liver or kidneys, tumors may use low oxygen conditions to escape senescence (Huang et al., 2009; Welford & Giaccia, 2011), and stem cells may use lack of oxygen as a differentiation signal



both in vitro and in vivo (Chow et al., 2001; Ezashi et al., 2005; D. W. Wang et al., 2005; F. Zhao et al., 2005; Hermitte et al., 2006). In contrast, cells and tissues not normally exposed to low oxygen conditions but stressed hypoxically in cultures can experience increased free radical formation, changes in tyrosine kinase phosphorylation mechanisms, and onset of pathological or necrotic conditions (Radisky et al., 2005; Wojciak-Stothard et al., 2005). Thus, a general rule for culture oxygenation across all cells and tissues, as well as culture methods, may not be appropriate. A better approach might be to focus on developing new “customized” culture models that mimic specific tissue metabolic demands or elicit characteristic pathological mechanisms using in vivo-relevant conditions. Improved oxygenation solutions involving active transport and engineered bioreactors (Zhang et al., 2010) seek to address these issues. This bioprocess engineering approach is critical, for example, in high-throughput cell growth systems used in commercial protein expression systems (e.g., CHO cell bioreactors) for optimizing protein production.

### 3. In vitro cell culture models: review, strengths, and limitations

The principal purpose of any in vitro model is to simplify experimental variables to effectively isolate different components of organs or organ structures for study under well-controlled and easily assessed conditions. How accurately these conditions must duplicate in vivo conditions depends on the study design and desired outcomes. Not every in vitro assay must necessarily recapitulate in vivo physiology. Different in vitro models may reflect different levels of cellular organization and behavior, and provide different degrees of in vivo-relevant information. Exploitation of in vitro cell culture systems has proven to be a valuable tool to study cell biological, physiological and pathological processes for over a century, but as any tool, is subject to limitations, distractions, artifacts, and misleading results when removed from physiological context without validation or justification. Intact functional organs in vivo exhibit extensive interrelationships and crosstalk from multiple different cell types and dynamics that modulate all physiological processes. This feedback mechanism is lost when individual cell types are cultured in vitro. All cell, tissue, or organ cultures seek a minimalist approach that on one hand facilitates their simplified assessment isolated from the dynamic in vivo context, but on the other hand restricts the depth of conclusions that can be drawn from the work. General agreement exists that no in vitro culture will ever completely represent whole animal experiments, and there are many cases in basic science where such fidelity is unnecessary.

However, for cellular toxicity assessments, many pathologies observed in animal and human studies are poorly understood on molecular and biochemical levels. Furthermore, toxicity, broadly defined, includes many pre-apoptotic cellular events that rely on models with faithful representation of in vivo cellular mechanisms, and cannot be tested with much reliability on oversimplified mimics. Therefore, selection of any in vitro culture for toxicity studies should reflect the complexity of the questions being asked. Additionally, determining idiosyncratic toxicities or cell responses to new drug candidates lacking much structure–toxicity information best relies on cultured cellular models exhibiting reliable, known and intact biochemical pathways and structural elements most likely able to detect toxicity signals. As different mechanisms within cellular microenvironments control basic cell functions in vivo (vide supra), in vitro models currently used in basic science and toxicology assessment each have distinct advantages and limitations in detecting clinically-relevant cellular changes, depending on their application to specific research questions, and their intrinsic ability to control cultured cells through their culture environmental factors.

#### 3.1. Organ/explant culture

Organ culture preserves whole or partial (explant) histological architecture of a surgically removed organ, allowing study of in vivo

processes ex vivo, and thus popular with basic scientists. The explanted primary tissue is usually localized near the air–liquid interface using a support (e.g., raft, mesh, gel, or grid) (see Fig. 5). Organ culture is one of the oldest tissue culture techniques, dating to 1897 when Loeb sustained liver, kidney, thyroid, and ovary in vitro on small plasma clots for up to three days (Loeb, 1897). Organ culture has been shown to be successful for studying the role of hormones and hormone therapies (Lasfargues, 1957; Rivera et al., 1963), as well as environmental insults such as radiation (Borghese, 1961; Lasnitzki, 1961a, 1961b; Trowell, 1961a, 1961b) or carcinogens (Lasnitzki, 1958; Lasnitzki & Lucy, 1961). Organ explant slices or precision-cut tissue slices (PCTS) are also extremely popular in developmental and toxicological studies. Similar to organ culture, PCTS can be maintained in vitro while preserving local histology, representing the majority of different cell types and intracellular interactions. Preservation of local cellular microenvironment in terms of both ECM and neighboring cells allows PCTS use for metabolic P450, enzymatic (e.g., alkaline phosphatase, alanine transaminase, and GGT), and drug transport pharmacotherapy studies that are not possible using immortalized cell lines.

The tissue slice system has several advantages over whole organ culture in toxicology; specifically, organ slices (explants) are suitable for assays that may require visual analysis or scoring, immunohistochemistry, or live imaging. Furthermore, with current advancements in tissue slicing techniques, significant improvements in the number of PCTS that can be obtained from each organ (also known as precision cut tissue chips) and slice precision became possible (Catania et al., 2007). The main restrictions of using the organ culture and PCTS in practice are careful and laborious preparation, lack of protocols that guarantee high viability upon freeze–thaw cycles, and short-term survival in culture. Due to these issues, both cultures have low applicability for HTS drug screening techniques.

Despite the drawbacks with most current organ culture models, advances in tissue engineering and regenerative medicine are leading to the creation of organ-like constructs ex vivo that are then implanted. For example, tissue engineered bladders have been produced in vitro and implanted into patients (Atala et al., 2006). Bladder-like tissues were constructed using autologous cells seeded onto scaffolds made from polyglycolic acid and collagen. Similarly, since 2008 several successful tracheal replacements have used autologous cells seeded onto decellularized tracheas from donors to create complete tracheal tissue engineered replacements (Naik, 2011). Such advances in tissue engineered organ cultures provide insight into preserving or recapitulating cell-based in vivo interactions, also with bio-material supports, ECM and matrices. The approach of preserving the native microenvironment and use of primary cells in combination with tissue engineering techniques as key methods in creating complex and in vivo-relevant models can be extended to drug development and screening innovations, thereby developing organ culture techniques for toxicological and target HTS screening.

#### 3.2. Organotypic culture

Organotypic culture is an in vitro technique using multiple different cell types to recapitulate in vivo-like cell heterogeneity (see Fig. 5). The approach can use either primary or immortalized cell lines. Organotypic cultures can incorporate different aspects of other models described here; for example, they can use supporting matrices to mimic organ cultures or use 3-D scaffolds to produce in vivo-like tissue architectures and morphologies. Use of multiple cell types in production of these models has been shown to be critical in producing in vivo-relevant cellular organization and function.

Skin models are the most well-characterized organotypic system and are suitable examples of how multi-cellular culture with native tissue architecture and biochemistry yield in vivo-relevant characteristics and even clinical tissue-replacement applications. Skin models

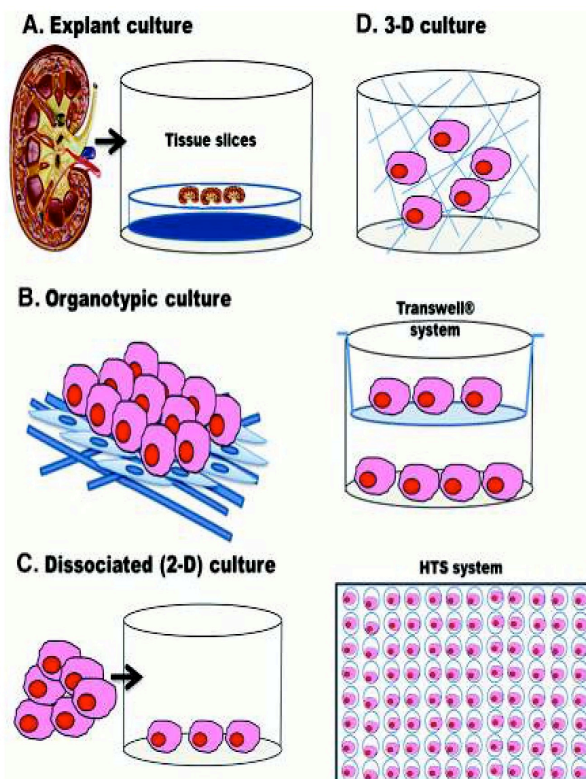


**Fig. 5.** In vitro cell-based models used for toxicity assessments. (A) Explant culture; (B) examples of organotypic culture: artificial skin and co-culture on Transwell® inserts; (C) dissociated cell culture maintained on 2-D surfaces; (D) 3-D cell culture in a supporting matrix. Kidney image from <http://www.ohsu.edu/nephrology>, accessed December, 2011.

have been used for the last two decades in a variety of toxicological, pharmacological, and pharmacokinetic studies, as well as the source for standard clinical treatments for burn victims (e.g., Apligraf, Dermagraft-TC, Integra Artificial Skin and Original BioBrane). The most commonly used and commercially available skin organotypic models include the EpiDerm™ skin model (MatTek), EpiSkin® (L'Oréal) and SkinEthic® (SkinEthic Laboratories). These models are tissue-engineered cultures used to replace skin organ cultures in vitro. Although skin is a rather amiable organ to be sustained in vitro, wide accessibility of human breast and abdomen tissue for research remains a challenge. Furthermore, because most laboratories do not typically have control over skin donors, samples might represent a wide variety of skin types and qualities, adding to the source of data noise in small studies. Hence, the ability to produce an equivalent for a variety of cosmetic, toxicological, drug formulation, and basic research studies is of great benefit.

The EpiDerm™ commercial skin model has been marketed since 1993 and used in a variety of studies in the United States, Europe, and Japan ([www.mattek.com](http://www.mattek.com)). The model uses primary human epithelial keratinocytes grown to a tissue-like monolayer structure or a combination of keratinocytes with fibroblasts to create skin-like tissue models ([www.mattek.com](http://www.mattek.com)). EpiSkin® is created by overlaying 2nd-passage human primary keratinocytes cultured for 13 days on a bovine collagen I matrix coated with a film of human type IV collagen (Tinois et al., 1991). Alternatively, SkinEthic® is a model created by culturing human keratinocytes for 17 days at the air–liquid interface

on polycarbonate filters (Rosdy & Clauss, 1990). Both SkinEthic® and EpiSkin® resemble the structure of epidermis rather than full skin and are therefore more likely to be relevant for non-absorption type of studies. All models exhibit skin ultrastructural features such as keratohyalin granules, tonofilament bundles, and desmosomes, and biochemical hallmarks such as lipid composition, protein composition (keratin 1, 10, small proline-rich protein, involucrin and transglutaminase), although small variations between all of these models and in vivo features have been observed (Netzlaff et al., 2005; [www.mattek.com](http://www.mattek.com)). Furthermore, all models showed good correlations to the in vitro organ culture equivalent in terms of chemical bio-conversion, cytokine (interleukin (IL)-8 and IL-1α) release in response to UV radiation, corrosive indicators (EpiSkin®) according to the European Center for the Validation of Alternative Methods, and cell damage (Netzlaff et al., 2005).

The biggest difference in properties between real skin and skin replacement models continues to be transport characteristics; specifically, most models are much more permeable than their in vivo counterpart. Full skin models are more representative for studies that study skin penetration/absorption, with their well-developed basement membrane. Evaluation of other models with more extensive dermal layers, such as EpiDerm FT™, Apligraf, and EpiSkin® model with fibroblasts cultured for 20 days instead of 13 days (Roguet et al., 1994; Ponc et al., 2002), might be better suited for more clinically-relevant transport characteristics. Nevertheless, the skin organotypic model represents a useful example of 3-D tissue



models that mimic *in vivo* structure through carefully constructed cell–cell and cell–matrix interactions and biochemistry, employing primary cells in 3-D constructs instead of oversimplifying single cell monolayers, producing *in vitro* data relevant to toxicity and drug distribution information obtained *in vivo*.

### 3.3. Dissociated cell culture

The first publication that described dissociation of explanted cells for cell culture purposes was nearly a century ago (Rous & Jones, 1916). Currently, use of dissociated culture in the form of primary culture (i.e., cultures of cells derived directly from tissue harvests) and immortalized cell lines (primary cells genetically transformed to produce rapidly proliferative, passaged, and easily cultured artificial phenotypes) expanded on 2-D tissue culture treated plastic surfaces is the primary model used for cell biology and testing research. In many fields this technique is synonymous with the term “*in vitro* culture”. The overall success of dissociated cells is attributed to the fact that the majority of mammalian cells can be expanded on culture plastics as adherent colonies. Nonetheless, the popularity of the technique as the cellular experimentation tool of choice is greatly influenced by: 1) relative ease of cell maintenance and manipulation; 2) low cost in comparison to whole animal studies; 3) the number of commercial cell maintenance products, kits, and assessment equipment on the market dedicated to dissociated cell culture evaluation; 4) establishment of recently commercialized molecular techniques that allow for genetic cellular manipulation (gene transfer, insertion, deletion, and silencing; cell fusion; gene sequencing); 5) manipulation of gene and protein expression; 6) possibility of HTS testing in academic or industrial settings; and 7) relatively low-cost sterile, pyrogen-free disposables and commercialized cell lines across diverse tissue types. The next two sections will discuss advantages and limitations of both culturing both cell sources using standard 2-D methods on generally rigid commercial thermoplastic flat sterile plates surface-treated to oxidize their surface chemistry for adsorptive uptake of cell adhesion molecules from media.

#### 3.3.1. Primary cells

Primary cell harvests from fresh tissue sources (e.g., insect, mammalian, fish, avian) first involves empirical methods for disaggregation from host tissues using mechanical, enzymatic, or chemical dispersion methods, followed by subsequent plating onto tissue culture-appropriate surfaces. Primary cells are often preferred due to their wild-type, unadulterated nature, which translates to *in vitro* cultures with cells preserving better structural and biochemical complexity found *in vivo*. Unfortunately, given the diversity of cells found together in most tissues, most primary cells are hard to extract from tissue as a homogeneous population. Many primary isolates are expected to be contaminated by minority cells of distinct origins and phenotypes from the targeted cell type. Additionally, isolated primary cells begin to de-differentiate within hours to days when cultured on 2-D surfaces in a process that is difficult to control, requiring repeated host tissue isolation. Finally, primary cells are very sensitive to passaging, resulting in altered phenotypes, slow proliferation rates and metabolic capacities, and early senescence after only a few expansions. Hence, primary cell culture is by far more work- and cost-intensive. Furthermore, because primary cells are so sensitive to their surroundings post-harvest, their isolation, maintenance, passaging, and use require more sophisticated techniques and advanced tissue culture training.

#### 3.3.2. Immortalized (transformed) cell lines

Immortalized cells have their origins in primary cells that have been deliberately genetically modified to overcome the tedious problems of their primary cell counterparts. Immortalization is the result of oncogene introduction into the cell's genome to enable rapid

proliferation in culture (oncogenic phenotype), resistance to de-differentiation, improved passaging, and greater resilience in culture. Importantly, as a result of genetic transformations, these cells are no longer primary cells, are no longer phenotypically identical, and for some immortalized cell types, are only marginally similar to their original primary phenotype (D. D. Allen et al., 2005; Donato et al., 2008). Nonetheless, these cells are typically easy to maintain and propagate in culture in dilute serum or serum-free media, can be expanded and stored as frozen stocks, exhibit reproducible results when thawed and re-seeded, and are stable for up to 25–50 passages. Also, unlike primary cells often prepared from tissue harvests or purchased at high cost as frozen commercial stocks, immortalized cell lines can be obtained from private biological resource collection centers such as ATCC and expanded in the lab in a much more economical way. The convenience of not continuously making new primary cell stocks comes at a quality control price, however. Several published reports indicate that many of the frozen circulating secondary cell line stocks are cross-contaminated with other cells, such as HeLa, HT29, and PC-3, or have been misidentified in their cellular or species origins (Masters, 2002; Nardone, 2007; Capes-Davis et al., 2010). Rarely are commercially sourced transformed cell lines actually validated for phenotype or contamination in published literature.

The use of immortalized cells has greatly simplified abilities to conduct cell-based studies in the basic and applied sciences. Therefore, it is not surprising that cell lines have become models of choice for many experimental designs. For many studies one might argue that the convenience of using immortalized cells in many cases outweighs their disadvantages. However, very few reports actually justify use of a cell model that utilizes genetically altered cells with dissimilar phenotypic properties from the tissue-sourced cells. Importantly, even fewer explain their reasons for selecting such a model to provide physiologically relevant information, or demonstrate such a validation. Furthermore, growing number of publications suggest limited value of immortalized cell lines in induction of *in vivo*-relevant biomarkers, such as cytokines, genes associated with toxicity, and protein biomarkers in response to tissue injury. For example, rat proximal tubule immortalized cell line NRK-52E, unlike the *in vivo* rat model, had no significant up-regulation of kidney injury molecule-1, lipocalin-2, tissue inhibitor of metalloproteinases-1, clusterin, osteopontin, and vimentin after exposure to known toxin, ochratoxin A (Rached et al., 2008). Similarly, many secondary cell lines are not known to induce or show great variation in the most prominent markers of toxicity, such as kidney injury molecule-1 in the kidney (Ichimura et al., 2008) or interleukin-6, interleukin-8, and tissue necrosis factor in cutaneous toxicity (D. G. Allen et al., 2001).

The recognized problems with using immortalized cell line cultures are two-fold: 1) genetic transformation and sub-culturing procedures to isolate cells that have escaped senescence and exhibit up-regulated telomerase activity produces cells with significant changes in their differentiation potential, and 2) the majority of transformed immortalized cell lines have not been studied in depth to identify all the idiosyncratic changes imposed by genetic manipulation and multiple passages. Several examples of cell behavioral changes upon immortalization compared to homologous primary cells are reported. Specifically, immortalized cell lines have been shown to have altered genomic content (Yamasaki et al., 2009); abnormal expression of intracellular proteins (Prozialeck et al., 2006); complete lack or significant deterioration of key morphological features such as microvilli, tight junctions, ligands, transporters, mucin production, and important cellular receptors (McLarnon et al., 2002; Ciarimboli et al., 2005; Motoyoshi et al., 2008); and loss of cellular polarity (Prozialeck et al., 2006). Predictably, these changes also result in functional alterations such as loss of contact inhibition (Milyavsky et al., 2003; Holt et al., 2010), metabolic cytochrome P450 (CYP) potential (Cummings et al., 2000; Donato et al., 2008), induction of inflammatory mediators (Chamberlain et al., 2009),

## ARTICLE IN PRESS

16

A. Astashkina et al. / Pharmacology &amp; Therapeutics xxx (2012) xxx–xxx

paracellular transport, trans-epithelial electrical resistance, and proliferation rates in culture (P. Hughes et al., 2007; Avdeef, 2010; [www.mfbprog.org.uk/publications/publications\\_item.asp?intPublicationID=1365](http://www.mfbprog.org.uk/publications/publications_item.asp?intPublicationID=1365)). These changes highlight important genotypic and phenotypic inequities that might confound collection and interpretation of screening data if used blindly to compare to similar cells in tissue in vivo contexts, but especially in assessments that include many complex biochemical, metabolic, and signaling events, such as involved with cellular toxicity. Disparate levels of important cellular mechanisms involving drug penetration, accumulation, transformation, elimination and toxicity defense, such as endocytotic activities, transporters, endosomal metabolic processing, glutathione regulation mechanisms, and CYP enzymes, may result in systems that are overly sensitized to or defective in drug processing capacities, or intrinsically incapable of accurately reflecting in vivo toxicity profiles (Delcomenne & Streuli, 1995; Gomez-Lechon et al., 1998; McLarnon et al., 2002; Ghosh et al., 2005; Lim et al., 2005).

Important microenvironment-driven variables as determinants of cell behavior (see Section 2) are often lost in 2-D cell culture methods, contributing to the known limitations of culturing cells using 2-D tissue culture plastic. Notably, dissociated cell culture methods that use primary cells on 2-D surfaces lose the numerous benefits of 3-D ECM–cell interactions and intercellular communication between heterogeneous cell populations commonly found in vivo. This often results in rapid cell de-differentiation and poor passaging. Similarly, immortalized cells often have intrinsic genetic limitations, lack of ability to form tissue architectures, and recognized 2-D surface disadvantages of lacking proper cell signaling cues (e.g., plastic rigidity, ECM-deficient and chemo-mechanical compromised) from 3-D supports. Therefore, culture of both primary and immortalized dissociated cell cultures on 2-D culture surfaces under most routine conditions should be recognized as deficient in key, complex processes required for cell behaviors in assessing toxicity, drug metabolism, or drug-induced inflammatory pathways. Furthermore, cell culture media used in all in vitro models often do not reflect any actual in vivo context, comprising 5–10% serum as a fundamental nutrient component, or no serum and a proprietary list of supplemented cell nutrients in various buffered salines, but can impact resulting cell phenotype (Gerber & ap Gwynn, 2001; Kolbe et al., 2011). Justification for use of a specific cell culture media – beyond the observation that the selected cells proliferate in the media successfully – is rarely provided in published reports. Fidelity of these culture conditions and resulting cell phenotypes to the desired in vivo endpoints should be proven using validation protocols, rather than presumed under such gross over-simplifications. The degree of tolerance for relative agreement or concurrence between in vitro cell-based testing models and next-step preclinical animal testing for methods validation is obviously subject to the complexity of the questions being asked for such outcomes. Specifically for toxicity testing, HTS assessment of newly synthesized libraries of drugs with unknown toxicity-mediated pathways would necessitate the highest possible correspondence between in vivo and in vitro assessments. Furthermore, early tissue-specific toxicology and dose–response assessments require induction of biomarkers that are reliable, translatable and measurable in animal or human clinical studies, not just metrics for cell death or lack of proliferation in culture (see Section 1.1.2). Hence, dissociated cell culture is less likely to satisfy these specific requirements for identifying multi-factorial processes involved in cell-mediated drug toxicity.

### 3.4. Three-dimensional cell culture

3-D cell culture models can utilize cells, healthy or diseased tissue biopsies, or complete organ as their living components. Culture in 3-D has its roots in tissue engineering and regeneration studies, but techniques and innovation here are adopted increasingly as cellular techniques for disease modeling, toxicological, and molecular target

identification work. Tissue engineering literature typically refers to 3-D culture supports as “scaffolds”, and to culture systems as “bioreactors” (see Fig. 6). Excellent reviews of scaffold fabrication materials and methods, cellular responses, bioreactor designs, and 3-D vs. 2-D culture functional comparisons are available (Cukierman et al., 2001; Bhadriraju & Chen, 2002; Cukierman et al., 2002; Yamada et al., 2003; Ghosh et al., 2005; Griffith & Swartz, 2006; Keller et al., 2007; Pampaloni et al., 2007; J. Lee et al., 2008; Prestwich, 2008; Prestwich & Kuo, 2008; Badyalak et al., 2009; Justice et al., 2009; C. S. Hughes et al., 2010; Elliott & Yuan, 2011). Because many aspects of 3-D culture have been reviewed extensively in the literature, only select elements pertinent to culture model development and their in vivo significance for toxicological or drug target validation methods are included here.

3-D cell culture scaffolds and culture systems are usually made by suspending cells in compatible hydrogels that can be gently cross-linked in vitro to suspend cells within these materials in the presence of excess water, or by seeding cells on solid support matrices, typically spongy, high porosity polymer or ceramic solid foams, or growing cells on the surface of a non-planar support material (see Figs. 6 and 7). Scaffolds are physically and chemically diverse in nature: they can be fabricated from synthetic or natural polymers, with diverse mechanical properties, with and without ECM proteins or other adhesion molecule additions, and ranging from dimensions on the super-centimeter bulk solid scale to millimeter microsphere/bead encapsulates to microliter sizes on cell-based gel microarrays or 3-D pendant gel cultures. Artificial scaffolds have greater manufacturing precision, versatile engineered properties and reproducibility but require addition of some minimal ECM-like material components to promote specific receptor–ligand cell–microenvironment interactions. Hydrogels (e.g., polyethylene glycol, polyacrylamides, alginates, celluloses) and synthetic polymers (e.g., polyurethanes, vinyl polymers, poly(alpha-hydroxy acids)) fall into this category. Scaffolds comprising natural proteins like collagen I or fibrin already have endogenous cell adhesion sites, but require extensive processing for 3-D applications. Both synthetic and natural polymers have been used to create 3-D constructs in many physical forms (e.g., gels, fibers, weaves, meshes, sponges, foams and channels) with many hundreds of references to date published.

Many scaffold studies describe significant differences between cellular morphology, molecular signaling, function, and behavior between 2-D and 3-D supports, some of which have been described in Section 2.3, clearly demonstrating disconnects in performance between the two types of culture models. The potential for 3-D culture methods to investigate cellular processes not previously possible in 2-D studies, such as cellular organization into tissue-like structures (tubules, aggregates, and cysts), cancer propagation and metastasis, inflammatory toxicity-driven pathways, and angiogenesis (Gudjonsson et al., 2002; L. E. O'Brien et al., 2002; Ghosh et al., 2005; Levenberg et al., 2005; Pampaloni et al., 2007). But from the model assessment perspective, several 3-D cell culture practices diminish the significance of producing and preserving in vivo-like molecular interactions in retaining appropriate cell physiological responses. The first compromising approximation is that some commercially available tumor-derived ECM-like products (e.g., Matrigel®) are comparable to native ECM for eliciting and retaining adherent cell phenotype and tissue-like growth. A second operational approximation is the use of single major ECM components (e.g., collagen I) or addition of one adhesion ligand (e.g., arginine–glutamate–aspartic acid peptide) as a functional equivalent to a complete ECM matrix combining many proteins. A final approximation is the deliberate manipulation of many native proteins (e.g., extensive laboratory processing that alters protein conformation, structure, ligand exposures, and crosslinking density) as adsorbed matrices for 3-D culture, and the presumption that these perturbed proteins are functionally equivalent to their native ECM protein counterparts. Matrigel® is an



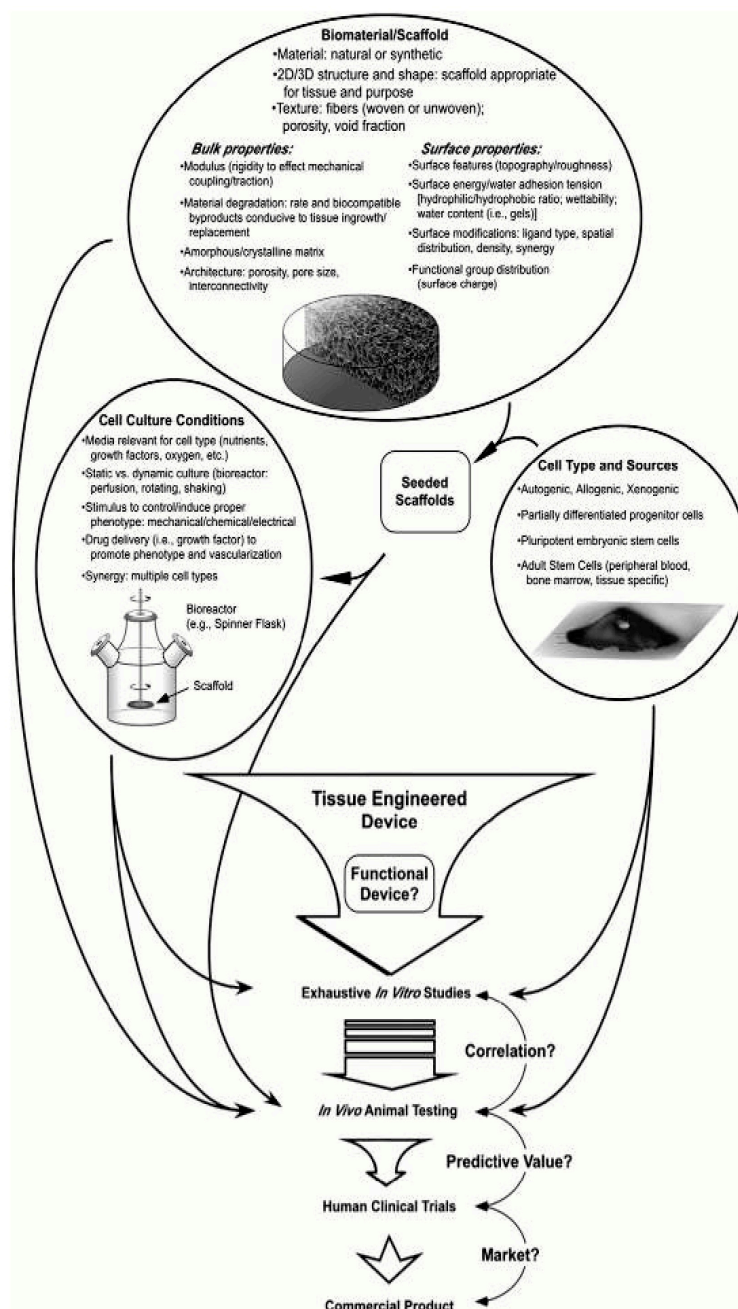


Fig. 6. Strategy for use of 3-D cell-support matrices and bioreactors for in vitro cellular toxicity assessment as part of tissue-engineered in vitro drug development process. From Harbers and Grainger (2006).

ECM replacement extracted from secretions of Engelbreth-Holm-Swarm mouse sarcoma cells, a complex mixture of proteins, growth factors, and other ECM components. Matrigel® is commonly used as an ECM surrogate because it is commercially available and easy to handle in the tissue culture lab (C. S. Hughes et al., 2010).

Unfortunately, Matrigel® as a tumor cell-derived ECM has characteristics highly dissimilar from normal ECM in terms of organization and structure (Larsen et al., 2006). Additionally, it has significant batch-to-batch variation and is susceptible to viral contamination as any other tissue-derived product. Therefore, even though it delivers

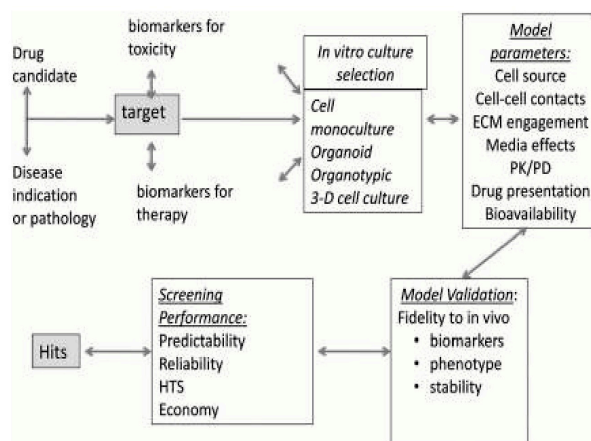


Fig. 7. Strategy for use of in vitro systems for prediction of in vivo toxicities in preclinical trials.

ECM-like complexity, this gelled tumor ECM might not always be the best choice for non-cancerous 3-D culture models for drug testing.

Similarly, single-protein component 3-D matrices and highly processed native protein adsorbed layers on scaffolds have analogous issues in their biological non-equivalence to normal native ECM. Adhesion molecules and cellular receptors of cell–matrix, cell–cell, and cell–soluble cues form part of the complex information superhighway that regulates all tissue physiological processes. As described in Section 2, these cell–matrix interactions depend on the presence/absence, activation state, and 3-D conformation of cell receptors with their targeted ECM proteins. Hence, ECM surrogate reductionist approaches in 3-D cell culture systems or their alterations from chemical or mechanical processing produce a distorted, incomplete molecular signaling scenario. In vitro, several examples of differences between 3-D cell cultures that use different types of ECM have been explored. For example, human fibroblasts cultured on tissue- and cell-derived 3-D matrices exhibited different cell–matrix adhesion composition and integrin (e.g., paxillin,  $\alpha_5$  integrin, fibronectin) localization than cells cultured on cell-derived flattened matrix or 3-D matrix composed of only fibronectin (Cukierman et al., 2001). Similarly, fibroblasts encapsulated in endogenous matrix showed 6-fold faster cell attachment than the same cells encapsulated in pure collagen I, laminin, or purified fibronectin (Cukierman et al., 2001). Additionally, cells in native matrix-derived gels exhibited 2-fold faster proliferation rates and increased migration rates compared to pure single protein gels (Cukierman et al., 2001). When the 3-D gels with native ECM were flattened using mechanical force (Cukierman et al., 2001) or solubilized by guanidine (Beacham et al., 2007), all the advantages of 3-D matrix disappeared, implying that neither 3-D nor matrix alone were responsible for the observed cell differences.

Chemically modified gel scaffolds also change cell migration within the matrix. In vivo or in vitro on native ECM substrates, cells colonize new spaces by clearing their migratory path by secreting metalloproteinases, serine proteases, and hyaluronidases that degrade matrix proteoglycans (Ikada, 2006). These processes are tightly controlled by the balance between active local ECM-bound proteases and their inhibitors. Scaffold modification through extensive chemical and/or mechanical processing results in ECM-replacements that are fundamentally different from native ECM, do not allow enzyme modification, and do not sustain in vivo-relevant cellular migration (Ikada, 2006). This further supports the hypothesis that both matrix

composition and its architecture are required for in vivo-like cellular interactions. Loss of appropriate matrix composition, topology, and biochemistry of the native ECM guarantees changes in cellular response. Whether these cell changes are important to the processes studied or can be ignored is a function of the research issues studied and the type of model.

Unfortunately, too many 3-D cell screening models have been introduced into the literature with little validation of distinguishing features, using simple cell adhesion and proliferation as the only reported characteristics asserting their biological relevance. In vitro, cells proliferate on many surfaces, independent of their differentiation states and genetic stability. Hence, seeding live cells in a 3-D matrix and establishing their viability cannot be the only assessment end-point. Furthermore, 3-D cell culture is commonly compared to in vitro 2-D culture as a measure of its validity. Although comparisons of traditional culture methods to new 3-D models have merit, they alone do not validate or justify 3-D cell culture in vivo relevance or significance as an improved culture method.

Similarly, significant commercial and academic efforts seek to create a “one-size-fits-all” matrix accommodating any cell type or cell line, applicable to many culture surfaces and cell types, instead of developing organ-specific or pathology-specific models that recapitulate and promote clinically relevant cell pathways. Under normal physiological conditions, ECM derived from different tissues exhibit their own unique tissue architectures, mechanical properties (e.g. elastic energies, moduli), protein compositions, and molecular complexities (Geiger, 2001). These properties can be modulated as a function of normal processes such as wound healing, or via pathological manifestations such as cancer induction (Amatangelo et al., 2005). Hence, it seems that creative focus in this area should be more on producing easily-modified matrix components that can be mixed and matched to closely re-create native biochemistry and matrix rigidity than pursuing a universal master ECM mix. In any case, care should be taken in understanding the culture model, the validation processes, and the advantages and limitations prior to a model’s use in drug development, toxicology, and other related applied research.

#### 3.4.1. Use of bioreactors

Bioreactors enable controlled and reproducible handling of large quantities of tissue engineered 3-D constructs in vitro with engineered, programmed and computer-controlled inputs and outputs to help regulate the cell biology both in and on the construct (see Fig. 6). Bioreactors are capable of maintaining environmental

## ARTICLE IN PRESS

A. Astashkina et al. / Pharmacology &amp; Therapeutics xxx (2012) xxx–xxx

19

conditions such as pH, temperature, and oxygen tension, as well as mechanical stimulation such as flow rates and shear stress, while retaining aseptic operation (Portner & Giese, 2007). Feedback and automation loops with on-board intelligence are clearly possible. However, beyond media sensing and mass transport controls, specific cellular sensing inputs, analysis and adjustments are not yet possible to engineer into reactor designs. Development of more sophisticated bioreactor systems able to continuously interrogate or sample, and then support cell environments would be an important step towards development of reliable HTS conditions for toxicological and target-validation assays. Integration of engineered reactor designs based on biologically based inputs, cellular demands, and physiological and pathological parameters that respond to in vivo conditions is not exploited sufficiently to date. Large-scale screening systems should be able to dynamically sense and adjust cell culture conditions to best support cell phenotypes and culture-specific needs, not simply maintain viable cultures. Hence, bioreactors are currently not integrated to HTS approaches and offer little advantages yet to either the screening or the phenotypic fidelity needs in cell-based drug-target validation or toxicology assays.

The most common bioreactors used to propagate dissociated cells in culture are either fixed/fluidized bed bioreactors or membrane bioreactors. In both fixed-bed and fluidized-bed systems, cells are seeded and maintained on fibrous networks or porous supports that are either suspended (fluidized bed) or affixed (fixed bed) onto a column (Portner & Giese, 2007). The main advantage of this type of bioreactor is long-term cell maintenance in culture, and because of this they are fairly efficient in cultivating cells to produce antibodies, recombinant drugs, and recombinant retroviruses. In membrane bioreactors, cells are sustained in compartments (culture chambers) that contain permeable membranes capable of nutrient and gas exchange. Hollow-fiber systems (e.g., the miniPERM bioreactor from Greiner, and the Tecnomouse™ cell cultivation system, Integra Biosciences) are examples of membrane bioreactors. Commercially available and custom-modified bioreactors have been used to produce antibodies, and to maintain hepatocyte and skin cell cultures. The main drawbacks of many current bioreactors are their intrinsic inability to perform HTS-type cell assessment in parallel, and that most use batch mode media replacement, which leads to constant changes in media feed conditions, complicated drug dosing, and problematic intracellular communication in organotypic models. Replacement of this batch cultivation with continuous perfusion, as is used in tissue engineering bioreactor systems for growing artificial organs, as well as better organ- and HTS-specific bioreactor designs represent important steps to improve 3-D tissue-replacement systems that are exposed to constant, controlled environments. Currently, most HTS assays are run in multi-well plates, using suspended or adherent cell cultures and no real bioreactor enhancements that enable feedback on actual real-time cell “health” or phenotypes.

In summary, none of the common models of current cell-based in vitro toxicity assessment presented in this section, i.e., organ/explant, organotypic, dissociated and 3-D cultures completely recapitulate in vivo physiology. Yet, they do collectively represent a significant gradient in model complexity as described by their intra- and extra-cellular interactions, cellular heterogeneity, and tissue organization. The dissociated culture grown as a 2-D monolayer on a cell-conductive support is the simplest and easiest to use, but also the least relevant toxicity model to in vivo cell damage processes. These cells are cultured using a minimalist approach that eliminates tissue-relevant cell–cell and cell–matrix interactions. Furthermore, use of transformed cell lines known to be missing major pathways responsible for drug accumulation and biotransformation makes it less likely that 2-D dissociated models can accurately predict in vivo cellular toxicity. Some specific examples include lack of gene induction in response to toxic exposure, and cytokine expression due to inflammatory processes associated with tissue damage (Yang et al., 2007; Rached et al., 2008; Akcay et al., 2009; Bonventre et al., 2010). On

the other hand, this model is an excellent starting point for drug-associated pharmacology assessments due to its simplicity, and ease of cellular transfection procedures for introducing known transporters, cellular ligands and metabolizing enzymes. This artificial response can be of great importance in initial in vitro screens that target specific modes of cell toxicity, such as interactions with common drug metabolizing CYP enzymes or validation of specific transporter roles in drug accumulation. More complex models, such as organ explant, organoid or 3-D cultures that include different cell types and attempt to retain and recapitulate multi-cellular interactions can be of greater value to in vivo toxicity prediction. This comes at some cost in terms of high-throughput limitations, and costly, tedious preparations. For any model, the expected degree of in vitro–in vivo correlation depends on the simplicity of the organ or tissue under simulation and complexity of the cellular microenvironment recapitulated in the model. Organotypic models of human skin and its 3-D models with heterogeneous cell populations as one example have provided successful tools for predicting drug penetration, inflammatory toxicity-driven pathway up-regulation, and toxicity assessments by establishing tissue-like complexity. Experimental data suggest that translating significant in vivo predictions in vitro requires a departure from minimalist cell culture approaches and thorough introduction of more physiologically relevant tissue-like models. However, as described, such culture selection and assays designs for toxicity predictions should be guided by biological principles that guide and sustain cell phenotype and tissue physiological performance in vivo. Based on this discussion, Fig. 7 summarizes the decision flow diagram to facilitate selection criteria for cell-based assays.

#### 3.4.2. Induced pluripotent stem cell culture opportunities

Opportunities have emerged for improving cell-based screening capabilities by exploiting recent developments in cellular reprogramming. The 2007 creation of human induced pluripotent stem cells (iPS cells) by skin cell transfections with c-Myc, Oct-4, Sox-2, and Klf4 (Takahashi et al., 2007) allowed subsequent differentiation of these former skin cells into many new cell types. Deliberate reversion of somatic cells to pseudo-embryonic states and selective differentiation into desired lineages (so-called “cell reprogramming”) can now be combined with as a new tool for in vitro drug and toxicity screening. Since iPS cell programming technology facilitates rapid culture access to cell types typically difficult for in vitro study (e.g., neurological cells like neurons, oligodendrocytes associated with long-latency in vivo neuronal pathologies) these iPS-derived cells may be used to better recapitulate normal as well as aging and longer-term pathological cellular states in vitro.

Significantly, multiple cell types derived from a single human source (e.g., a diseased patient) and proposed to interact in producing a given pathology might be co-cultured as iPS-derived products differentiated from that patient, complete with the patient's genotype and “personalized” biomarkers. Comparisons of both disease states and drug candidate responses across multiple iPS-reprogrammed cell culture sources from multiple patients with their intrinsic genetic diversity yet common disease states represent an untapped potential for iPS-based personalized drug response and screening. Analogous strategies using iPS-derived patient-specific cultures in toxicogenomics are equally viable. Toxicity-sensitized and disease-specific iPS-derived cells have attractive features for assessing drug and toxic compound libraries, especially using patient-specific cells prior to clinical evaluations. Genomic analysis of these cells could be cross-referenced to in vitro screening results, rationally guiding target elucidation, toxicogenomic pathway identification, and therefore clinical profiles for patients best benefiting (or most risk averse) from new trials of lead compounds. In vitro toxicity tests can also be conducted on the same patient. For example, liver hepatocytes central to most first-pass and other drug metabolism are critical for toxicity screening since drug-induced liver injury represents the single-most



cause of safety-related drug withdrawals in the past half-century (Research, 2009). However, immortalized HepG2 cell lines commonly used for in vitro screening assays exhibit the expected anomalies from their transformation from primary hepatocytes, while primary hepatocytes are difficult to culture beyond a few passages, and must be derived from fresh tissue sources continuously. iPS-derived hepatocyte sourcing (and also many other analogous toxicity-relevant cell types, including kidney, myocardium and bone marrow) would be a significant new and impacting innovation to address this long-standing problem. This strategy would also provide both donor-specific cell-based toxicity screens, correlated to toxicogenomic profiles, as well as consistent sourcing that would eliminate tissue donor source variability. Challenges exist in directing iPS differentiation into cell types of interest at high efficiency and at reliability. This includes iPS culture methods, media cocktails, transfection success and differential outcomes where standard methods are only just emerging (Chu et al., 2001; Menasche, 2011).

Combined with emerging 3-D cell culture and co-culture methods, this iPS-guided in vitro screening approach is a powerful opportunity for improving retention of specific cell phenotypes, modeling tissue complexity and agent response, as well as for correlating many genotypes to both disease progression and therapeutic outcomes. A versatile, improved, standardized and when desired, personalized, source of cells for drug and toxicity screening is becoming available for in vitro use. Nonetheless, as with all other cells in culture, appreciating the iPS microenvironment is critical to eliciting proper cellular contextual responses to bioactive agents in vitro. This means that the same cell culture arguments (vida supra) for placing these reprogrammed cells into appropriate culture matrices best representative of tissue states are essential to evoke accurate, predictive in vitro responses for these assays.

#### 4. Conclusions

Cellular models have a proven record as powerful tools for drug screening for toxicity assessments. But as in any field, these models are only as good as their ability to recapitulate explicit in vivo physiologic and pathologic processes and cell properties specific to the context under study. Toxicity is an organ-specific, sometimes species-specific, multi-factorial process that involves dynamic drug accumulation in the cells via uptake/efflux transporters and passive diffusion, apoptosis, cell dedifferentiation, metabolite and reactive oxygen production, drug biotransformation by intracellular/extracellular enzymes and protein-binding, interactions with the immune system, and tissue regeneration. But toxicity often has cell-specific etiologies and drug-specific mechanisms for each cell type: well-intended “one-size-fits-all” screening and reporting solutions cannot often discriminate these differences. Furthermore, many processes that contribute to induction of toxicity, such as inflammation as well as tissue and ECM pathological changes, require normal cellular communication with native ECM proteins or other cell control systems in the body. The cumulative results of these intracellular pathways and interactions lead to reversible or irreversible tissue damage. Hence, generalized or simplified mimics of in vivo processes such as immortalized cell lines grown on 2-D surfaces with their general lack of drug transporters, cell ligands, and appropriate ECM–cell adhesion molecule interactions, might be grossly insufficient to reproduce many of these essential processes.

The possibility for success is especially grim for cases of toxicity screening of new compound libraries with unknown modes of toxicity. One goal of this review was to summarize the current understanding of how different variables contribute to cellular changes in the context of environmentally imposed toxicity. Although some research remains at early stages of development, the realization that cell communication with its environment as a key to most differences between 2-D and 3-D systems as well as between different 3-D

systems is becoming more apparent. Restoration of these native-like lines of cell communication by providing primary cells with scaffolds that resemble native microenvironment, supply appropriate topology, and provide mechanical stimulation similar to that present in vivo has been shown to result in partial or short-term (in weeks) reinstatement of cellular functions. These results further support the overall hypothesis that cell–cell and cell–matrix interactions in the context of tissue architecture are often critical for guiding and maintaining specific attachment-dependent cellular identities in vivo. Therefore, full endowment of culture systems with native interactions instead of employing a minimalist’s approach to cell–materials interactions should better ensure that biological requirements for creating and sustaining tissue replacement models that promote cell viability and functionality in vitro similar to the in vivo counterparts are reliably attained.

Several specific reasons for the current inability to reliably screen toxicity biomarkers in vitro that consistently predict in vivo responses all have the same basic, central problem in common: most current methods assess cellular damage in cultured cell lines instead of trying to measure indicators that better inform toxicity in humans. Precise comparison of systemic drug exposure in vivo to drug dosing in vitro might be impossible, but lack of success in predicting toxicity is guaranteed by continuing to use models that do not reveal or reliably trigger clinically relevant toxicity indicators. Several recent developments including “human on the chip” or “organ on a chip” cell-based assays were able to sustain primary liver phase I and phase II drug metabolism for several weeks, augmentation of gene expression, induction of leukocyte adhesion molecules (ICAMs) that could stimulate adhesion and diapedesis of neutrophils, and were capable of predicting toxicity for known toxic pharmacological agents or reflect inflammatory processes associated with nanoparticle exposure (Khetani & Bhatia, 2008; Huh et al., 2010). These models closely reflect older data obtained from organ slices and whole organ models that accurately exhibited in vivo-like behavior in hormonal stimulation and drug toxicity. These models are promising examples of how fostering organotypic intracellular interactions as well as native mechanical stimulation can result in tissue replacement systems with toxicity pathway-specific assessment.

The importance of acquiring accurate, predictive pathway-specific in vivo-relevant information from cell cultures is three-fold. First, models that respond with biomarkers commonly tested in animal/human studies could be used to assess pre-lethal molecular and histological changes associated with tissue toxicity. Collected model data can be compared to extensive data already known from animal experiments on specific histological and physiological alterations that accompany toxicity, serving as the basis for in vitro–in vivo comparisons. It is likely that a battery of tests that include both morphological, gene and protein expression, as well as molecular signaling and protein-based assessment can be developed that may serve as the source for a multi-factorial toxicity scoring system in vitro. Empirical validation using current and failed pharmaceuticals of the most predictive assays and of the scoring system might be required. Second, 3-D assays that respond with organ-specific biomarkers can be used to assess doses that organs might be exposed to in vivo. Although no direct pharmacokinetic correlations between in vivo and in vitro models currently exist, development of PBPK in parallel with clinically relevant models might foster predictive relationships that can elucidate such doses. Advances in dose correlations will be critical for therapeutic window establishment as well as for correct dosing of in vitro models. The Paracelsus doctrine regarding the relationship between dose and toxicity implies that all cells can be killed or damaged in vitro, but whether the toxic dose is relevant to the clinical dose must be assessed beforehand. Additionally, development of new bioreactors that facilitate dose tracking in vitro may be critical for in vivo-like cellular exposure when testing pharmaceutical agents. Third, establishment of tissue replacement models might be



important for use in new next-generation biological developments, for example, in studies that involve toxicity pathway prediction using systems biology algorithms. System biology uses process integration instead of common reductionist model approaches to draw conclusions about how the properties of complex physiological systems emerge, using analytical and computer modeling (Pujol et al., 2010). Its assessment protocols require comprehensive datasets that may include genomic, proteomic, and metabolomics data (Pujol et al., 2010). Current systems biology methods are primarily applied to data obtained from animal studies due to lack of reliable assessments using traditional cell monolayer culture approaches (Pujol et al., 2010). Hence, only in vitro models with direct, accurate resemblance to native tissue might provide data of sufficient quality to be used to assert testable hypotheses about biological systems using systems biology methods.

All of these advantages attributed to in vitro cell culture systems that can reliably yield better-quality, more accurate, and tissue-specific information could also significantly improve the technical output, predictive value, and translation efficiencies between in vitro, animal, and clinical human studies. Moreover, such capabilities would open new avenues for application of in vitro cell-based research in terms of integrated data utilization, improved drug screening results, and higher quality pharmacokinetic assessments. Further developments using 3-D models that focus on production and preservation of native (not minimalist equivalent) ECM, relevant tissue architectures, and restoration of both chemical and mechanical tissue-like stimulation with bioreactors will be critical for advancing in vitro experimental capabilities to obtain clinically relevant data.

#### Acknowledgments

We thank J. Herron (University of Utah) for valuable drug–protein interactions discussions and Dr. Ben Brooks (University of Utah) for help with figures. This work was partially supported by the University of Utah's Office of Vice President for Research SEED grant and the University's Technology Commercialization Office Microgrant.

#### References

- Abraham, V. C., Towne, D. L., Waring, J. F., Warrior, U., & Burns, D. J. (2008). Application of a high-content multiparameter cytotoxicity assay to prioritize compounds based on toxicity potential in humans. *J Biomol Screen* 13, 527–537.
- Adkins, J. N., Varnum, S. M., Auberry, K. J., Moore, R. J., Angell, N. H., Smith, R. D., et al. (2002). Toward a human blood serum proteome: analysis by multidimensional separation coupled with mass spectrometry. *Mol Cell Proteomics* 1, 947–955.
- Akca, A., Nguyen, Q., & Edelstein, C. L. (2009). Mediators of inflammation in acute kidney injury. *Mediators Inflamm* 2009, 137072.
- Albelda, S. M. (1991). Endothelial and epithelial cell adhesion molecules. *Am J Respir Cell Mol Biol* 4, 195–203.
- Albini, A., Pennesi, G., Donatelli, F., Cammarota, R., De Flora, S., & Noonan, D. M. (2010). Cardiotoxicity of anticancer drugs: the need for cardio-oncology and cardio-oncological prevention. *J Natl Cancer Inst* 102, 14–25.
- Allen, D. D., Caviedes, R., Cardenas, A. M., Shimahara, T., Segura-Aguilar, J., & Caviedes, P. A. (2005). Cell lines as in vitro models for drug screening and toxicity studies. *Drug Dev Ind Pharm* 31, 757–768.
- Allen, D. G., Riviere, J. E., & Monteiro-Riviere, N. A. (2001). Cytokine induction as a measure of cutaneous toxicity in primary and immortalized porcine keratinocytes exposed to jet fuels, and their relationship to normal human epidermal keratinocytes. *Toxicol Lett* 119, 209–217.
- Amatangelo, M. D., Bassi, D. E., Klein-Szanto, A. J., & Cukierman, E. (2005). Stroma-derived three-dimensional matrices are necessary and sufficient to promote desmoplastic differentiation of normal fibroblasts. *Am J Pathol* 167, 475–488.
- Amin, R. P., Vickers, A. E., Sistare, F., Thompson, K. L., Roman, R. J., Lawton, M., et al. (2004). Identification of putative gene based markers of renal toxicity. *Environ Health Perspect* 112, 465–479.
- Anderson, L., & Anderson, N. G. (1977). High resolution two-dimensional electrophoresis of human plasma proteins. *Proc Natl Acad Sci U S A* 74, 5421–5425.
- Angst, B. D., Marozzi, C., & Magee, A. I. (2001). The cadherin superfamily: diversity in form and function. *J Cell Sci* 114, 629–641.
- Arndt, M., Lendeckel, U., Rocken, C., Nepple, K., Wolke, C., Spiess, A., et al. (2002). Altered expression of ADAMs (a disintegrin and metalloproteinase) in fibrillating human atria. *Circulation* 105, 720–725.
- Atala, A., Bauer, S. B., Soker, S., Yoo, J. J., & Retik, A. B. (2006). Tissue-engineered autologous bladders for patients needing cystoplasty. *Lancet* 367, 1241–1246.
- Avdeef, A. (2010). Leakiness and size exclusion of paracellular channels in cultured epithelial cell monolayers—interlaboratory comparison. *Pharm Res* 27, 480–489.
- Badyal, S. F., Freytes, D. O., & Gilbert, T. W. (2009). Extracellular matrix as a biological scaffold material: structure and function. *Acta Biomater* 5, 1–13.
- Balis, F. M. (2002). Evolution of anticancer drug discovery and the role of cell-based screening. *J Natl Cancer Inst* 94, 78–79.
- Beacham, D. A., Amatangelo, M. D., & Cukierman, E. (2007). Preparation of extracellular matrices produced by cultured and primary fibroblasts. *Curr Protoc Cell Biol* (Chapter 10, Unit 10.19).
- Bernard, A., Lauwerys, R., Gengoux, P., Mahieu, P., Foidart, J. M., Druet, P., et al. (1984). Anti-laminin antibodies in Sprague–Dawley and brown Norway rats chronically exposed to cadmium. *Toxicology* 31, 307–313.
- Bhadraju, K., & Chen, C. S. (2002). Engineering cellular microenvironments to improve cell-based drug testing. *Drug Discov Today* 7, 612–620.
- Bienz, M. (1999). APC: the plot thickens. *Curr Opin Genet Dev* 9, 595–603.
- Bissell, M. J., & Radisky, D. (2001). Putting tumours in context. *Nat Rev Cancer* 1, 46–54.
- Bissell, M. J., Radisky, D. C., Rizki, A., Weaver, V. M., & Petersen, O. W. (2002). The organizing principle: microenvironmental influences in the normal and malignant breast. *Differentiation* 70, 537–546.
- Bonventre, J. V., Vaidya, V. S., Schmoeder, R., Feig, P., & Dieterle, F. (2010). Next-generation biomarkers for detecting kidney toxicity. *Nat Biotechnol* 28, 436–440.
- Borghese, E. (1961). The effect of ionizing radiations on mouse embryonic lungs developing in vitro. *Ann N Y Acad Sci* 95, 866–872.
- Brosnan, C. F., Scemes, E., & Spray, D. C. (2001). Cytokine regulation of gap junction connectivity: an open-and-shut case or changing partners at the Nexus? *Am J Pathol* 158, 1565–1569.
- Brown, J. D., & Moon, R. T. (1998). Wnt signaling: why is everything so negative? *Curr Opin Cell Biol* 10, 182–187.
- Canton, L., Cole, D. M., Kemp, E. H., Watson, P. F., Chuntapong, J., Ryan, A. J., et al. (2010). Development of a 3D human in vitro skin co-culture model for detecting irritants in real-time. *Biotechnol Bioeng* 106, 794–803.
- Capes-Davis, A., Theodosopoulos, G., Atkin, I., Drexler, H. G., Kohara, A., MacLeod, R. A., et al. (2010). Check your cultures! A list of cross-contaminated or misidentified cell lines. *Int J Cancer* 127, 1–8.
- Carter, W. G., Wayner, E. A., Bouchard, T. S., & Kaur, P. (1990). The role of integrins alpha 2 beta 1 and alpha 3 beta 1 in cell–cell and cell–substrate adhesion of human epidermal cells. *J Cell Biol* 110, 1387–1404.
- Casadevall, N., Nataf, J., Viron, B., Kolta, A., Kiladjian, J. J., Martin-Dupont, P., et al. (2002). Pure red-cell aplasia and antierythropoietin antibodies in patients treated with recombinant erythropoietin. *N Engl J Med* 346, 469–475.
- Casasnovas, J. M., Bickford, J. K., & Springer, T. A. (1998). The domain structure of ICAM-1 and the kinetics of binding to rhinovirus. *J Virol* 72, 6244–6246.
- Catania, J. M., Pershing, A. M., & Gandolfi, A. J. (2007). Precision-cut tissue chips as an in vitro toxicology system. *Toxicol In Vitro* 21, 956–961.
- Chakraborty, P. K., Lee, W. K., Molitor, M., Wolff, N. A., & Thevenod, F. (2010). Cadmium induces Wnt signaling to upregulate proliferation and survival genes in sub-confluent kidney proximal tubule cells. *Mol Cancer* 9, 102.
- Chambard, M., Verrier, B., Gabrion, J., & Mauchamp, J. (1984). Polarity reversal of inside-out thyroid follicles cultured within collagen gel: reexpression of specific functions. *Biol Cell* 51, 315–325.
- Chamberlain, L. M., Godek, M. L., Gonzalez-Juarrero, M., & Grainger, D. W. (2009). Phenotypic non-equivalence of murine (monocyte-) macrophage cells in biomaterial and inflammatory models. *J Biomed Mater Res A* 88, 858–871.
- Chaudhary, K. R., Batchu, S. N., & Seubert, J. M. (2009). Cytochrome P450 enzymes and the heart. *IUBMB Life* 61, 954–960.
- Chen, C. S. (2008). Mechanotransduction – a field pulling together? *J Cell Sci* 121, 3285–3292.
- Chipman, J. K., Mally, A., & Edwards, G. O. (2003). Disruption of gap junctions in toxicity and carcinogenicity. *Toxicol Sci* 71, 146–153.
- Chow, D. C., Wenning, L. A., Miller, W. M., & Papoutsakis, E. T. (2001). Modeling pO<sub>2</sub> distributions in the bone marrow hematopoietic compartment. II. Modified Kroghian models. *Biophys J* 81, 685–696.
- Chu, V., Noble, A., & Rollins, L. (2001). Cellular reprogramming: opportunities and challenges. *Am Lab* 43, 40–43.
- Ciarimboli, G., Ludwig, T., Lang, D., Pavenstadt, H., Koepsell, H., Piechota, H. J., et al. (2005). Cisplatin nephrotoxicity is critically mediated via the human organic cation transporter 2. *Am J Pathol* 167, 1477–1484.
- Cromwell, M. E., Hilario, E., & Jacobson, F. (2006). Protein aggregation and bioprocessing. *AAPS J* 8, E572–E579.
- Crosby, L. M., & Waters, C. M. (2010). Epithelial repair mechanisms in the lung. *Am J Physiol Lung Cell Mol Physiol* 298, L715–L731.
- Cukierman, E., Pankov, R., Stevens, D. R., & Yamada, K. M. (2001). Taking cell–matrix adhesions to the third dimension. *Science* 294, 1708–1712.
- Cukierman, E., Pankov, R., & Yamada, K. M. (2002). Cell interactions with three-dimensional matrices. *Curr Opin Cell Biol* 14, 633–639.
- Cummings, B. S., Lasker, J. M., & Lash, L. H. (2000). Expression of glutathione-dependent enzymes and cytochrome P450s in freshly isolated and primary cultures of proximal tubular cells from human kidney. *J Pharmacol Exp Ther* 293, 677–685.
- Daley-Yates, P. T., & McBrien, D. C. (1984). Cisplatin metabolites in plasma, a study of their pharmacokinetics and importance in the nephrotoxic and antitumour activity of cisplatin. *Biochem Pharmacol* 33, 3063–3070.
- Dasgupta, A., & Timmerman, T. G. (1996). In vitro displacement of phenytoin from protein binding by nonsteroidal antiinflammatory drugs tolmetin, ibuprofen, and naproxen in normal and uremic sera. *Ther Drug Monit* 18, 97–99.
- Delcommenne, M., & Streuli, C. H. (1995). Control of integrin expression by extracellular matrix. *J Biol Chem* 270, 26794–26801.

## ARTICLE IN PRESS

22

A. Astashkina et al. / Pharmacology &amp; Therapeutics xxx (2012) xxx–xxx

- Dermietzel, R., Yancey, S. B., Traub, O., Willecke, K., & Revel, J. P. (1987). Major loss of the 28-kD protein of gap junction in proliferating hepatocytes. *J Cell Biol* 105, 1925–1934.
- DiMasi, J. A., Hansen, R. W., & Grabowski, H. G. (2003). The price of innovation: new estimates of drug development costs. *J Health Econ* 22, 151–185.
- Dirix, L. Y., Van Dam, P., Prove, A., & Vermeulen, P. B. (2006). Inflammatory breast cancer: current understanding. *Curr Opin Oncol* 18, 563–571.
- Donato, M. T., Lahoz, A., Castell, J. V., & Gomez-Lechon, M. J. (2008). Cell lines: a tool for in vitro drug metabolism studies. *Curr Drug Metab* 9, 1–11.
- Dorato, M. A., & Buckley, L. A. (2001). Toxicology testing in drug discovery and development. *Current protocols in toxicology*. John Wiley & Sons, Inc.
- Duflo-Dancer, A., Mesnil, M., & Yamasaki, H. (1997). Dominant-negative abrogation of connexin-mediated cell growth control by mutant connexin genes. *Oncogene* 15, 2151–2158.
- Elliott, N. T., & Yuan, F. (2011). A review of three-dimensional in vitro tissue models for drug discovery and transport studies. *J Pharm Sci* 100, 59–74.
- Engler, A. J., Sen, S., Sweeney, H. L., & Discher, D. E. (2006). Matrix elasticity directs stem cell lineage specification. *Cell* 126, 677–689.
- Essani, N. A., Fisher, M. A., Farhood, A., Manning, A. M., Smith, C. W., & Jaeschke, H. (1995). Cytokine-induced upregulation of hepatic intercellular adhesion molecule-1 messenger RNA expression and its role in the pathophysiology of murine endotoxin shock and acute liver failure. *Hepatology* 21, 1632–1639.
- Ezashi, T., Das, P., & Roberts, R. M. (2005). Low O<sub>2</sub> tensions and the prevention of differentiation of hES cells. *Proc Natl Acad Sci U S A* 102, 4783–4788.
- Fainaru, O., Adini, I., Benny, O., Bazinet, L., Pravda, E., D'Amato, R., et al. (2008). Doxycycline induces membrane expression of VE-cadherin on endothelial cells and prevents vascular hyperpermeability. *FASEB J* 22, 3728–3735.
- Farhood, A., McGuire, G. M., Manning, A. M., Miyasaka, M., Smith, C. W., & Jaeschke, H. (1995). Intercellular adhesion molecule 1 (ICAM-1) expression and its role in neutrophil-induced ischemia-reperfusion injury in rat liver. *J Leukoc Biol* 57, 368–374.
- FDA (2009). Guidance for industry: assay development for immunogenicity testing of therapeutic proteins. In F.A.D. Administration (Ed.).
- Fisher, G. J., Duell, E. A., Nickloff, B. J., Annesley, T. M., Kowalke, J. K., Ellis, C. N., et al. (1988). Levels of cyclosporin in epidermis of treated psoriasis patients differentially inhibit growth of keratinocytes cultured in serum free versus serum containing media. *J Invest Dermatol* 91, 142–146.
- Fukumoto, M., Kujirakawa, T., Hara, M., Shibasaki, T., Hosoya, T., & Yoshida, M. (2001). Effect of cadmium on gap junctional intercellular communication in primary cultures of rat renal proximal tubular cells. *Life Sci* 69, 247–254.
- Gallagher, W. M., Tweats, D., & Koenig, J. (2009). Omic profiling for drug safety assessment: current trends and public-private partnerships. *Drug Discov Today* 14, 337–342.
- Gasparini, G., Brooks, P. C., Biganzoli, E., Vermeulen, P. B., Bonaldi, E., Dirix, L. Y., et al. (1998). Vascular integrin alpha(v)beta3: a new prognostic indicator in breast cancer. *Clin Cancer Res* 4, 2625–2634.
- Geier, A., Fickert, P., & Trauner, M. (2006). Mechanisms of disease: mechanisms and clinical implications of cholestasis in sepsis. *Nat Clin Pract Gastroenterol Hepatol* 3, 574–585.
- Geiger, B. (2001). Cell biology. Encounters in space. *Science* 294, 1661–1663.
- Geiger, B., & Bershadsky, A. (2002). Exploring the neighborhood: adhesion-coupled cell mechanosensors. *Cell* 110, 139–142.
- Geiger, B., Bershadsky, A., Pankov, R., & Yamada, K. M. (2001). Transmembrane crosstalk between the extracellular matrix–cytoskeleton crosstalk. *Nat Rev Mol Cell Biol* 2, 793–805.
- Geisbrecht, E. K., & Montell, D. J. (2002). Myosin VI is required for E-cadherin-mediated border cell migration. *Nat Cell Biol* 4, 616–620.
- Gerber, I., & Gwynn, I. (2001). Influence of cell isolation, cell culture density, and cell nutrition on differentiation of rat calvarial osteoblast-like cells in vitro. *Eur Cell Mater* 2, 10–20.
- Ghosh, S., Spagnoli, G. C., Martin, I., Ploegert, S., Demougin, P., Heberer, M., et al. (2005). Three-dimensional culture of melanoma cells profoundly affects gene expression profile: a high density oligonucleotide array study. *J Cell Physiol* 204, 522–531.
- Giesen, T. J., Mantel-Teeuwisse, A. K., Straus, S. M., Schellekens, H., Leufkens, H. G., & Egberts, A. C. (2008). Safety-related regulatory actions for biologicals approved in the United States and the European Union. *JAMA* 300, 1887–1896.
- Gomez-Lechon, M. J., Jover, R., Donato, T., Ponsoda, X., Rodriguez, C., Stenzel, K. G., et al. (1998). Long-term expression of differentiated functions in hepatocytes cultured in three-dimensional collagen matrix. *J Cell Physiol* 177, 553–562.
- Griffith, L. G., & Swartz, M. A. (2006). Capturing complex 3D tissue physiology in vitro. *Nat Rev Mol Cell Biol* 7, 211–224.
- Gudjonsson, T., Ronnov-Jessen, L., Villadsen, R., Rank, F., Bissell, M. J., & Petersen, O. W. (2002). Normal and tumor-derived myoepithelial cells differ in their ability to interact with luminal breast epithelial cells for polarity and basement membrane deposition. *J Cell Sci* 115, 39–50.
- Gumbiner, B. M. (1996). Cell adhesion: the molecular basis of tissue architecture and morphogenesis. *Cell* 84, 345–357.
- Gumbiner, B. M. (1998). Propagation and localization of Wnt signaling. *Curr Opin Genet Dev* 8, 430–435.
- Gumbiner, B. M. (2005). Regulation of cadherin-mediated adhesion in morphogenesis. *Nat Rev Mol Cell Biol* 6, 622–634.
- Guppy, M., Leedman, P., Zu, X., & Russell, V. (2002). Contribution by different fuels and metabolic pathways to the total ATP turnover of proliferating MCF-7 breast cancer cells. *Biochem J* 364, 309–315.
- Gupta, S., Indelicato, S. R., Jethwa, V., Kawabata, T., Kelley, M., Mire-Sluis, A. R., et al. (2007). Recommendations for the design, optimization, and qualification of cell-based assays used for the detection of neutralizing antibody responses elicited by biological therapeutics. *J Immunol Methods* 321, 1–18.
- Harbers, G., & Grainger, D. W. (2006). Cell–materials interactions: fundamental design issues for tissue engineering and clinical considerations. In J. O. Hollinger, & S. Guelcher (Eds.), *An Introduction to Biomaterials* (pp. 15–45). Boca Raton, FL: CRC Press.
- Hartmann, F., & Bissell, D. M. (1982). Metabolism of heme and bilirubin in rat and human small intestinal mucosa. *J Clin Invest* 70, 23–29.
- Hermitte, F., Brunet de la Grange, P., Belloc, F., Praloran, V., & Ivanovic, Z. (2006). Very low O<sub>2</sub> concentration (0.1%) favors G0 return of dividing CD34+ cells. *Stem Cells* 24, 65–73.
- Hoefkens, J. (2011). Use of integrated data analysis to gain an advantage in biomarker discovery and personalized medicine. *Am Lab* 43, 39–41.
- Hoffmann, D., Adler, M., Vaidya, V. S., Rached, E., Mulrane, L., Gallagher, W. M., et al. (2010). Performance of novel kidney biomarkers in preclinical toxicity studies. *Toxicol Sci* 116, 8–22.
- Holt, D. J., Chamberlain, L. M., & Grainger, D. W. (2010). Cell–cell signaling in co-cultures of macrophages and fibroblasts. *Biomaterials* 31, 9382–9394.
- Huang, X., Ding, L., Bennewith, K. L., Tong, R. T., Welford, S. M., Ang, K. K., et al. (2009). Hypoxia-inducible mir-210 regulates normoxic gene expression involved in tumor initiation. *Mol Cell* 35, 856–867.
- Hughes, P., Marshall, D., Reid, Y., Parkes, H., & Gelber, C. (2007). The costs of using unauthenticated, over-passaged cell lines: how much more data do we need? *Biotechniques* 43 (575), 577–578 (581–572 passim).
- Hughes, C. S., Postovit, L. M., & Lajoie, G. A. (2010). Matrigel: a complex protein mixture required for optimal growth of cell culture. *Proteomics* 10, 1886–1890.
- Huh, D., Matthews, B. D., Mammoto, A., Montoya-Zavala, M., Hsin, H. Y., & Ingber, D. E. (2010). Reconstituting organ-level lung functions on a chip. *Science* 328, 1662–1668.
- Hulpiau, P., & van Roy, F. (2009). Molecular evolution of the cadherin superfamily. *Int J Biochem Cell Biol* 41, 349–369.
- Humphries, M. J., Travis, M. A., Clark, K., & Mould, A. P. (2004). Mechanisms of integration of cells and extracellular matrices by integrins. *Biochem Soc Trans* 32, 822–825.
- Huo, W., Zhang, K., Nie, Z., Li, Q., & Jin, F. (2010). Kidney injury molecule-1 (KIM-1): a novel kidney-specific injury molecule playing potential double-edged functions in kidney injury. *Transplant Rev (Orlando)* 24, 143–146.
- Hynes, R. O. (1999). Cell adhesion: old and new questions. *Trends Cell Biol* 9, M33–M37.
- Hynes, R. O. (2002). Integrins: bidirectional, allosteric signaling machines. *Cell* 110, 673–687.
- Ichimura, T., Asselton, E. J., Humphreys, B. D., Gunaratnam, L., Duffield, J. S., & Bonventre, J. V. (2008). Kidney injury molecule-1 is a phosphatidylserine receptor that confers a phagocytic phenotype on epithelial cells. *J Clin Invest* 118, 1657–1668.
- Ichimura, T., Bonventre, J. V., Bailly, V., Wei, H., Hession, C. A., Cate, R. L., et al. (1998). Kidney injury molecule-1 (KIM-1), a putative epithelial cell adhesion molecule containing a novel immunoglobulin domain, is up-regulated in renal cells after injury. *J Biol Chem* 273, 4135–4142.
- Ikada, Y. (2006). Scope of tissue engineering. In Y. Ikada (Ed.), *Tissue engineering: fundamentals and applications* Vol. 8. (pp. 33): Elsevier Ltd.
- Imamdi, R., de Grauw, M., & van de Water, B. (2004). Protein kinase C mediates cisplatin-induced loss of adherens junctions followed by apoptosis of renal proximal tubular epithelial cells. *J Pharmacol Exp Ther* 311, 892–903.
- Ishii, I., Tomizawa, A., Kawachi, H., Suzuki, T., Kotani, A., Koshushi, I., et al. (2001). Histological and functional analysis of vascular smooth muscle cells in a novel culture system with honeycomb-like structure. *Atherosclerosis* 158, 377–384.
- Jacobs, J. M., Adkins, J. N., Qian, W. J., Liu, T., Shen, Y., Camp, D. G., 2nd, et al. (2005). Utilizing human blood plasma for proteomic biomarker discovery. *J Proteome Res* 4, 1073–1085.
- Jaeschke, H. (1997). Cellular adhesion molecules: regulation and functional significance in the pathogenesis of liver diseases. *Am J Physiol* 273, G602–G611.
- Jiang, J., Dean, D., Burghardt, R. C., & Parrish, A. R. (2004). Disruption of cadherin/catenin expression, localization, and interactions during HgCl<sub>2</sub>-induced nephrotoxicity. *Toxicol Sci* 80, 170–182.
- Jones, C. F., & Grainger, D. W. (2009). In vitro assessments of nanomaterial toxicity. *Adv Drug Deliv Rev* 61, 438–456.
- Justice, B. A., Badr, N. A., & Felder, R. A. (2009). 3D cell culture opens new dimensions in cell-based assays. *Drug Discov Today* 14, 102–107.
- Kamgang, E., Peyret, T., & Krishnan, K. (2008). An integrated QSPR-PBPK modelling approach for in vitro-in vivo extrapolation of pharmacokinetics in rats. *SAR QSAR Environ Res* 19, 669–680.
- Katsumi, A., Orr, A. W., Tzima, E., & Schwartz, M. A. (2004). Integrins in mechanotransduction. *J Biol Chem* 279, 12001–12004.
- Kauly, T., Kaufman-Francis, K., Lesman, A., & Levenberg, S. (2009). Vascularization – the conduit to viable engineered tissues. *Tissue Eng Part B Rev* 15, 159–169.
- Keller, P. J., Pampaloni, F., & Stelzer, E. H. (2007). Three-dimensional preparation and imaging reveal intrinsic microtubule properties. *Nat Methods* 4, 843–846.
- Kellner, K., Liebsch, G., Klimant, I., Wolfbeis, O. S., Blunk, T., Schulz, M. B., et al. (2002). Determination of oxygen gradients in engineered tissue using a fluorescent sensor. *Biotechnol Bioeng* 80, 73–83.
- Khetani, S. R., & Bhatia, S. N. (2008). Microscale culture of human liver cells for drug development. *Nat Biotechnol* 26, 120–126.
- Kendigand, D. M., & Tarloff, J. B. (2007). Inactivation of lactate dehydrogenase by several chemicals: Implications for in vitro toxicology studies. *Toxicology in Vitro* 21, 125–132.
- Kim, S. H., Jen, W. C., De Robertis, E. M., & Kintner, C. (2000). The protocadherin PAPC establishes segmental boundaries during somitogenesis in *Xenopus* embryos. *Curr Biol* 10, 821–830.
- Kishimoto, T. K., Jutila, M. A., Berg, E. L., & Butcher, E. C. (1989). Neutrophil Mac-1 and MEL-14 adhesion proteins inversely regulated by chemotactic factors. *Science* 245, 1238–1241.



- Kobel, S., & Lutolf, M. (2010). High-throughput methods to define complex stem cell niches. *Biotechniques* 48 (ix–xxii).
- Kola, I., & Landis, J. (2004). Can the pharmaceutical industry reduce attrition rates? *Nat Rev Drug Discov* 3, 711–715.
- Kolaja, K. L., Engelken, D. T., & Klaassen, C. D. (2000). Inhibition of gap-junctional-intercellular communication in intact rat liver by nongenotoxic hepatocarcinogens. *Toxicology* 146, 15–22.
- Kolaja, K. L., Petrick, J. S., & Klaassen, C. D. (2000). Inhibition of gap-junctional-intercellular communication in thyroid-follicular cells by propylthiouracil and low iodine diet. *Toxicology* 143, 195–202.
- Kolbe, M., Xiang, Z., Dohle, E., Tonak, M., Kirkpatrick, C. J., & Fuchs, S. (2011). Paracrine effects influenced by cell culture medium and consequences on microvessel-like structures in cocultures of mesenchymal stem cells and outgrowth endothelial cells. *Tissue Eng Part A* 17, 2199–2212.
- Kwon, O., Nelson, W. J., Sibley, R., Huie, P., Scandling, J. D., Dafeo, D., et al. (1998). Backleak, tight junctions, and cell-cell adhesion in postschismic injury to the renal allograft. *J Clin Invest* 101, 2054–2064.
- Ladoux, B., Anon, E., Lambert, M., Rabodzey, A., Hersen, P., Buguin, A., et al. (2010). Strength dependence of cadherin-mediated adhesions. *Biophys J* 98, 534–542.
- Lafite, P., Dijols, S., Buisson, D., Macherey, A. C., Zeldin, D. C., Dansette, P. M., et al. (2006). Design and synthesis of selective, high-affinity inhibitors of human cytochrome P450 2J2. *Bioorg Med Chem Lett* 16, 2777–2780.
- Lafite, P., Dijols, S., Zeldin, D. C., Dansette, P. M., & Mansuy, D. (2007). Selective, competitive and mechanism-based inhibitors of human cytochrome P450 2J2. *Arch Biochem Biophys* 464, 155–168.
- Larsen, M., Artym, V. V., Green, J. A., & Yamada, K. M. (2006). The matrix reorganized: extracellular matrix remodeling and integrin signaling. *Curr Opin Cell Biol* 18, 463–471.
- Lasfargues, E. Y. (1957). Cultivation and behavior in vitro of the normal mammary epithelium of the adult mouse. II. Observations on the secretory activity. *Exp Cell Res* 13, 553–562.
- Lasnitzki, I. (1958). Observations on the effects of condensates from cigarette smoke on human foetal lung in vitro. *Br J Cancer* 12, 547–552.
- Lasnitzki, I. (1961). The effect of radiation on the normal and oestrone-treated mouse vagina grown in vitro. *Br J Radiol* 34, 356–361.
- Lasnitzki, I. (1961). The effect of x rays on cellular differentiation in organ culture. *Ann N Y Acad Sci* 95, 873–881.
- Lasnitzki, I., & Lucy, J. A. (1961). Amino acid metabolism and arginase activity in mouse prostate glands grown in vitro with and without 20-methylcholanthrene. *Exp Cell Res* 24, 379–392.
- Lasser, K. E., Allen, P. D., Woolhandler, S. J., Himmelstein, D. U., Wolfe, S. M., & Bor, D. H. (2002). Timing of new black box warnings and withdrawals for prescription medications. *JAMA* 287, 2215–2220.
- Lee, J., Cuddihy, M. J., & Kotov, N. A. (2008). Three-dimensional cell culture matrices: state of the art. *Tissue Eng Part B Rev* 14, 61–86.
- Lee, J. W., Kelley, M., King, L. E., Yang, J., Salimi-Moosavi, H., Tang, M. T., et al. (2011). Bioanalytical approaches to quantify “total” and “free” therapeutic antibodies and their targets: technical challenges and PK/PD applications over the course of drug development. *AAPS J* 13, 99–110.
- Legate, K. R., Wickstrom, S. A., & Fassler, R. (2009). Genetic and cell biological analysis of integrin outside-in signaling. *Genes Dev* 23, 397–418.
- Leussink, B. T., Litvinov, S. V., de Heer, E., Slikkerveer, A., van der Voet, G. B., Bruijn, J. A., et al. (2001). Loss of homotypic epithelial cell adhesion by selective N-cadherin displacement in bismuth nephrotoxicity. *Toxicol Appl Pharmacol* 175, 54–59.
- Levenberg, S., Rouwkema, J., Macdonald, M., Garfein, E. S., Kohane, D. S., Darland, D. C., et al. (2005). Engineering vascularized skeletal muscle tissue. *Nat Biotechnol* 23, 879–884.
- Lewinski, N., Colvin, V., & Drezek, R. (2008). Cytotoxicity of nanoparticles. *Small* 4, 26–49.
- Li, A. P. (2004). Accurate prediction of human drug toxicity: a major challenge in drug development. *Chem Biol Interact* 150, 3–7.
- Lim, S. W., Li, C., Ahn, K. O., Kim, J., Moon, I. S., Ahn, C., et al. (2005). Cyclosporine-induced renal injury induces toll-like receptor and maturation of dendritic cells. *Transplantation* 80, 691–699.
- Lin, J. H., Weigel, H., Cotrina, M. L., Liu, S., Bueno, E., Hansen, A. J., et al. (1998). Gap-junction-mediated propagation and amplification of cell injury. *Nat Neurosci* 1, 494–500.
- Loeb, L. (1897). Ueber die Entstehung von Bindegewebe, Leukocyten und roten Blutkörperchen aus Epithel und ueber eine Methode, isolierte Gewebsteile zu zuechten. Chicago: M. Stern and Co.
- Loewenstein, W. R. (1981). Junctional intercellular communication: the cell-to-cell membrane channel. *Physiol Rev* 61, 829–913.
- Loppnow, H., Werdan, K., & Buerke, M. (2008). Vascular cells contribute to atherosclerosis by cytokine- and innate-immunity-related inflammatory mechanisms. *Innate Immun* 14, 63–87.
- Lu, L., Payvandi, F., Wu, L., Zhang, L. H., Hariri, R. J., Man, H. W., et al. (2009). The anti-cancer drug lenalidomide inhibits angiogenesis and metastasis via multiple inhibitory effects on endothelial cell function in normoxic and hypoxic conditions. *Microvasc Res* 77, 78–86.
- Maaser, K., Wolf, K., Klein, C. E., Niggemann, B., Zanker, K. S., Brocker, E. B., et al. (1999). Functional hierarchy of simultaneously expressed adhesion receptors: integrin alpha2beta1 but not CD44 mediates MV3 melanoma cell migration and matrix reorganization within three-dimensional hyaluronan-containing collagen matrices. *Mol Cell Biol* 10, 3067–3079.
- McKeague, A. L., Wilson, D. J., & Nelson, J. (2003). Staurosporine-induced apoptosis and hydrogen peroxide-induced necrosis in two human breast cell lines. *British journal of cancer* 88, 125–131.
- Mally, A., & Chipman, J. K. (2002). Non-genotoxic carcinogens: early effects on gap junctions, cell proliferation and apoptosis in the rat. *Toxicology* 180, 233–248.
- Mally, A., Decker, M., Bektreshi, M., & Dekant, W. (2006). Ochratoxin A alters cell adhesion and gap junction intercellular communication in MDCK cells. *Toxicology* 223, 15–25.
- Masters, J. R. (2002). HeLa cells 50 years on: the good, the bad and the ugly. *Nat Rev Cancer* 2, 315–319.
- Matsunaga, M., Hatta, K., Nagafuchi, A., & Takeichi, M. (1988). Guidance of optic nerve fibres by N-cadherin adhesion molecules. *Nature* 334, 62–64.
- Mattana, J., Margiloff, L., Sharma, P., & Singhal, P. C. (1998). Oxidation of the mesangial matrix metalloproteinase-2 impairs gelatinolytic activity. *Inflammation* 22, 269–276.
- McEver, R. P., Moore, K. L., & Cummings, R. D. (1995). Leukocyte trafficking mediated by selectin-carbohydrate interactions. *J Biol Chem* 270, 11025–11028.
- McLarnon, S., Holden, D., Ward, D., Jones, M., Elliott, A., & Riccardi, D. (2002). Aminoglycoside antibiotics induce pH-sensitive activation of the calcium-sensing receptor. *Biochem Biophys Res Commun* 297, 71–77.
- Mehendale, H. M., Roth, R. A., Gandolfi, A. J., Klaunig, J. E., Lemasters, J. J., & Curtis, L. R. (1994). Novel mechanisms in chemically induced hepatotoxicity. *FASEB J* 8, 1285–1295.
- Menasche, P. (2011). Stem cell therapy for chronic heart failure: lessons from a 15-year experience. *C R Biol* 334, 489–496.
- Milyavsky, M., Shats, I., Erez, N., Tang, X., Senderovich, S., Meerson, A., et al. (2003). Prolonged culture of telomerase-immortalized human fibroblasts leads to a premalignant phenotype. *Cancer Res* 63, 7147–7157.
- Mistry, P., Lee, C., & McBrien, D. C. (1989). Intracellular metabolites of cisplatin in the rat kidney. *Cancer Chemother Pharmacol* 24, 73–79.
- Molina, A., Sanchez-Madrid, F., Bricio, T., Martin, A., Barat, A., Alvarez, V., et al. (1994). Prevention of mercuric chloride-induced nephritis in the brown Norway rat by treatment with antibodies against the alpha 4 integrin. *J Immunol* 153, 2313–2320.
- Moorby, C., & Patel, M. (2001). Dual functions for connexins: Cx43 regulates growth independently of gap junction formation. *Exp Cell Res* 271, 238–248.
- Moran, S. M., & Myers, B. D. (1985). Pathophysiology of protracted acute renal failure in man. *J Clin Invest* 76, 1440–1448.
- Motoyoshi, Y., Matsusaka, T., Saito, A., Pastan, I., Willnow, T. E., Mizutani, S., et al. (2008). Megalin contributes to the early injury of proximal tubule cells during nonselective proteinuria. *Kidney Int* 74, 1262–1269.
- Myers, B. D., Chui, F., Hilberman, M., & Michaels, A. S. (1979). Transtubular leakage of glomerular filtrate in human acute renal failure. *Am J Physiol* 237, F319–F325.
- Naciri, M., Kuystermans, D., & Al-Rubeai, M. (2008). Monitoring pH and dissolved oxygen in mammalian cell culture using optical sensors. *Cytotechnology* 57, 245–250.
- Nagel, S. C., vom Saal, F. S., & Welshons, W. V. (1998). The effective free fraction of estradiol and xenoestrogens in human serum measured by whole cell uptake assays: physiology of delivery modifies estrogenic activity. *Proc Soc Exp Biol Med* 217, 300–309.
- Naik, G. (2011). Lab-made trachea saves man. *Wall Street Journal health*. : Dow Jones & Company, Inc.
- Nardone, R. M. (2007). Eradication of cross-contaminated cell lines: a call for action. *Cell Biol Toxicol* 23, 367–372.
- Netzlaff, F., Lehr, C. M., Wertz, P. W., & Schaefer, U. F. (2005). The human epidermis models EpiSkin, SkinEthic and EpiDerm: an evaluation of morphology and their suitability for testing phototoxicity, irritancy, corrosivity, and substance transport. *Eur J Pharm Biopharm* 60, 167–178.
- Nony, P. A., & Schnellmann, R. G. (2003). Mechanisms of renal cell repair and regeneration after acute renal failure. *J Pharmacol Exp Ther* 304, 905–912.
- O'Brien, P., & Haskins, J. R. (2007). In vitro cytotoxicity assessment. *Methods Mol Biol* 356, 415–425.
- O'Brien, L. E., Jou, T. S., Pollack, A. L., Zhang, Q., Hansen, S. H., Yurchenco, P., et al. (2001). Rac1 orientates epithelial apical polarity through effects on basolateral laminin assembly. *Nat Cell Biol* 3, 831–838.
- O'Brien, L. E., Zegers, M. M., & Mostov, K. E. (2002). Opinion: building epithelial architecture: insights from three-dimensional culture models. *Nat Rev Mol Cell Biol* 3, 531–537.
- Ojakian, G. K., & Schwimmer, R. (1994). Regulation of epithelial cell surface polarity reversal by beta 1 integrins. *J Cell Sci* 107(Pt 3), 561–576.
- Ozog, M. A., Stushansian, R., & Naus, C. C. (2002). Blocked gap junctional coupling increases glutamate-induced neurotoxicity in neuron-astrocyte co-cultures. *J Neuropathol Exp Neurol* 61, 132–141.
- Pampaloni, F., Reynaud, E. G., & Stelzer, E. H. (2007). The third dimension bridges the gap between cell culture and live tissue. *Nat Rev Mol Cell Biol* 8, 839–845.
- Parrish, A. R., Catania, J. M., Orozco, J., & Gandolfi, A. J. (1999). Chemically induced oxidative stress disrupts the E-cadherin/catenin cell adhesion complex. *Toxicol Sci* 51, 80–86.
- Paszek, M. J., Zahir, N., Johnson, K. R., Lakins, J. N., Rozenberg, G. I., Gefen, A., et al. (2005). Tensional homeostasis and the malignant phenotype. *Cancer Cell* 8, 241–254.
- Pelham, R. J., Jr., & Wang, Y. (1997). Cell locomotion and focal adhesions are regulated by substrate flexibility. *Proc Natl Acad Sci U S A* 94, 13661–13665.
- Pelham, R. J., Jr., & Wang, Y. L. (1998). Cell locomotion and focal adhesions are regulated by the mechanical properties of the substrate. *Biol Bull* 194, 348–349 (discussion 349–350).
- Peracchia, C., Wang, X. G., & Peracchia, L. L. (2000). Chemical gating of gap junction channels. *Methods* 20, 188–195.
- Perini, P., Facchinetti, A., Bulian, P., Massaro, A. R., Pascalis, D. D., Bertolotto, A., et al. (2001). Interferon-beta (INF-beta) antibodies in interferon-beta1a- and interferon-beta1b-treated multiple sclerosis patients. Prevalence, kinetics, cross-reactivity, and factors enhancing interferon-beta immunogenicity in vivo. *Eur Cytokine New* 12, 56–61.
- Petersen, O. W., Ronnov-Jessen, L., Howlett, A. R., & Bissell, M. J. (1992). Interaction with basement membrane serves to rapidly distinguish growth and differentiation

- pattern of normal and malignant human breast epithelial cells. *Proc Natl Acad Sci U S A* 89, 9064–9068.
- Plucienik, F., Verrecchia, F., Bastide, B., Herve, J. C., Joffre, M., & Deleze, J. (1996). Reversible interruption of gap junctional communication by testosterone propionate in cultured Sertoli cells and cardiac myocytes. *J Membr Biol* 149, 169–177.
- Pokutta, S., & Weis, W. I. (2007). Structure and mechanism of cadherins and catenins in cell–cell contacts. *Annu Rev Cell Dev Biol* 23, 237–261.
- Ponec, M., Boelsma, E., Gibbs, S., & Mommaas, M. (2002). Characterization of reconstructed skin models. *Skin Pharmacol Appl Skin Physiol* 15(Suppl. 1), 4–17.
- Porter, S. (2001). Human immune response to recombinant human proteins. *J Pharm Sci* 90, 1–11.
- Portner, R., & Giese, C. (2007). An overview on bioreactor design, prototyping and process control for reproducible three-dimensional tissue culture. In U. Marx, & V. Sandig (Eds.), *Drug testing in vitro: breakthroughs and trends in cell culture technology* (pp. 53–78). : WILEY-VCH Verlag GmbH&Co.
- Prentis, R. A., Lis, Y., & Walker, S. R. (1988). Pharmaceutical innovation by the seven UK-owned pharmaceutical companies (1964–1985). *Br J Clin Pharmacol* 25, 387–396.
- Prestwich, G. D. (2008). Evaluating drug efficacy and toxicology in three dimensions: using synthetic extracellular matrices in drug discovery. *Acc Chem Res* 41, 139–148.
- Prestwich, G. D., & Kuo, J. W. (2008). Chemically-modified HA for therapy and regenerative medicine. *Curr Pharm Biotechnol* 9, 242–245.
- Prozialeck, W. C., Edwards, J. R., Lamar, P. C., & Smith, C. S. (2006). Epithelial barrier characteristics and expression of cell adhesion molecules in proximal tubule-derived cell lines commonly used for in vitro toxicity studies. *Toxicol In Vitro* 20, 942–953.
- Prozialeck, W. C., Lamar, P. C., & Lynch, S. M. (2003). Cadmium alters the localization of N-cadherin, E-cadherin, and beta-catenin in the proximal tubule epithelium. *Toxicol Appl Pharmacol* 189, 180–195.
- Pujol, A., Mosca, R., Farres, J., & Aloy, P. (2010). Unveiling the role of network and systems biology in drug discovery. *Trends Pharmacol Sci* 31, 115–123.
- Qin, J., Vinogradova, O., & Plow, E. F. (2004). Integrin bidirectional signaling: a molecular view. *PLoS Biol* 2, e169.
- Rached, E., Hoffmann, D., Blumberg, K., Weber, K., Dekant, W., & Mally, A. (2008). Evaluation of putative biomarkers of nephrotoxicity after exposure to ochratoxin A in vivo and in vitro. *Toxicol Sci* 103, 371–381.
- Racusen, L. C., Fivush, B. A., Li, Y. L., Slatnik, L., & Solez, K. (1991). Dissociation of tubular cell detachment and tubular cell death in clinical and experimental "acute tubular necrosis". *Lab Invest* 64, 546–556.
- Radisky, D. C., Levy, D. D., Littlepage, L. E., Liu, H., Nelson, C. M., Fata, J. E., et al. (2005). Rac1 and reactive oxygen species mediate MMP-3-induced EMT and genomic instability. *Nature* 436, 123–127.
- Reilly, G. C., & Engler, A. J. (2010). Intrinsic extracellular matrix properties regulate stem cell differentiation. *J Biomech* 43, 55–62.
- Research, C. F. B. E. a. (2009). Guidance for industry [electronic resource]: drug-induced liver injury, premarketing clinical evaluation. Rockville, MD: U.S. Dept. of Health and Human Services, Food and Drug Administration, Center for Drug Evaluation and Research; Center for Biologics Evaluation and Research.
- Rivera, E. M., Elias, J. J., Bern, H. A., Napalkov, N. P., & Pitelka, D. R. (1963). Toxic effects of steroid hormones on organ cultures of mouse mammary tumors, with a comment on the occurrence of viral inclusion bodies. *J Natl Cancer Inst* 31, 671–687.
- Roguet, R., Cohen, C., Dossou, K. G., & Rougier, A. (1994). Episkin, a reconstituted human epidermis for assessing in vitro the irritancy of topically applied compounds. *Toxicol In Vitro* 8, 283–291.
- Ronzitti, G., Callegari, F., Malaguti, C., & Rossini, G. P. (2004). Selective disruption of the E-cadherin–catenin system by an algal toxin. *Br J Cancer* 90, 1100–1107.
- Rosdy, M., & Claus, L. C. (1990). Terminal epidermal differentiation of human keratinocytes grown in chemically defined medium on inert filter substrates at the air–liquid interface. *J Invest Dermatol* 95, 409–414.
- Rosenberg, A. S. (2006). Effects of protein aggregates: an immunologic perspective. *AAPS J* 8, E501–E507.
- Rous, P., & Jones, F. S. (1916). A method for obtaining suspensions of living cells from the fixed tissues, and for the plating out of individual cells. *J Exp Med* 23, 549–555.
- Saelman, E. U., Keely, P. J., & Santoro, S. A. (1995). Loss of MDCK cell alpha 2 beta 1 integrin expression results in reduced cyst formation, failure of hepatocyte growth factor/scatter factor-induced branching morphogenesis, and increased apoptosis. *J Cell Sci* 108(Pt 11), 3531–3540.
- Saez, J. C., Connor, J. A., Spray, D. C., & Bennett, M. V. (1989). Hepatocyte gap junctions are permeable to the second messenger, inositol 1,4,5-trisphosphate, and to calcium ions. *Proc Natl Acad Sci U S A* 86, 2708–2712.
- Sanchez, S., Barger, T., Zhou, L., Hale, M., Mytych, D., Gupta, S., et al. (2011). Strategy to confirm the presence of anti-erythropoietin neutralizing antibodies in human serum. *J Pharm Biomed Anal* 55, 1265–1274.
- Sastry, S. K., & Burridge, K. (2000). Focal adhesions: a nexus for intracellular signaling and cytoskeletal dynamics. *Exp Cell Res* 261, 25–36.
- Scadden, D. T. (2006). The stem-cell niche as an entity of action. *Nature* 441, 1075–1079.
- Schick, C. S., & Haller, C. (1999). Comparative cytotoxicity of ionic and non-ionic radiocontrast agents on MDCK cell monolayers in vitro. *Nephrol Dial Transplant* 14, 342–347.
- Schwimmer, R., & Ojakian, G. K. (1995). The alpha 2 beta 1 integrin regulates collagen-mediated MDCK epithelial membrane remodeling and tubule formation. *J Cell Sci* 108(Pt 6), 2487–2498.
- Shen, J., Behrens, C., Wistuba, I. I., Feng, L., Lee, J. J., Hong, W. K., et al. (2006). Identification and validation of differences in protein levels in normal, premalignant, and malignant lung cells and tissues using high-throughput Western Array and immunohistochemistry. *Cancer Res* 66, 11194–11206.
- Sheridan, A. M., & Bonventre, J. V. (2000). Cell biology and molecular mechanisms of injury in ischemic acute renal failure. *Curr Opin Nephrol Hypertens* 9, 427–434.
- Shizukuda, Y., & Buttrick, P. M. (2002). Oxygen free radicals and heart failure: new insight into an old question. *Am J Physiol Lung Cell Mol Physiol* 283, L237–L238.
- Sivridis, E., Giatromanolaki, A., & Koukourakis, M. I. (2004). "Stromatogenesis" and tumor progression. *Int J Surg Pathol* 12, 1–9.
- Smith, D. A. (1991). Species differences in metabolism and pharmacokinetics: are we close to an understanding? *Drug Metab Rev* 23, 355–373.
- Staunton, D. E., Marlin, S. D., Stratowa, C., Dustin, M. L., & Springer, T. A. (1988). Primary structure of ICAM-1 demonstrates interaction between members of the immunoglobulin and integrin supergene families. *Cell* 52, 925–933.
- Storer, R. D., McKelvey, T. W., Kraynak, A. R., Elia, M. C., Barnum, J. E., Harmon, L. S., Nichols, W. W., & DeLuca, J. G. (1996). Revalidation of the in vitro alkaline elution/rat hepatocyte assay for DNA damage: improved criteria for assessment of cytotoxicity and genotoxicity and results for 81 compounds. *Mutat Res* 368, 59–101.
- Sudlow, G., Birkett, D. J., & Wade, D. N. (1976). Further characterization of specific drug binding sites on human serum albumin. *Mol Pharmacol* 12, 1052–1061.
- Swierenga, S. H., & Yamasaki, H. (1992). Performance of tests for cell transformation and gap-junction intercellular communication for detecting nongenotoxic carcinogenic activity. *IARC Sci Publ*, 165–193.
- Tadokoro, S., Shattil, S. J., Eto, K., Tai, V., Liddington, R. C., de Pereda, J. M., et al. (2003). Talin binding to integrin beta tails: a final common step in integrin activation. *Science* 302, 103–106.
- Takahashi, K., Tanabe, K., Ohnuki, M., Narita, M., Ichisaka, T., Tomoda, K., et al. (2007). Induction of pluripotent stem cells from adult human fibroblasts by defined factors. *Cell* 131, 861–872.
- Tan, T. W., Lai, C. H., Huang, C. Y., Yang, W. H., Chen, H. T., Hsu, H. C., et al. (2009). CTGF enhances migration and MMP-13 up-regulation via alphavbeta3 integrin, FAK, ERK, and NF-kappaB-dependent pathway in human chondrosarcoma cells. *J Cell Biochem* 107, 345–356.
- Tang, Y., Olufemi, L., Wang, M. T., & Nie, D. (2008). Role of Rho GTPases in breast cancer. *Front Biosci* 13, 759–776.
- Tepass, U., Godt, D., & Winklbauer, R. (2002). Cell sorting in animal development: signalling and adhesive mechanisms in the formation of tissue boundaries. *Curr Opin Genet Dev* 12, 572–582.
- Tinois, E., Tiollier, J., Gaucherand, M., Dumas, H., Tardy, M., & Thivolet, J. (1991). In vitro and post-transplantation differentiation of human keratinocytes grown on the human type IV collagen film of a bilayered dermal substitute. *Exp Cell Res* 193, 310–319.
- Trowell, O. A. (1961). Cytocidal effects of radiation on organ cultures. *Ann N Y Acad Sci* 95, 849–865.
- Trowell, O. A. (1961). Radiosensitivity of the cortical and medullary lymphocytes in the thymus. *Int J Radiat Biol* 4, 163–173.
- Troxell, M. L., Loftus, D. J., Nelson, W. J., & Marrs, J. A. (2001). Mutant cadherin affects epithelial morphogenesis and invasion, but not transformation. *J Cell Sci* 114, 1237–1246.
- Vinken, M., Doktorova, T., Decroock, E., Leybaert, L., Vanhaecke, T., & Rogiers, V. (2009). Gap junctional intercellular communication as a target for liver toxicity and carcinogenicity. *Crit Rev Biochem Mol Biol* 44, 201–222.
- Wang, D. W., Fermor, B., Gimble, J. M., Awad, H. A., & Guilak, F. (2005). Influence of oxygen on the proliferation and metabolism of adipose derived adult stem cells. *J Cell Physiol* 204, 184–191.
- Wang, L., Lee, J. F., Lin, C. Y., & Lee, M. J. (2008). Rho GTPases mediated integrin alpha v beta 3 activation in sphingosine-1-phosphate stimulated chemotaxis of endothelial cells. *Histochem Cell Biol* 129, 579–588.
- Wang, A. Z., Ojakian, G. K., & Nelson, W. J. (1990). Steps in the morphogenesis of a polarized epithelium. I. Uncoupling the roles of cell–cell and cell–substratum contact in establishing plasma membrane polarity in multicellular epithelial (MDCK) cysts. *J Cell Sci* 95(Pt 1), 137–151.
- Wang, A. Z., Ojakian, G. K., & Nelson, W. J. (1990). Steps in the morphogenesis of a polarized epithelium. II. Disassembly and assembly of plasma membrane domains during reversal of epithelial cell polarity in multicellular epithelial (MDCK) cysts. *J Cell Sci* 95(Pt 1), 153–165.
- Wang, L., Sun, J., Horvat, M., Koutalistras, N., Johnston, B., & Ross Sheil, A. G. (1996). Evaluation of MTS, XTT, MIT and 3HTdR incorporation for assessing hepatocyte density, viability and proliferation. *Methods in Cell Science* 18, 249–255.
- Wang, A. Z., Wang, J. C., Ojakian, G. K., & Nelson, W. J. (1994). Determinants of apical membrane formation and distribution in multicellular epithelial MDCK cysts. *Am J Physiol* 267, C473–C481.
- Wang, F., Weaver, V. M., Petersen, O. W., Larabell, C. A., Dedhar, S., Briand, P., et al. (1998). Reciprocal interactions between beta1-integrin and epidermal growth factor receptor in three-dimensional basement membrane breast cultures: a different perspective in epithelial biology. *Proc Natl Acad Sci U S A* 95, 14821–14826.
- Wang, L. M., Wong, M., Lightwood, J. M., & Cheng, C. M. (2010). Black box warning contraindicated comedications: concordance among three major drug interaction screening programs. *Ann Pharmacother* 44, 28–34.
- Welford, S. M., & Giaccia, A. J. (2011). Hypoxia and senescence: the impact of oxygenation on tumor suppression. *Mol Cancer Res* 9, 538–544.
- Wells, P. S., Holbrook, A. M., Crowther, N. R., & Hirsh, J. (1994). Interactions of warfarin with drugs and food. *Ann Intern Med* 121, 676–683.
- Wojciak-Stothard, B., Tsang, L. Y., & Haworth, S. G. (2005). Rac and Rho play opposing roles in the regulation of hypoxia/reoxygenation-induced permeability changes in pulmonary artery endothelial cells. *Am J Physiol Lung Cell Mol Physiol* 288, L749–L760.
- Wozniak, M. A., Desai, R., Solski, P. A., Der, C. J., & Keely, P. J. (2003). ROCK-generated contractility regulates breast epithelial cell differentiation in response to the physical properties of a three-dimensional collagen matrix. *J Cell Biol* 163, 583–595.
- [www.mattek.com](http://www.mattek.com). The EpiDerm™ Skin Model. In.

## ARTICLE IN PRESS

A. Astashkina et al. / Pharmacology &amp; Therapeutics xxx (2012) xxx–xxx

25

- Xu, J. J., Diaz, D., & O'Brien, P. J. (2004). Applications of cytotoxicity assays and pre-lethal mechanistic assays for assessment of human hepatotoxicity potential. *Chem Biol Interact* 150, 115–128.
- Yamada, K. M., Pankov, R., & Cukierman, E. (2003). Dimensions and dynamics in integrin function. *Braz J Med Biol Res* 36, 959–966.
- Yamasaki, K., Kawasaki, S., Young, R. D., Fukuoka, H., Tanioka, H., Nakatsukasa, M., et al. (2009). Genomic aberrations and cellular heterogeneity in SV40-immortalized human corneal epithelial cells. *Invest Ophthalmol Vis Sci* 50, 604–613.
- Yang, A., Trajkovic, D., Illanes, O., & Ramiro-Ibanez, F. (2007). Clinicopathological and tissue indicators of para-aminophenol nephrotoxicity in Sprague–Dawley rats. *Toxicol Pathol* 35, 521–532.
- Zahran, W. A., Ghonaim, M. M., Koura, B. A., El-Banna, H., Ali, S. M., & El-Sheikh, N. (2006). A study of the role of IL-12 in pulmonary tuberculosis using the whole blood flowcytometry technique. *Egypt J Immunol* 13, 53–65.
- Zhang, H., Wang, W., Quan, C., & Fan, S. (2010). Engineering considerations for process development in mammalian cell cultivation. *Curr Pharm Biotechnol* 11, 103–112.
- Zhao, F., Pathi, P., Grayson, W., Xing, Q., Locke, B. R., & Ma, T. (2005). Effects of oxygen transport on 3-d human mesenchymal stem cell metabolic activity in perfusion and static cultures: experiments and mathematical model. *Biotechnol Prog* 21, 1269–1280.
- Zhao, P., Zhang, L., Grillo, J. A., Liu, Q., Bullock, J. M., Moon, Y. J., et al. (2011). Applications of physiologically based pharmacokinetic (PBPK) modeling and simulation during regulatory review. *Clin Pharmacol Ther* 89, 259–267.
- Zhou, S. F. (2008). Drugs behave as substrates, inhibitors and inducers of human cytochrome P450 3A4. *Curr Drug Metab* 9, 310–322.
- Zimmerhackl, L. B., Mesa, H., Kramer, F., Kolmel, C., Wiegele, G., & Brandis, M. (1997). Tubular toxicity of cyclosporine A and the influence of endothelin-1 in renal cell culture models (LLC-PK1 and MDCK). *Pediatr Nephrol* 11, 778–783.
- Zuk, A., & Matlin, K. S. (1996). Apical beta 1 integrin in polarized MDCK cells mediates tubulocyst formation in response to type I collagen overlay. *J Cell Sci* 109(Pt 7), 1875–1889.

## CHAPTER 3

### A 3-D ORGANOID KIDNEY CULTURE MODEL ENGINEERED FOR HIGH THROUGHPUT NEPHROTOXICITY ASSAYS<sup>1</sup>

#### Abstract

Cell-cell and cell-matrix interactions control cell phenotypes and functions *in vivo*. Maintaining these interactions *in vitro* is essential to both produce and retain cultured cell fidelity to normal phenotype and function in the context of drug efficacy and toxicity screening. Two-dimensional (2-D) cultures on culture plastics rarely recapitulate any of these desired conditions. Three-dimensional (3-D) culture systems provide a critical junction between traditional, yet often irrelevant, *in vitro* cell cultures and more accurate, yet costly, *in vivo* models. This study describes development of an organoid-derived 3-D culture of kidney proximal tubules (PTs) that maintains native cellular interactions in tissue context, regulating phenotypic stability of primary cells *in vitro* for up to 6 weeks. Furthermore, unlike immortalized cells on plastic, these 3-D organoid kidney cultures provide a more physiologically relevant response to nephrotoxic agent exposure, with production of toxicity biomarkers found *in vivo*. This biomimetic primary kidney model has broad applicability to high-throughput drug and biomarker nephrotoxicity screening, as well as more mechanistic drug toxicology, pharmacology, and metabolism studies.

---

<sup>1</sup> Reprinted with permission from *Biomaterials*: Anna Astashkina, Brenda Mann, Glenn Prestwich, David Grainger. A 3-D organoid kidney culture model engineered for high throughput nephrotoxicity assays, 2012

### Introduction

*In vivo* cell-cell interactions, and more broadly, the contextual communication characteristics of the tissue microenvironment (i.e., matrix-mediated, haptotactic, chemotactic, biomechanic, paracrine, autocrine signals), dictate cell phenotype and are required to produce and maintain tissue-like responses *in vitro* (1-8). Many physiological variables including cell-cell interactions, cell-matrix communication, matrix chemical composition, matrix mechanics, matrix porosity, chemotactic gradients of soluble cell signals, cell oxygenation, and 3-D matrix architectures are critical for producing *in vivo*-like cell behavior (1, 4-6, 9). Cell proliferation, polarization, migration, signaling, and gene expression *in vitro* depend on both presence and proper presentation of these signals. However, no single variable alone achieves tissue-like organization to elicit tissue-like functions; many (if not all) of these chemical, mechanical and structural parameters must be satisfied in any *in vitro* culture to recapitulate *in vivo* cell responses. Available *in vitro* bioreactors using highly sophisticated control systems and dynamic inputs to control cell growth in 3-D scaffold systems (10) is not informed at the appropriate cell level with requisite design criteria to recapitulate *in vivo* complexity in several tissue types, particularly at levels of organ heterogeneity. Hence, a compelling need remains for improved cellular models that capture the complexity of tissue organization *in vitro* in a reproducible manner to reproduce key traits (e.g., responses to drugs, regenerative tissue function) and study processes only accessible currently in mammalian animal models.

Development of a physiologically accurate and functionally high-fidelity kidney tissue surrogate is of particular interest for kidney transplant clinical demands (11-14). Another impact



lies in pharmaceutical drug development needs, as many drugs and new drug candidates inadvertently cause kidney toxicity (15). Currently, commercially marketed drugs account for 25% of acute kidney injury in critical care patients (16). Next to liver toxicity, kidney toxicity is the second leading indicator for drug candidate attrition (16). Furthermore, since current clinical methods such as blood urea nitrogen (BUN) and creatinine measurements suffer from an intrinsic inability to recognize early signs of kidney damage (17, 18), a great need exists for cell-based systems capable of reliable and sensitive assessment of kidney toxicity. Such systems would benefit from numerous advances in high-throughput (HTS) assessment as well as recent developments in biomarker validation using toxicogenomics, proteomics, and metabolomics (15). The few extensive biomarker studies conducted -- the Innovative Medicines for Europe (InnoMed) PredTox project, ILSI Health and Environmental Sciences Institute initiative, Predictive Safety Testing Consortium -- were limited by their reliance on costly *in vivo* models due to limitations inherent in *in vitro* cell culture screens. Additionally, these efforts required consortia of pharmaceutical industry, academia, and regulatory agencies due to the excessive expenses and workload associated with the studies (15). Hence, development of improved *in vitro* culture approaches better reflective of *in vivo* cell behaviors and reactions to drugs would significantly impact both the cost and accessibility of future HTS work.

Reliable kidney toxicity assessment requires retention of cellular structural and biochemical pathways; nephrotoxicity is a complex process involving drug metabolism using cytochrome (CYP) P450, biotransformation using intra- and extracellular enzymes, dynamic changes in cellular accumulation as a function of uptake and drug removal via specific transporters and inflammatory



process regulation (19-21). Currently, the gold standard for kidney-like culture models involves use of primary or immortalized cell lines grown on conventional 2-D tissue culture plastic surfaces. Although convenient and relatively simple to employ, the 'petri dish' approach leads to quick de-differentiation of primary cells *in vitro*, most probably through loss of tissue-like interactions on 2-D plastic (22, 23). Furthermore, transformed kidney cell lines have limited cellular machinery, including transporters, ligands associated with endocytosis, enzymes involved in biotransformation of molecules, and CYP P450 metabolism, making them intrinsically incapable of reacting to complex external pathophysiological stimuli with *in vivo*-relevant biomarkers (5, 7, 23-27). Due to the limiting functional cell equivalence on 2-D surfaces, cell assay data obtained in response to toxic drug and environmental agents are typically limited to simple observations of changes in cell viability and proliferation, both of which have little predictive value *in vivo*. Furthermore and perhaps most importantly, no tangible improvements of 2-D cell culture are feasible as studies will always be constrained by the fundamental limitations of rudimentary cell monolayer and (frequently) monoculture interactions on tissue culture plastic. More complex *in vitro* cell cultures that preserve tissue-like 3-D cell-cell interactions, tissue architecture and communicative biochemistry are needed to better assess complex cellular mechanisms in a clinically significant fashion.

The current nephrotoxicity assay design focused on toxicity processes associated with the PT, an essential central component of the functional nephron. The PT is a hollow tube comprising a basement membrane lined by epithelial cells, and is the primary site of clinical kidney toxicity instigated by external stimuli, such as heavy metals, dyes and drugs (28). Susceptibility of PTs to

environmental assaults is most likely due to the significant epithelial surface area provided in this part of the nephron, as well as the large number of active transporters possibly hijacked by small molecules entering the nephron. Encapsulation of harvested viable intact PTs, and not simply the epithelial cells that line their lumens, directly into a well-characterized biologically derived matrix avoids unpredictable, confounding cell-polymer matrix interactions, while preserving native 3-D cell matrix environments and cell-cell physiological interfaces. Together this cellular context ensures cell maintenance, signaling and more accurate, extended *in vivo*-like epithelial cell responses.

Hyaluronic acid (HA)-based hydrogels used to encapsulate PTs are already well-established in preserving tissue-like architectures and cell interactions in several tissue regeneration and 3-D bioreactor culture models (29-32). Furthermore, HA is a natural polymer present in almost all bodily tissues, including the kidney. Primary proximal tubule epithelial cell viability, differentiation potential and functionality were all used to assess and validate this newly developed 3-D organoid culture for up to 2 months. This culture response to known nephrotoxic agents compared cytochrome P450 enzyme induction, metabolite production, and kidney injury-1 (Kim-1) protein up-regulation – accepted markers for typical drug toxicity screens.

## Methods

### Construct preparation

Male C57BL/6 mice (6-8 weeks) were purchased from Jackson Laboratory (Bar Harbor, USA). All animals were euthanized using carbon dioxide according to approved University of Utah

IACUC protocols and PTs were isolated immediately following literature-established procedures using standard aseptic conditions in a BSL2-certified laminar flow hood (33). Briefly, murine kidneys were removed surgically and cleaned of the kidney capsule, blood vessels and ureter. Between all steps tissue was stored in ice-cold KREBS solution (145 mM NaCl, 10 mM HEPES, 5 mM KCl, 1 mM  $\text{NaH}_2\text{PO}_4$ , 2.5 mM  $\text{CaCl}_2$ , 1.8 mM  $\text{MgSO}_4$ , 5 mM glucose, pH 7.3) (34). The tissue was then mechanically disrupted using sharp razor blades and enzymatically digested for 30 min in enzyme solution (10ml KREBS, 2mg/ml hyaluronidase (Worthington Biochemical Corporation, USA), 3mg/ml collagenase IV (Worthington Biochemical Corporation, USA), 0.1mg/ml DNase I (Sigma-Aldrich Chemical, USA)) at 37°C (34). PTs were enriched by sequential 250 $\mu\text{M}$  and 80  $\mu\text{M}$  sieving of the resulting digested nephron sections. PTs were then pelleted from the resulting suspension in KREBS by centrifugation for 15 min at 12,000 rpm. Proximal tubule yield was estimated using a hemocytometer.

The 3-D organoid proximal tubule cultures were fabricated by combining purified PTs with 1.5% commercial thiol-modified carboxymethylated hyaluronic acid (HA) (carboxymethyl, thiol modified: CMHA-S) and 7.5% commercial poly(ethylene glycol) diacrylate (PEGDA) bifunctional polymer electrophile (30, 32, 35). Both gel-forming GMP biomedical grade polymers were generously provided by Sentrx Animal Care (Salt Lake City, USA). CMHA-S and PEGDA were resuspended in  $\text{PBS}^{++}$ , sterile filtered using 0.22  $\mu\text{m}$  cell culture syringe filters (ISC Bioexpress, USA), and mixed in 4:1 ratio with PTs. Constructs were made by casting 50  $\mu\text{L}$  of PT/gel mixture into Teflon-AF® -coated 96 well plates (see below). Then the 3-D organoid gel precursor matrix was crosslinked for 35 min in a cell incubator at 37°C (5%  $\text{CO}_2$  and 95% air). Proximal tubule

media consisting of 1% fetal calf serum (Invitrogen, USA), 5% sodium pyruvate (Invitrogen, USA), 10% non-essential amino acids (Invitrogen, USA), 10% insulin/transferrin/selenium (Invitrogen, USA), 1% antibiotic-antimycotic (Invitrogen, USA), 0.9 µg of hydrocortisone (Invitrogen, USA), and Dulbecco's modified Eagle medium (DMEM)-Ham's F-12 with 4-(2-hydroxyethyl)-1-piperazineethanesulfonic acid (HEPES) and L-glutamine (Invitrogen, USA) (33) was then added to final HA hydrogel constructs containing viable tubules (100 µL/well) and exchanged every 2 days for maximum cell viability.

The Teflon AF®-coated 96-well culture plates (150 µL/well) were prepared according to previously published protocols (36) using non-tissue culture polystyrene plates (ISC Bioexpress, USA) and Teflon-AF® (Dupont, USA) dissolved in FC-40 (3M, USA) organic solvent. Solvent was removed using vacuum drying in elevated temperature (56°C), and coated plates were sterilized using UV for 30 min before use (36).

#### Analysis of cell viability

Proximal tubule epithelial cell viability in the 3-D organoid constructs was assessed using CyQuant NF® (Invitrogen, USA) and MTS (Fisher, USA) viability assays. All solutions for both assays were prepared according to each manufacturer's instructions. All constructs were treated for 1 hour with 0.01 mM peroxide in proximal tubule media in the incubator to oxidize all remaining non-crosslinked thiols in the CMHA-S-based HA gel. MTS and CyQuant NF® reagents were then applied directly on top of the 3-D organoid cultures and incubated for 1 hour at 37°C. When using CyQuant NF®, the supernatant over the gel was fluorometrically analyzed, and with MTS, the

optical density of the entire construct was analyzed, both using a Synergy 2 microplate reader (CyQuant NF® fluorescence at 485 nm excitation and 530 nm emission; MTS absorbance at 490 nm). HA hydrogel without cells was used as background control.

#### Analysis of cell differentiation status

Proximal epithelial cell differentiation status was assessed using reverse-transcriptase polymerase chain reaction (RT-PCR) and immunofluorescence. RT-PCR for common nephron markers was performed at 0-8 weeks of 3-D organoid culture: AQP1 (proximal tubule gene marker), AQP2 (distal tubule gene marker), NCC (collective tubule gene marker), GAPDH (housekeeping gene), megalin (functional ligand). RNA was extracted by solubilizing the entire construct in TRIzol® (Invitrogen, USA), flash freezing it in liquid nitrogen, homogenizing the construct using mortar and pestel, and extracting RNA using the standard TRIzol® protocol. RNA was reverse-transcribed into cDNA using a Superscript III kit (Invitrogen, USA) and message for the genes of interest was isolated using PCR with gene-specific primers (see Supplementary Tables). RT-PCR was performed on an iCycler (Bio-Rad, USA) using GoTaq Green mastermix (Promega, USA) following the manufacturer's suggestions. All PCR samples were run with 40 denaturation cycles under the following conditions: 30 sec at 95°C; 30 sec annealing at 60°C (Megalin, AQP1), 60.7°C (GAPDH), 65°C (AQP2), 55°C (NCC), 1 min elongation at 72°C. PCR products were visualized on a 1.5% agarose gel (Fisher, USA) containing ethidium bromide using a Bio-Rad gel imager.

Immunofluorescence was performed on the entire 3-D organoid construct. Scaffolds were fixed using 4% paraformaldehyde overnight at 4°C, blocked using anti-goat serum for 2 hours at room temperature (RT), stained with primary antibody or lectin for 3 days in the 4°C, and incubated with secondary Alexa-488 goat-antimouse IgG antibody and PI for 1 hour at RT. Primary AQP1 antibody (Chemicon, USA) and PHA-E-FITC (Vector Labs, USA) were used at 1:2000, and OAT-1 antibody (Abbiotec, USA), connexin 43 (Millipore, USA), and  $\alpha_3$  antibody (Santa Cruz Biotechnology) at 1:1000 dilution. Constructs were imaged using an AR1 Nikon inverted microscope (University of Utah Imaging Core facilities).

#### Analysis of cell functionality

Cell functions in the 3-D organoid hydrogel cultures were analyzed by measuring cell-specific enzymatic functions and their ability to endocytose drugs. Cathepsin B, alkaline phosphatase, and  $\gamma$ -glutamyl-transferase were assessed at 0-8 weeks of culture. Cathepsin B in the 3-D organoid constructs was measured using a fluorescence-based kit (BioVision, USA). All solutions were prepared according to manufacturer's protocol. Cells in PTs were lysed by adding 50  $\mu$ L of chilled lysis solution/well and vigorous mixing with the gel for 10 min in the hood at RT. The reaction was initiated by adding 50  $\mu$ L of the reaction solution provided and 2  $\mu$ L of substrate provided in the kit. Identical hydrogel with no cells was used as a control. All samples were read fluorescently using 400 nm excitation and 505 nm emission filters (slit width 2nm) on a spectrophotometer (Synergy 2).

Alkaline phosphatase activity was measured in 3-D cell constructs using SensoLyte® kit (AnaSpec, USA). All solutions were prepared according to the manufacturer's instructions.

Reaction mixture from the kit (50  $\mu$ L) was added directly to the construct and incubated for 30 min at 37°C. Chromogenic product was estimated using a spectrophotometer at  $A_{405}$  and referenced against the provided optical standard. Identical hydrogel without cells was used as background.

$\gamma$ -glutamyl-transferase activity was assessed according to standard chromogenic assay protocols (37). Each construct was preincubated with 50  $\mu$ L of assay solution (150 mM NaCl and 10 mM Tris-HCl, pH 8.5) for 5 min at RT. The assay reaction was begun by adding 50  $\mu$ L 5mM  $\gamma$ -glutamyl-p-nitroaniline (Sigma Aldrich, USA) with 100mM glycylglycine (Sigma Aldrich, USA) chromogenic substrate. The reaction proceeded for 20 min in the incubator and then stopped using 10% acetic acid. Amounts of chromogenic product produced were determined using a spectrophotometer at  $A_{405}$  and referenced against that for 1mM p-nitroanilide (Sigma Aldrich, USA).

PT epithelial cell ability to endocytose was determined by estimating cell viability upon exposure to drug neomycin (Sigma Aldrich, USA) in the presence of endocytosis inhibitor colchicine (Sigma Aldrich, USA). Neomycin was directly resuspended in the proximal tubule media. Colchicine was diluted from 20 mM stock solution in 100% dimethyl sulfoxide (DMSO) using proximal tubule media. Both drugs were sterile filtered prior to exposure to constructs. Cell viability was assessed using CyQuant NF® as specified above.

#### Analysis of cell senescence and gluconeogenesis

Proximal tubule epithelial cell senescence was quantified using  $\beta$ -galactosidase activity according to a published protocol (38). Briefly, cells within the hydrogel were lysed using 250  $\mu$ L of lysis buffer (5 mM 3-[(3-cholamidopropyl)dimethylammonio]-1-propanesulfonate, 40 mM citric acid,

40 mM sodium phosphate, 0.5 mM benzamidine, and 0.25 mM phenylmethanesulfonyl fluoride, pH 6.0), decellularized by vortexing and collecting the supernatant. The reaction was initiated with 150  $\mu$ L of reaction buffer with 1.7 mM of 4-methylumbelliferyl-  $\beta$ -galactopyranoside) to 100  $\mu$ L of cell lysate and 50  $\mu$ L of lysis buffer, and then stopped by adding 500  $\mu$ L of sodium carbonate after 2 hours. Fluorescence (ex: 360 nm, em: 465 nm) was read against HA blank control gel without cells as background.

Glucose concentration was determined using a HK kit (Sigma Aldrich, USA), which quantifies the amount of glucose present as a function of its phosphorylation by adenosine triphosphate (ATP) to glucose-6-phosphate (G6P) and concurrent reduction of oxidized nicotinamide adenine dinucleotide (NAD) to NADH. All reagents were reconstituted and calculations were performed according to manufacturer's instructions. An internal glucose standard of known concentration was used as a positive calibration control.

#### Analysis of nephrotoxicity

Proximal tubule epithelial cell expression of CYP2E1 and Kim-1 was determined using immunofluorescence. Hydrogel scaffolds containing organoids were exposed to 1% acetone (Fisher, USA) or 1.7 mM cisplatin for 3 days. Cisplatin (Sigma Aldrich, USA) was stored as 200 mM stock solution in DMSO, diluted to its final concentration, and sterile filtered using 0.22 $\mu$ m filter prior to application to cell constructs. After culture exposure to drug, 3-D organoid cultures were fixed using 4% paraformaldehyde overnight at 4°C, blocked using signal enhancer (Invitrogen, USA) for 1 hour at RT, stained with primary antibody for 3 days at 4°C, and incubated with secondary 1:1000



Alexa-488 goat-antimouse IgG antibody (Invitrogen, USA) for 2 hours at RT. CYP2E1 antibody (Millipore, USA) was used at 1:1000 and R9 Kim-1 antibody used at 1:500 dilution. Cell constructs were imaged using an Olympus FV1000 spectral confocal microscope (University of Utah Imaging Core facilities).

#### Analysis of cisplatin metabolites

Metabolite production was assessed using HPLC after both 1 hour and 6 hours of 3-D culture incubation with 1.7 mM cisplatin. Cisplatin was resuspended in DMEM-Ham's F-12 protein-free media from a 200 mM DMSO stock solution. Media with platinum species were analyzed directly. Hydrogel constructs were weighed, suspended in 4 times w/v 0.25 M sucrose solution, homogenized, and centrifuged at 9000g following by 19000g for 15 min each time. Samples (10 $\mu$ L) of supernatants from constructs and media were then loaded onto an Atlantis dC18 3  $\mu$ m column (2.1x30mm). The column was pre-equilibrated in 50 mM potassium phosphate buffer, pH 6.0 (mobile phase A). Samples were eluted at 0.2 ml/min rate by a linear gradient starting from 100% mobile phase A and reaching 100% solvent B (0.45% acetonitrile in mobile phase A) after 10 min, followed by 5 min wash in mobile phase A at 1ml/min for 5 min. Platinum species were detected at 280nm using a Finnigan Surveyor HPLC system (Waters, USA). Protein-cisplatin controls were prepared by mixing 2 mM cisplatin with 2 mM NAC (Sigma Aldrich, USA), Cys-Gly (Sigma Aldrich, USA), GSH (Sigma Aldrich, USA), cysteine (Sigma Aldrich, USA) and incubation for 1 hour at 37°C.

### Analysis of proximal tubule cell cytokine expression

MCP-1, TNF $\alpha$ , RANTES, MIP-1 $\alpha$ , IL-6 and IL-1 $\beta$  cytokine release was assessed in the proximal tubule media samples after 3 days of drug incubation at the corresponding EC<sub>50</sub> concentrations for each drug (doxorubicin (DOX) at 1.4  $\mu$ M, colchicine (Col) at 24.4  $\mu$ M, PAP at 24.9  $\mu$ M, cisplatin (Cisp) at 0.42 mM). Cytokines were captured using a commercial cytometric bead array kit (BD™ Biosciences, USA) according to manufacturer's instructions and their concentrations were measured by averaging fluorescence of at least 300 beads per analyte. All protein concentrations were calculated by comparing measured sample values to the analyte fluorescence standard curve run (see Supplementary Figures) with every assay using commercially provided cytokine controls. Only values that fell into standard curves' dynamic range were considered for sample evaluation. Data acquisition was performed using 5-color FACScan Analyzer (BD™ Biosciences, USA) with a benchtop analyzer using two lasers for fluorochrome excitation (15 mW argon (488 nm) and 25 mW red diode (637 nm)). Free Weasel (Walter & Eliza Hall Institute) software was used to import and quantify collected for CBA data.

### Statistical analysis

GraphPad Prism 5 (GraphPad Software, Inc.) and Excel 2010 (Microsoft, Inc.) statistical software packages were used for data analysis. Independent samples used cells isolated from separate mice. Experiments that produced data and their corresponding normalization values were expressed as mean $\pm$ S.E (standard error). Experiments that used normalization values from separate measurements appear as mean $\pm$ 95% confidence intervals. CBA data were analyzed

using unpaired student t-test and adjusted for multiple comparisons using Hochberg's procedure. A post-hoc student's t-test was used to determine statistically significant differences between samples ( $p < 0.05$ ).

## Results

### Proximal tubule isolation purity and efficiency

The protocol to isolate proximal tubule-enriched subpopulations from freshly harvested intact C57BL/6 murine kidneys was reliable and efficient. PTs were extracted from whole kidneys via enzymatic digestion and mechanical, size-based sieving based on published protocols (33, 34) (see Supplementary Figures). Average PT isolation efficiency and viability was assessed using hemocytometer cell counts as well as live-dead Hoechst and propidium iodine (PI) staining, respectively (see Supplementary Figures). PT isolation purity was verified using RT-PCR for known proximal tubule biomarker aquaporin 1 (AQP1), distal tubule marker aquaporin 2 (AQP2), and collective ducts (Na-Cl co-transporter (NCC)) (see Supplementary Figures) (33). The procedure yielded approximately  $95,200 \pm 34,460$  tubule fragments per kidney with  $85 \pm 8\%$  viability ( $n=3$ ) at high isolate purity as verified by RT-PCR (see Supplementary Figures).

### Engineering congruent 3-D organoid proximal tubule constructs

Organoid 3-D cultures were created by encapsulating intact murine (C56BL/6 mice) proximal tubule fragments within commercial biomedical-grade HA hydrogels. Importantly, PT cell viability in these 3-D organoid hydrogel constructs requires 1) gentle gel encapsulation conditions, 2) consistent diffusion of oxygen and nutrients throughout the gel-tubule construct, and 3)

miniaturized construct size and optimized geometry to facilitate nutrient transport. The thiol-modified HA covalently crosslinks to form a hydrogel spontaneously within the cell incubator when combined with PEG-diacrylate electrophile for ~35 min. Nine different HA formulations were evaluated for their ability to encapsulate PTs (see Supplementary Tables). HA formulation consisting of 1.5% CMHA-S-7.5% PEGDA was chosen due to relatively fast gelation and network stability during 2-month incubation in the cell culture hood. Each construct was formed by 50  $\mu$ L of gel with PTs (the smallest technically feasible volume) to improve diffusion of oxygen and media. HA gels containing PTs were fabricated in polystyrene 96-well plates coated with TeflonAF® to reduce the wetting meniscus between the gel and plate wall, yielding symmetrical, uniform cylindrical gel constructs with roughly equal oxygenation gradients throughout the 3-D culture in the plate (Fig. 3.1A). Cell survival was analyzed in the meniscus zone at 1-week time points to verify that symmetrical gel constructs produced significantly less cell death than gel constructs with high menisci (data not shown). Furthermore, selected HA formulations produced a highly porous biopolymer gel matrix that accommodated encapsulated organoid oxygen delivery requirements, metabolite transport, and cell survival in culture with requisite integrity for up to 2 months (Fig. 3.1B).

#### Proximal tubule culture viability, differentiation, and functionality

In addition to preservation of appropriate 3D tubule organization, HA constructs containing PTs were characterized for viability, differentiation, and functionality. Data for PT epithelial cell viability, differentiation state and functionality in 3-D HA hydrogel cultures showed that viable

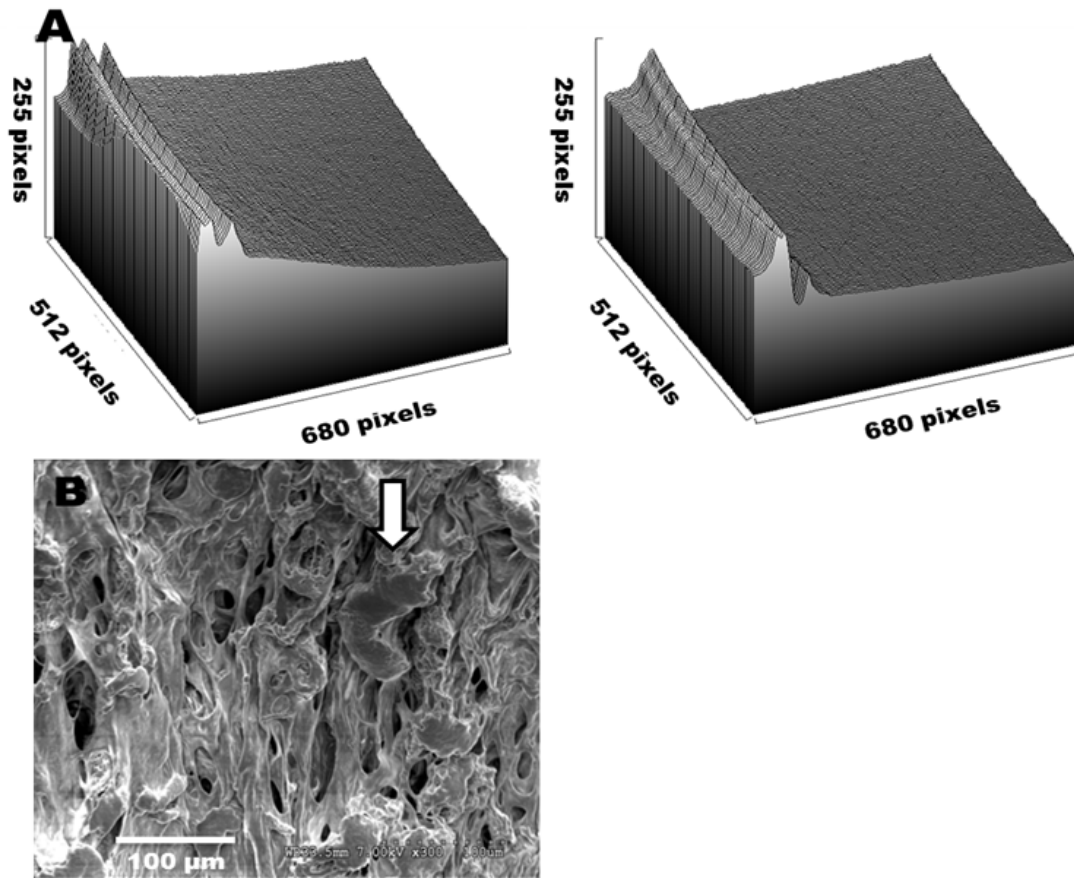


**Figure 3.1 I** Optimization of 96-well plates and gel formulation for 3-D organoid cultures. A) Profile of meniscus of polymerized HA hydrogels in TCPS microwell plates (left), and in TeflonAF®-coated non-TCPS microwell plates (right); B) SEM of the desiccated HA hydrogel containing PTs (arrow points at a PT).

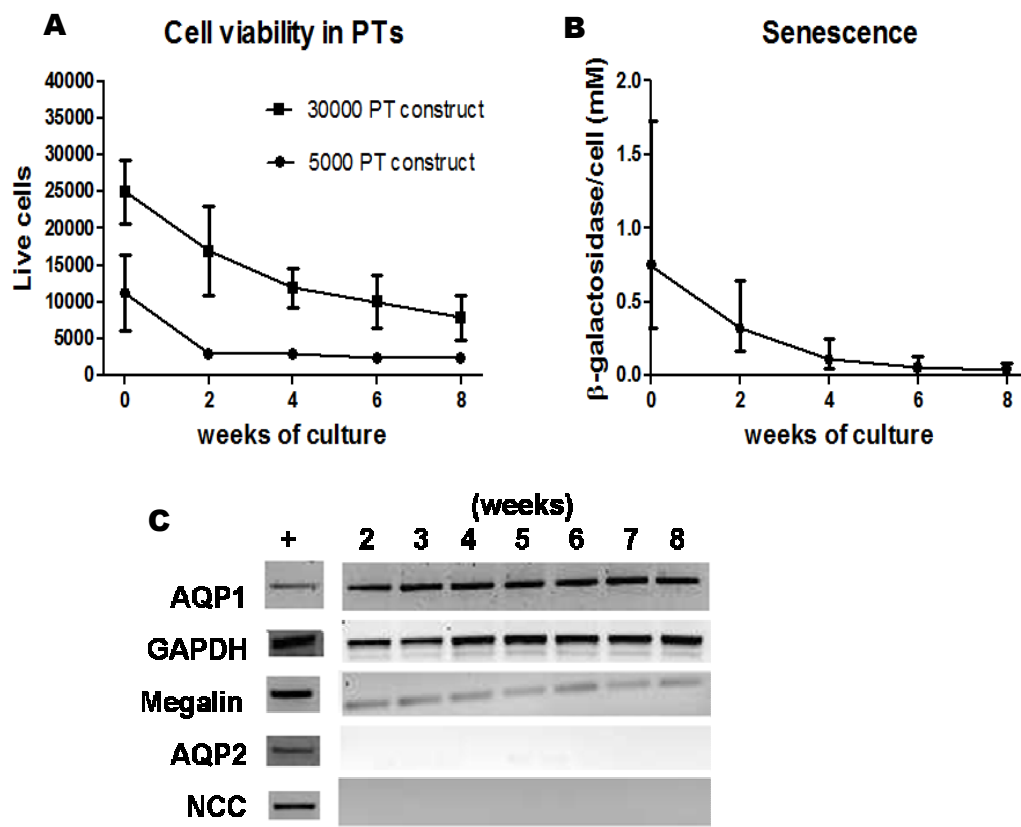


**Figure 3.2 |** Cellular characterization in 3-D organoid cultures during 2 months of incubation. A) Cell viability in proximal tubule fragments encapsulated by HA (n=3 (2 technical replicas), mean±SE), B) Senescence in the 3-D organoid culture (n=3 (2 technical replicas), mean±95%CI), C) RT-PCR for nephron markers: AQP1 - proximal tubule aquaporin, AQP2 - distal tubule aquaporin, GAPDH - housekeeping gene, megalin - functional ligand, NCC – Na<sup>+</sup>-Cl<sup>-</sup> co-transporter of the collective duct.



epithelial cells populated the 3-D organoid cultures for up to 2 months (Fig. 3.2A). Cell viability was evaluated at 5000 PTs/gel construct/well using CyQuant NF® assays, and at  $3 \times 10^4$  PTs per gel construct per well using MTS assays. Both assays are common approaches to evaluate cell viability *in vitro*. Different seeding densities were used to understand if the PT construct viability was limited by cell-to-gel ratio. Both assays were consistent in demonstrating that cell viability dropped two-fold in the PT constructs within the first 2 weeks, after which time it stabilized, reaching a plateau for the remainder of the culture period (Fig. 3.2A). Cell senescence was also evaluated (Fig. 3.2B) to test the hypothesis that the initial cell death in the 3-D organoid cultures was potentially the result of acute insufficient oxygen diffusion post-harvest. No increase in cell senescence in culture (Fig. 3.2B) was observed for 2 months.

Although viability in 3D organoid cultures is a critical parameter, equally valuable for functional equivalence is the cell differentiation status. During the 2 months of culture, cell differentiation was gauged by RT-PCR and immunofluorescence assays. RT-PCR was performed bi-weekly using nephron-specific markers, AQP1, AQP2, NCC, and megalin, with the housekeeping gene, GAPDH. Proximal tubule-specific aquaporin (AQP1) and megalin but no other general nephron transcripts were found to be expressed in PTs encapsulated in the HA hydrogel for 2 months (Fig. 3.2C). Furthermore, these mRNA data were confirmed with immunofluorescence specific for AQP1 and *Phaseolus vulgaris* erythroagglutinin labeled with FITC (PHA-E) at 2 months (Fig. 3.3A,B). Differentiation markers for structurally important proximal tubule characteristics were further supported by continuous expression of cytochrome P450 enzymes in the long-term 3D organoid culture (Fig. 3.2C,D). PTs -- analogous to liver -- are

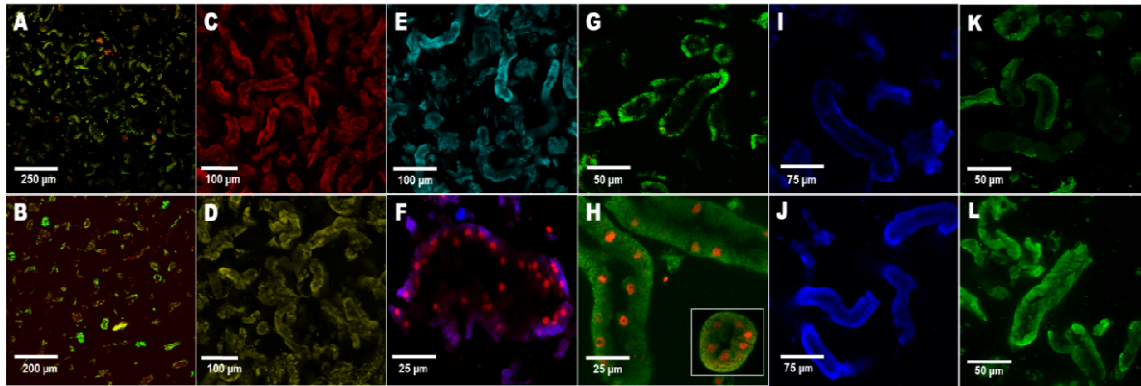
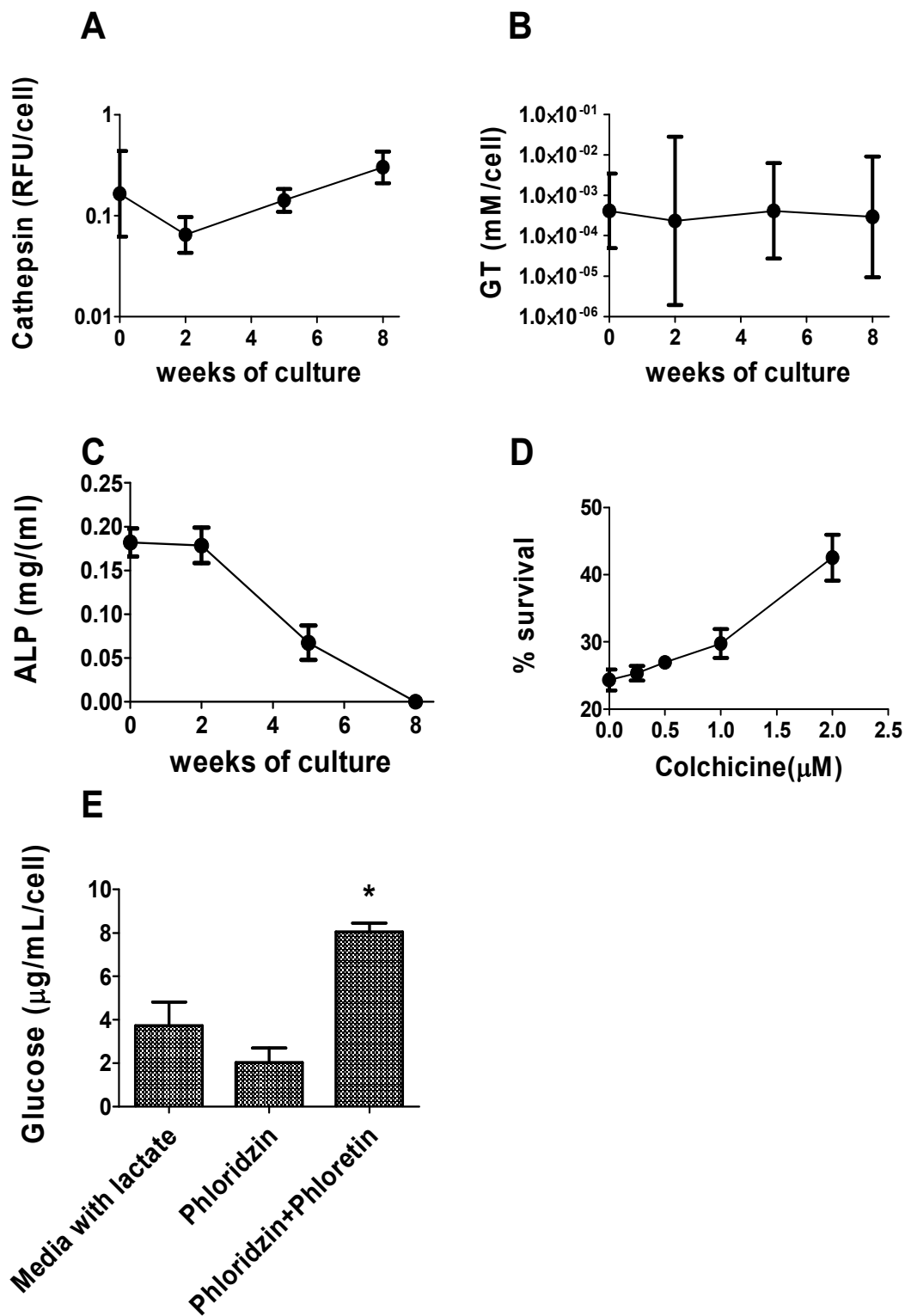


**Figure 3.3** | Staining for cell differentiation markers: A) AQP1 staining after 2 months' culture, B) PHA-E staining after 2 months' culture, C) CYP2B1 staining after 2 months' culture, D) CYP2E1 staining after 2 months' culture, E) gap junctions staining after 2 months' culture, F) OAT1 staining after 2 months' culture, G)  $\alpha_3$  integrin staining after 2 months' culture, H) PHA-E staining 2 days, I) CYP2E1 control well (no drugs) staining at 3 days, J) CYP2E1 staining after 1% acetone treatment for 3 days, K) Kim-1 staining of control well, L) Kim-1 staining after cisplatin treatment for 3 days.

metabolically active, with CYP2E1 one of the most strongly expressed biotransformation enzymes (39). Although CYP2E1 protein is not present in the human kidney, it has been implicated in rodent proximal tubule cell damage associated with bioactive molecules and environmental agents (40). Overall, both immunofluorescence for differentiation markers and RT-PCR suggest that all cells that remained in the HA hydrogel for 2 months retained their differentiation status for the entire culture period.

Proximal tubule epithelial cells phenotypic functionality inside PTs was evaluated as a series of enzymatic activity assays that tested their capability to process proteins from the media (cathepsin B (41)), maintain ligands for biotransformation ( $\gamma$ -glutamyl-transferase (42)) and endocytosis (megalin (27, 43, 44)), and continue signaling molecule dephosphorylation (alkaline phosphatase (AP) (45)). It was established that all measured enzymes, proteases, and ligands were present in cells over 6-8 weeks of culture (Fig. 3.2C, and 3.4A-C). Furthermore, it was confirmed that megalin ligand on the cell surface could assist in drug uptake similar to *in vivo* behavior in the presence of increasing gradients of the endocytosis inhibitor, colchicine (Fig. 3.4D). Another important difference between 2-D and *in vivo* proximal epithelial cell physiology is ability to oxidize lactic acid as a part of gluconeogenesis (46-49). Gluconeogenesis is a metabolic pathway that converts non-carbohydrate substrates, such as pyruvate, lactate and other non-glucidic precursors, into glucose. Specifically, immortalized proximal tubule-like cell lines lack gluconeogenic potential (47) and primary proximal tubule epithelial cells grown in static 2-D monolayer approach rapidly lose their gluconeogenic potential (49-51). Since gluconeogenesis is an important and distinctive feature of fully differentiated proximal tubule cells (52, 53), cellular

**Figure 3.4 I** Enzyme expression in the 3-D organoid culture: A) cathepsin B ((n=3 (2 technical replicas), mean $\pm$ 95% CI), B)  $\gamma$ -glutamyl-transferase (n=3 (2 technical replicas), mean $\pm$ 95% CI), C) alkaline phosphatase (n=3 (2 technical replicas), mean $\pm$ SE) D) neomycin endocytosis in the presence of endocytosis inhibitor colchicine (n=3 (2 technical replicas), mean $\pm$ SE), E) gluconeogenesis in the 3-D organoid cultures at 3 days (n=3 (2 technical replicas), mean $\pm$ SE).





ability to oxidize one of the possible non-carbohydrate substrates, lactate, to glucose was assessed in the presence of phloridzin, an inhibitor of glucose transport across the apical cell side, and phloridzin with phloretin, an inhibitor of glucose transport across the basolateral membrane (49) (Fig. 3.4E). Addition of both inhibitors resulted in significant net glucose increases in 3-D cultures grown in the presence of lactate (Fig. 3.4E).

#### Preservation of 3-D organoid cell organization

A major objective of this study was to assess cell-cell and cell-matrix interactions and 3-D organization in preserving cultured cell phenotypic behaviors most consistent with *in vivo* traits. Specifically in the kidney, maintenance of both accessible luminal and basal epithelial cell membranes in PTs is critical in obtaining accurate *in vivo*-equivalent cell data, since both PT cell surfaces require direct accessibility to signaling stimuli through diffusion, transporters, and ligands. This is naturally limited in cell monocultures on plastic. Native PT microenvironment biomarkers assessed were gap junctions (connexin 43), integrins ( $\alpha_3$ ), and cell polarization (transporter localization) using immunofluorescence assays. Antibodies against connexin 43,  $\alpha_3$ , and organic anion transporter 1 (OAT 1) revealed extensive labeling of epithelial PT cells after 2 months of culture within the HA gels (Fig. 3.3C-E). OAT 1 transporter was clearly associated with the basal side of PTs, suggesting that prolonged culture in 3-D HA gel did not affect cell polarization. Moreover, immunofluorescence using proximal tubule-specific lectin, PHA-E, indicated that PTs in the gel constructs maintained their tubular shape, with open lumens accessible to external stimuli (Fig. 3.3F) such as nutrients and drugs.

#### Culture responses to nephrotoxins; PT biomarker induction

The 3-D culture's capacity to respond to nephrotoxic agent exposures with toxicity indicators only measurable *in vivo* was determined by assessing its ability to up-regulate CYP P450 enzymes and the Kim-1 protein in response to acetone and cisplatin, respectively. Antibody-based staining for CYP2E1 (Fig. 3.3 I,J) and Kim-1 (Fig. 3.3 K,L) in response to acetone and cisplatin showed presence of both biomarkers in the tested conditions.

#### Culture response to nephrotoxins: drug metabolite production

Cisplatin toxicity *in vivo* is at least partially attributed to formation of metabolites in the PT epithelial cells (54-58). To assess the 3-D culture's ability to process drugs similarly to that reported *in vivo*, metabolite production was assessed in the media and cytosol of PTs in protein-free media after 1h (see Supplemental Figures) and 6h (see Supplemental Figures) of incubation with cisplatin. In 3-D organoid cultures collected, protein-free PT media contained unchanged cisplatin drug (peak B), aquated cisplatin cation ( $[\text{Pt}(\text{NH}_3)_2(\text{Cl})(\text{H}_2\text{O})]^{1+}$  and/or  $[\text{Pt}(\text{NH}_3)_2(\text{H}_2\text{O})_2]^{2+}$ , peak E), and cisplatin- *N*-acetylcysteine (NAC, peaks F,G). Cytosol of the cells had the above peaks as well as peaks A and C. Peak A eluted at the same time as cisplatin-glutathione (GSH) and cisplatin-cysteine (Cys), and peak C had similar retention times to cisplatin-NAC and cisplatin-Cys-Gly.

#### Culture response to nephrotoxins: inflammatory protein production

Pro-inflammatory soluble proteins TNF $\alpha$ , MCP-1, IL-6, IL-1 $\beta$ , MIP-1 $\alpha$ , and RANTES were measured after 3 days of exposure to nephrotoxic drugs to evaluate 3-D culture's ability to elicit

immune response. Nephrotoxic compounds, cisplatin and doxorubicin, 4-aminophenol (PAP), and colchicine exhibited significant up-regulation of IL-6 and MCP-1 with all drug exposures, RANTES and MIP-1 $\alpha$  for all drugs except PAP, and IL-1 $\beta$  for cisplatin and doxorubicin only (Figure 3.5).

### Discussion

Nephrotoxicity is a complex pathology that combines tissue damage through interference with biochemical, metabolic, and nuclear processes. Furthermore, this form of toxicity has poor structure-toxicity predictions, making nephrotoxicity almost an idiosyncratic occurrence in clinical drug use. Hence, its prediction by oversimplified systems, such as immortalized cell lines that lack important structural elements or are limited in their ability to respond with physiologically-relevant indicators, is highly compromised and unreliable. For example, most transformed cells are missing OAT (1-3), organic cation (OCT 1-2), peptide (PEPT 1-2), and P-glycoprotein transporters critical for drug accumulation in cells, have poor levels of AP and  $\gamma$ -glutamyl-transferase that play roles in cell signaling and drug biotransformation. Additionally, transformed cells express different native tissue adhesion molecules such as E-cadherin instead of N-cadherin critical in chemical and mechanical sensing of intracellular and cell-ECM bi-directional signal transduction, and lack or exhibit limited morphological features such as microvilli, tight junctions, and ligands important in the development of cellular pathologies *in vivo*. This lack of ability to sense and respond to cellular microenvironmental cues unsurprisingly results in significant differences in cell damage biomarker induction. Specifically, no immortalized cell lines have been reported to induce Kim-1 protein, the most promising early kidney injury indicator *in vivo*, metabolize drugs, induce genes associated

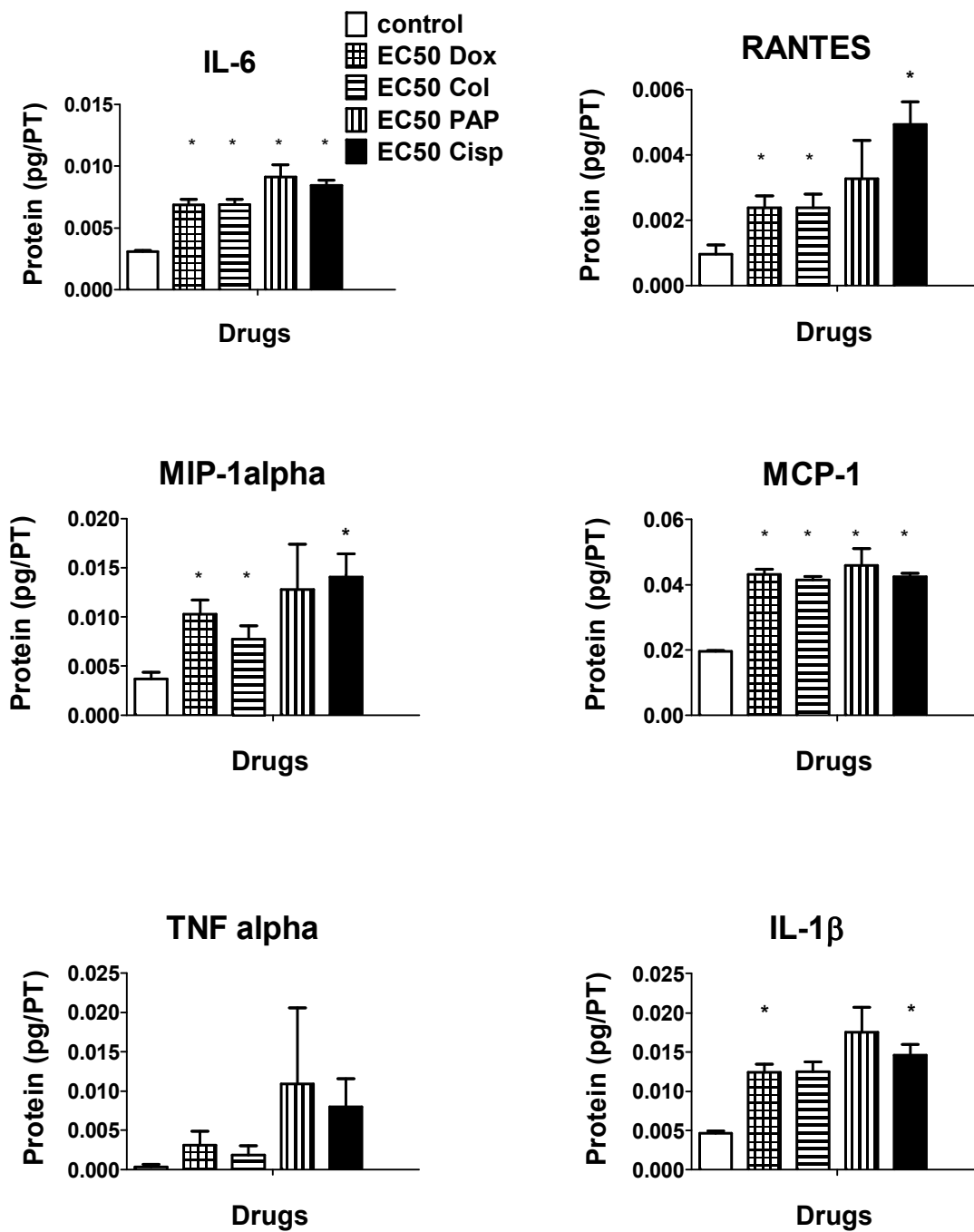


**Figure 3.5 I** Inflammatory cytokine release into culture media at drugs' EC<sub>50</sub> values: doxorubicin (DOX) at 1.4  $\mu$ M, colchicine (Col) at 24.4  $\mu$ M, PAP at 24.9  $\mu$ M, cisplatin (Cisp) at 0.42 mM (n=6, mean $\pm$ SE).

with toxicity, or produce extensive paracrine cytokine production in response to chemical injury. Therefore, use of primary cells in a culture environment that supports their native interactions and retains their tissue-like differentiation state is critical for producing *in vitro* models capable of clinically relevant toxicological data collection.

Our design combines now-routine tissue engineering approaches for 3-D scaffold-supported cell culture with highly accepted and validated use of isolated PT harvests (33, 34) to validate a new 3-D organoid PT culture system that preserves PT tubule epithelial cell functions and phenotypes for several months (18). The protocol to isolate proximal tubule-enriched subpopulations from freshly harvested intact C57BL/6 murine kidneys was reliable and efficient, which was verified by staining (see Supplementary Figures) as well as RT-PCR for known nephron biomarkers (see Supplementary Figures) (33). Isolated PTs were sustained in culture using biomedical-grade HA polymer that was previously used to differentiate and maintain multiple different cell types. As a natural glycan-based biopolymer found in most human tissues, commercial HA-derived hydrogel recognized for its mild gelation conditions, cell and tissue compatibility due to its compatibility with soft tissues' elastic modulus (similar formulation was found to have  $G'$  of 3500 Pa) (35) and high network porosity (large mesh size). This thiol-modified HA covalently crosslinks to form a hydrogel spontaneously within the cell incubator at physiological pH and without harmful chemistry. Nine different HA formulations with varying thiol concentrations, molecular weights of co-added PEG-acrylate electrophile, and HA thiol:PEGacrylate ratios were evaluated for their ability to encapsulate PTs (see Supplementary Tables). Changing these matrix variables resulted in different gel network porosities, stabilities, stiffnesses, and gelation times. HA



gels comprising 1.5% CMHA-S-7.5% PEGDA were chosen due to relatively fast gelation (35 min) and network stability during prolonged incubation. This selected HA formulation allowed the maintenance of PTs inside of the gel in their native tubular shape with open lumens, which was verified both by immunohistochemistry (Fig. 3.3F) and ability of nephrotoxic drugs to gain access to the proximal epithelial cells inside of PTs (Fig. 3.4D). The smallest technically feasible volume of this HA biopolymer was mixed directly with PT harvests to form encapsulated cell constructs with diffusion accessibility for oxygen and media. *In vivo*, the average distance between blood vessels carrying oxygen and cells that consume it is 150-200 nm (59). Lack of blood vessels and technical complexity of making 3-D cultures with mm thickness, including the 3-D organoid culture presented here, remains one of the primary challenges of the field. In this work cell viability dropped two-fold in the PT constructs within the first 2 weeks (Fig. 2A) most likely due to cell death as a result insufficient oxygen in the deepest gel layers in the plates. In future studies, cell viability in the 3-D organoid cultures may be improved using active perfusion rather than static diffusion-limited cultures.

Despite the imperfect diffusion of oxygen throughout the culture, the 3-D organoid PT constructs in their native environment proved to retain markers of cellular differentiation, such as AQP1 and megalin expression in PTs and histological staining with PHA-E, for 2 months of construct culturing *in vitro* (Fig. 3.2C and 3.3A,B). Similarly, biomarkers that reflect conservation of intracellular connections, such as gap junctions and integrins, and cellular polarization were sustained for the same amount of time within the HA gels (Fig. 3.3C-E). Furthermore, the epithelial proximal tubule cells that line PTs proved to be able to oxidize lactic acid to glucose proving to

maintain more *in vivo*-like rather than 2-D cell culture properties (Fig. 3.4E). *In vivo*, proximal tubule cells generate their energy primarily through oxidative metabolism, converting non-carbohydrate substrates such as lactate into glucose (48, 60-62). *In vitro*, cells cultured using traditional monolayer approaches suffer from reduction of gluconeogenesis and even complete reversal to glycolysis (49). Previous data show metabolic reversal in 2-D cell monolayers as a result of hypoxia and high glucose concentrations in the culture media (49, 53, 63, 64). Organoid cultures were assayed for glucose net production in the media in the presence of phloridzin, an inhibitor of glucose transport across the apical cell side (49), and phloridzin with pleretin, an inhibitor of glucose transport across the basolateral membrane (49) (Fig. 3.4E). Both inhibitors elicited significant net glucose increases in proximal tubule 3-D cultures grown in the presence of lactate, indicating important retention of glucose conversion and up-take mechanisms in 3-D organoid cultures. These data further indicate that primary proximal tubule epithelial cells in the 3-D proximal tubule organoid cultures maintain metabolic profiles similar to cells *in vivo*.

Retention of cellular architecture, organization, and gluconeogenic potential *in vitro* in the 3-D organoid cultures were accompanied by maintenance of proximal tubule epithelial cells' phenotypic functionality. Specifically, cells conserved structural capability to process proteins from the media via cathepsin B (41), maintained enzymes involved in drug biotransformation ( $\gamma$ -glutamyl-transferase (42)) and endocytosis (megalin (27, 43, 44)), and retained proteins that are responsible for signaling molecule dephosphorylation (AP (45)). Cathepsin B is a protease critical for lysosomal protein degradation in normal protein metabolism (41). AP is a brush border enzyme essential for cell signaling (41, 45). Megalin is a cell ligand that extracts proteins such as

albumin from the glomerular filtrate and transports them back into proximal tubule epithelial cells for re-absorption or degradation (65).  $\gamma$ -glutamyl-transferase is an enzyme located on proximal tubule microvilli responsible for amino acid uptake (42). Besides functions associated with normal PT cell physiology, megalin and  $\gamma$ -glutamyl-transferase are also implicated in drug transport and biotransformation in the proximal tubule epithelial cells (19, 66). It was established that all measured enzymes, proteases, and ligands were present in cells over 6-8 weeks of culture (Fig. 3.2C, and 3.4A-C). Furthermore, it was confirmed that megalin ligand on the cell surface could assist in drug uptake similar to *in vivo* behavior. To achieve this, proximal tubule 3-D organoid constructs were exposed to neomycin, a toxic aminoglycoside drug well-known to enter PT cells via interaction with megalin (67), in the presence of increasing gradients of the endocytosis inhibitor, colchicine. As expected, decreased neomycin accumulation in cells due to abrogated endocytosis resulted in reduced cell death in the 3-D organoid culture, further supporting the proposal that these culture conditions support functional PT epithelial cells (Fig. 3.4D). These data cumulatively suggest that preservation of native microenvironment leads to significant improvements in cells' long-term functionality maintenance *in vitro*.

To capitalize on advances of the developed 3-D organoid culture, cellular capacity to respond to nephrotoxic agent exposures with toxicity indicators only measurable *in vivo* was determined. Specifically, 3-D cultures' ability to up-regulate CYP P450 enzymes and Kim-1 protein in response to known nephrotoxins, acetone (40, 68) and cisplatin (69, 70), was assessed. Cytochrome CYP2E1 was chosen because it is one of the most abundantly expressed enzymes in murine kidneys and a common target for exogenous agent detoxification (39). Furthermore, *in vivo*

acetone induces nephrotoxicity in rodents and is also a well-established substrate for CYP2E1 biotransformation (39). Similarly, Kim-1 is one of the most sensitive markers of nephrotoxicity and commonly used as a hallmark of general kidney injury *in vivo* (71). Kim-1 up-regulation in response to cisplatin-induced toxicity is a well-characterized phenomenon in both rodents and humans (70, 72). Cisplatin, a potent chemotherapeutic drug limited in clinical use by severe PT toxicity (73), was applied to the 3-D organoid culture in this work at a concentration corresponding to the common mouse clinical dose (20 mg/kg) that causes kidney damage in mice in 3 days to ensure more relevant *in vivo*-to-*in vitro* comparison (73). Positive staining for CYP2E1 (Fig. 3.3 I,J) and Kim-1 (Fig. 3.3 K,L) in response to acetone and cisplatin, respectively, confirmed previously published whole animal nephrotoxicity data and ascertained 3-D organoid culture's ability to respond to endogenous toxicants with *in vivo*-relevant biomarkers.

Validation of the improved predictive power of the 3-D PT organoid culture is required to assert its relevance to predicting clinically important outcomes. In this work production of drug's metabolites was assessed using previously published protocols on the example of cisplatin (see Supplemental Figures). Seven platinum-containing metabolized chemical species were previously reported in rodent kidneys (56, 58), from which cisplatin adducts with glutathione (GSH), *N*-acetylcysteine (NAC), and cysteinyl-glycine (Cys-Gly) were reported to be toxic to cells *in vitro* (54). Similarly to *in vivo* data (56, 58), 3-D constructs produced unchanged drug (peak B), aquated cisplatin cation ( $[\text{Pt}(\text{NH}_3)_2(\text{Cl})(\text{H}_2\text{O})]^{1+}$  and  $[\text{Pt}(\text{NH}_3)_2(\text{H}_2\text{O})_2]^{2+}$ , peak E), and cisplatin-NAC (peaks F,G) in the proximal tubule media, and additional peaks A and C in the harvested cytosol. Comparing 3-D culture elution peaks with standards for drug-enzyme incubations, peak A eluted at

the same time as cisplatin-GSH and cisplatin-cysteine, and peak C had similar retention times to cisplatin-NAC and cisplatin-Cys-Gly. These data indicate that primary proximal tubule cells cultured in their native proximal tubule environment are capable of transforming a drug as expected *in vivo*.

Besides drug-specific detoxification pathways in the kidneys, 3-D organoid cultures were assessed for ability to induce pro-inflammatory events associated with toxicity leading to acute kidney injury (AKI) (3). Several studies have suggested that *in vivo* initial insult on PT epithelium sets up a cascade of events that produces morphological and molecular changes in the kidney, resulting in production of cytokines and chemokines that attract macrophages, natural killer cells, neutrophils, and leukocytes to the site of injury. In the nephrotoxic model of AKI, TNF $\alpha$ , MCP-1, IL-6, IL-1 $\beta$ , MIP-1 $\alpha$ , and RANTES proteins are mediators of inflammation that are either released or regulated by epithelial cells (3). In this work, IL-6, TNF, MCP-1, IL-1 $\beta$ , MIP-1 $\alpha$ , and RANTES secretion by primary cells was tested in response to common clinically used nephrotoxic drugs, cisplatin and doxorubicin, drug metabolite PAP, and suspected nephrotoxin, colchicine. After 3-day incubations with each drug, the 3-D culture model exhibited significant up-regulation of IL-6 and MCP-1 with all drug exposures, RANTES and MIP-1 $\alpha$  for all drugs except PAP, and IL-1 $\beta$  for cisplatin and doxorubicin only (Figure 3.5). These data matched well to cytokine profiles associated with nephrotoxicity in AKI models (3). For example, TNF $\alpha$ , unlike all other inflammatory proteins tested here, is up-regulated but is not cleaved from the epithelial surface, and hence not commonly found in the urine *in vivo* (74). In this work, TNF $\alpha$  release into the media was not significant for any drugs, similar to published animal data. Furthermore, cisplatin-induced protein induction of TNF $\alpha$ , IL-1 $\beta$ , MCP-1, IL-6 and RANTES corresponded directly to an *in vivo* model of



cisplatin-induced AKI (75). In addition to the cytokines and chemokines listed (*vide supra*), MIP-1 $\alpha$  was found to be significantly increased in 3-D cell cultures exposed to cisplatin. Although MIP-1 $\alpha$  has not been specifically studied in association with the drug, it is a ligand that binds to the same receptor as RANTES in the ischemic model of AKI and has been previously shown to be up-regulated together with MCP-1 under regulation of IL-1 $\beta$  in proximal epithelial cells (3, 76). Hence, MCP-1 is a likely chemokine candidate in the cisplatin model of AKI. Taken together, these data collectively point to significant similarities in cytokine and chemokine production between *in vivo* and the *in vitro* 3-D organoid endpoints of drug toxicity.

Presented data on functional equivalency between the 3-D organoid culture and *in vivo* available information from the literature confirm the hypothesis that preservation of native cellular microenvironment that houses PT epithelial cells within their endogenous matrix, sustaining the native cell-cell, cell-matrix, and biochemical cues, while limiting non-native cell-polymer interactions and 2-D culture artifacts, better retains essential cellular responses relevant to *in vivo* kidney pathophysiology. This 'proof of concept' has answered fundamental questions about the role of the primary cell microenvironment on cell long-term viability, differentiation stability, and contextual functionality of cells in an *in vitro* culture system. Furthermore, the study provides important value as support for the future potential of such *in vitro* culture designs in replicating the necessary physiological features for more accurately predicting *in vivo*-like processes. This includes the ability of these organoid cultures to respond to environmental stimuli with clinically important indicators not usually observed in traditional 2-D monolayer cell monocultures.

### Conclusions

The 3-D organoid culture developed in this study provides the technical capability to sustain the complex nature of primary cell interactions during prolonged culture conditions by manipulating a cell's direct, natural microenvironment. By preserving native cell organization and intracellular interactions in organoid harvests, no re-introduction of such tissue complexity needs to be built back into a 3-D culture system or fabricated *de novo*. The PT primary epithelial cells retain their natural contextual environment as found *in vivo*, and therefore their extended *in vitro* culture sustains and extends cell phenotypic and functional stability for almost 2 months. This method should provide a platform for improved assessment and validation of kidney-related disease and toxicity biomarkers for HTS 96-well screening, as well as serve as a model for basic molecular biology studies in drug-drug interactions, drug-induced toxicity, and metabolism. Additionally, further exploration using the 3-D organoid model may provide insight that would lead to greater understanding of cell organizational and communication roles in tissue functional maintenance. This level of understanding further informs the design parameters for improved bioreactor models for 3-D cell scaffolds popular in regenerative medicine and tissue engineering. The model should also facilitate establishment of cell culture models better suited to directly assess and contrast different *in vivo* and *in vitro* pathophysiology and tissue damage biomarkers.

### Acknowledgements

We thank Dr. J.V. Bonventre, Brigham and Women's Hospital/Harvard Medical School (USA), for generous donation of the R9 Kim-1 antibody; Dr. B. Jurgen, NIDDK/NIH (USA), for gift of the

OAT-1 antibody; and Dr. R. Hitchcock (Utah) for contributing connexin 43,  $\alpha 3$ , and secondary Alexa-488 antibodies. We further thank G. Stoddard, University of Utah Statistical Core, for helpful discussion of statistical analyses, Paul Hoglebe for SEM, and Dr. C. Rodesch, University of Utah Imaging Facility, for assistance with 3-D imaging. Partial financial support for this work was provided by SEED and Micro grants from the University of Utah. The University of Utah Study Design and Biostatistics Center, is supported by UL1-RR025764 and C06-RR11234 grants from the National Center for Research Resources.

### References

1. M.J. Bissell, D.C. Radisky, A. Rizki, V.M. Weaver, and O.W. Petersen. The organizing principle: microenvironmental influences in the normal and malignant breast. *Differentiation; Research in Biological Diversity*. 70:537-546 (2002).
2. J. Chunthapong, I. Cantón, E. Kemp, A. Ryan, S. MacNeil, and J. JW Haycock. A 3D skin tissue-engineered model for inflammatory and toxicity testing. *European Cells and Materials*. 16:42 (2008).
3. A. Akcay, Q. Nguyen, and C.L. Edelstein. Mediators of inflammation in acute kidney injury. *Mediators of inflammation*. 2009:137072 (2009).
4. E. Cukierman, R. Pankov, D.R. Stevens, and K.M. Yamada. Taking cell-matrix adhesions to the third dimension. *Science (New York, NY)*. 294:1708-1712 (2001).
5. F. Hartmann and D.M. Bissell. Metabolism of heme and bilirubin in rat and human small intestinal mucosa. *J Clin Invest*. 70:23-29 (1982).
6. B. Geiger, A. Bershadsky, R. Pankov, and K.M. Yamada. Transmembrane crosstalk between the extracellular matrix--cytoskeleton crosstalk. *Nat Rev Mol Cell Biol*. 2:793-805 (2001).
7. S. Ghosh, G.C. Spagnoli, I. Martin, S. Ploegert, P. Demougin, M. Heberer, and A. Reschner. Three-dimensional culture of melanoma cells profoundly affects gene expression profile: a high density oligonucleotide array study. *J Cell Physiol*. 204:522-531 (2005).
8. F. Pampaloni, E.G. Reynaud, and E.H. Stelzer. The third dimension bridges the gap between cell culture and live tissue. *Nat Rev Mol Cell Biol*. 8:839-845 (2007).

9. J. Chunthapong, I. Canton, E.H. Kemp, A.J. Ryan, S. Mac Neil, and J.W. Haycock. A 3D skin tissue-engineered model for inflammatory and toxicity testing. *European Cells and Materials*. 16:42 (2008).
10. R. Portnerand and C. Giese. An overview on bioreactor design, prototyping and process control for reproducible three-dimensional tissue culture In M.U.a.S. V (ed.), *Drug testing in vitro: breakthroughs and trends in cell culture technology*, WILEY-VCH Verlag GmbH&Co., 2007, pp. 53-78.
11. S. Bayat, M. Kessler, S. Briancon, and L. Frimat. Survival of transplanted and dialysed patients in a French region with focus on outcomes in the elderly. *Nephrol Dial Transplant*. 25:292-300 (2010).
12. S.P. McDonaldand and G.R. Russ. Survival of recipients of cadaveric kidney transplants compared with those receiving dialysis treatment in Australia and New Zealand, 1991-2001. *Nephrol Dial Transplant*. 17:2212-2219 (2002).
13. G.C. Oniscu, H. Brown, and J.L. Forsythe. Impact of cadaveric renal transplantation on survival in patients listed for transplantation. *J Am Soc Nephrol*. 16:1859-1865 (2005).
14. C.G. Rabbat, K.E. Thorpe, J.D. Russell, and D.N. Churchill. Comparison of mortality risk for dialysis patients and cadaveric first renal transplant recipients in Ontario, Canada. *J Am Soc Nephrol*. 11:917-922 (2000).
15. D. Hoffmann, M. Adler, V.S. Vaidya, E. Rached, L. Mulrane, W.M. Gallagher, J.J. Callanan, J.C. Gautier, K. Matheis, F. Staedtler, F. Dieterle, A. Brandenburg, A. Sposny, P. Hewitt, H. Ellinger-Ziegelbauer, J.V. Bonventre, W. Dekant, and A. Mally. Performance of novel kidney biomarkers in preclinical toxicity studies. *Toxicol Sci*. 116:8-22 (2010).
16. S. Olson, S. Robinson, and R. Giffin. Accelerating the Development of Biomarkers for Drug Safety: Workshop Summary *Forum on Drug Discovery, Development, and Translation: National Academy of Science: Institute of Medicine* 2009.
17. S.C. Tseng, P.C. Lee, P.F. Ells, D.M. Bissell, E.A. Smuckler, and R. Stern. Collagen production by rat hepatocytes and sinusoidal cells in primary monolayer culture. *Hepatology*. 2:13-18 (1982).
18. J.W. Davis, 2nd, F.M. Goodsaid, C.M. Bral, L.A. Obert, G. Mandakas, C.E. Garner, 2nd, N.D. Collins, R.J. Smith, and I.Y. Rosenblum. Quantitative gene expression analysis in a nonhuman primate model of antibiotic-induced nephrotoxicity. *Toxicology and Applied Pharmacology*. 200:16-26 (2004).
19. N. Pablaand and Z. Dong. Cisplatin nephrotoxicity: mechanisms and renoprotective strategies. *Kidney International*. 73:994-1007 (2008).
20. V. Pinzani, F. Bressolle, I.J. Haug, M. Galtier, J.P. Blayac, and P. Balmes. Cisplatin-induced renal toxicity and toxicity-modulating strategies: a review. *Cancer Chemotherapy and Pharmacology*. 35:1-9 (1994).

21. X. Yao, K. Panichpisal, N. Kurtzman, and K. Nugent. Cisplatin nephrotoxicity: a review. *The American Journal of the Medical Sciences*. 334:115-124 (2007).
22. W. Li, M. Lam, D. Choy, A. Birkeland, M.E. Sullivan, and J.M. Post. Human primary renal cells as a model for toxicity assessment of chemo-therapeutic drugs. *Toxicol In Vitro*. 20:669-676 (2006).
23. L. Rebelo, M. Carmo-Fonseca, and T.F. Moura. Redistribution of microvilli and membrane enzymes in isolated rat proximal tubule cells. *Biology of the Cell / under the Auspices of the European Cell Biology Organization*. 74:203-209 (1992).
24. M. Delcommenneand and C.H. Streuli. Control of integrin expression by extracellular matrix. *J Biol Chem*. 270:26794-26801 (1995).
25. S.W. Lim, C. Li, K.O. Ahn, J. Kim, I.S. Moon, C. Ahn, J.R. Lee, and C.W. Yang. Cyclosporine-induced renal injury induces toll-like receptor and maturation of dendritic cells. *Transplantation*. 80:691-699 (2005).
26. S. McLarnon, D. Holden, D. Ward, M. Jones, A. Elliott, and D. Riccardi. Aminoglycoside antibiotics induce pH-sensitive activation of the calcium-sensing receptor. *Biochem Biophys Res Commun*. 297:71-77 (2002).
27. Y. Motoyoshi, T. Matsusaka, A. Saito, I. Pastan, T.E. Willnow, S. Mizutani, and I. Ichikawa. Megalin contributes to the early injury of proximal tubule cells during nonselective proteinuria. *Kidney international*. 74:1262-1269 (2008).
28. J.B. Hook. Toxic responses of the kidney. In J. Doull, C.D. Klaassen, and M.O. Amdur (eds.), *Casarett and Doull's toxicology: the basic science of poisons*, Macmillan, New York, 1980.
29. S. Gerecht, J.A. Burdick, L.S. Ferreira, S.A. Townsend, R. Langer, and G. Vunjak-Novakovic. Hyaluronic acid hydrogel for controlled self-renewal and differentiation of human embryonic stem cells. *Proceedings of the National Academy of Sciences of the United States of America*. 104:11298-11303 (2007).
30. G.D. Prestwich. Evaluating drug efficacy and toxicology in three dimensions: using synthetic extracellular matrices in drug discovery. *Accounts of Chemical Research*. 41:139-148 (2008).
31. Y. Liu, X. Zheng Shu, and G.D. Prestwich. Biocompatibility and stability of disulfide-crosslinked hyaluronan films. *Biomaterials*. 26:4737-4746 (2005).
32. G.D. Prestwich. Hyaluronic acid-based clinical biomaterials derived for cell and molecule delivery in regenerative medicine. *J Control Release*. 155:193-199 (2011).
33. S. Terryn, F. Jouret, F. Vandenabeele, I. Smolders, M. Moreels, O. Devuyst, P. Steels, and E. Van Kerkhove. A primary culture of mouse proximal tubular cells, established on collagen-coated membranes. *Am J Physiol Renal Physiol*. 293:F476-485 (2007).



34. R.L. Miller, P. Zhang, T. Chen, A. Rohrwasser, and R.D. Nelson. Automated method for the isolation of collecting ducts. *Am J Physiol Renal Physiol*. 291:F236-245 (2006).
35. J.L. Vanderhooft, M. Alcoutlabi, J.J. Magda, and G.D. Prestwich. Rheological properties of cross-linked hyaluronan-gelatin hydrogels for tissue engineering. *Macromol Biosci*. 9:20-28 (2009).
36. M.L. Godek, R. Michel, L.M. Chamberlain, D.G. Castner, and D.W. Grainger. Adsorbed serum albumin is permissive to macrophage attachment to perfluorocarbon polymer surfaces in culture. *Journal of Biomedical Materials Research*. 88:503-519 (2009).
37. L. Naftalin, M. Sexton, J.F. Whitaker, and D. Tracey. A routine procedure for estimating serum gamma-glutamyltranspeptidase activity. *Clin Chim Acta*. 26:293-296 (1969).
38. R.K. Garyand and S.M. Kindell. Quantitative assay of senescence-associated beta-galactosidase activity in mammalian cell extracts. *Analytical biochemistry*. 343:329-334 (2005).
39. C. Fang, M. Behr, F. Xie, S. Lu, M. Doret, H. Luo, W. Yang, K. Aldous, X. Ding, and J. Gu. Mechanism of chloroform-induced renal toxicity: non-involvement of hepatic cytochrome P450-dependent metabolism. *Toxicology and Applied Pharmacology*. 227:48-55 (2008).
40. E. Gonzalez-Jasso, T. Lopez, D. Lucas, F. Berthou, M. Manno, A. Ortega, and A. Albores. CYP2E1 regulation by benzene and other small organic chemicals in rat liver and peripheral lymphocytes. *Toxicology Letters*. 144:55-67 (2003).
41. C.J. Olbricht, M. Fink, and E. Gutjahr. Alterations in lysosomal enzymes of the proximal tubule in gentamicin nephrotoxicity. *Kidney International*. 39:639-646 (1991).
42. B.Y. Hsu, J.W. Foreman, S.M. Corcoran, K. Ginkinger, and S. Segal. Absence of a role of gamma-glutamyl transpeptidase in the transport of amino acids by rat renal brushborder membrane vesicles. *The Journal of Membrane Biology*. 80:167-173 (1984).
43. E.I. Christensen and J. Gburek. Protein reabsorption in renal proximal tubule-function and dysfunction in kidney pathophysiology. *Pediatric Nephrology (Berlin, Germany)*. 19:714-721 (2004).
44. A.L. Negri. Proximal tubule endocytic apparatus as the specific renal uptake mechanism for vitamin D-binding protein/25-(OH)D3 complex. *Nephrology (Carlton, Vic)*. 11:510-515 (2006).
45. U. Schmid and U.C. Dubach. Alkaline phosphatase: a marker enzyme for brush border membrane? *Experientia*. 28:385-386 (1972).
46. H.J. Adrogué. Glucose homeostasis and the kidney. *Kidney International*. 42:1266-1282 (1992).

47. G. Gstraunthaler and J.S. Handler. Isolation, growth, and characterization of a gluconeogenic strain of renal cells. *The American Journal of Physiology*. 252:C232-238 (1987).
48. H.A. Krebs, D.A. Bennett, P. De Gasquet, P. Gasquet, T. Gascoyne, and T. Yoshida. Renal gluconeogenesis. The effect of diet on the gluconeogenic capacity of rat-kidney-cortex slices. *Biochem J*. 86:22-27 (1963).
49. G. Nowak and R.G. Schnellmann. Improved culture conditions stimulate gluconeogenesis in primary cultures of renal proximal tubule cells. *The American Journal of Physiology*. 268:C1053-1061 (1995).
50. M.D. Aleo and R.G. Schnellmann. Regulation of glycolytic metabolism during long-term primary culture of renal proximal tubule cells. *The American Journal of Physiology*. 262:F77-85 (1992).
51. M.J. Tang and R.L. Tannen. Relationship between proliferation and glucose metabolism in primary cultures of rabbit proximal tubules. *The American Journal of Physiology*. 259:C455-461 (1990).
52. W.G. Guder and B.D. Ross. Enzyme distribution along the nephron. *Kidney International*. 26:101-111 (1984).
53. S.R. Gullans, P.C. Brazy, V.W. Dennis, and L.J. Mandel. Interactions between gluconeogenesis and sodium transport in rabbit proximal tubule. *The American Journal of Physiology*. 246:F859-869 (1984).
54. D.M. Townsend, J.A. Marto, M. Deng, T.J. Macdonald, and M.H. Hanigan. High pressure liquid chromatography and mass spectrometry characterization of the nephrotoxic biotransformation products of cisplatin. *Drug Metab Dispos*. 31:705-713 (2003).
55. M.H. Hanigan, E.D. Lykissa, D.M. Townsend, C.N. Ou, R. Barrios, and M.W. Lieberman. Gamma-glutamyl transpeptidase-deficient mice are resistant to the nephrotoxic effects of cisplatin. *Am J Pathol*. 159:1889-1894 (2001).
56. P.T. Daley-Yates and D.C. McBrien. Cisplatin metabolites in plasma, a study of their pharmacokinetics and importance in the nephrotoxic and antitumour activity of cisplatin. *Biochemical Pharmacology*. 33:3063-3070 (1984).
57. P.T. Daley-Yates and D.C. McBrien. Enhancement of cisplatin nephrotoxicity by probenecid. *Cancer Treat Rep*. 68:445-446 (1984).
58. P. Mistry, C. Lee, and D.C. McBrien. Intracellular metabolites of cisplatin in the rat kidney. *Cancer Chemotherapy and Pharmacology*. 24:73-79 (1989).
59. T. Kaully, K. Kaufman-Francis, A. Lesman, and S. Levenberg. Vascularization--the conduit to viable engineered tissues. *Tissue Eng Part B Rev*. 15:159-169 (2009).

60. D.C. Bradley and H.R. Kaslow. Radiometric assays for glycerol, glucose, and glycogen. *Analytical Biochemistry*. 180:11-16 (1989).
61. E. Leal-Pinto, H.C. Park, F. King, M. MacLeod, and R.F. Pitts. Metabolism of lactate by the intact functioning kidney of the dog. *The American Journal of Physiology*. 224:1463-1467 (1973).
62. M.J. Weidemann and H.A. Krebs. The fuel of respiration of rat kidney cortex. *Biochem J*. 112:149-166 (1969).
63. R.S. Balaban and L.J. Mandel. Metabolic substrate utilization by rabbit proximal tubule. An NADH fluorescence study. *The American Journal of Physiology*. 254:F407-416 (1988).
64. K.G. Dickman and L.J. Mandel. Glycolytic and oxidative metabolism in primary renal proximal tubule cultures. *The American Journal of Physiology*. 257:C333-340 (1989).
65. J.A. Jefferson, S.J. Shankland, and R.H. Pichler. Proteinuria in diabetic kidney disease: a mechanistic viewpoint. *Kidney International*. 74:22-36 (2008).
66. M.H. Hanigan and P. Devarajan. Cisplatin nephrotoxicity: molecular mechanisms. *Cancer Therapy*. 1:47-61 (2003).
67. J. Nagai, H. Tanaka, N. Nakanishi, T. Murakami, and M. Takano. Role of megalin in renal handling of aminoglycosides. *Am J Physiol Renal Physiol*. 281:F337-344 (2001).
68. W.R. Hewitt and G.L. Plaa. Dose-dependent modification of 1,1-dichloroethylene toxicity by acetone. *Toxicology Letters*. 16:145-152 (1983).
69. J.A. Broomhead, D.P. Fairlie, and M.W. Whitehouse. cis-Platinum(II) amine complexes: some structure-activity relationships for immunosuppressive, nephrotoxic and gastrointestinal (side) effects in rats. *Chem Biol Interact*. 31:113-132 (1980).
70. J.V. Bonventre. Kidney injury molecule-1 (KIM-1): a urinary biomarker and much more. *Nephrol Dial Transplant*. 24:3265-3268 (2009).
71. J.V. Bonventre and L. Yang. Kidney injury molecule-1. *Curr Opin Crit Care* (2010).
72. R.P. Amin, A.E. Vickers, F. Sistare, K.L. Thompson, R.J. Roman, M. Lawton, J. Kramer, H.K. Hamadeh, J. Collins, S. Grissom, L. Bennett, C.J. Tucker, S. Wild, C. Kind, V. Oreffo, J.W. Davis, 2nd, S. Curtiss, J.M. Naciff, M. Cunningham, R. Tennant, J. Stevens, B. Car, T.A. Bertram, and C.A. Afshari. Identification of putative gene based markers of renal toxicity. *Environmental Health Perspectives*. 112:465-479 (2004).
73. P. Devarajan, R. Tarabishi, J. Mishra, Q. Ma, A. Kourvetaris, M. Vougiouka, and T. Boulikas. Low renal toxicity of lipoplatin compared to cisplatin in animals. *Anticancer Research*. 24:2193-2200 (2004).
74. C. van Kooten, M.R. Daha, and L.A. van Es. Tubular epithelial cells: a critical cell type in the regulation of renal inflammatory processes. *Exp Nephrol*. 7:429-437 (1999).

75. G. Ramesh and W.B. Reeves. TNF-alpha mediates chemokine and cytokine expression and renal injury in cisplatin nephrotoxicity. *The Journal of Clinical Investigation*. 110:835-842 (2002).
76. K. Furuichi, T. Wada, Y. Iwata, S. Kokubo, A. Hara, J. Yamahana, T. Sugaya, Y. Iwakura, K. Matsushima, M. Asano, H. Yokoyama, and S. Kaneko. Interleukin-1-dependent sequential chemokine expression and inflammatory cell infiltration in ischemia-reperfusion injury. *Crit Care Med*. 34:2447-2455 (2006).

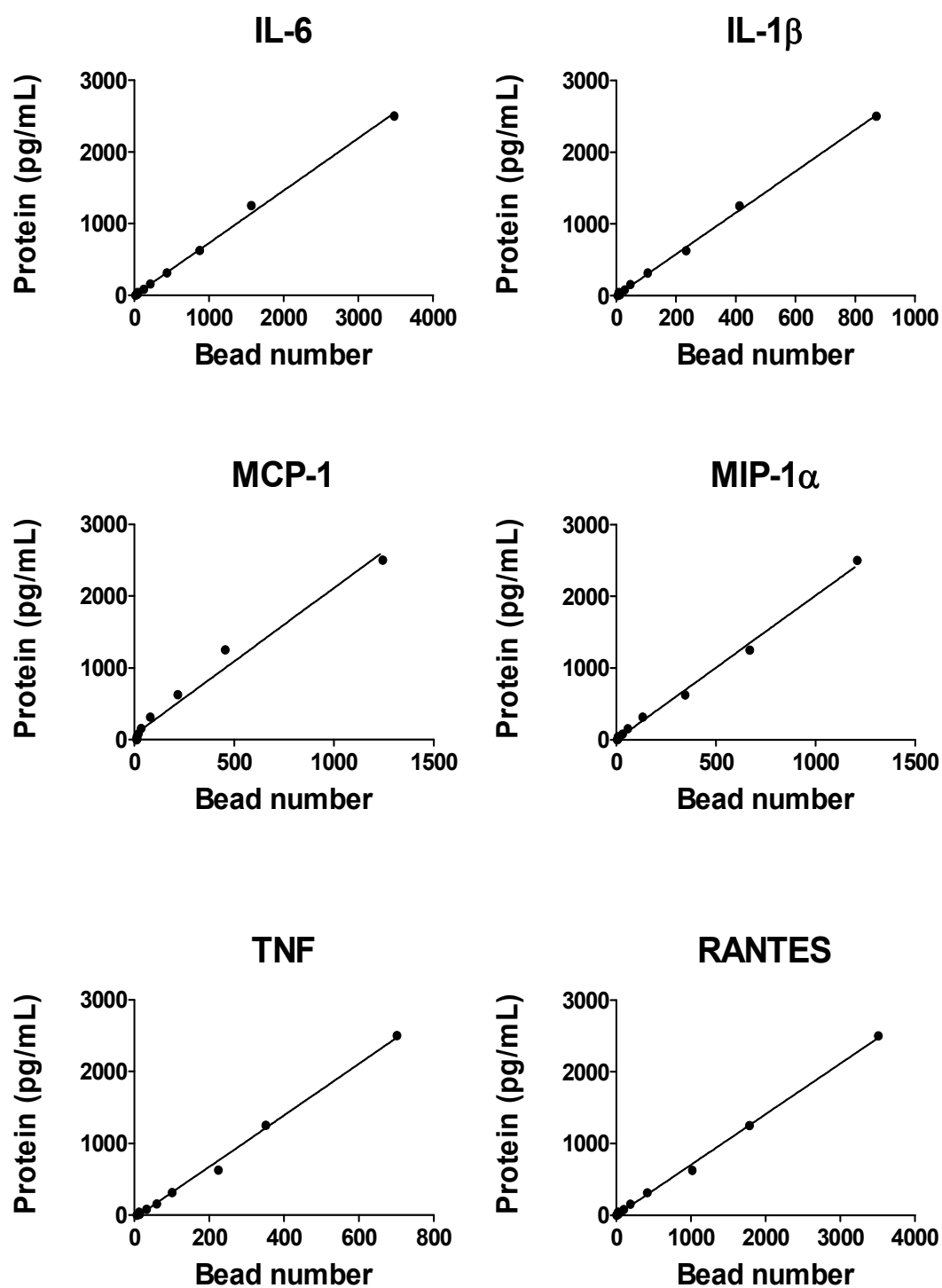
**Supplementary Table 3.1** RT-PCR primers used.

|         |         |                          |
|---------|---------|--------------------------|
| GAPDH   | Forward | TCTACATGTTCCAGTATGACTCCA |
|         | Reverse | AGTCCATGCCATCACTGCCACCC  |
| AQP1    | Forward | TCCCCTAACTTTCCCCTTTG     |
|         | Reverse | TGGCAAGGAAGGGATAGCTTT    |
| AQP2    | Forward | GAGAGAGGGAGGGAGGAAGA     |
|         | Reverse | GGTCAGGAAGAGCTCCACAG     |
| NCC     | Forward | CTGGAGAACCTGTTCGCTTC     |
|         | Reverse | CAGAGGCATCTCTCACCACA     |
| Megalín | Forward | GGTTCGTTATGGCAGTCGTT     |
|         | Reverse | GGTCACATCCCGTAGCAAGT     |

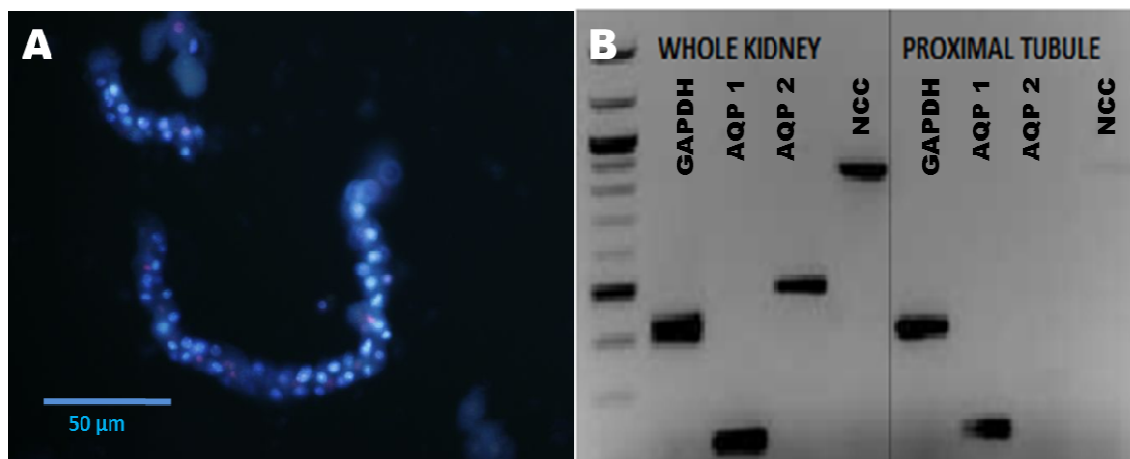
**Supplementary Table 3.2** Hydrogel formulations tested for use in proximal tubule encapsulation.

| <b>GEL<br/>FORMULATION</b> | <b>CMHA-S<br/>THIOL<br/>LEVEL</b> | <b>PEGDA<br/>MW</b> | <b>CMHA-S FINAL<br/>CONC (MG/ML)</b> | <b>PEGDA<br/>FINAL<br/>CONC<br/>(MG/ML)</b> | <b>THIOL:ACRYL<br/>RATIO</b> |
|----------------------------|-----------------------------------|---------------------|--------------------------------------|---|------------------------------|
| 1                          | high                              | 3350                | 16                                   | 16  | 1.26 : 1                     |
| 2                          | high                              | 3350                | 16                                   | 20  | 1 : 1                        |
| 3                          | high                              | 6000                | 16                                   | 16  | 2.26 : 1                     |
| 4                          | high                              | 6000                | 16                                   | 36  | 1 : 1                        |
| 5                          | low                               | 3350                | 20                                   | 10  | 1 : 1                        |
| 6                          | low                               | 6000                | 20                                   | 18  | 1 : 1                        |
| 7                          | high                              | 3350                | 8                                    | 10  | 1 : 1                        |
| 8                          | high                              | 3350                | 12                                   | 15  | 1 : 1                        |
| 9                          | high                              | 3350                | 16                                   | 8   | 2.52 : 1                     |

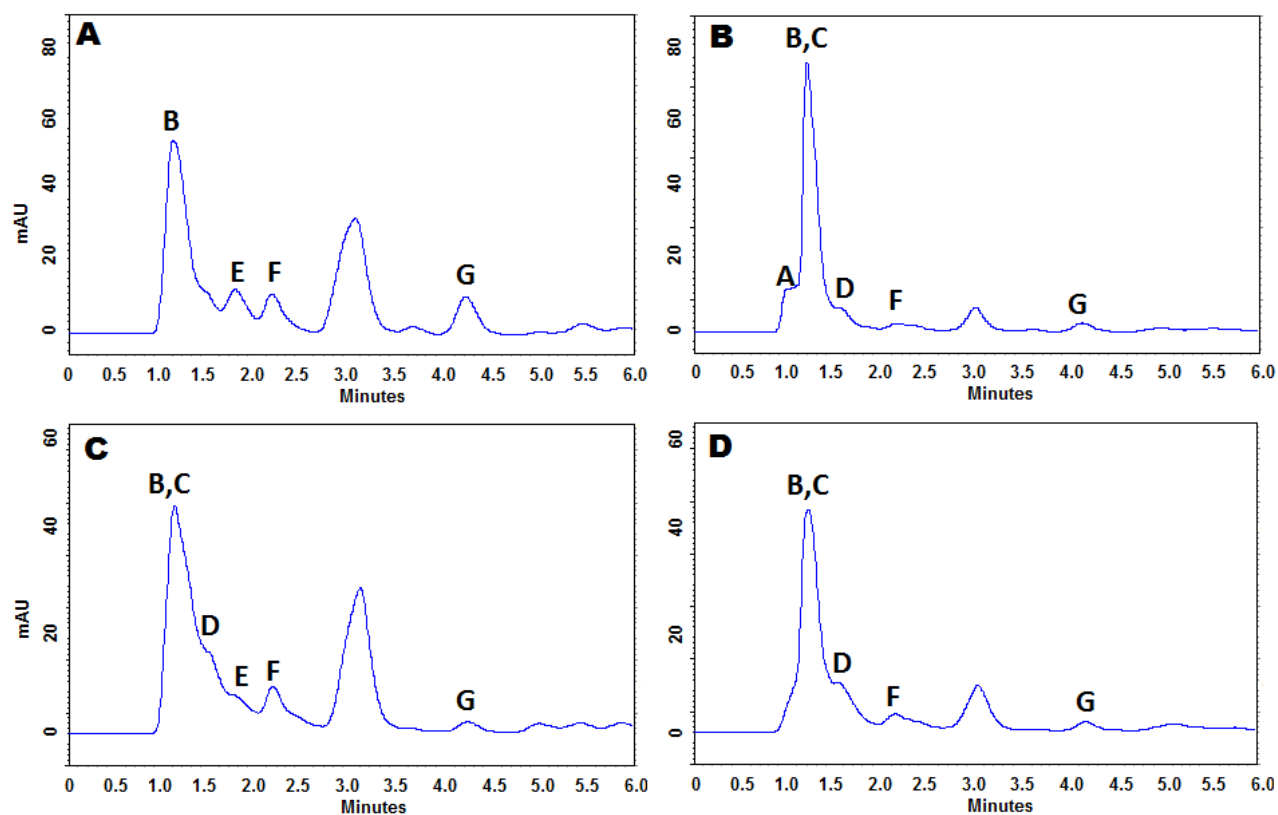




**Supplementary Figure 3.1** FACS standard curves for measured soluble proteins.



**Supplementary Figure 3.2** Isolation purity of proximal tubules. A) Isolated proximal tubule fragments stained with PI and Hoechst for assessment of live and dead cells in PTs; B) PCR results for nephron markers showing high yield of proximal tubule isolation procedure: GAPDH-housekeeping gene, AQP1- proximal tubule marker, AQP2-distal tubule, NCC-collective duct.



**Supplementary Figure 3.3** Cisplatin metabolite production in 3-D organoid proximal tubule culture in: A) media after 1 hour of incubation with the drug, B) epithelial cell cytosol after 1h incubation with the drug, C) media after 6h incubation with the drug, D) epithelial cell cytosol after 6h incubation with the drug.

## CHAPTER 4

# INFLUENCE OF DRUG HYDROPHOBICITY, CELL CONFLUENCE, AND ASSAY SELECTION ON TOXICITY ASSESSMENT IN VITRO IN PRIMARY AND TRANSFORMED KIDNEY CELL CULTURES<sup>1</sup>

### Abstract

Primary and immortalized kidney cell lines are used interchangeably in the scientific literature for toxicity assessment of pharmaceutical agents, drug delivery vehicles, and biomaterials without much reported validation of their fidelity to each other or to actual *in vivo* cell responses. Two immortalized kidney-derived cell lines (HEK293 cells and LLC-PK1), each with different phenotypes resembling epithelial cells, were compared in drug toxicity assays. Results were shown to vary widely based on incubation time, drug partition coefficient, culture confluence, and viability assays. Specifically, immortalized cell lines showed non-monotonic dose response curve (NMDRC) toxicity behavior for hydrophobic but not hydrophilic drugs, when tested on cultures at low cell seeding densities, at early time points of drug exposure, and different viability assessment assays. Unlike transformed kidney cell lines, primary kidney epithelial cells in 3-D hydrogel cultures produced *in vivo*-like dose-toxicity relationships to the same drugs. Collective data indicate that

---

<sup>1</sup> Submitted to *AAPS Journal*: Anna Astashkina, David Grainger. Influence of drug hydrophobicity, cell confluence, and assay selection on toxicity assessment in vitro in primary and transformed kidney cell culture, 2012

only primary cell cultures should be used in this context for reliable *in vivo*-relevant toxicity screening that recapitulates key aspects of cell behaviors *in vivo*.

### Introduction

The majority of lead compound identification, drug delivery vehicle optimization, or drug discovery target validation is accomplished using cell-based *in vitro* assays both in industry and academia. Such assays can serve to measure drug-cell permeability routes and transport kinetics as well as dose-response relationships in toxicity studies. Use of both primary and immortalized cell lines is quite common, often applied interchangeably, based on the presumption that data collected from either cell type are physiologically relevant to *in vivo* cellular responses. Historically, use of immortalized or transformed cell lines has been the preferred method of drug development and screening (1, 2). The approach can be explained by convenience, ease-of-use, as well as reproducibility of data between different laboratories (1, 2). Specifically, transformed cell lines are readily sourced, easily expanded using common culture conditions, maintained in culture for 40-50 generations, and readily handled in high through-put screening (HTS) methods using automation and robotic dispensing (2). In contrast, primary cells de-differentiate *in vitro* in days or weeks depending on the complexity of the native phenotype, are costly, tedious, and ethically challenging to extract from living tissue sources using a diverse array of tissue-specific cell isolation protocols, with resulting heterogeneous cell populations. Inherent difficulties associated with maintaining primary cell cultures often outweigh the disadvantages of using transformed cell lines. The phenotypic and genetic alterations from genetic transformation using oncogene insertions and

multiple passaging produce distinct cellular differences compared to their native source (1). Genetic transformation is often achieved to increase culture convenience, at the expense of losing molecular, structural, and biochemical cell identifiers, resulting in reduced or completely altered processes in these cells and overall functional non-equivalence between the immortalized and *in vivo* cells (3-14). Hence, careful characterization of cellular behaviors, phenotypes, and specific processes relevant to those under investigation is required prior to model selection. Lack of validation and understanding of a cell culture model's limitations makes interpretation of results and their physiological relevance highly tentative and possibly irreproducible.

Nonetheless, transformed cell lines remain an important scientific tool for studies on drug receptors and transporters, ligand-substrate binding, and drug signaling pathways, where expression of all key molecular components for a particular study are controlled using targeted transfection or siRNA techniques to create specific mutations (1, 2). However, a growing body of literature reflects the limitations of these systems in providing accurate, reliable insight into highly complex and poorly understood physiological processes such as pharmacological studies (15-18), inflammation (16, 19-21), and cell signaling (22-25) in response to environmental stimuli. Often, a simplistic monocultured cell model, despite controlled phenotypic features, cannot reflect the complexity of host physiology in drug-tissue interactions, pharmacokinetics, pharmacodynamics, metabolic processing, toxicity, and therapy. Their use in pharmacological and toxicological translation is often presumed, empirically determined and often unreliable.

Assessing kidney toxicity (nephrotoxicity) of exogenous agents likely succumbs to this problem. Nephrotoxicity is a complex process induced primarily in proximal tubule epithelial cells



that line proximal tubules (PTs) in the kidney nephron (26). PT toxicity is a cumulative compounding sequence of events that includes drug accumulation, biotransformation, and apoptosis induction. PT drug uptake is achieved via drug-specific active transporters (i.e., organic cation transporter 2 (OCT2) for cisplatin (27), P-glycoprotein for doxorubicin (28) and colchicine (29)), ligands (e.g., megalin for aminoglycoside drugs (7)) and microvilli surface area-assisted passive diffusion. Drug biotransformation occurs as a series of biochemical interactions with brush border enzymes (e.g.,  $\gamma$ -glutamyl-transferase for cisplatin (27)), intracellular enzymes (i.e., glutathione for cisplatin (27)) and P450 cytochromes (27, 30). The active metabolites of biotransformation, protein-drug conjugates, and free drug accumulated in the cytoplasm then initiate cellular apoptosis and necrosis. All of these components play a compound, complex role to induce nephrotoxicity, and, hence, their functional preservation *in vitro* in culture is critical to achieve kidney toxicology assays with any relevance to *in vivo* nephrotoxicity.

Basic studies of different immortalized kidney cells lines *in vitro* support a current, clear understanding that transformed cell lines lack clinically relevant markers such as toxicity-related gene up-regulation, ion-sensing receptors that serve as drug agonists, endocytic scavenger receptors implicated in drug uptake and early injury, biosynthesis of drug metabolizing enzymes, and Toll-like receptors mediating inflammation in drug toxicity (3-9, 31). Hence, immortalized kidney cell lines would likely be intrinsically incapable of producing *in vivo*-relevant toxicity responses. Yet after decades, validation of their utility and accuracy in such nephrotoxicity assessments beyond correlative anecdotes and historical precedent is not published.

This study compares immortalized kidney cell lines to differentially stable primary proximal tubule cell cultures in cellular toxicity studies using known drugs with different pharmacological indications and formulations but importantly, known nephrotoxicity *in vivo*. Furthermore, these cell toxicity data were collected as a function of exposure (incubation times) and cell densities commonly used in the literature and replicated using different assessment methodologies. Results show similar toxicity profiles between primary and immortalized cell lines for highly water-soluble drugs. However, almost any toxicity endpoint could be achieved with hydrophobic drugs and immortalized kidney cell lines -- but not with primary cells -- just by changing the cell culture conditions.

## Methods

### Chemicals

Drugs except for rifampicin and ciprofloxacin were purchased from Sigma-Aldrich Chemical Co. (St. Louis, USA). Ciprofloxacin and rifampicin were purchased from LKT Laboratories, Inc. (St. Paul, USA) and Gold Biotechnology Co. (St. Louis, USA), respectively. Doxorubicin (doxorubicin hydrochloride, Sigma 44584), colchicine (Sigma C9754), dexamethasone (Sigma D4902), neomycin (neomycin trisulfate salt hydrate, Sigma N6386), rifampicin (LKT R3220), ciprofloxacin (LKT C3262) were dissolved in dimethyl sulfoxide (DMSO) (Fisher Scientific) as 20 or 200mM stock solutions. Stocks were protected from light and stored at -20°C.

### Immortalized cell resources and cell culture

Porcine secondary LLC-PK1 renal proximal tubule epithelial cells were purchased from ATCC (Manassas, USA). Human secondary HEK293 renal proximal tubule epithelial cells were generously donated by Dr. A. Cheung, University of Utah. Cell lines were expanded using aseptic techniques in DMEM (Invitrogen, USA) with 10% FBS (Invitrogen) and 1% anti-anti (Invitrogen). Both cell lines were kept in cell culture incubator with 5% CO<sub>2</sub> and 95% air at 37°C.

For all experiments, cells were seeded in 96-well tissue culture plates (Fisher Scientific, USA) at either 170,750 cells/well or 10,000 cells/well concentrations and allowed to adhere for 2 hours using DMEM media with 10% FBS. Cultures with lower cell numbers were used to assess inter-epithelial transport in the uptake of drugs (see Supplemental Figures). Higher cell numbers were chosen to create monolayer-like cultures (see Supplemental Figures). All drugs were diluted to their final concentrations (except for the no-FCS control experiment) in proximal tubule complete media (1% FCS, 5% sodium pyruvate, 1% non-essential amino acids, 1% insulin/transferrin/selenium, 1% anti-anti, 0.9 µg of hydrocortisone, phenol red-free DMEM-Ham's F-12 with L-glutamine) and sterilized using 0.22µm pore filtration. Experiments without growth factors used incomplete PT media (5% sodium pyruvate, 1% non-essential amino acids, 1% insulin/transferrin/selenium, 1% anti-anti, 0.9 µg of hydrocortisone, phenol red-free DMEM-Ham's F-12 with L-glutamine). Phenol red-free media was used in all experiments to avoid optical interference with luminescence and fluorescence assays.

### 3-D organoid constructs preparation

All 3-D constructs were made using Teflon-AF® (Dupont)-coated non-tissue culture polystyrene plates (ISC Bioexpress, USA). Teflon-AF® was resuspended in FC-40 (3M, USA) organic solvent and applied to culture surfaces per previously published protocols (32, 33). Solvent was removed using heated vacuum drying. Plates were sterilized using UV irradiation in the cell culture hood for 30 min before use. All 3-D cultures were made using primary PTs from male C57BL/6 mice 6-8 weeks old that were purchased from Jackson Laboratory (Bar Harbor, USA). PTs were isolated according to our lab's published method (32). Briefly, isolated kidneys were prepared by removal of kidney capsule, blood vessels, and ureter using standard aseptic conditions in BSL2 laminar flow hood. Tissues were finely mechanically disrupted and enzymatically digested in collagenase IV (Worthington Biochemical Corporation, USA), DNase I (Sigma-Aldrich, USA), and HAse (Worthington Biochemical Corporation, USA) enzyme KREBS solution (145 mM NaCl, 10 mM HEPES, 5 mM KCl, 1 mM NaH<sub>2</sub>PO<sub>4</sub>, 2.5 mM CaCl<sub>2</sub>, 1.8 mM MgSO<sub>4</sub>, 5 mM glucose, pH 7.3) at 37°C (34). Digested sections of the kidney were put through a series 80 µm and 250 µm of sieves (35). The resulting suspension of PTs resuspended in 1.5% thiol-modified carboxymethylated HA (CMHA-S, Sentrx Animal Care, Salt Lake City, USA) in PBS<sup>++</sup>, and cross-linked using 7.5% poly(ethylene glycol) diacrylate (PEGDA) bifunctional electrophile (4:1 v/v CMHA-S:PEGDA, total volume 50 µL, SentrX Animal Care, Salt Lake City, USA) into 3-D constructs (36). Crosslinking was done for 35 min in the incubator followed by full PT media addition. The 3-D constructs were made using ~5000 PTs/well and used within 1 week

after preparation. The constructs were maintained in the incubator with 5% CO<sub>2</sub> with culture media exchanged every other day for optimum viability.

#### Cytotoxicity measurements

Cytotoxicity due to various chemicals in LLC-PK1 and HEK293 cells was assessed using the DNA-labeling assay, CyQuant NF® (Invitrogen, USA); necrosis measured using the ToxiLight® (Lonza, USA) assay, and the metabolic MTS assay (Fisher, USA). Linear assay responses were verified using standard curves (see Supplemental Figures). All cell lysis standard curves for ToxiLight® assays were determined for each time point using ToxiLight® 100% Lysis Reagent Set (Lonza, USA). All assays were performed in triplicate using two technical replicas in each experiment.

After incubating drug solutions for the indicated culture periods, cells and media were separated for further analysis. Cells were assessed for cell viability using MTS or CyQuant NF®. Media from the cells was assayed for cell necrosis using ToxiLight®. For MTS assays, MTS reagent was diluted according to manufacturer's instructions and stored at -20°C. Prior to cell exposure, 20µL of defrosted MTS reagent was mixed with 100µL of PT complete media for each tested well. Cells were incubated with final media-diluted reagent for 1 hour in the incubator. For CyQuant NF®, cells were exposed to 100µL of dye prepared according to manufacture's instructions for 1 hour in the cell culture incubator. For ToxiLight®, 20µL of cell media was transferred to opaque 96-well plates (Dynex Microlite, USA), cooled at room temperature (RT) for at least 5 minutes, and exposed to 100µL of ToxiLight® reagent for 5 minutes. CyQuant NF®

fluorescence (using 485nm excitation and 529nm emission wavelengths, respectively), MTS absorbance (490nm) and ToxiLight® luminescence were measured using a Synergy 2 plate reader (BioTek, USA). CyQuant NF® and MTS data were expressed as a percent of cell survival through normalization to wells containing cells not exposed to any drugs, and ToxiLight® data were expressed as percent cell death compared to 100% cell lysis as measured by ToxiLight® 100% Lysis Reagent Set.

#### Drug aggregation assay in culture media

Colchicine aggregation in PT complete media was assessed using a Nano-ZS Zetasizer (Malvern Instruments, USA). Final drug concentrations in the PT complete media were incubated at RT in a 96-well tissue culture polystyrene plate. Drug aggregation detected as particle formation in the media was assessed at 2 hours for colchicine, rifampicin, dexamethasone, and ciprofloxacin and every 20 min for 3-hours for colchicine (see Supplemental Tables).

#### Statistical analyses

All data analysis was performed using Excel 2010 (Microsoft) and GraphPad Prism 5 (GraphPad Software, Inc., USA). All cell experiments were performed using three independent samples with two technical replicas. All data in the paper were presented as mean±S.E (standard error). Significant differences in binary comparisons were determined using one-way analysis of variance (ANOVA).

## Results

### Drug effects on cell viability as a function of cell assay

Three common commercial cells assays -- CyQuant NF®, MTS, and ToxiLight® -- were used to assess cell viability as an indicator of toxicity *in vitro*. For all time points tested, CyQuant NF® and ToxiLight® were found to be significantly more sensitive at detecting drug-induced damage than MTS. Specifically, MTS was able to detect cell death in culture, but failed to distinguish cell death changes below 10% mortality from either doxorubicin and colchicine at most measured time points (likely confounded by these assays' intrinsic lack of sensitivity at low percent cell death). Increasing the incubation time from 3 hours to 3 days did not change this trend, showing little cell damage due to exposure to both drugs (Figures 4.1 and 4.2). Furthermore, the luminescence-based necrosis assay, ToxiLight®, was shown to be highly susceptible to presence of residual organic solvent, DMSO, used in the drug stock solutions. Presence of DMSO above 5% in solutions tested reduced assay luminescence signal by more than 10-fold (data not shown). Hence, all data presented for ToxiLight® assays used 0.5%-2% DMSO final concentrations with cells. Furthermore, continuously releasing substrate assays, such as ToxiLight®, lose their ability to discern between the 100% cell lysis as measured by ToxiLight® 100% Lysis Reagent Set and cell death due to drug exposure as a function of time. Both HEK293 and LLC-PK1 cells dropped from 5-fold to less than 2-fold in ToxiLight® assay sensitivity between 3 hours and 48 hours of cell incubation (Figure 4.3). Unlike ToxiLight® and MTS assays, CyQuantNF® assays seemed to be relatively insensitive to media additives and therefore more applicable for testing of many different



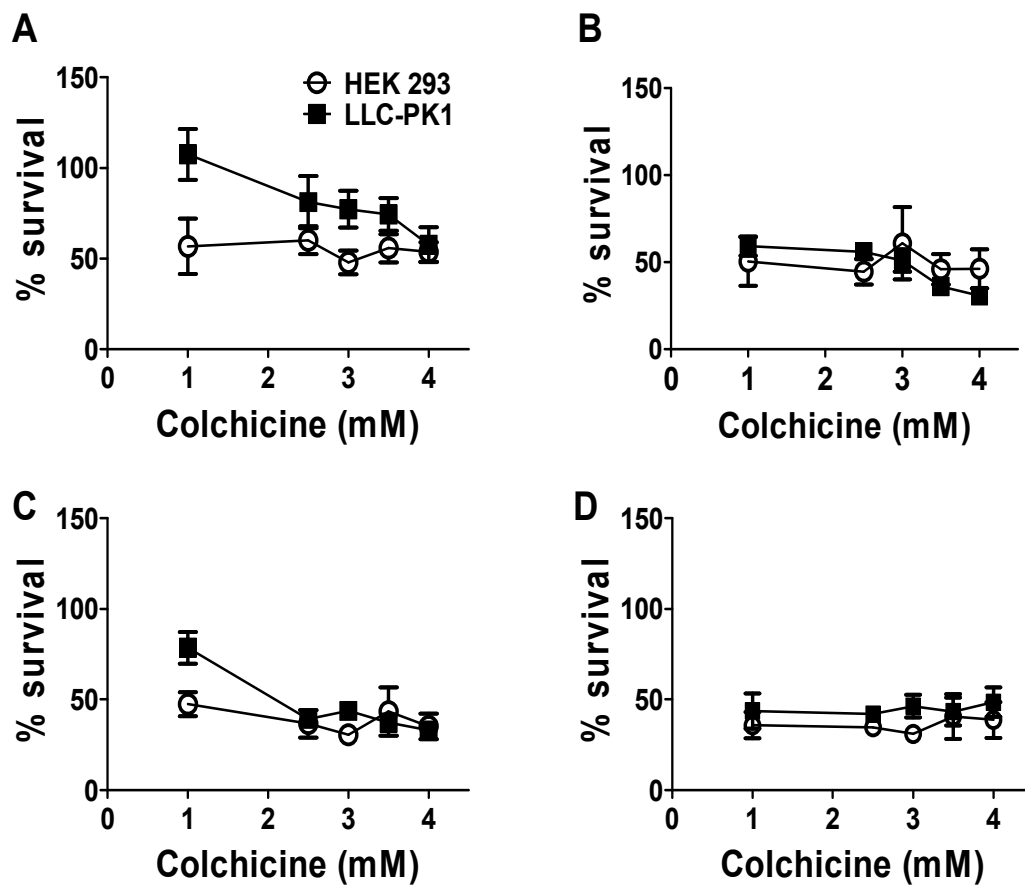


**Figure 4.1.** MTS cell viability assay from continuous incubation of HEK293 and LLC-PK1 cells with increased concentrations of colchicine: (A) 3 hours, (B) 24 hours, (C) 48 hours of incubation, and (D) 72 hours of incubation.

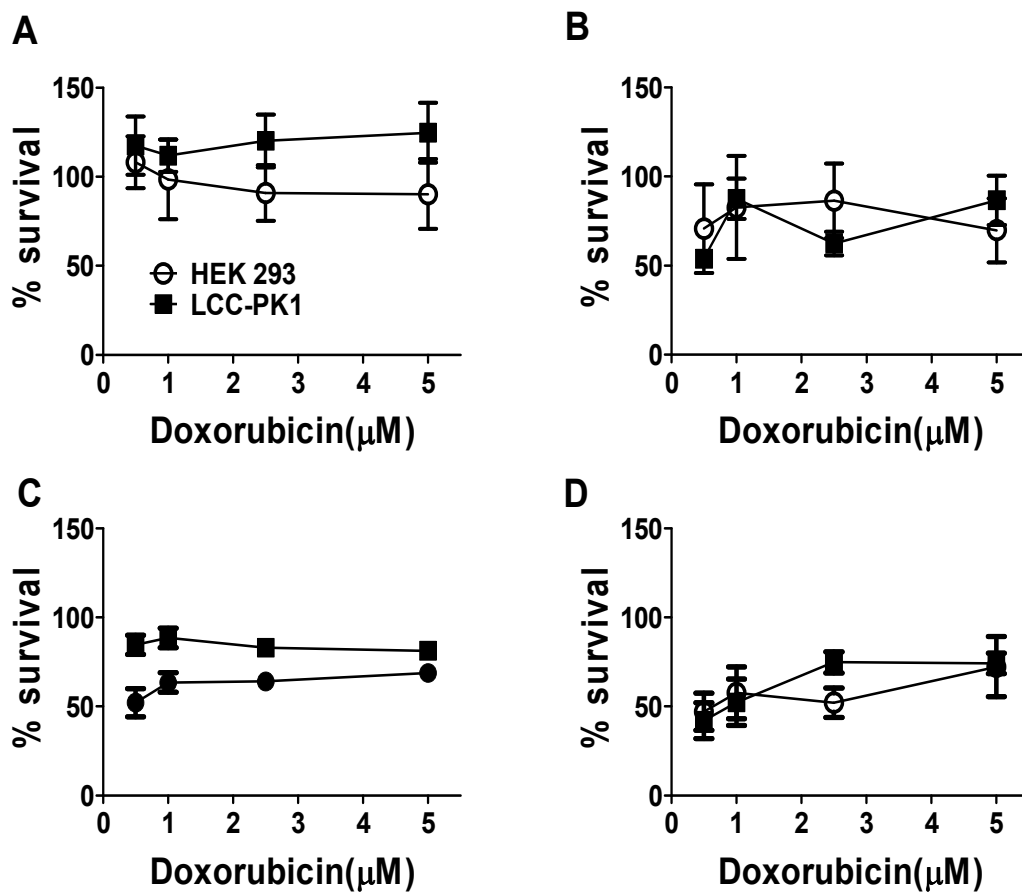


**Figure 4.2.** MTS cell viability assay for continuous incubation of HEK293 and LLC-PK1 cells with increasing concentrations of doxorubicin in cell culture media: (A) 3 hours, (B) 24 hours, (C) 48 hours, and (D) 72 hours of incubation.

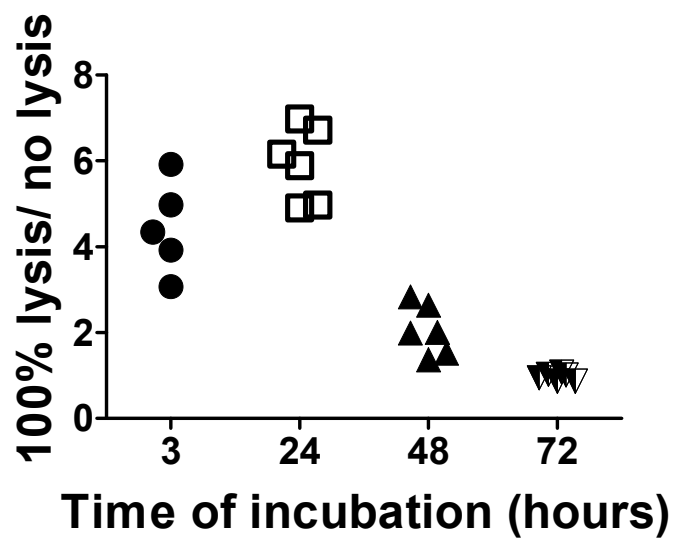


**Figure 4.3.** Loss of ToxiLight® assay sensitivity with prolonged cell incubation: (A) HEK293 cells and (B) LLC-PK1 cells measured by ToxiLight® assay signal.

time points. Furthermore, this assay was not confounded by drugs' intrinsic fluorescent signatures or optical density (see Supplemental Figures).

#### Drug effects on cell viability as a function of incubation time

Drug toxicity using CyQuant NF®, MTS, and ToxiLight® assays were measured after 3 hours, 6 hours, 24 hours, 48 hours, and 72 hours of drug incubation with HEK293 and LLC-PK1 cells using 170,750 cell/well seeding density. MTS assays detected no changes in cell viability at most measured time points and for all tested chemical agents (Figures 4.1 and 4.2). CyQuant NF® and ToxiLight® assays showed an expected trend of higher cell survival at lower doxorubicin hydrochloride and neomycin trisulfate salt hydrate concentrations at all tested time points. Within the first 3 hours of incubation, both drugs produced discernable changes in cell viability as a function of drug concentration. Differences in cell viability did not change significantly for the entire 3 days of culture, although cell recovery was noticeable after 6 hours of cell incubation with doxorubicin and neomycin salts (Figure 4.4). These data matched previously *in vitro* published observations (37). In contrast to incubation with doxorubicin and neomycin salts, both CyQuant NF® and ToxiLight® assays detected increased cell survival at high colchicine concentrations and low cell survival at low colchicine concentrations at 3 hours for HEK293 and both 3 and 6 hours for LLC-PK1 cells (Figure 4.5). This observation was reversed with increasing incubation time. Notably, this toxicity-dose inversion occurs in a gradient manner for both cell lines tested by these two assays. Colchicine exposure of 24 hours was required with both HEK293 and LLC-PK1 cells to establish the expected high drug concentration-high cell death correlation. To evaluate if this

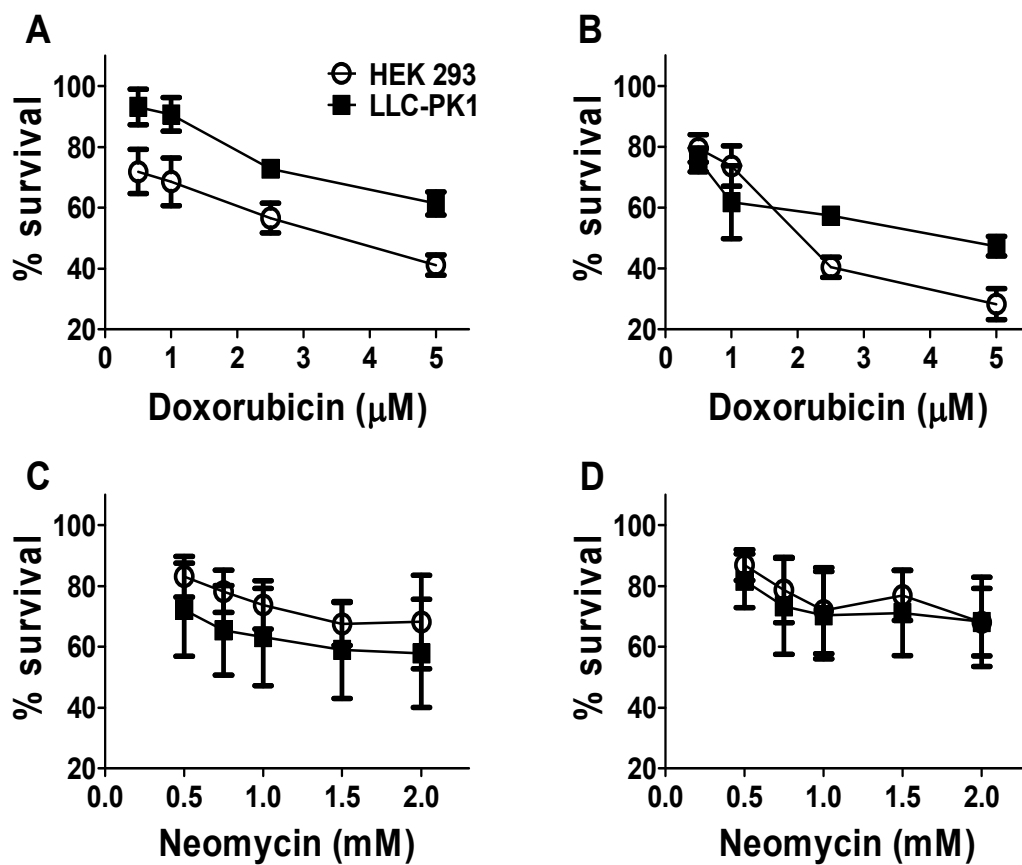


**Figure 4.4.** CyQuant NF® cell toxicity assay of HEK293 and LLC-PK1 cells with doxorubicin and neomycin drugs showing expected dose-dependent high drug concentration-low cell survival: (A) doxorubicin, 3 hours, (B) doxorubicin, 72 hours, (C) neomycin, 3 hours, and (D) neomycin, 24 hours of incubation.

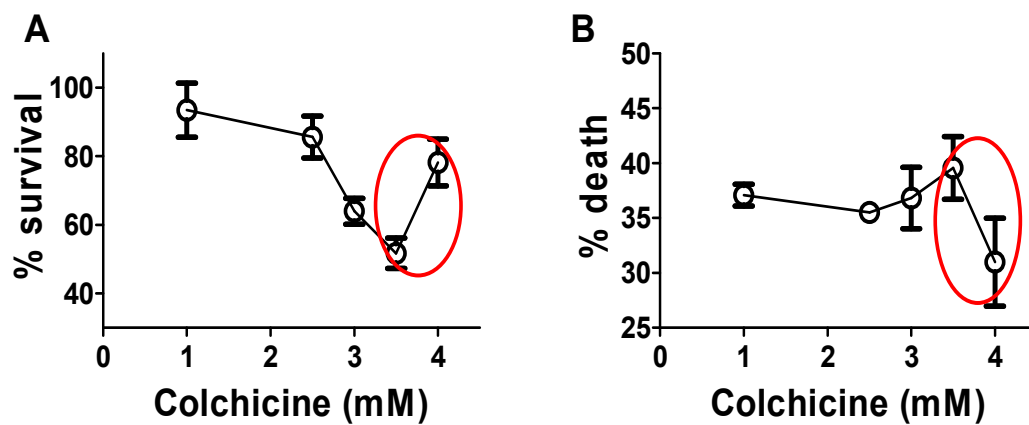


**Figure 4.5.** HEK293 cell viability after 3 hour incubations with colchicine showing increased cell viability at higher drug concentrations measured using (A) CyQuant NF® (% cell survival) and (B) ToxiLight® (% cell death) assays. Red circles indicate NMDRC cytotoxicity.

effect was specific to colchicine, both immortalized cell lines were also exposed to rifampicin and ciprofloxacin. Rifampicin showed a “normal” toxicity relationship (i.e., increasing dose produces corresponding increases in toxicity), whereas ciprofloxacin exhibited a non-monotonic dose response curve (NMDRC (38)) for toxicity, similar also to that from colchicine, for all cell types and all time points tested (Figure 4.6). Primary PT cell cultures exposed to colchicine, dexamethasone, and ciprofloxacin produced the expected normal toxicity curves where increased cell death was observed at higher drug concentrations for all time points tested (Figure 4.7).

#### Drug aggregation studies in media

Aggregation kinetics for colchicine, rifampicin, dexamethasone, and ciprofloxacin in protein-containing cell culture media were explored after 2 hours of incubation. This exploited a commercial Zetasizer instrument capable of detecting particles as small as 4nm in diameter as a standard approach to assessing particle sizes and size distributions in solute environments. Additionally, colchicine was evaluated every 20 min for 2 hours (corresponding to the first measured cell toxicity time point). No drug aggregation was detected in all samples tested (see Supplemental Tables).

#### Facilitated drug-cell permeation studies

To assess whether the observed lack of cell response to drugs at high concentration in culture resulted from limited drug penetration, cell experiments were repeated using increased amounts of DMSO added to media. DMSO is known to increase drug permeation into cells (39). Higher DMSO concentrations in culture media produced no statistically significant changes in cell

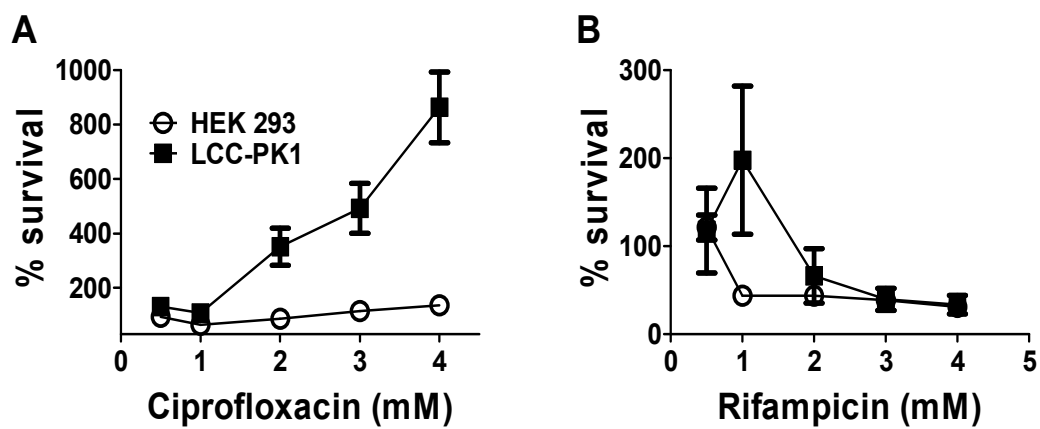


**Figure 4.6.** CyQuant NF® assay of cell line culture viability treated with (A) ciprofloxacin and (B) rifampicin in the media with low (<2%) DMSO after 24 hours of exposure.



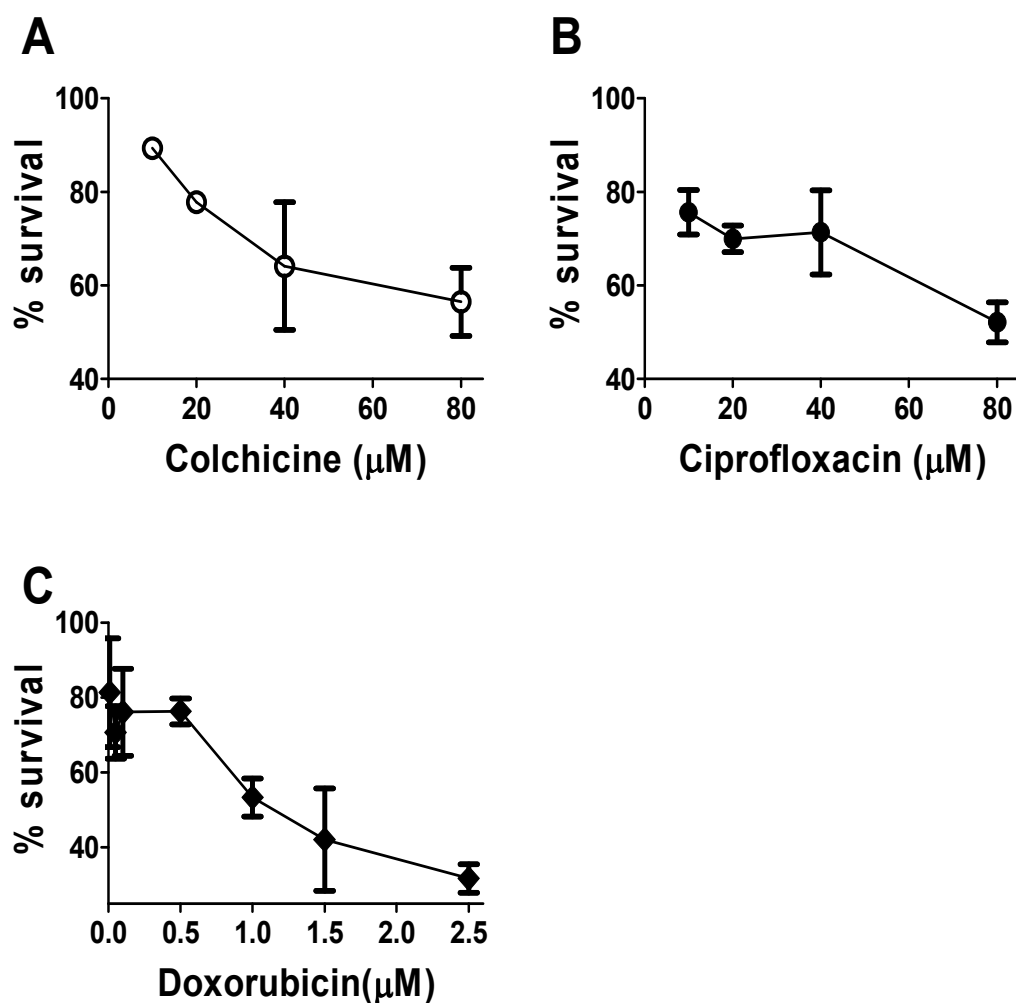


**Figure 4.7.** Viability of primary proximal tubule cells with increasing concentrations of drugs in the culture media as measured by CyQuantNF®: (A) colchicine after 6 hours, (B) ciprofloxacin after 24 hours, and (C) doxorubicin after 72 hours of incubation. See data in Supplemental Figures showing that these drugs do not interfere with the assay.

viability in control cells (i.e., cells exposed to no drug) (see Supplemental Figures). Due to DMSO interference with the ToxiLight® assay and lack of sensitivity associated with the MTS assay, all experiments were performed using the CyQuant NF® assays against new standard curves run in the presence of DMSO. Increased DMSO fractions in the media further exaggerated the NMDRC drug toxicity curves for HEK293 cells and increased cell proliferation in LLC-PK1 cell lines (Figure 4.8). Increasing colchicine incubation time from 3 hours to 72 hours shows gradual reversion of the high drug dose-high cell survival curves back to the expected high drug dose-low cell survival relationship (Figure 4.9). To test whether this phenomenon was specific to colchicine, the same experiments were repeated using dexamethasone, ciprofloxacin, and rifampicin. Dexamethasone produced very similar NMDRC toxicity curves using HEK293 cells starting 3 hours of incubation time point and at 2 days using LLC-PK1 cells (Figure 4.10). Ciprofloxacin toxicity exhibited NMDRC drug toxicity for both cell lines in the media (Figure 4.10). Rifampicin had the expected conventional drug toxicity vs. drug concentration relationship for all cell types (Figure 4.10).

#### Drug effects on cultured cell viability as a function of media-supplied

##### growth factors

The presence of endogenous growth factors in cell culture media in combination with microtubule-destabilizing drugs were previously reported to significantly increase proximal tubule cell proliferation rates in initial stages of cell incubation (40). To explore whether the apparent lack of cell death at high colchicine concentrations resulted from this growth factor presence in cell culture media, experiments were repeated using incomplete PT media (PT media lacking FCS).

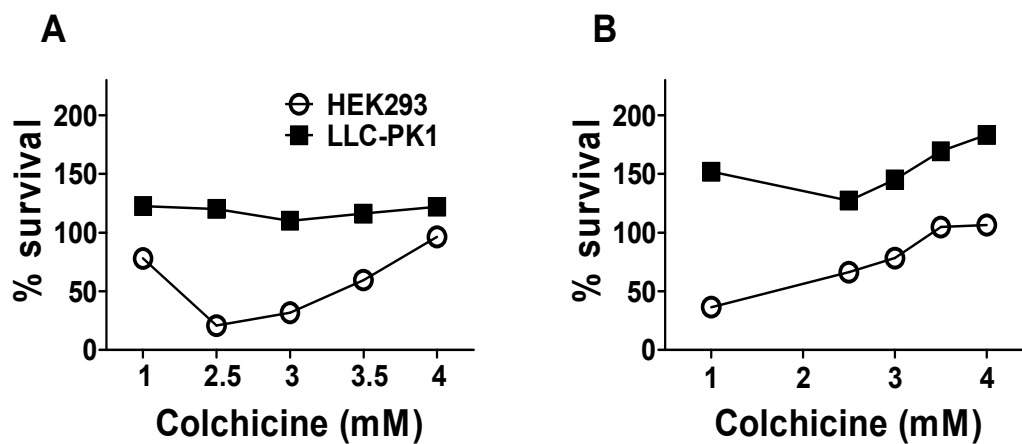


**Figure 4.8.** CyQuant NF® assay of immortalized cell culture viability after (A) 3 and (B) 6 hours of incubation with colchicine in increasing concentrations, showing NMDRC cell toxicity curves for HEK293 cells and increased proliferation for LLC-PK1 cells.

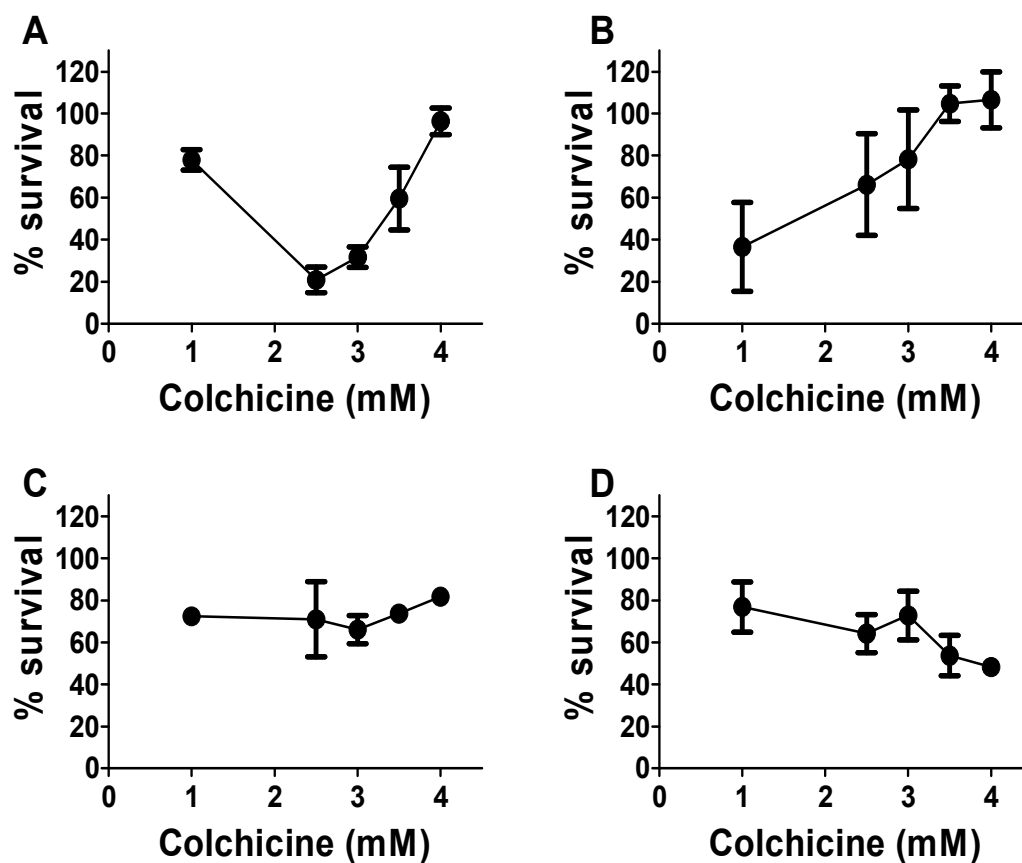


**Figure 4.9.** Time-dependent cell toxicity for HEK 293 cells from (A) 3, (B) 6, (C), 24 and (D) 72 hours of incubation with increasing amounts of colchicine dispensed to culture with increased amounts of DMSO (20%), displaying gradual time-dependent reversal of cell toxicity curves.

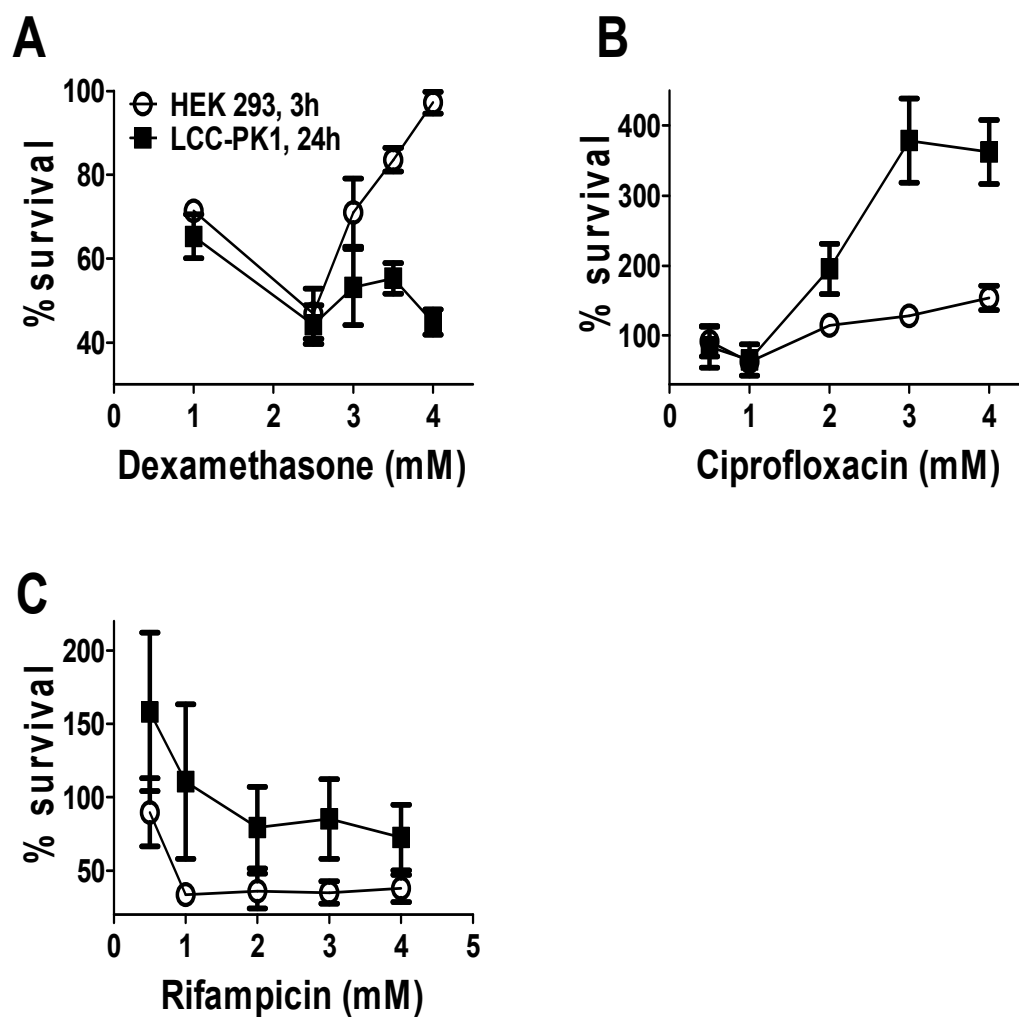


**Figure 4.10.** Cell survival after incubation of the two immortalized cell lines with increasing concentrations of dexamethasone, ciprofloxacin, and rifampicin and increased DMSO over time: (A) dexamethasone after 3 hours of incubation for HEK 293 and 24 hours for LLC-PK1 cells, (B) ciprofloxacin after 24 hours of incubation, (C) rifampicin after 24 hours of incubation.

Early time points – at 3 and 6 hours -- were chosen to ensure that cell death would not be significantly induced by lack of proteins and growth factors associated with FCS absence (see Supplemental Figures). Lack of media-supplied growth factors did not ameliorate or change the observed trend of the NMDRC drug toxicity (Figure 4.11).

#### Drug effects on cell viability as a function of culture confluence

To ascertain whether the observed NMDRC toxicity trends observed resulted from lack of cell-cell interactions in culture, experiments with reduced and increased DMSO in the drug-containing media were repeated on HEK293 and LLC-PK1 cultures using low cell seeding densities of 10,000 cells/well. Considering significant (almost 18-fold) reduction of cell density in these cultures, drug toxicity was assessed at 10-fold lower concentrations as well as concentrations comparable to the high-density cell cultures. All colchicine dose exposures to sub-confluent culture revealed cell toxicity induction at a slower rate than in high-cell density cultures. Even when secondary cell cultures were treated with colchicine in millimolar concentrations (with low DMSO additions), cell death induction required days of continuous drug incubation (Figure 3.12). For example, after 2 days of incubation with 2mM colchicine, both HEK293 and LLC-PK1 cells showed ~20% cell death as compared to untreated controls. Furthermore, these data in general had much more noise reflected by larger standard error bars (see Figure 4.12). All drug incubations produced no observed NMDRC drug dose-cell toxicity behavior (Figure 4.12 and 4.13). Unlike colchicine, ciprofloxacin and rifampicin produced significant (20-70%) changes in cell death after 3 hours of drug incubation in sub-confluent

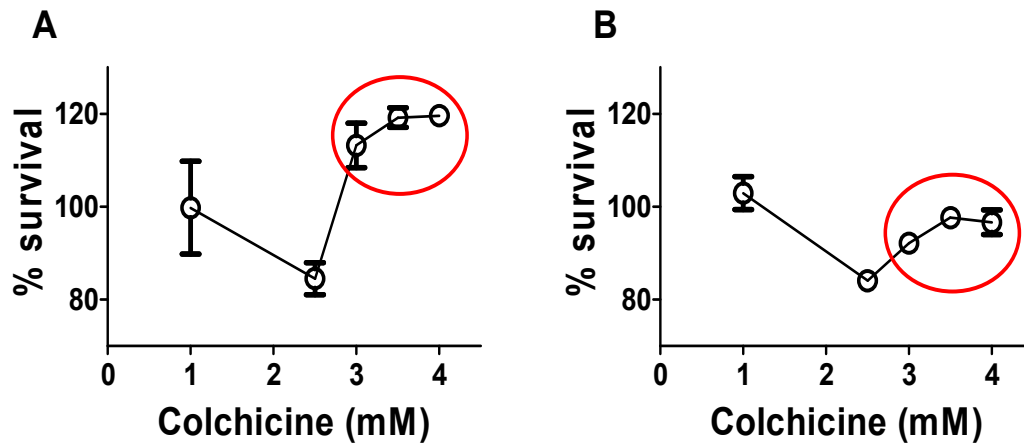


**Figure 4.11.** Cell toxicity due to increasing colchicine concentrations in cell culture media lacking FCS (no endogenous growth factors) at (A) 3 hours with HEK293 cells, and (B) 6 hours with LLC-PK1 cells. Red inserts indicate NMDRC cytotoxicity.

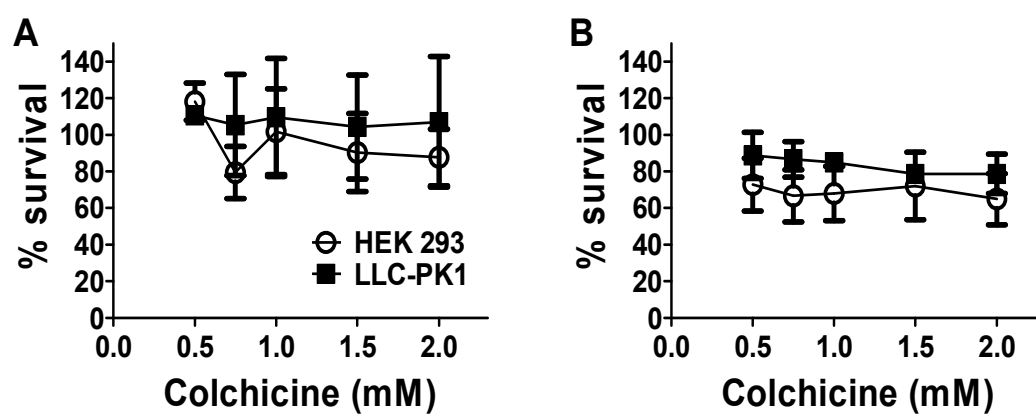


**Figure 4.12.** Cell survival during incubation of increasing colchicine concentrations with  $10^4$  cells/well in culture (A) and (B) with low DMSO additions to media (<2%).



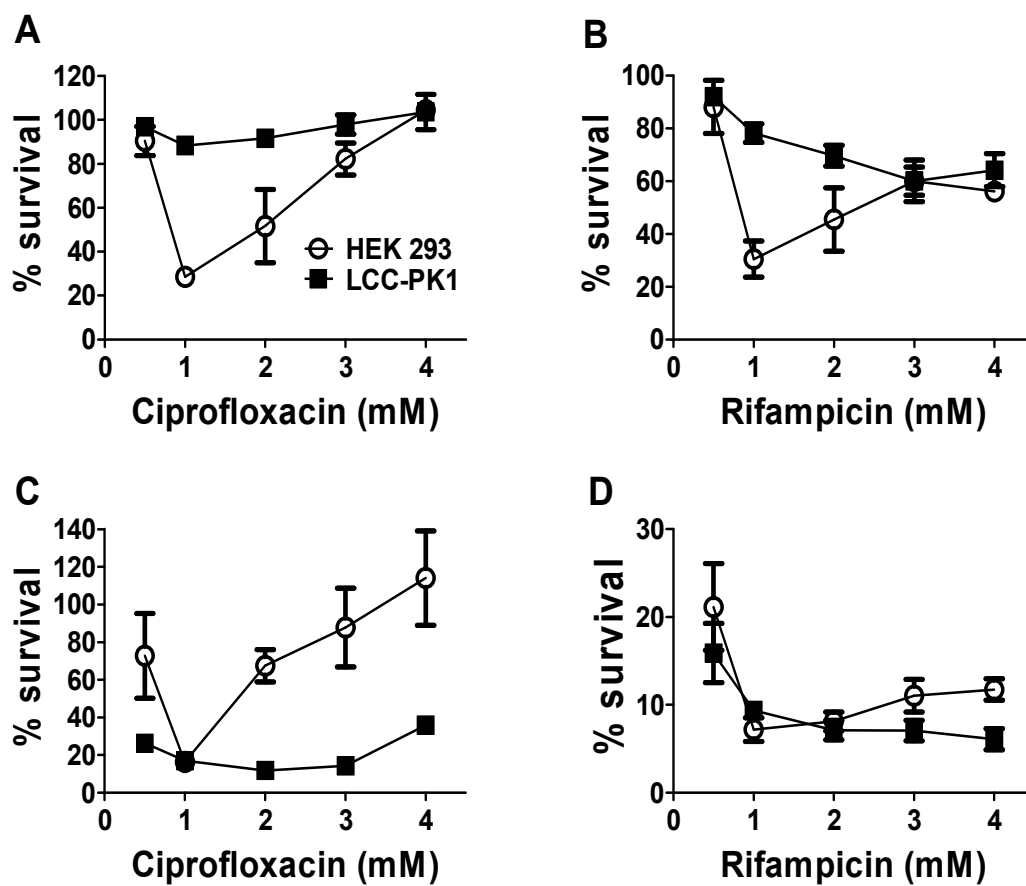


**Figure 4.13.** Cell survival with increasing ciprofloxacin and rifampicin concentrations in low density-seeded ( $10^4$  cells/well) cultures. (A) and (C): ciprofloxacin at 3 and 24 hours of incubation. (B) and (D): rifampicin at 3 and 24 hours of incubation.

cultures. Ciprofloxacin and rifampicin exhibited pronounced NMDRC drug dose-cell toxicity behavior in HEK293 cell cultures at 3 hours, 24 hours, 48 hours, and 72 hours, with little amelioration in cell viability during prolonged incubation. Cell death appeared to be constant at different tested time points for ciprofloxacin, and progressive for rifampicin in this cell line. Amelioration of observed NMDRC drug toxicity with rifampicin in HEK293 cells was noticeable after prolonged drug incubation, but was not fully resolved at 72 hours. No change in NMDRC toxicity curves was observed with ciprofloxacin. Similar to HEK293 cells, LLC-PK1 cells exposed to ciprofloxacin in sub-confluent cultures showed low cell death at high drug concentrations for all tested time points. But unlike HEK293 cell responses, LLC-PK1 cells continued to show reduced cell numbers over the duration of study. Furthermore, LLC-PK1 cells cultured with rifampicin produced no noticeable inversion in drug toxicity kinetics at all the time points (Figure 4.13).

### Discussion

Numerous reports on the use of immortalized kidney cells lines to measure toxicity of new compounds, drug delivery systems, and biomaterials continue to appear annually. Most reports do not explain the choice of cell models or conditions used for their toxicity or biocompatibility assessments, often assuming that transformed cell line monocultures *in vitro* on plastic respond to environmental stimuli similarly to their cellular counterparts *in vivo*. In this work we chose to test this assumption using two transformed kidney cell lines, HEK293 and LLC-PK1, and commonly employed cell culture conditions. Drug-induced cell toxicity was chosen as the simplest comparative endpoint. HEK293 and LLC-PK1 were selected due to their common use by both

industry and academic labs, as well as due to the spectrum of cellular differentiation that these cell lines claim to represent. HEK293 is a human embryonic kidney cell line with non-established kidney cell origin (41, 42). HEK293 cells exhibit no significant brush border, contain no or low amounts of brush border enzymes (for example, gamma-glutamyl-transpeptidase (43) and alkaline phosphatase (44)) or known characteristic kidney cell ligands (e.g., megalin), low endogenous expression of P-glycoprotein efflux pumps, and little or no expression of epithelial cell-characteristic transporters of charged molecules, such as OCT2 (45), organic anionic transporters 1-3 (OAT 1-3) (46-48), and H<sup>+</sup>/peptide intestinal peptide transporters 1 and 2 (PepT1-2) (49, 50). Furthermore, HEK293 cells were found to exhibit neural cell characteristics, such as expression of many neuronal-specific proteins including neurofilament subunits NF-L, NF-M, NF-H and  $\alpha$ -internexin (51). Overall, HEK293 can be categorized as a poorly differentiated kidney cell line with low endogenous expression of relevant epithelial cell markers. Dissimilar to HEK293, LLC-PK1 is an immortalized cell line with far greater resemblance to kidney proximal tubule epithelial cells. LLC-PK1 was originally derived from porcine kidney tissue (52) and found to retain some brush border cellular protrusions (53), cell ligands (53, 54), gamma-glutamyl-transpeptidase and alkaline phosphatase enzymes, and a Na<sup>+</sup>-dependent transport system (11, 53, 55-57). But as for HEK293 cells, LLC-PK1 cells lack glucocorticoid receptors (10), and small molecule transporters (11, 12). LLC-PK1 has been shown to bear many similarities to *in vivo* proximal tubule cells regarding transcellular transport mechanisms, and is considered to be a model of fully differentiated adult epithelial cells (11, 53, 55, 56). In this study, these two immortalized kidney cell line cultures were also compared in parallel drug toxicity assays

with primary mouse kidney proximal tubule epithelial cell cultures *in vitro*. Cells within proximal tubules were isolated and cultured in a 3-D cell culture system previously shown to retain cell differentiation and functional potential (32). Freshly isolated proximal tubule epithelial cells are known to start losing their polarization as quickly as 20 min after extraction (9). Hence, a more complex 3-D culture was chosen to retain epithelial cell character and ensure the phenotypically stable primary vs. immortalized cell comparison to various nephrotoxic drug doses and times. HEK293 and LLC-PK1 cells were also exposed to hydrophobic drugs from different classes and with different pharmacological indications to assess cell toxicity as a function of cell type and not specific drug characteristics. Furthermore, cell titer assays with different modes of optical detection -- absorbance, fluorescence, and luminescence -- were selected to reduce the possibility of drug interference with assay read-out.

A first important finding was recognition that assay sensitivity as well as intrinsic mechanisms of the assay signal production could significantly impact the data obtained. For example, the MTS cell titer assay, among the most abundantly used cell viability methods, was found to be relatively insensitive to small changes in cell numbers (Figures 3.1 and 3.2). MTS is an absorbance-based metabolic enzyme activity assay that estimates the number of viable cells on the assumption that only living cells are capable of reducing the redox-sensitive MTS dye, and that the cell treatment does not change the cellular metabolic rate (58, 59). MTS-obtained toxicity data did not discriminate cell types or drug responses with prolonged drug incubation, pointing towards intrinsic lack of sensitivity independent of culture conditions or drug physicochemical characteristics. ToxiLight® -- a luminescence-based assay -- should suffer from little interference between the

drugs and assay reagents by measuring ATP escaping from cell cytosol during cell rupture (60, 61). Cell necrosis was estimated relative to the 100% cell lysis control performed as a separate experiment. ToxiLight® proved to be more sensitive in this respect than MTS (Figure 4.5), but was also found to suffer from interference with water-miscible DMSO commonly used to dissolve hydrophobic pharmacological agents in media (data not shown). Furthermore, because ToxiLight® is an ATP accumulation-based assay, upon prolonged incubation, its sensitivity drops 5-7 fold after 3 days depending on the cell line (Figure 4.3). Overall, ToxiLight® was found to be a sensitive assay for time points below 24 hours of cell assessment in culture. The CyQuant NF® fluorescence-based assay measures cell number as a function of a DNA-binding dye (62). The assay was not confounded by the drugs' intrinsic fluorescence (see Supplemental Figures). This optical assay was found to be as sensitive as ToxiLight® without being affected by DMSO additions or cell culture conditions.

Drug-induced toxicity in kidney proximal tubule cells *in vivo* is complex, involving drug accumulation in the cell, drug interaction with its targets, as well as possible drug biotransformation by cellular enzymes and metabolism by cytochrome P450 (CYPs) (27, 30, 63). Many influx and efflux transporters, as well as the drug's cellular targets, are missing in immortalized cell lines. Hence, we sought to explore and compare cell lines' abilities to respond to known drug toxicities using known pharmacological agents. Six different drugs -- neomycin, doxorubicin, dexamethasone, colchicine, rifampicin, and ciprofloxacin -- were selected for toxicity assessments in cell cultures. Neomycin and doxorubicin were purchased as soluble salt formulations, and hence had better solubility in media than other drugs used in their native free

base or acid hydrophobic form. These differences in physicochemical properties of the tested agents provided additional insight into toxicity dose-response characteristics between primary and immortalized cells. To ensure that cell toxicity was not affected by drugs' abilities to enter cells, all hydrophobic drugs employed had partition coefficient ( $\log P$ ) values below 2.0 (see Supplemental Tables, ref. (64-68)), reducing possible aggregation in full cell culture media (69). Drug-media aggregation potential was further reduced by using kinetic instead of thermodynamic solubility conditions, achieved by re-suspending drugs in DMSO prior to addition to cell culture media (70). Furthermore, drug aggregation was directly assessed for all drugs that showed NMDRC cell toxicity behavior (see Supplemental Figures). No significant aggregates above the instrument's 4nm sensitivity limit were observed in full media by particle size analysis, consistent with previous reports of low drug aggregation for molecules with  $\log P$  values below 5 (69).

Exposing HEK293 and LLC-PK1 cell lines and primary PT epithelial cells to the six drugs selected for this study revealed distinctive differences in cell toxicity between different formulations for transformed cell lines, as well as between primary vs. immortalized cell lines. Both immortalized cell lines produced cell toxicity proportional to drug exposure for water soluble drug formulations -- neomycin and doxorubicin (Figure 4.4), but exhibited non-monotonic dose response toxicity curves for high drug concentrations for all hydrophobic drugs but rifampicin (Figures 4.5, 4.6, 4.8). NMDRC drug toxicity was replicated by titer assays with different assessment mechanisms (Figure 4.5), and therefore is not likely to be an artifact of drug-assay interactions. Unlike immortalized cells, primary PT epithelial cells in a 3-D hydrogel culture (32) that deters rapid de-differentiation seen in these cells on 2-D surfaces (35), produced cell death

proportional to drug amounts applied to cultures, independent of drug formulation or duration of drug exposure (Figure 4.7). NMDRC behavior is a newly documented anomalous dose-response behavior observed both *in vivo* and *in vitro* (38). It is characterized by both 'U-shape' and 'inverted U-shape' dose-cell toxicity curves and is most commonly exhibited by endocrine-disrupting drugs and DNA-reactive carcinogens (71). To date over 1600 cases of chemicals responding with NMDRC dose-toxicity curves have been published (71). Although NMDRC and its clinical significance are still highly debated, several modes of NMDRC induction have been proposed: 1. a membrane transporter model where different subtypes of the same receptor have different affinities for the ligand and opposing downstream function, 2. increased DNA-repair model that is induced upon drug exposure, 3. increased rate of mutation model where there is cell cycle acceleration after toxic damage, 4. induction of proliferation model upon low drug stimulation (38). Current NMDRC scenarios show the breadth of possibilities that can result in atypical drug-toxicity relationships and these most likely do not describe all of the possible outcomes, only specific cases for which NMDRC behavior has been scientifically explained. From all the tested drugs in this study, doxorubicin was the only drug with a well-recognized DNA-damaging profile yet lacking NMDRC-type behavior. Furthermore, since NMDRC was prominent in these short-term culture experiments, proliferation and induction of mutations seems to be unlikely explanations. Hence, NMDRC in immortalized cell lines was mediated possibly by some form of membrane transporter or downstream intracellular drug detoxification mechanism. Immortalized cell lines exhibit lack of *in vivo*-relevant transporters and intracellular receptors for the tested drugs, but since NMDRC toxicity patterns cannot easily be explained by passive diffusion, some form of active transport is

plausible.

To evaluate whether the drugs' intrinsic inability to enter cells prompted the observed NMDRC toxicity behavior in transformed cell lines, experiments were repeated with increased DMSO in the media to enhance cell permeation (39). The NMDRC cell toxicity behavior was retained for both HEK293 and LLC-PK1 cells (Figure 4.9, 4.10). Additionally, more pronounced NMDRC drug concentration-cell toxicity behavior was also observed at lower drug concentrations (Figure 4.9). Prolonged cell incubation with these drugs revealed that this NMDRC cell toxicity over time and concentration could be reversed for some drugs, like colchicine (Figure 4.9), but not others (i.e., ciprofloxacin, data not shown). Because both immortalized cell lines were affected and only LLC-PK1 cells are known to induce P-glycoprotein upon prolonged drug exposure (72), and at least one drug reverted to normal toxicity curves within 24 hours, it was not likely that efflux pumps were responsible for changing the mechanism of cell-drug toxicity profiles. The DMSO-enhanced drug permeability experiments were not specific enough to pinpoint membrane transporter mechanisms that elicit the observed NMDRC response. However, they showed that lack of both drug intracellular penetration and efflux were not likely reasons for atypical behavior observed.

Drugs that showed NMDRC toxicity behavior in media *in vitro* -- colchicine, dexamethasone, and ciprofloxacin -- share some known capability to induce toxicity through microtubule disruption in mammalian cells (73-75). Previously, microtubule inhibitor drugs were shown to induce cell proliferation when administered with growth factors (40). Since some hydrophobic drugs induced cell proliferation *in vitro* (Figures 4.6 and 4.8), and full cell culture media contains endogenous



growth factors (76), the hypothesis that observed lack of cell death at high drug concentrations might alternatively be attributed to confounding induction of cell proliferation. Drug toxicity experiments with colchicine, a classic microtubule-disrupting drug, in media that contained no growth factors were repeated at 3 and 6 hours of culture. Early time points were selected to reduce cell stress from depleted media-based starvation (see Supplemental Figures) and because previously published results ascertained early time points to be the most significant in growth factor-microtubule inhibitor drug synergy (40). No changes in the NMDRC drug toxicity behavior of colchicine were observed in the absence of serum-supplied growth factors (Figure 4.11), indicating that media components were not responsible for NMDRC cell toxicities.

*In vivo*, paracellular transport (transport between epithelial cells) can supplement transcellular epithelial cell drug up-take and might be significant *in vivo* in kidney PT cell polarization-dependent toxicity mechanisms (i.e., apical vs. basal membrane drug uptake pathways) (26). Paracellular/transcellular comparisons for transport-aided drug accumulation and toxicity is irrelevant in non-confluent cell cultures lacking tight junctions. Therefore, to evaluate possible contributions to basal-apical receptor-facilitated drug uptake and resultant NMDRC toxicity, cell culture confluence effects were also explored. Methods for assessing *in vitro* cellular toxicity vary significantly in the published literature, with many methods using seeded cells sufficient to create a monolayer, or as few as 10,000 cells/well, which eliminates immediate cell-cell interactions even in a 96-well format (77-82). Data discussed to this point in this study used cells initially seeded/cultured at nearly 80% confluence, and producing 100% confluence for controls (i.e., seeded wells not exposed to drugs) after 3 days of culture (see Supplemental

Figures). Experiments with low and high DMSO concentrations (i.e., less than 2% DMSO (low DMSO) and less than 20% (high DMSO) at highest tested concentrations) in media additions were repeated for colchicine, ciprofloxacin, and rifampicin with cell cultures that were seeded at 10,000 cells/well (i.e., low density) for both LLC-PK1 and HEK293 cells. Both sub-confluent and confluent cultures required nearly the same drug concentration to induce toxicity. Furthermore, sub-confluent cultures were much slower responding to drugs with observable toxicity than confluent cultures for select drugs (Figure 4.12). Nonetheless, no significant changes in NMDRC toxicity were observed between sub-confluent and confluent cultures: drugs that exhibited pronounced anomalous NMDRC toxicities retained this profile, and drugs that exhibited normal toxicities with increasing drug concentration maintained this normal behavior in 10,000 cell/well cultures (Figure 4.13). These data indicate that paracellular drug uptake of hydrophobic drugs might be important to PT toxicity *in vivo*, but is not responsible for the NMDRC toxicity observed in the HEK293 and LLC-PK1 transformed cell lines *in vitro*.

### Conclusions

This study considered several parameters commonly varied in published reports of *in vitro*-based drug toxicity assays: primary and immortalized cell lines, cell culture confluence, and different toxicity assessment assays. All drugs in this study have been extensively used *in vivo* with known dose-response behaviors and toxicities (83-87). Primary PT-derived cells cultured and tested in their native-like 3-D environment produced expected dose-response curves unperturbed by 2-D culture conditions. Unlike their primary counterparts, immortalized cells showed NMDRC

toxicity profiles with increasing drug concentrations for three out of four tested hydrophobic drugs. Interestingly, all three of these drugs - colchicine, dexamethasone, and ciprofloxacin -- rely *in vivo* and in primary epithelial cultures on carrier-mediated transport (colchicine (88)), active transport (ciprofloxacin (89, 90)), and cellular targets (glucocorticoid receptor for dexamethasone (91)) that are notably absent in both LLC-PK1 and HEK293 cells (10, 92). Furthermore, rifampicin, the only hydrophobic drug that did not produce NMDRC toxicity in immortalized cell lines, is taken up by cells via passive transport pathways ubiquitous to all cells (93, 94). These data cannot distinguish whether observed NMDRC cell toxicity resulted from alterations to cellular drug accumulation seen in transformed cell lines as a result of their missing influx and efflux transporters, or due instead to altered ability of these secondary cells to process toxic agents due to their missing intracellular targets. Nonetheless, these data clearly support the need for using validated cell models that provide the appropriate complexity, congruence, and analogous molecular structures and functional pathways as primary cells as required for predicting drug interactions. Only primary proximal tubule epithelial cells exhibited *in vivo*-relevant toxicity profiles for all drugs, all formulations, and all time points. The LLC-PK1 immortalized cell line with many features of the primary proximal tubule cells showed NMDRC toxicity behavior for hydrophobic agents, but this atypical response was far less significant than that seen in HEK293 cells. HEK293 cells carry little resemblance to primary kidney cells, and exhibited atypical toxicity behavior that was not cell culture technique-, cell media-, or cell assay-dependent. Results from this study clearly indicate: 1) inability of immortalized cell lines to respond normally to toxicities imposed by many hydrophobic agents, including common drugs, and 2) high variability of results -- spanning from 'non-toxic' to

'highly toxic' -- for transformed cell lines experiencing the same agent under simple modifications to cell culture conditions, including seeding density (confluence), toxic drug exposure assay time point, drug log P value, or type of cell assay.

Significant differences between primary PT and immortalized HEK293 and LLC-PK1 cell cultures in their ability to assess toxicity of hydrophobic agents were shown. Changes in cell culture methods or cell evaluation conditions produced highly variable outcomes for the same agents in transformed kidney cell lines versus primary proximal tubule epithelial cells. Immortalized kidney cell lines used for *in vitro* testing novel therapeutics with unknown toxicity modalities demonstrated little reliability to predict *in vivo* drug toxicity behaviors.

#### Acknowledgements

A. Cheung and H. Herd (University of Utah, USA) are thanked for providing HEK293 cell lines and useful guidance with particle sizing, respectively. Prof. B. Mann and Prof. G. Prestwich (Univ. Utah, USA) are thanked for gifts of polymer hydrogel precursors and technical guidance in their use.

#### References

1. Lash L.H. Principles and methods for renal toxicology. In: Hayes AW, editor. Principles and Methods of Toxicology 5th ed. New York, NY: Informa Heath Care USA, Inc.; 2007. p. 1529-30.
2. Zhang K. and Rayburn E.R. Linkage between toxicology of drugs and metabolism. In: Gad SM, editor. Preclinical Development Handbook: ADME and Biopharmaceutical Properties. Hoboken, NJ: John Wiley&Sons, Inc.; 2008. p. 995-1000.
3. Delcommenne M. and Streuli C.H. Control of integrin expression by extracellular matrix. J Biol Chem. 1995 Nov 10;270(45):26794-801.

4. Ghosh S., Spagnoli G.C., Martin I., Ploegert S., Demougin P., and Heberer M., et al. Three-dimensional culture of melanoma cells profoundly affects gene expression profile: a high density oligonucleotide array study. *Journal of Cellular Physiology*. 2005 Aug;204(2):522-31.
5. Gomez-Lechon M.J., Jover R., Donato T., Ponsoda X., Rodriguez C., and Stenzel K.G., et al. Long-term expression of differentiated functions in hepatocytes cultured in three-dimensional collagen matrix. *J Cell Physiol*. 1998 Dec;177(4):553-62.
6. Lim S.W., Li C., Ahn K.O., Kim J., Moon I.S., and Ahn C., et al. Cyclosporine-induced renal injury induces toll-like receptor and maturation of dendritic cells. *Transplantation*. 2005 Sep 15;80(5):691-9.
7. McLarnon S., Holden D., Ward D., Jones M., Elliott A., and Riccardi D. Aminoglycoside antibiotics induce pH-sensitive activation of the calcium-sensing receptor. *Biochemical and Biophysical Research Communications*. 2002 Sep 13;297(1):71-7.
8. Motoyoshi Y., Matsusaka T., Saito A., Pastan I., Willnow T.E., and Mizutani S., et al. Megalin contributes to the early injury of proximal tubule cells during nonselective proteinuria. *Kidney Int*. 2008 Nov;74(10):1262-9.
9. Rebelo L., Carmo-Fonseca M., and Moura T.F. Redistribution of microvilli and membrane enzymes in isolated rat proximal tubule cells. *Biology of the cell / under the auspices of the European Cell Biology Organization*. 1992;74(2):203-9.
10. Gowda B., Sar M., Mu X., Cidlowski J., and Welbourne T. Coordinate modulation of glucocorticoid receptor and glutaminase gene expression in LLC-PK1-F+ cells. *Am J Physiol*. 1996 Mar;270(3 Pt 1):C825-31.
11. Grundemann D., Babin-Ebell J., Martel F., Ording N., Schmidt A., and Schomig E. Primary structure and functional expression of the apical organic cation transporter from kidney epithelial LLC-PK1 cells. *J Biol Chem*. 1997 Apr 18;272(16):10408-13.
12. Leibach F.H. and Ganapathy V. Peptide transporters in the intestine and the kidney. *Annu Rev Nutr*. 1996;16:99-119.
13. Avdeef A. Leakiness and size exclusion of paracellular channels in cultured epithelial cell monolayers-interlaboratory comparison. *Pharm Res*. 2010 Mar;27(3):480-9.
14. Hughes P., Marshall D., Reid Y., Parkes H., and Gelber C. The costs of using unauthenticated, over-passaged cell lines: how much more data do we need? *Biotechniques*. 2007 Nov;43(5):575,

7-8, 81-2 passim.

15. Thonemann B., Schmalz G., Hiller K.A., and Schweikl H. Responses of L929 mouse fibroblasts, primary and immortalized bovine dental papilla-derived cell lines to dental resin components. *Dent Mater*. 2002 Jun;18(4):318-23.

16. Allen D.G., Riviere J.E., and Monteiro-Riviere N.A. Cytokine induction as a measure of cutaneous toxicity in primary and immortalized porcine keratinocytes exposed to jet fuels, and their relationship to normal human epidermal keratinocytes. *Toxicol Lett*. 2001 Mar 8;119(3):209-17.

17. Pan C., Kumar C., Bohl S., Klingmueller U., and Mann M. Comparative proteomic phenotyping of cell lines and primary cells to assess preservation of cell type-specific functions. *Mol Cell Proteomics*. 2009 Mar;8(3):443-50.

18. Kagan L. and Rieck P.W. [A comparative in vitro analysis of primary and immortalized keratocytes]. *Ophthalmologe*. 2010 Apr;107(4):341-6.

19. Chamberlain L.M., Godek M.L., Gonzalez-Juarrero M., and Grainger D.W. Phenotypic non-equivalence of murine (monocyte-) macrophage cells in biomaterial and inflammatory models. *J Biomed Mater Res A*. 2009 Mar 15;88(4):858-71.

20. Holt D.J., Chamberlain L.M., and Grainger D.W. Cell-cell signaling in co-cultures of macrophages and fibroblasts. *Biomaterials*. 2010 Dec;31(36):9382-94.

21. Yamanishi Y., Kitaura J., Izawa K., Kaitani A., Komeno Y., and Nakamura M., et al. TIM1 is an endogenous ligand for LMIR5/CD300b: LMIR5 deficiency ameliorates mouse kidney ischemia/reperfusion injury. *J Exp Med*. 2010 Jul 5;207(7):1501-11.

22. Cukierman E., Pankov R., Stevens D.R., and Yamada K.M. Taking cell-matrix adhesions to the third dimension. *Science*. 2001 Nov 23;294(5547):1708-12.

23. Geiger B. and Bershadsky A. Exploring the neighborhood: adhesion-coupled cell mechanosensors. *Cell*. 2002 Jul 26;110(2):139-42.

24. Geiger B., Bershadsky A., Pankov R., and Yamada K.M. Transmembrane crosstalk between the extracellular matrix--cytoskeleton crosstalk. *Nat Rev Mol Cell Biol*. 2001 Nov;2(11):793-805.

25. Sastry S.K. and Burridge K. Focal adhesions: a nexus for intracellular signaling and cytoskeletal dynamics. *Exp Cell Res*. 2000 Nov 25;261(1):25-36.

26. Rush G.F. and Hook J.B. The kidney as a target organ for toxicity. In: Cohen GM, editor.

Target organ toxicity. Boca Raton, FL: CRC Press, Inc.; 1986. p. 6-10.

27. Pabla N. and Dong Z. Cisplatin nephrotoxicity: mechanisms and renoprotective strategies. *Kidney Int.* 2008 May;73(9):994-1007.

28. Shiraki N., Hamada A., Ohmura T., Tokunaga J., Oyama N., and Nakano M. Increase in doxorubicin cytotoxicity by inhibition of P-glycoprotein activity with lomerizine. *Biological & Pharmaceutical Bulletin.* 2001 May;24(5):555-7.

29. Druley T.E., Stein W.D., Ruth A., and Roninson I.B. P-glycoprotein-mediated colchicine resistance in different cell lines correlates with the effects of colchicine on P-glycoprotein conformation. *Biochemistry.* 2001 Apr 10;40(14):4323-31.

30. Pinzani V., Bressolle F., Haug I.J., Galtier M., Blayac J.P., and Balmes P. Cisplatin-induced renal toxicity and toxicity-modulating strategies: a review. *Cancer Chemother Pharmacol.* 1994;35(1):1-9.

31. Hartmann F. and Bissell D.M. Metabolism of heme and bilirubin in rat and human small intestinal mucosa. *J Clin Invest.* 1982 Jul;70(1):23-9.

32. Astashkina A., Mann B., Prestwich G., and Grainger D.W. A 3-D organoid kidney culture model engineered for high throughput nephrotoxicity assays. *Biomaterials.* Epub 2012.

33. Godek M.L., Michel R., Chamberlain L.M., Castner D.G., and Grainger D.W. Adsorbed serum albumin is permissive to macrophage attachment to perfluorocarbon polymer surfaces in culture. *J Biomed Mater Res A.* 2009 Feb;88(2):503-19.

34. Miller R.L., Zhang P., Chen T., Rohrwasser A., and Nelson R.D. Automated method for the isolation of collecting ducts. *Am J Physiol Renal Physiol.* 2006 Jul;291(1):F236-45.

35. Terryn S., Jouret F., Vandenabeele F., Smolders I., Moreels M., and Devuyst O, et al. A primary culture of mouse proximal tubular cells, established on collagen-coated membranes. *Am J Physiol Renal Physiol.* 2007 Aug;293(2):F476-85.

36. Prestwich G.D. Evaluating drug efficacy and toxicology in three dimensions: using synthetic extracellular matrices in drug discovery. *Accounts of Chemical Research.* 2008 Jan;41(1):139-48.

37. Hickey C.W., Blaise C., and Costan G. Microtesting appraisal of ATP and cell recovery toxicity end points after acute exposure of *Selenastrum capricornutum* to selected chemicals. *Environmental Toxicology and Water Quality.* 1991;6(4):383-403.

38. Conolly R.B. and Lutz W.K. Nonmonotonic dose-response relationships: mechanistic basis, kinetic modeling, and implications for risk assessment. *Toxicol Sci.* 2004 Jan;77(1):151-7.
39. Kurihara-Bergstrom T., Flynn G.L., and Higuchi W.I. Physicochemical study of percutaneous absorption enhancement by dimethyl sulfoxide: dimethyl sulfoxide mediation of vidarabine (ara-A) permeation of hairless mouse skin. *J Invest Dermatol.* 1987 Sep;89(3):274-80.
40. Otto A.M., Zumbe A., Gibson L., Kubler A.M. and Jimenez de Asua L. Cytoskeleton-disrupting drugs enhance effect of growth factors and hormones on initiation of DNA synthesis. *Proc Natl Acad Sci U S A.* 1979 Dec;76(12):6435-8.
41. Graham F.L., Smiley J., Russell W.C., and Nairn R. Characteristics of a human cell line transformed by DNA from human adenovirus type 5. *J Gen Virol.* 1977 Jul;36(1):59-74.
42. Louis N., Eveleigh C., and Graham F.L. Cloning and sequencing of the cellular-viral junctions from the human adenovirus type 5 transformed 293 cell line. *Virology.* 1997 Jul 7;233(2):423-9.
43. Benesic A., Schwerdt G., Mildenberger S., Freudinger R., Gordjani N., and Gekle M. Disturbed Ca<sup>2+</sup>-signaling by chloroacetaldehyde: a possible cause for chronic ifosfamide nephrotoxicity. *Kidney International.* 2005 Nov;68(5):2029-41.
44. Lenz W., Herten M., Gerzer R., and Drummer C. Regulation of natriuretic peptide (urodilatin) release in a human kidney cell line. *Kidney Int.* 1999 Jan;55(1):91-9.
45. Chen Y., Li S., Brown C., Cheatham S., Castro R.A., and Leabman M.K., et al. Effect of genetic variation in the organic cation transporter 2 on the renal elimination of metformin. *Pharmacogenet Genomics.* 2009 Jul;19(7):497-504.
46. Hagos Y., Krick W., Bräulke T., Mühlhausen C., Burckhardt G., and Burckhardt B.C. Organic anion transporters OAT1 and OAT4 mediate the high affinity transport of glutarate derivatives accumulating in patients with glutaric acidurias. *Pflugers Arch.* 2008 Oct;457(1):223-31.
47. Sato M., Mamada H., Anzai N., Shirasaka Y., Nakanishi T., Tamai I. Renal secretion of uric acid by organic anion transporter 2 (OAT2/SLC22A7) in human. *Biol Pharm Bull.* 2010;33(3):498-503.
48. Erdman A.R., Mangravite L.M., Urban T.J., Lagpacan L.L., Castro R.A., and de la Cruz M., et al. The human organic anion transporter 3 (OAT3; SLC22A8): genetic variation and functional genomics. *Am J Physiol Renal Physiol.* 2006 Apr;290(4):F905-12.
49. Anderle P., Nielsen C.U., Pinsonneault J., Krog P.L., Brodin B., and Sadee W. Genetic



variants of the human dipeptide transporter PEPT1. *J Pharmacol Exp Ther.* 2006 Feb;316(2):636-46.

50. Noshiro R., Anzai N., Sakata T., Miyazaki H., Terada T., and Shin H.J., et al. The PDZ domain protein PDZK1 interacts with human peptide transporter PEPT2 and enhances its transport activity. *Kidney Int.* 2006 Jul;70(2):275-82.

51. Shaw G., Morse S., Ararat M., and Graham F.L. Preferential transformation of human neuronal cells by human adenoviruses and the origin of HEK293 cells. *FASEB J.* 2002 Jun;16(8):869-71.

52. Hull R.N., Cherry W.R., and Weaver G.W. The origin and characteristics of a pig kidney cell strain, LLC-PK. *In Vitro.* 1976 Oct;12(10):670-7.

53. Nielsen R., Birn H., Moestrup S.K., Nielsen M., Verroust P., and Christensen E.I. Characterization of a kidney proximal tubule cell line, LLC-PK1, expressing endocytotic active megalin. *J Am Soc Nephrol.* 1998 Oct;9(10):1767-76.

54. Verkoelen C.F., van der Boom B.G., Kok D.J., Houtsmuller A.B., Visser P., and Schroder F.H., et al. Cell type-specific acquired protection from crystal adherence by renal tubule cells in culture. *Kidney International.* 1999 Apr;55(4):1426-33.

55. Rabito C.A. Occluding junctions in a renal cell line (LLC-PK1) with characteristics of proximal tubular cells. *Am J Physiol.* 1986 Apr;250(4 Pt 2):F734-43.

56. Gstraunthaler G., Pfaller W., and Kotanko P. Biochemical characterization of renal epithelial cell cultures (LLC-PK1 and MDCK). *Am J Physiol.* 1985 Apr;248(4 Pt 2):F536-44.

57. Amsler K., Murray J., Cruz R., and Chen J.L.. Chronic TPA treatment inhibits expression of proximal tubule-specific properties by LLC-PK1 cells. *The American Journal of Physiology.* 1996 Jan;270(1 Pt 1):C332-40.

58. Cory A.H., Owen T.C., Barltrop J.A., and Cory J.G. Use of an aqueous soluble tetrazolium/formazan assay for cell growth assays in culture. *Cancer Commun.* 1991 Jul;3(7):207-12.

59. Mosmann T. Rapid colorimetric assay for cellular growth and survival: application to proliferation and cytotoxicity assays. *J Immunol Methods.* 1983 Dec 16;65(1-2):55-63.

60. Crouch S.P., Kozlowski R., Slater K.J., and Fletcher J. The use of ATP bioluminescence as a measure of cell proliferation and cytotoxicity. *J Immunol Methods.* 1993 Mar 15;160(1):81-8.

61. Olsson T., Gulliksson H., Palmeborn M., Bergstrom K., and Thore A. Leakage of adenylate kinase from stored blood cells. *J Appl Biochem.* 1983 Dec;5(6):437-45.
62. Jones L.J., Gray M., Yue S.T., Haugland R.P., and Singer V.L. Sensitive determination of cell number using the CyQUANT cell proliferation assay. *J Immunol Methods.* 2001 Aug 1;254(1-2):85-98.
63. Yao X., Panichpisal K., Kurtzman N., and Nugent K. Cisplatin nephrotoxicity: a review. *The American Journal of the Medical Sciences.* 2007 Aug;334(2):115-24.
64. Mora P., Eperon S., Felt-Baeyens O., Gurny R., Sagodira S., and Breton P., et al. Trans-scleral diffusion of triamcinolone acetonide. *Curr Eye Res.* 2005 May;30(5):355-61.
65. Tang-Wai D.F., Brossi A., Arnold L.D., and Gros P. The nitrogen of the acetamido group of colchicine modulates P-glycoprotein-mediated multidrug resistance. *Biochemistry.* 1993 Jun 29;32(25):6470-6.
66. Beck R., van Keyserlingk J., Fischer U., Guthoff R., and Drewelow B. Penetration of ciprofloxacin, norfloxacin and ofloxacin into the aqueous humor using different topical application modes. *Graefes Arch Clin Exp Ophthalmol.* 1999 Feb;237(2):89-92.
67. Mehta S.K., Kaur G., and Bhasin K.K. Analysis of Tween based microemulsion in the presence of TB drug rifampicin. *Colloids Surf B Biointerfaces.* 2007 Oct 15;60(1):95-104.
68. Al-Hiari Y., Qandil A., Al-Zoubi R., Alzweiri M., Darwish R., and Shattat G., et al. Synthesis and antibacterial activity of novel 7-haloanilino-8-nitrofluoroquinolone derivatives. *Medicinal Chemistry Research.* 1-7.
69. Doak A.K., Wille H., Prusiner S.B., and Shoichet B.K. Colloid formation by drugs in simulated intestinal fluid. *J Med Chem.* 2010 May 27;53(10):4259-65.
70. Dehring K.A., Workman H.L., Miller K.D., Mandagere A., and Poole S.K. Automated robotic liquid handling/laser-based nephelometry system for high throughput measurement of kinetic aqueous solubility. *J Pharm Biomed Anal.* 2004 Nov 15;36(3):447-56.
71. Calabrese E.J. and Baldwin L.A. Hormesis: a generalizable and unifying hypothesis. *Crit Rev Toxicol.* 2001 Jul;31(4-5):353-424.
72. van der Sandt I.C., Blom-Roosemalen M.C., de Boer A.G., and Breimer D.D. Specificity of doxorubicin versus rhodamine-123 in assessing P-glycoprotein functionality in the LLC-PK1,

LLC-PK1:MDR1 and Caco-2 cell lines. *Eur J Pharm Sci.* 2000 Sep;11(3):207-14.

73. Craddock V.M., Hill R.J., and Henderson A.R. Stimulation of DNA replication in rat esophagus and stomach by the trichothecene mycotoxin diacetoxyscirpenol. *Cancer Lett.* 1987 Dec;38(1-2):199-208.

74. O'Brien E.T., Perkins S.L., Roberts B.C., and Epstein D.L. Dexamethasone inhibits trabecular cell retraction. *Exp Eye Res.* 1996 Jun;62(6):675-88.

75. Sanchez-Alcazar J.A., Rodriguez-Hernandez A., Cordero M.D., Fernandez-Ayala D.J., Brea-Calvo G., and Garcia K., et al. The apoptotic microtubule network preserves plasma membrane integrity during the execution phase of apoptosis. *Apoptosis.* 2007 Jul;12(7):1195-208.

76. Chen L., Mao S.J., and Larsen W.J. Identification of a factor in fetal bovine serum that stabilizes the cumulus extracellular matrix. A role for a member of the inter-alpha-trypsin inhibitor family. *J Biol Chem.* 1992 Jun 15;267(17):12380-6.

77. Li W., Lam M., Choy D., Birkeland A., Sullivan M.E., and Post J.M. Human primary renal cells as a model for toxicity assessment of chemo-therapeutic drugs. *Toxicol In Vitro.* 2006 Aug;20(5):669-76.

78. Clement M.V., Hirpara J.L., Chawdhury S.H., and Pervaiz S. Chemopreventive agent resveratrol, a natural product derived from grapes, triggers CD95 signaling-dependent apoptosis in human tumor cells. *Blood.* 1998 Aug 1;92(3):996-1002.

79. Carmichael J., DeGraff W.G., Gazdar A.F., Minna J.D., and Mitchell J.B. Evaluation of a tetrazolium-based semiautomated colorimetric assay: assessment of radiosensitivity. *Cancer Res.* 1987 Feb 15;47(4):943-6.

80. Moser T.L., Stack M.S., Asplin I., Enghild J.J., Hojrup P., and Everitt L., et al. Angiostatin binds ATP synthase on the surface of human endothelial cells. *Proc Natl Acad Sci U S A.* 1999 Mar 16;96(6):2811-6.

81. Frater-Schroder M., Risau W., Hallmann R., Gautschi P., and Bohlen P. Tumor necrosis factor type alpha, a potent inhibitor of endothelial cell growth in vitro, is angiogenic in vivo. *Proc Natl Acad Sci U S A.* 1987 Aug;84(15):5277-81.

82. Hodis H.N., Kramsch D.M., Avogaro P., Bittolo-Bon G., Cazzolato G., and Hwang J., et al. Biochemical and cytotoxic characteristics of an in vivo circulating oxidized low density lipoprotein (LDL-). *J Lipid Res.* 1994 Apr;35(4):669-77.

83. Scherrmann J.M., Urtizbarea M., Pierson P., and Terrien N. The effect of colchicine-specific active immunization on colchicine toxicity and disposition in the rabbit. *Toxicology*. 1989 Jun 1;56(2):213-22.
84. Doroshow J.H., Locker G.Y., Ifrim I., and Myers C.E. Prevention of doxorubicin cardiac toxicity in the mouse by N-acetylcysteine. *J Clin Invest*. 1981 Oct;68(4):1053-64.
85. Koutsandrea C.N., Miceli M.V., Peyman G.A., Farahat H.G., and Niesman M.R.. Ciprofloxacin and dexamethasone inhibit the proliferation of human retinal pigment epithelial cells in culture. *Curr Eye Res*. 1991 Mar;10(3):249-58.
86. Vignati L.A., Bogni A., Grossi P., and Monshouwer M. A human and mouse pregnane X receptor reporter gene assay in combination with cytotoxicity measurements as a tool to evaluate species-specific CYP3A induction. *Toxicology*. 2004 Jun 1;199(1):23-33.
87. Shaikh B., Jackson J., Guyer G., and Ravis W.R. Determination of neomycin in plasma and urine by high-performance liquid chromatography. Application to a preliminary pharmacokinetic study. *J Chromatogr*. 1991 Nov 15;571(1-2):189-98.
88. Wierzba K., Sugiyama Y., Okudaira K., Iga T., and Hanano M. Uptake of colchicine, a microtubular system disrupting agent, by isolated rat hepatocytes. *Pharm Res*. 1989 Mar;6(3):235-8.
89. Griffiths N.M., Hirst B.H., and Simmons N.L. Active intestinal secretion of the fluoroquinolone antibacterials ciprofloxacin, norfloxacin and pefloxacin; a common secretory pathway? *J Pharmacol Exp Ther*. 1994 May;269(2):496-502.
90. Dautrey S., Felice K., Petiet A., Lacour B., Carbon C., and Farinotti R. Active intestinal elimination of ciprofloxacin in rats: modulation by different substrates. *Br J Pharmacol*. 1999 Aug;127(7):1728-34.
91. Pujols L., Mullol J., Perez M., Roca-Ferrer J., Juan M., and Xaubet A., et al. Expression of the human glucocorticoid receptor alpha and beta isoforms in human respiratory epithelial cells and their regulation by dexamethasone. *Am J Respir Cell Mol Biol*. 2001 Jan;24(1):49-57.
92. Gumy C., Chandsawangbhuwana C., Dzyakanchuk A.A., Kratschmar D.V., Baker M.E., and Odermatt A. Dibutyltin disrupts glucocorticoid receptor function and impairs glucocorticoid-induced suppression of cytokine production. *PLoS One*. 2008;3(10):e3545.
93. Hoger P.H., Seger R.A., Schaad U.B., and Hitzig W.H. Chronic granulomatous disease: uptake and intracellular activity of fosfomycin in granulocytes. *Pediatr Res*. 1985 Jan;19(1):38-44.

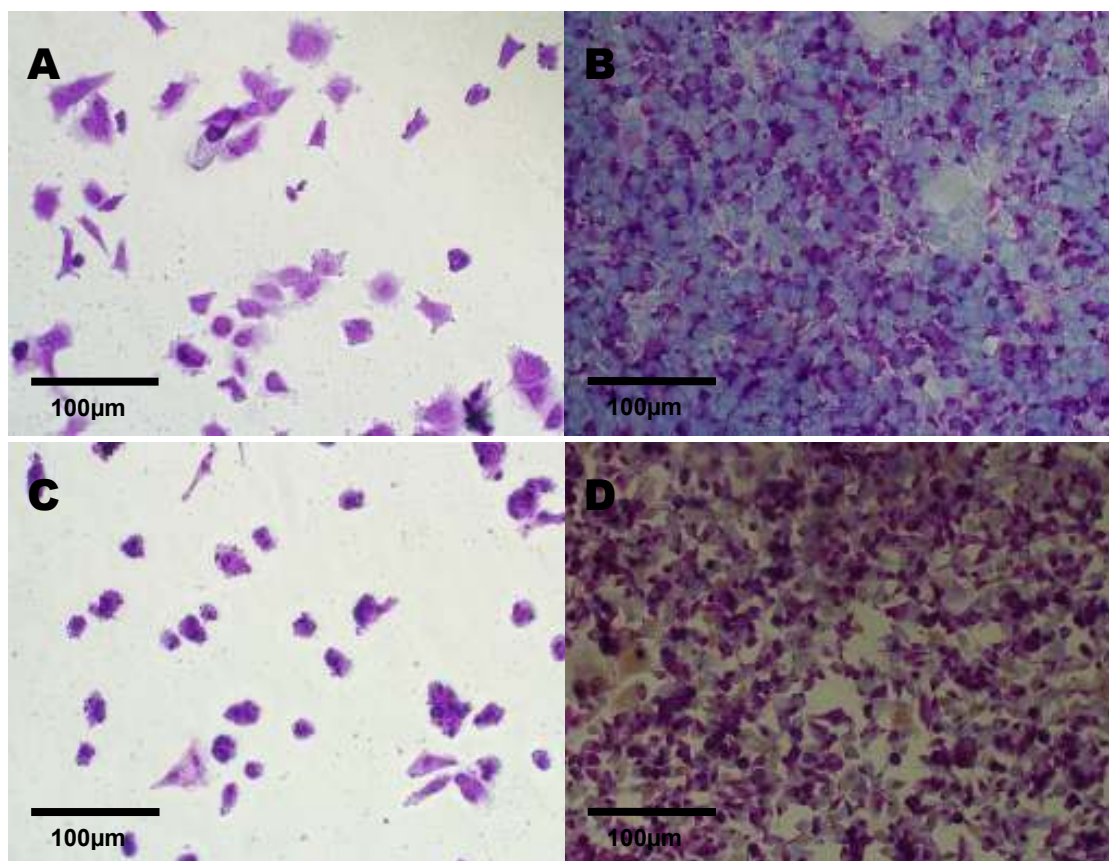
94. Ranaldi G., Islam K., and Sambuy Y. Epithelial cells in culture as a model for the intestinal transport of antimicrobial agents. *Antimicrob Agents Chemother.* 1992 Jul;36(7):1374-81.
95. Medical Economics Data. Physicians desk reference: Montvale, N.J.:Medical Economics Data; 1998.
96. Boman G. and Ringberger V.A. Binding of rifampicin by human plasma proteins. *Eur J Clin Pharmacol.* 1974 Aug 23;7(5):369-73.
97. Discher D.E., Janmey P. and Wang Y.L. Tissue cells feel and respond to the stiffness of their substrate. *Science.* 2005 Nov 18;310(5751):1139-43.
98. Lange U., Schumann C., and Schmidt K.L. Current aspects of colchicine therapy -- classical indications and new therapeutic uses. *Eur J Med Res.* 2001 Apr 20;6(4):150-60.
99. Hansch C., Telzer B.R., and Zhang L. Comparative QSAR in toxicology: examples from teratology and cancer chemotherapy of aniline mustards. *Crit Rev Toxicol.* 1995;25(1):67-89.
100. Yalkowsky S.H. and Patel S.D. Acceleration of heat transfer in vial freeze-drying of pharmaceuticals. II. A fluid cushion device. *Pharm Res.* 1992 Jun;9(6):753-8.
101. Yang L., Panetta J.C., Cai X., Yang W., Pei D., and Cheng C., et al. Asparaginase may influence dexamethasone pharmacokinetics in acute lymphoblastic leukemia. *J Clin Oncol.* 2008 Apr 20;26(12):1932-9.
102. Gordon R.C., Regamey C., and Kirby W.M. Serum protein binding of the aminoglycoside antibiotics. *Antimicrob Agents Chemother.* 1972 Sep;2(3):214-6.

**Supplemental Table 4.1.** Lack of detectable drug aggregation in culture media solutions containing 4mM colchicine after 2 hours of incubation in different media.

| <b>Sample</b>                       | <b>Average particle size (nm)</b> | <b>Polydispersity index</b> |
|-------------------------------------|-----------------------------------|-----------------------------|
| <b>Water</b>                        | 0                                 | 0                           |
| <b>50nm particles</b>               | 33                                | 0.131                       |
| <b>0.5X PBS</b>                     | 13.46                             | 0.843                       |
| <b>Proximal tubule media</b>        | 136.2                             | 0.882                       |
| <b>4mM colchicine (t=0)</b>         | 138                               | 0.772                       |
| <b>4mM colchicine (t=30min)</b>     | 133.8                             | 0.831                       |
| <b>4mM colchicine (t=1 hour)</b>    | 159.8                             | 0.824                       |
| <b>4mM colchicine (t=1.5 hours)</b> | 54.27                             | 1                           |
| <b>4mM colchicine (t=2 hours)</b>   | 123                               | 0.855                       |

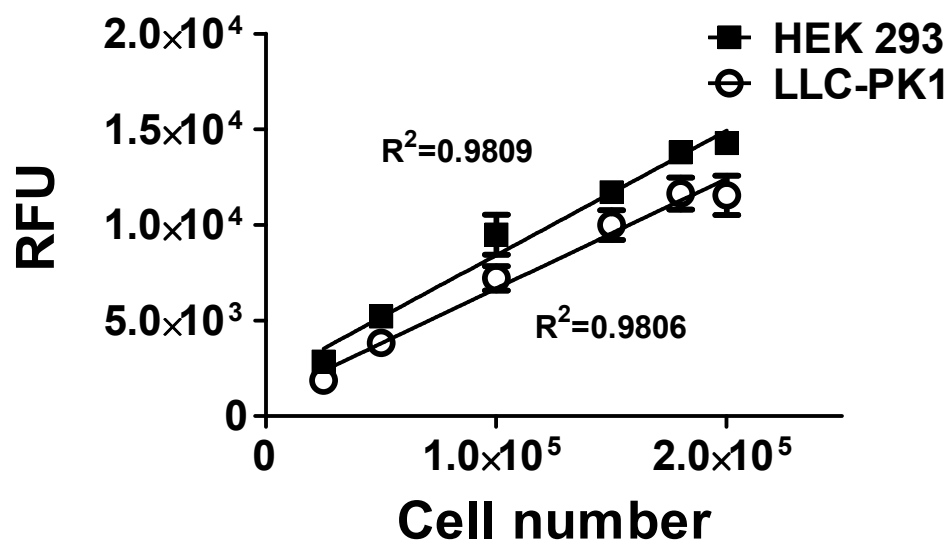
**Supplemental Table 4.2.** General properties for drugs taken from the literature (parentheses are references)

| <b>Drug</b>                             | <b>Empirical formula</b>                           | <b>LogP value</b> | <b>Aqueous solubility</b> | <b>Serum binding fraction</b> |
|---|--|-------------------|---------------------------|-------------------------------|
| <b>Ciprofloxacin</b>                    | $C_{17}H_{18}FN_3O_3$                              | 1.32 (68)         | insoluble                 | 20-40%(95)                    |
| <b>Rifampicin</b>                       | $C_{43}H_{58}N_4O_{12}$                            | 1.1 mg/mL (67)    | 2.5 mg/mL (67)            | 87-91%(96)                    |
| <b>Doxorubicin hydrochloride</b>        | $C_{27}H_{29}NO_{11} \cdot HCl$                    | N/A               | 50 mg/mL                  | 50%(97)                       |
| <b>Colchicine</b>                       | $C_{22}H_{25}NO_6$                                 | 1.03 (65)         | 10 mg/mL                  | 50%(98)                       |
| <b>Dexamethasone</b>                    | $C_{22}H_{29}FO_5$                                 | 1.83 (99)         | 0.89 mg/mL (100)          | 80% (101)                     |
| <b>Neomycin trisulfate salt hydrate</b> | $C_{23}H_{46}N_6O_{13} \cdot 3H_2SO_4 \cdot xH_2O$ | N/A               | 50 mg/mL                  | 0-30%(102)                    |

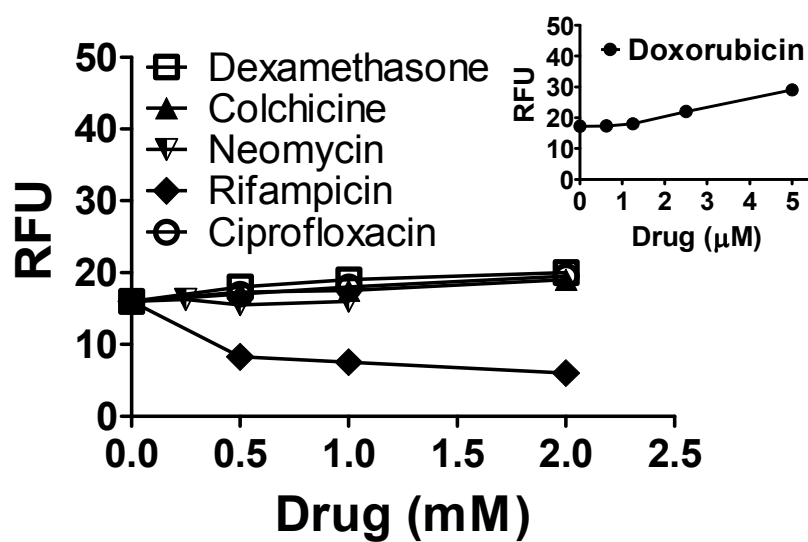


**Supplemental Figure 4.1.** Appearance of low-confluence and high-confluence cell cultures used in this work showing presence or absence of cell-cell interactions important to assess drug influences by paracellular transport and cell polarization-dependent drug uptake. Microscopy of hematoxylin and eosin staining of HEK 293 and LLC-PK1 cell cultures after 5 hours of incubation (representative of the first 3 hour drug assessment time point, 200X): A) HEK 293 seeded at 10,000 cells/well, B) HEK 293 seeded at 175,750 cells/well, C) LLC-PK1 seeded at 10,000 cells/well, D) LLC-PK1 seeded at 175,750 cells/well.

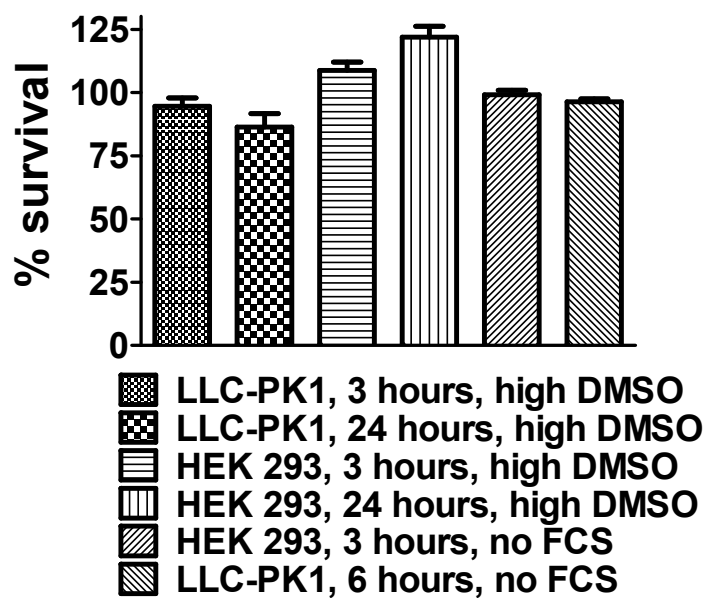




**Supplemental Figure 4.2.** Fluorescence signal standard curves for HEK 293 and LLC-PK1 cultures as a function of cell number showing that CyQuant NF® is sensitive to distinguish optical signals from high cell concentrations (symbols: experimental data, lines: regression fits to data). All experiments were done with n=3 and 2 technical replicas.



**Supplemental Figure 4.3.** Lack of detectable interference between CyQuantNF® assay signal and several drug concentrations. Inset shows interference of doxorubicin with the assay.



**Supplemental Figure 4.4.** Control cell cultures with high DMSO content (20%) and without FCS on 170,750 cells/well, showing lack of observed cell stress or mortality increases under these culture conditions.

## CHAPTER 5

### COMPARING PREDICTIVE DRUG NEPHROTOXICITY BIOMARKERS IN KIDNEY

#### 3-D PRIMARY ORGANOID CULTURE AND IMMORTALIZED CELL LINES<sup>1</sup>

##### Abstract

The cellular microenvironment is recognized to play a key role in stabilizing cell differentiation states and phenotypes in culture. This study addresses the hypothesis that preservation of *in vivo*-like tissue architecture *in vitro* produces a cell culture more capable of responding to environmental stimuli with clinically relevant toxicity biomarkers. This was achieved using kidney proximal tubules in three-dimensional organoid hydrogel culture, with comparisons to conventional monolayer kidney cell cultures on plastic. Kidney proximal tubule cultures and two immortalized kidney cell line monolayer cultures exposed to known nephrotoxic drugs were evaluated for inflammatory cytokines, nephrotoxicity-associated genes, Kim-1 protein, cytochrome enzymes, and characteristic cellular enzyme shedding. Significant similarities are shown for these traditional biomarkers of kidney toxicity between *in vivo* and 3-D organoid endpoints of drug toxicity, and significantly, a consistent lack of clinically relevant endpoints produced by traditional 2-D kidney cell cultures. These findings impact both *in vitro* bioreactor-based kidney functional and

---

<sup>1</sup> Reprinted with permission from *Biomaterials*: Anna Astashkina, Brenda Mann, Glenn Prestwich, David Grainger. Comparing predictive drug nephrotoxicity biomarkers in kidney 3-D primary organoid culture and immortalized cell lines, 2012

regenerative medicine models, as well as high-throughput cell-based drug screening validations.

### Introduction

Tissue-like cell interactions, cell organization, and communication in time and space in three-dimensions (3-D) are key *in vivo* variables that elicit and maintain distinct cell lineages and phenotypes in tissues required for tissue structure and function. Few if any of these important factors are incorporated into conventional cell culture monolayer systems on tissue culture plastic. Hence, many unanswered questions remain about the equivalence of cell monolayer cultures on plastic with their 3-D cultures in terms of phenotypic stability, biomarker production, or their respective fidelities to corresponding cells in tissues *in vivo*. Addressing such questions remains critical to asserting the validity of *in vitro* cell-based test systems in drug screening, toxicology, and models of cell signal transduction pathways required to confidently elucidate important physiological and pathological issues.

A wealth of knowledge accumulated by tissue engineering and regenerative models in the last two decades underscores the importance of restoring or maintaining native cellular interactions and endogenous matrix in preserving *in vivo*-like cell phenotypes, behavior, and signaling; and tissue function and architecture (1). Specifically, matrix chemistry and mechanics, cell-cell paracrine signaling, and cell-matrix interactions are known to be critical for sustaining tissue-like activities including cell organization, proliferation, attachment, polarization, signaling, gene expression, morphogenesis, and homeostasis (1). New 3-D culture methods that promote, facilitate and sustain such natural cell-cell relationships and native behaviors better recapitulate

tissue-like architectures and functions, laying the basis for improved *in vivo*-relevant cell culture models (2, 3). Broad technical advances in tissue engineering have benefited multiple fields, including fundamental cell biology and physiology, organ regeneration, wound healing, drug development and cancer research. We describe tissue-like cultures for studying and validating toxicity mechanisms associated with common clinically relevant, pharmaceutically active agents.

Drug and bioactive compound toxicity remains a major health and drug development issue: estimates are that only 8% of all drug candidates reach the market and almost 20% of all failures are attributed to some form of toxicity (4, 5). Unlike other reasons for drug candidate attrition in clinical trials, toxicity failure rates have not changed in the last two decades, reflecting a poor understanding of *in vivo* drug-host interactions and lack of appropriate cellular models (5). Nephrotoxicity, or kidney toxicity, is the second-leading cause of drug-induced damage after hepatotoxicity in critically ill patients and is thought to cause as many as 25% of all kidney failures in this group (6). Nephrotoxicity describes a complex process of tissue damage due to active and passive agent accumulation in the kidneys and their chemical alterations through interactions with cellular enzymes, particularly cytochrome (CYP) P450 enzymes (7). The compound nature of kidney cellular injury *in vivo* requires that simpler cell-based models intended to recapitulate its mechanisms with any fidelity should retain cellular structures involved in toxicity induction. Specifically, preservation of brush border and intracellular enzymes  $\gamma$ -glutamyl-transferase and glutathione known to process chemotherapeutic platinum drugs (8); ligands involved in endocytosis of small molecules such as megalin-induced endocytosis of aminoglycosides (9); active transporters implicated in charged species re-uptake from blood such as cisplatin

accumulation using organic cationic transporter 2 (OCT 2) (7); and stable cytP450 expression capable of drug biotransformation to metabolites (8) are minimal competences for such models in drug toxicity testing. We have previously shown that 3-D proximal tubule (PT) organoid cultures in hyaluronic acid (HA) hydrogels retain all of these *in vivo*-toxicity relevant cellular bioactivities through maintenance of 3-D cell architecture and cell-cell interactions. This work probes the relationships between 3-D cellular organization and production of clinically relevant cellular biomarkers of toxicity *in vitro*, as well as comparison of the 3-D organoid cultures to the cell culture “gold standard”: 2-D cultured monolayers of kidney secondary cells on rigid tissue culture thermoplastic.

## Methods

### Drugs and bioactive agents

All bioactive agents were purchased from Sigma-Aldrich (USA). Doxorubicin (doxorubicin hydrochloride), colchicine, cisplatin (cis-diaminedichloro-platinum II) and PAP were dissolved in dimethyl sulfoxide (DMSO, Fisher Scientific, USA) to stock solutions and stored at -20°C. Doxorubicin was resuspended at 1 mM concentration and all other molecules were used from 20mM stock solutions. Prior to cell application, all drugs were diluted to their final concentrations in proximal tubule media (1% fetal calf serum, 5% sodium pyruvate, 1% non-essential amino acids, 1% insulin/transferrin/selenium, 1% antibiotic-antimycotic, 0.9 µg of hydrocortisone, phenol red-free Dulbecco's modified Eagle medium (DMEM)-Ham's F-12 with L-glutamine and 4-(2-hydroxyethyl)-1-piperazineethanesulfonic acid (HEPES)) and sterilized using a 0.22µm

pore-sized sterile filter (ISC Bioexpress, USA). Phenol red-free media was used in order to avoid color interference with luminescence and fluorescence cell viability measurements. All reagents for cell culture were purchased from Invitrogen (USA).

#### Culture plate preparation for PT 3-D organoid constructs

Non-tissue culture polystyrene plates (96-well, ISC Bioexpress) were coated with transparent, non-toxic Teflon-AF® (Dupont, USA) thin films in FC-40 (3M, USA) solvent per published protocols (10). Solvent was removed using heated vacuum drying and plates sterilized using UV irradiation for 30 min before use.

#### PT isolation and 3-D hydrogel construct fabrication

Male C57BL/6 mice 6-8 weeks old were purchased from Jackson Laboratories (Bar Harbor, USA). PTs were isolated according to published methods (11). Briefly, animals were euthanized using carbon dioxide according to approved University of Utah IACUC protocols. All procedures used *standard* aseptic conditions in a BSL2 laminar flow hood. Freshly harvested kidneys were isolated by removal of the kidney capsule, blood vessels, and ureter. Cleaned kidneys were finely mechanically disrupted and enzymatically digested in collagenase IV (Worthington Biochemical Corporation, USA), DNase I (Sigma Aldrich, USA), and hyaluronidase (HAse, Worthington Biochemical Corporation) enzyme KREBS solution (145 mM NaCl, 10 mM HEPES, 5 mM KCl, 1 mM NaH<sub>2</sub>PO<sub>4</sub>, 2.5 mM CaCl<sub>2</sub>, 1.8 mM MgSO<sub>4</sub>, 5 mM glucose, pH 7.3) at 37°C (12). Digested sections of the nephron were then enriched for PTs using serial 80 µm and 250 µm sized sieves (11). The resulting suspension of PTs in KREBS was pelleted, resuspended in 1.5% thiol-modified



biomedical grade carboxymethylated HA (CMHA-S, SentrX Animal Care, Salt Lake City, USA) in PBS<sup>++</sup>, and crosslinked chemically and directly in situ by addition of 7.5% poly(ethylene glycol) diacrylate (PEGDA, SentrX Animal Care, Salt Lake City, USA) bifunctional electrophile (4:1 v/v CMHA-S:PEGDA, total volume 50 $\mu$ L) into the 3-D constructs (2, 3). Crosslinking was performed for 35 min in 96-well TeflonAF®-coated culture plates in an incubator followed by PT media addition, producing soft hydrogels under conditions that do not affect cell viability or function (2). Culture constructs comprised approximately 5000 PTs/well and were used within 2 weeks of preparation. The 3-D constructs were maintained in a cell culture incubator under 5% CO<sub>2</sub> and 95% air and culture media were exchanged every other day for optimum PT viability.

#### Immortalized kidney cell line monolayer cultures

Immortalized transformed porcine LLC-PK1 renal PT epithelial cells were purchased from ATCC, USA. Immortalized transformed human embryonic kidney (HEK 293) renal proximal tubule epithelial cells were generously donated by Dr. Alfred Cheung (University of Utah, USA). Cell lines were expanded using aseptic techniques in DMEM with 10% fetal bovine serum (FBS) and 1% antibiotic-antimycotic. Both cell lines were maintained in cell culture incubators under 5% CO<sub>2</sub> and 95% air at 37°C.

All studies but the cytochrome 2-D culture monolayer experiments used cells seeded in 96-well tissue culture plates (Fisher Scientific, USA) at 170,750 cells/well density, approximately equivalent to 5000 PTs/well. Cells were adhered for 2 hours in DMEM with 10% FBS and 1% antibiotic-antimycotic media prior to drug application. For cytochrome expression experiments,

cells cultured as 2-D monolayer and 3-D organoid culture used 96-well tissue culture treated imaging plates (BD Falcon, USA). Immortalized cells were seeded at 170,750 cells/well and allowed to adhere overnight prior to drug exposure on imaging plates for the cytochrome induction due to inferior cell adhesion compared to regular tissue culture polystyrene substrates.

#### EC<sub>50</sub> determinations

The EC<sub>50</sub> values for 3-D and 2-D cultures exposed to nephrotoxic drugs were determined after 3 days of incubation with each drug. This time point was chosen to provide cells both grown as monolayers and suspended in HA gels sufficient time for uniform drug diffusion and exposure. Drug diffusion in the HA gel was first tested using cisplatin as a model since all drugs had comparable molecular weights, but basic, amine-bearing cisplatin had the greatest electrostatic interaction with the HA gels. Cisplatin was resuspended in water and placed on an HA gel surface without cells, cast over transwell microporous inserts (Corning, USA). Transwell® inserts with diameters compatible with 96-well plates were placed in a 24-well plate (Flow Laboratories, USA) with 500µL of water/well. The entire volume of the well was removed at 1-24 hour time points and appearance of cisplatin below the Transwell® filter was assayed spectrophotometrically (Synergy 2) at A<sub>260</sub> and A<sub>280</sub>.

The commercial CyQuant NF® (Invitrogen, USA) assay was used to measure cell numbers for 2-D and 3-D cultures through nucleic acid labeling. For 2-D experiments, cell concentration was assessed using the standard manufacturer's protocol. For 3-D experiments, HA gel constructs were pretreated with 10µM peroxide in PT media to oxidize all non-crosslinked thiols of

the gel for 1 hour in the incubator. CyQuant NF® solution was prepared according to manufacturer's instructions and applied directly to the constructs. Supernatant was analyzed using a fluorescence microplate reader (Synergy 2, USA). CyQuant NF® measurements for blank HA gel without cells were subtracted from 3-D organoid constructs as a background. Amount of drug trapped by the HA gel was estimated using depletion methods for all tested drugs. Specifically, gels without cells were incubated with EC<sub>50</sub> drug concentrations in water for 3 days in the incubator. Amounts of drug both prior to and post gel incubation in the medium were measured using a Cary 400 Bio UV-VIS spectrophotometer (Varian, USA) and a Nanodrop instrument (Thermosciences, USA). Drug presence was evaluated at A<sub>290</sub> for cisplatin, A<sub>340</sub> for colchicine, A<sub>219</sub> for PAP, and A<sub>489</sub> for doxorubicin. Solutions removed from the gel were adjusted for evaporation in final concentration determinations.

#### Shedding of cellular enzymes

NAG and  $\gamma$ -glutamyl-transferase shedding into urine are clinical indications of drug-induced nephrotoxicity (13, 14). Enzyme concentrations in the media from 2-D primary cells and 3-D organoid cultures were assessed after 3 days of drug incubation at corresponding EC<sub>50</sub> values. Optical absorbance of drugs in the media was subtracted as background.

NAG is an intracellular enzyme measured in the media according to published chromogenic protocols (13, 14). Briefly, 100  $\mu$ L of the media was incubated for 10 min at room temperature (RT) with 100  $\mu$ L of 2.24mM *p*-nitrophenyl-*N*-acetyl- $\beta$ -D-glucosaminide (Sigma Aldrich, USA) dissolved in citrate/phosphate buffer (0.1 M citric acid, 0.1 M Na<sub>2</sub>HPO<sub>4</sub>, pH 4.5). Absorbance was read at

405 nm on the microplate reader and referenced against a 1 mM 4-nitrophenol standard (Sigma Aldrich, USA). Negative values for NAG concentration were shown as zeros.

Gamma-glutamyl-transferase is a brush border enzyme assessed according to a standard chromogenic protocol (15). Briefly, 50µL of media from each construct was pre-incubated with 50µL of assay solution (150mM NaCl and 10mM Tris-HCL, pH 8.5) for 5 min at RT. The reaction was initiated by adding 50µL of 5mM L-glutamyl-p-nitroaniline (Sigma Aldrich, USA) chromogenic substrate with 100mM glycylglycine (Sigma Aldrich, USA). The reaction was allowed to proceed for 20 min in the incubator and stopped using 200µL of 10% acetic acid. Amount of the chromogenic product was assessed using a spectrophotometer at  $A_{405}$  and referenced against a 1 mM reading of p-nitroanilide (Sigma Aldrich, USA).

#### Staining for cellular cytP450 ,TNF- $\alpha$ , and Kim-1 markers

Changes in of cytP450 enzyme expression is an indicator cell toxicity (16). LLC-PK1, HEK 293, and 3-D PT organoid cultures were assessed for expression of common mouse cytP450 enzymes, CYP2B2 and CYP2E2, after 3-day exposure to active molecules at their corresponding  $EC_{50}$  values using immunofluorescence. Both anti-mouse CYP2E2 and CYP2B1/2 antibodies were purchased from Millipore (USA).

TNF $\alpha$  and Kim-1 protein up-regulation on cell surface is another specific signature of nephrotoxicity (17, 18). TNF $\alpha$  and Kim-1 were analyzed on LLC-PK1, HEK 293, and 3D PT organoid cultures after 3 days of drug exposure at their corresponding  $EC_{50}$  values (see Table 5.1). Anti-mouse TNF $\alpha$ -PE antibody was purchased from eBiosciences. Kim-1 anti-rat R9 antibody

**Table 5.1.** Effective EC<sub>50</sub> values for nephrotoxic drugs in different kidney cell line (2-D HEK293, LLC-PK1 monolayers) and primary PT 3-D hydrogel cell cultures. Data reflect background subtraction of drug adsorption to HA gel matrix (see Materials and Methods).

| <b><i>Drug</i></b> | <b><i>2-D HEK293</i></b> | <b><i>2-D LLC-PK1</i></b> | <b><i>3-D PTs</i></b> |
|--------------------|--------------------------|---------------------------|-----------------------|
| <b>Cisplatin</b>   | 2.7mM                    | 2.0mM                     | 0.42mM                |
| <b>Doxorubicin</b> | 2.3μM                    | 1.9μM                     | 1.4μM                 |
| <b>Colchicine</b>  | 4mM                      | 2.1mM                     | 24.4μM                |
| <b>PAP</b>         | 0.63mM                   | 0.7mM                     | 24.9μM                |

was generously donated by Dr. Joseph V. Bonventre (Harvard University, USA). Both cells cultured in 2-D monolayers on plastic and in 3-D scaffolds as hydrogels were fixed using 4% paraformaldehyde. Monolayer cell culture was fixed for 30 min at RT and 3-D organoid PT constructs were fixed overnight in a 4°C refrigerator. Both 2-D and 3-D cell cultures were pretreated with 0.1% Triton X in the case of cytP450 CYPs and KIM-1, but not TNF- $\alpha$ , and blocked using Invitrogen's signal enhancer at RT for 30 min and 1 hour, respectively. Primary antibody was then applied for 2 hours at RT into cell monolayers and 3 days at 4°C on 3-D organoid cultures. Alexa-488 goat-anti-mouse IgG antibody (Invitrogen, USA) was used as a secondary antibody for all CYP proteins. Cells stained for Kim-1 and TNF- $\alpha$  were stained with secondary Alexa-488 anti-rabbit IgG. All primary antibodies were used at 1:1000 dilutions except for Kim-1 used at 1:500; secondary antibodies were used at 1:1000 concentrations. All cells were imaged at 400X magnification on an Olympus FV1000 Spectral confocal microscope. Each sample was evaluated as an average of 3 images for secondary cells and 4 images for primary cells. ImageJ free software was used to analyze fluorescence intensity and number of nuclei per sample.

#### Quantitative polymerase chain reaction (qPCR)

Several genes were identified *in vivo* as sensitive, specific biomarkers of kidney toxicity (19-23). Immortalized cell lines and primary 3-D PT organoid cultures were tested for induction of neutrophil gelatinase-associated lipocalin (NGAL), osteopontin (Spp1), clusterin (CLU), vimentin (VIM), heme oxygenase-1 (HO-1) at corresponding EC<sub>50</sub> values after 3 days of incubation with nephrotoxic drugs. Messenger RNA (mRNA) was isolated using the standard TRIzol® (Invitrogen,

USA) protocol. Final mRNA samples were treated with DNase I (Sigma-Aldrich) to eliminate genomic DNA contamination. RNA samples were diluted in nuclease-free water (Invitrogen, USA) to 300 ng/μL for primary cells and 100 ng/μL for immortalized cell lines. qPCR was performed using commercial TaqMan® Gene expression Assays (Applied Biosystems, USA): Mm9999915\_g1 for GAPDH, Mm01324470\_m1 for Lcn2 (NGAL), Mm004427773\_m1 for CLU, Mm00516005\_m1 for HO, Mm01333430\_m1 for VIM, Mm00436767\_m1 for Spp1. GAPDH was chosen as a housekeeping control due to low variation between drug-treated and control samples. Gene amplification was performed using RNA-C<sub>T</sub> Taqman Kit (Applied Biosystems, USA) on Step One Plus qPCR cycler (Applied Biosystems, USA). QPCR data were analyzed using the  $2^{-\Delta\Delta C_T}$  method (24). Samples that did not express genes after 40 cycles were assigned 41-cycle expression for calculations.

### Statistics

All data analysis used Excel 2010 (Microsoft) and GraphPad Prism 5 (GraphPad Software, Inc.). All cell experiments were performed using three to six independent samples with two technical replicas. For the 3-D PT organoid cultures, independent samples used cells isolated from different mice. Data were evaluated using unpaired student's test with Hochberg's post-hoc procedure to adjust for multiple comparisons. Observations were considered to be statistically significant with  $p < 0.05$ . All data in the paper were presented as mean ± S.E.

## Results

### EC<sub>50</sub> values in primary 3-D and cell line 2-D cultures

Apoptosis in *in vitro* cultures is a common measurement after toxic agent exposure. Although reduction of cell numbers has no corresponding values *in vivo*, it can be used for comparative purposes of relative toxicity between different compounds *in vitro*. EC<sub>50</sub> values were defined as the amounts of drug required to kill 50% of cells after 3-day incubations (see Supplemental Figures). HA gels were found to significantly interact with all drugs tested except doxorubicin; specifically, drug binding in the gel was measured to be 74% for cisplatin, 39% for colchicine, and 50% for PAP. The 3-day time point of drug exposure was selected to reduce diffusion differences between 2-D and 3-D cell culture, since drug diffusion experiments through the HA gel showed that drugs may take 1-4 hours to penetrate through these gels (data not shown). Quantification of cell apoptosis in cultures revealed 1.6-164-fold differences in EC<sub>50</sub> values between 3-D primary and cell line monolayer cultures, with primary 3-D organoid cultures exhibiting greater sensitivity to drug exposure (Table 5.1). Colchicine exhibited the greatest difference and cisplatin the least difference in toxicities between two cell culture conditions.

### NAG and $\gamma$ -glutamyl-transferase release into culture media

Shedding of intracellular and extracellular enzymes is a signature of proximal tubule cell damage and is commonly assessed in an *in vivo* setting (13, 14). NAG is a lysosomal enzyme and  $\gamma$ -glutamyl-transferase is an apical brush border enzyme highly expressed in PTs *in vivo*. Levels of



both NAG and  $\gamma$ -glutamyl-transferase in the media were determined after 3 days of incubation with drugs at drugs' corresponding  $EC_{50}$  values using colorimetric assays. Both HEK 293 and LLC-PK1 cell lines grown on 2-D plastic responded to toxic agents without a specific pattern (Figure 5.1). PAP and cisplatin did not elevate  $\gamma$ -glutamyl-transferase in a statistically significant way and all tested drugs had no effect on NAG production (Figure 5.1). Conversely, colchicine increased  $\gamma$ -glutamyl-transferase in HEK 293, while doxorubicin and colchicine elevated the same protein in LLC-PK1 (Figure 5.1). Organoid 3-D cell culture of PTs responded to nephrotoxic drug exposure by up-regulating both NAG and  $\gamma$ -glutamyl-transferase for all drug molecules (Figure 5.1). Increase in NAG was more consistent between the various drugs assayed in 3-D cultures, possibly reflecting greater responsiveness of the 3-D organoid culture to produce this protein in response to drug toxicity as *in vivo*.

#### Expression of TNF- $\alpha$

Inflammation and tissue damage are two processes common in drug toxicity (18, 25). TNF $\alpha$  was previously found to be up-regulated by proximal tubule cells in response to nephrotoxic drugs *in vivo* (18, 25). Cytokine production was tested at corresponding  $EC_{50}$  for different drugs after 3 day exposure. Surface-bound TNF $\alpha$  was up-regulated for PAP, doxorubicin, and cisplatin, but not for colchicine in the 3-D organoid culture and for doxorubicin and colchicine in LLC-PK1 cells (see Figure 5.2, Supplemental Figures). HEK 293 produced large changes in TNF $\alpha$  that were not statistically different due to large variations (see Figure 5.2, Supplemental Figures).

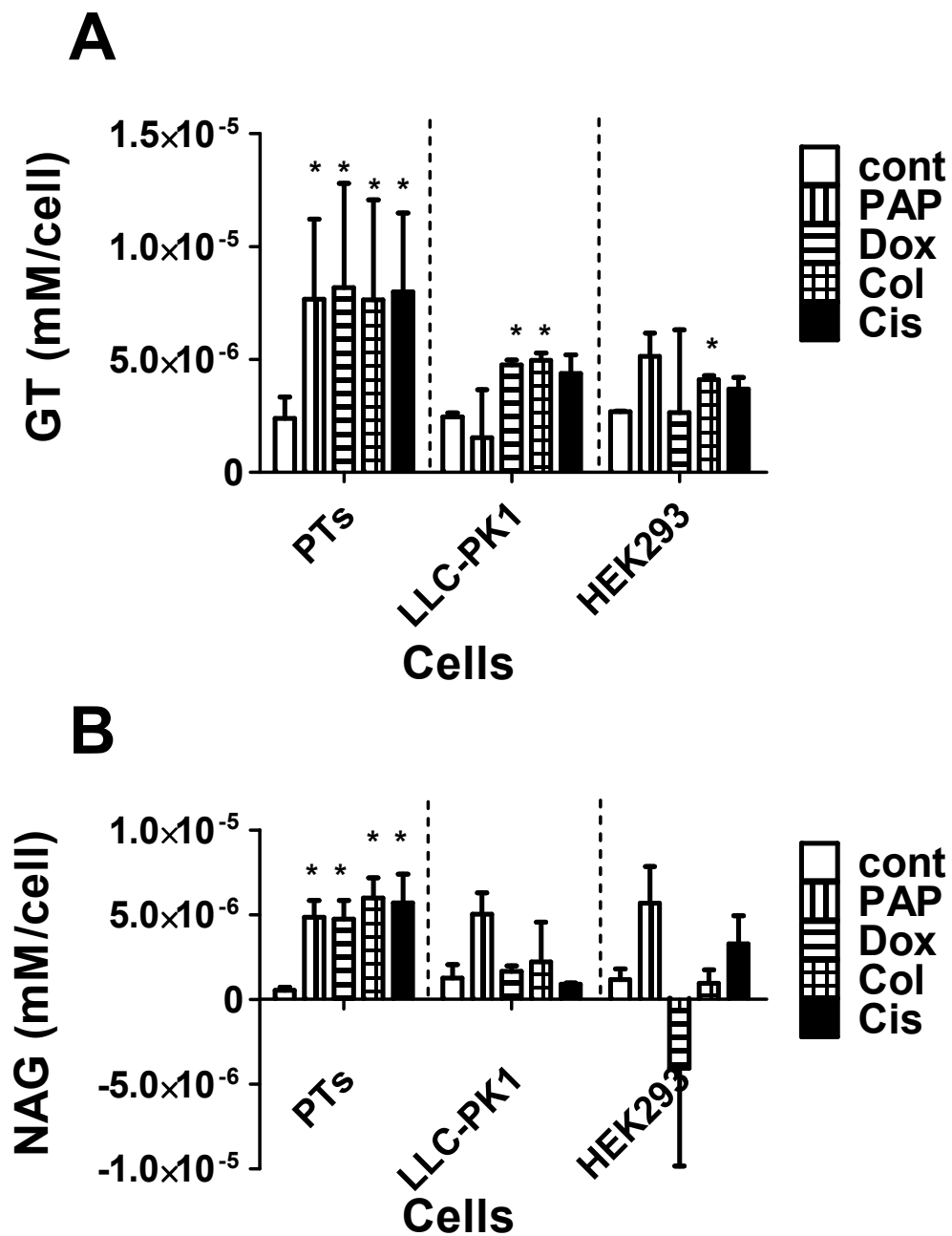


**Figure 5.1.**  $\gamma$ -glutamyl-transferase (GT) and NAG release into media at drugs' EC<sub>50</sub> values in different kidney cell cultures (PT = 3-D hydrogel; LLC-PK1 and HEK293 are 2-D monolayers on plastic) (n=3 for NAG and n=9 for  $\gamma$ -glutamyl-transferase, mean $\pm$ SE).

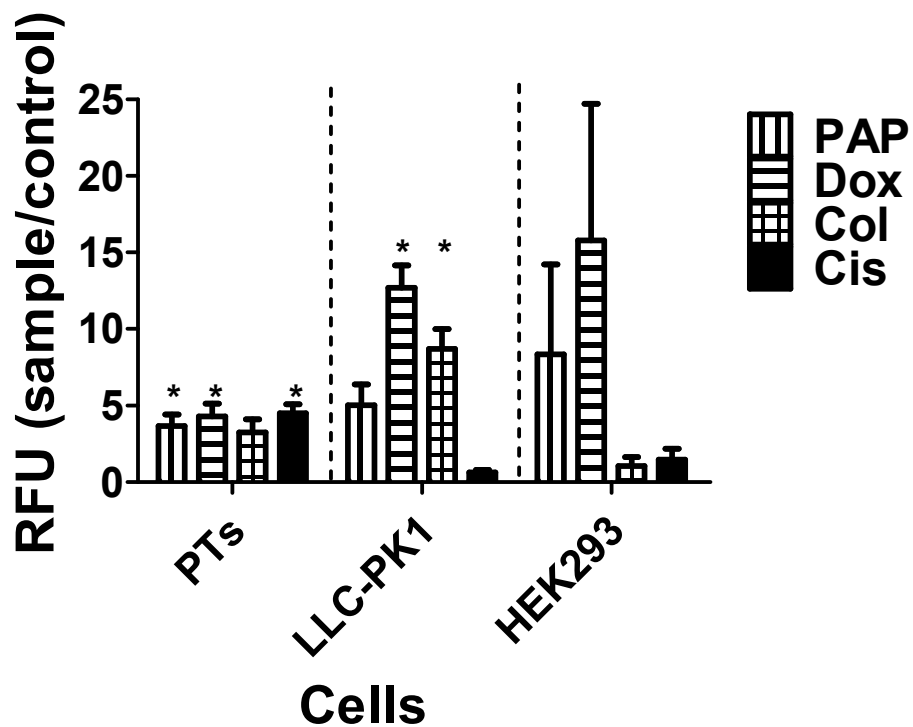


**Figure 5.2.** TNF- $\alpha$  expression on cultured cell surfaces at drugs'  $EC_{50}$  values in different kidney cell cultures normalized to control (PT = 3-D hydrogel; LLC-PK1 and HEK293 are 2-D monolayers on plastic; RFU=relative fluorescence units).

### Expression of CYP450 enzymes

Proximal tubule epithelial cells are metabolically active cells, with both CYP2E1 and CYP2B1 abundantly present in mouse kidney PTs (26). Furthermore, these two cytochromes are regulated by many endogenous agents (16). Changes in CYP2E1 and CYP2B1 levels were measured after 3 days culture at all drugs' corresponding  $EC_{50}$  values. CYP2B1 was up-regulated exposed to doxorubicin and colchicine in LLC-PK1; and with colchicine in HEK 293 cells (Figure 5.3). Very little expression of CYP2B1 was found in HEK 293 compared to LLC-PK1 immortalized cells (see Supplemental Figures). CYP2E1 was induced by cisplatin in PTs; doxorubicin in LLC-PK1; and colchicine in HEK 293 cells (Figure 5.4). Similar expression of CYP2E1 was detected in both transformed cell lines (see Supplemental Figures).

### Induction of Kim-1

Kim-1 up-regulation is associated with the kidney proximal tubule tissue damage *in vivo* (17, 27). Kim-1 protein assay used immunohistochemistry in 3-D organoid culture and LLC-PK1 and HEK 293 immortalized cells. No staining was achieved in transformed cell lines (data not shown). All drugs produced some up-regulation of Kim-1 in primary cells (Figure 5.5), with greatest staining in cisplatin and doxorubicin-treated cells. All Kim-1 drug-induced staining seemed to be cytosolic except for doxorubicin, where protein appeared to be nucleus-associated (Figure 5.5D).

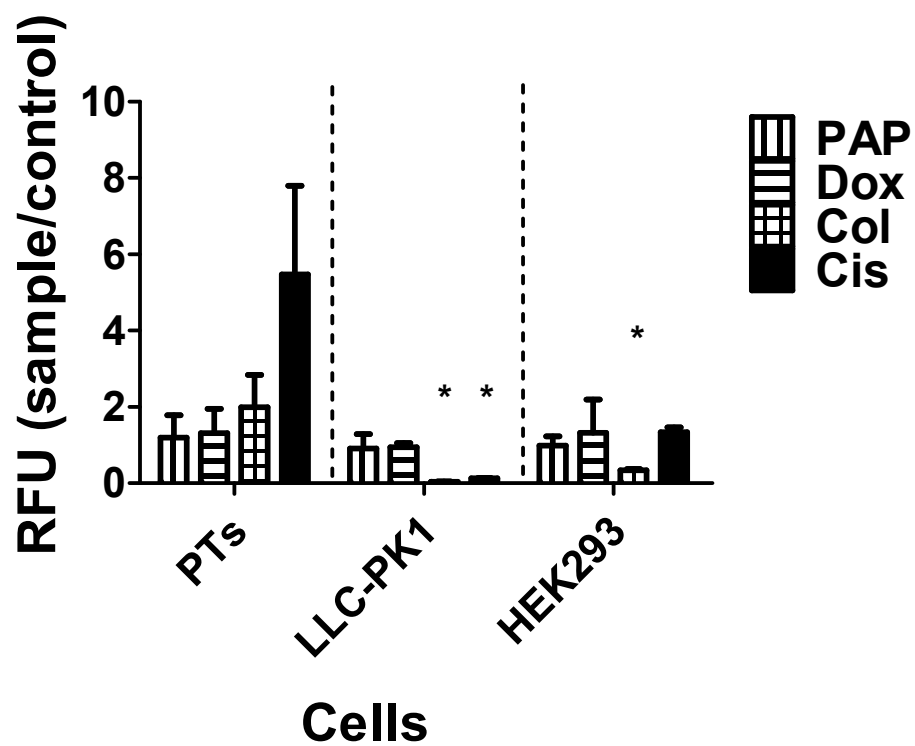


**Figure 5.3.** CYP2B1 intracellular expression at drugs'  $EC_{50}$  values in different kidney cell lines normalized to control (PT = 3-D hydrogel; LLC-PK1 and HEK293 are 2-D monolayers on plastic; RFU=relative fluorescence units).

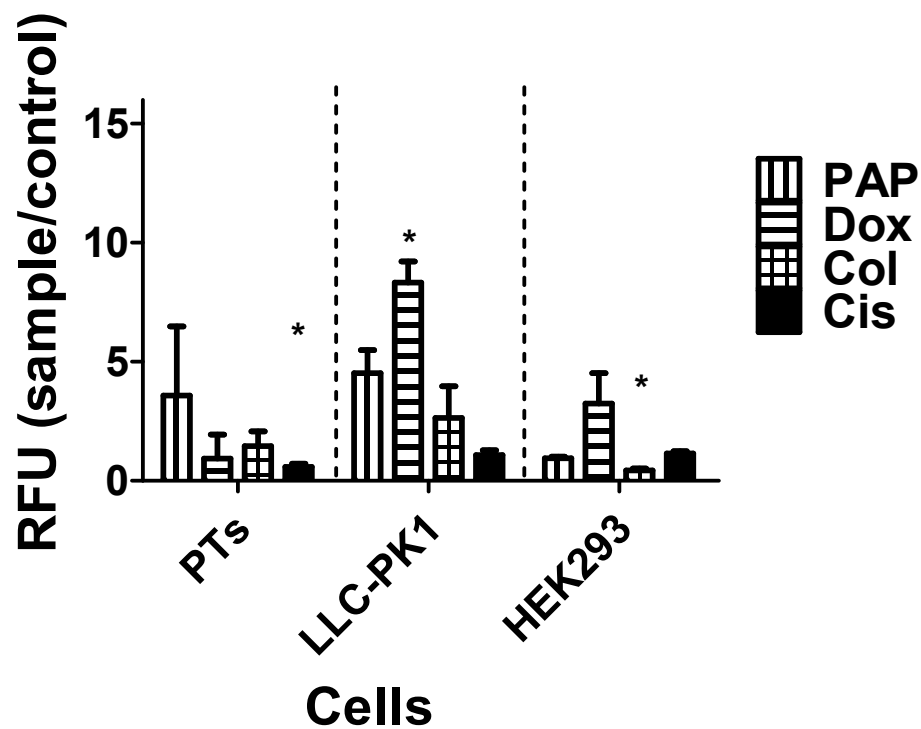
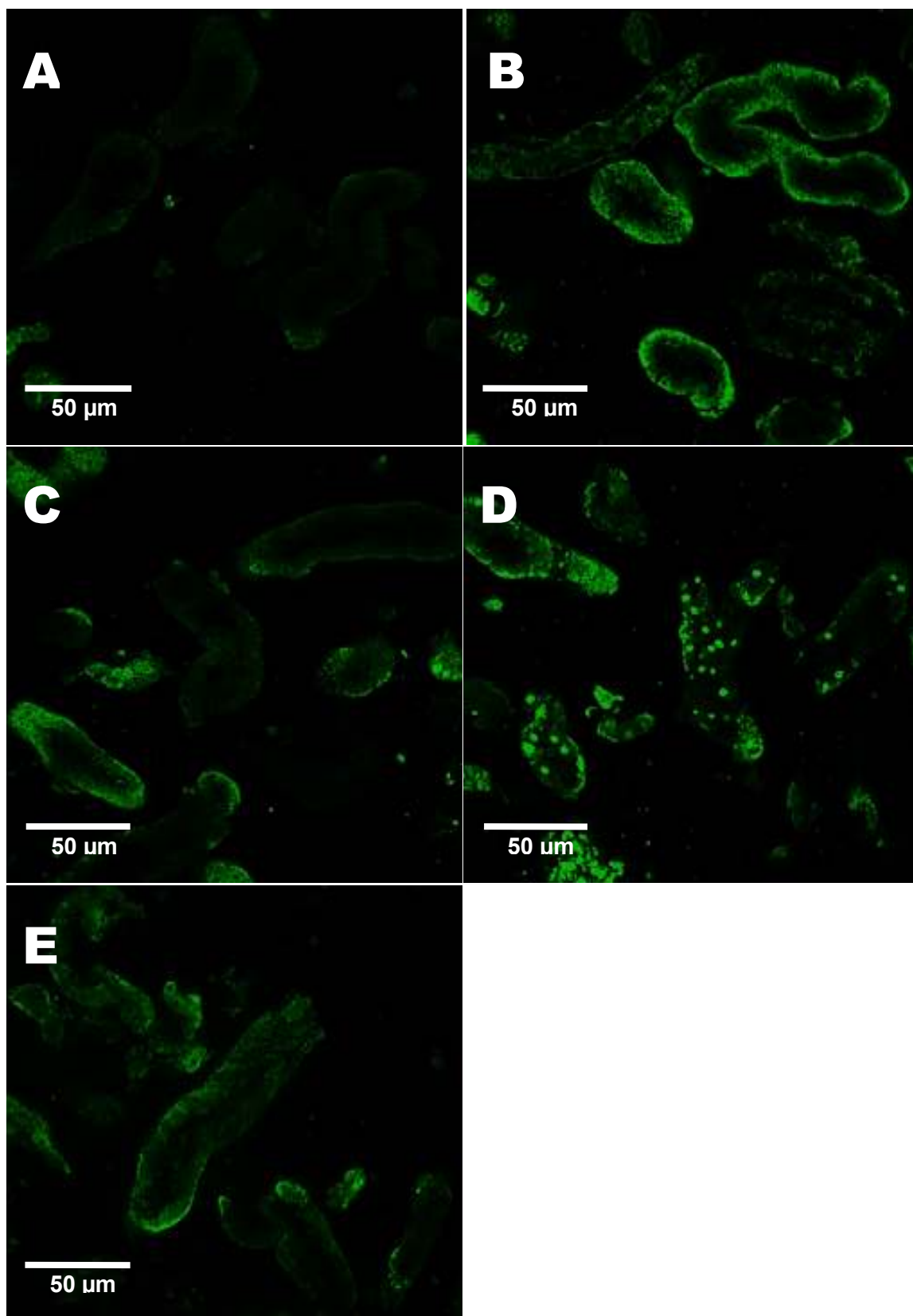


**Figure 5.4.** CYP2E1 intracellular expression at drugs' EC<sub>50</sub> values in different kidney cell cultures normalized to control (PT = 3-D hydrogel; LLC-PK1 and HEK293 are 2-D monolayers on plastic; RFU=relative fluorescence units).

**Figure 5.5.** Fluorescence microscopy of immuno-stained Kim-1 intracellular expression at drugs'  $EC_{50}$  values in 3-D PT cultures. A) PTs not treated with drugs (control), B-E) PTs treated with: B) cisplatin, C) colchicine, D) Dox, and E) PAP.





### Stimulation of nephrotoxic biomarker genes

Several genes are up-regulated with proximal tubule cell damage *in vivo*. Gene up-regulation in primary 3-D culture of PTs and monolayer cell lines was analyzed using qPCR. No up-regulation above 2-fold expression changes was observed in HEK 293 cells except for VIM in case of doxorubicin treatment (Figure 5.6). LLC-PK1 cell treated with drugs induced VIM for all drugs except PAP; NGAL and HO for PAP and cisplatin; and Spp1 for cisplatin (Figure 5.6). Primary 3-D organoid culture of PTs up-regulated all tested genes for all drugs (Figure 5.6). Lack of statistical significance for immortalized and primary cells was primarily attributed to large variations between samples.

### Discussion

Immortalized cell lines are commonly used for nephrotoxicity assessment due to the fact that primary epithelial kidney cells start to lose their cellular characteristics within 20 min. after isolation and completely de-differentiate within weeks in 2-D culture (11, 28). Unfortunately, immortalized cell lines have limited resemblance to their primary analogs and commonly lack essential molecular structures critical for toxicity induction with any clinical relevance (9, 28, 29). For example, the two transformed cell lines used on this study, HEK 293 and LLC-PK1, are reported to be missing small molecule transporters responsible for drug uptake, including organic cationic transporters 1-3 (OAT 1-3), OCT 2, and H<sup>+</sup>/peptide intestinal peptide transporters 1 and 2 (PepT 1-2), intracellular drug targets, such as glucocorticoid receptors, and low levels of drug efflux mechanisms, such as MDR1/P-glycoprotein. Furthermore, HEK 293 cells exhibit (i) few microvilli

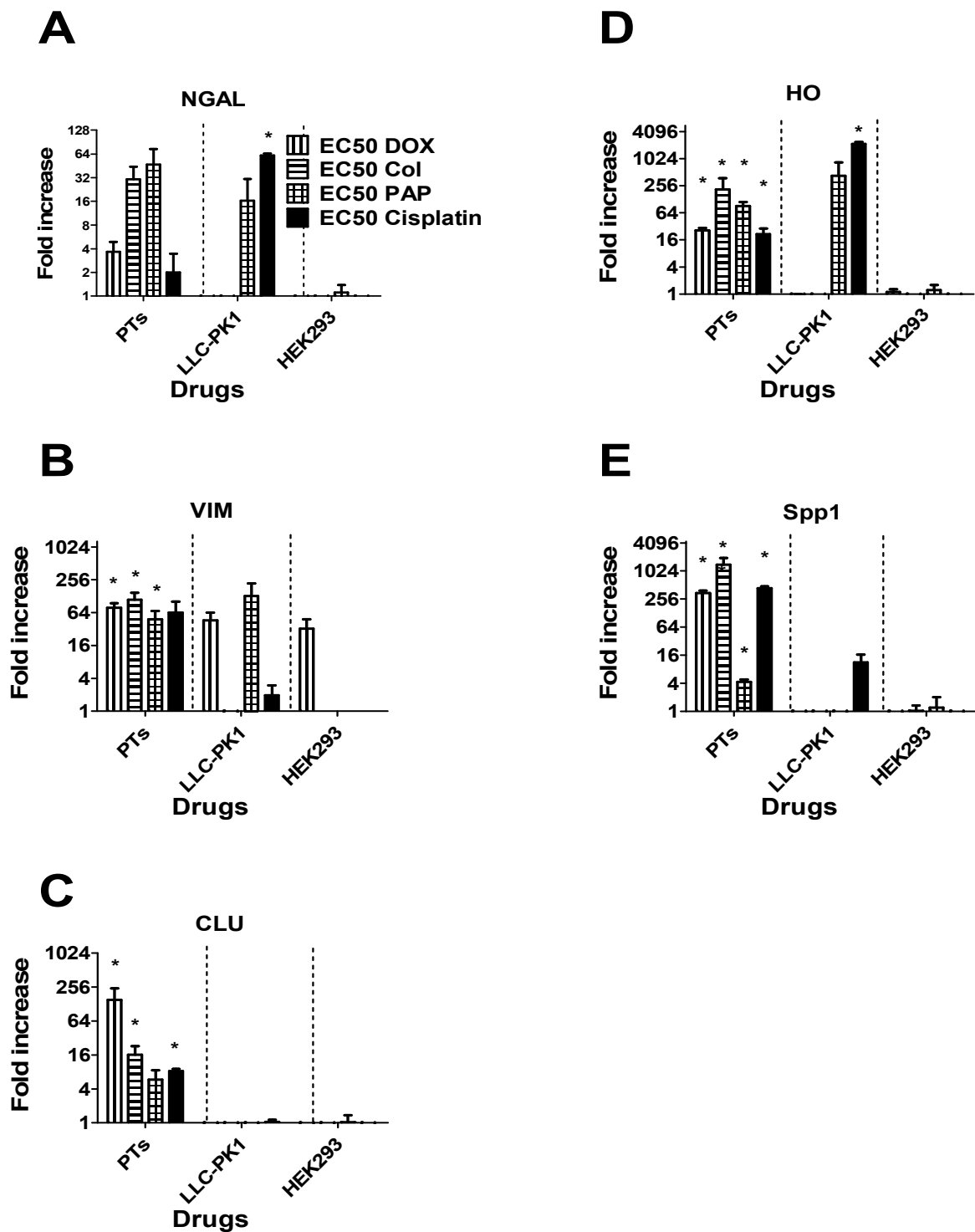


**Figure 5.6.** Distinctly different nephrotoxic gene expression profiles at drugs' EC<sub>50</sub> values in different kidney cell cultures (n=3-6, mean±SE): A) NGAL, B) VIM, C) CLU, D) HO, and E) Spp1. (PT = 3-D hydrogel; LLC-PK1 and HEK293 are 2-D monolayers on plastic).

(30), cellular extensions that promote molecule and water re-absorption, (ii) an absence of cellular ligands such as megalin, which are critical for albumin and aminoglycoside endocytosis (31), and (iii) minimal alkaline phosphatase activity, an apical enzyme essential for cell signaling induction (32). Lack of these (and possibly other) cellular components makes immortalized kidney cells poor models for toxicity assessment of novel drug compounds, drug delivery vehicles, and biomaterials with unknown modes of toxicity induction. Furthermore, absence of cellular complexity limits the type of toxicity biomarkers that might be correlated or discovered from transformed cell lines for drug development or clinical translation. Most *in vitro* studies report decreased cell viability or proliferation as endpoints for toxicity assays, data not easily translated to equivalent values *in vivo*. Ideally, *in vitro* cultures would respond to toxic agents by expressing clinically relevant biomarkers that facilitate direct comparisons between *in vitro* and *in vivo* results.

In this study, an organoid 3-D culture of kidney PT epithelial cells previously shown to retain primary cell differentiation status and functionality for weeks *in vitro* in culture was assessed for *in vivo*-relevant toxicity biomarkers after exposure to known nephrotoxic drugs. A well-published and extensively used, commercialized hyaluronic acid-based hydrogel biomaterial was used to encapsulate PT isolates exploiting mild Michael addition reactions (2,3). The advantages of this gel system are that HA gels: 1. do not contain proximal tubule cell adhesive sites, inhibiting PT cells from out-migrating from PTs and importantly, compelling them to remain associated within PTs during prolonged *in vitro* culture, 2. contain no catalyst/additives that affect cell viability, 3. quickly gel *in situ* around living cell or tissue isolates in the incubator or at room temperature, and 4. have an extensive publication record of characterization with both cultures of many different

primary and immortalized cell phenotypes.

A series of clinically used drugs -- cisplatin, doxorubicin, PAP, and colchicine -- with known and varying nephrotoxicity *in vivo* were chosen for evaluation. Cisplatin is a potent, platinum-based drug that kills cancer cells through crosslinking DNA, and a common chemotherapeutic agent used to treat several forms for cancers, including carcinomas, sarcomas, and lymphomas (7). Cisplatin's clinical use is primarily limited by its nephrotoxicity, affecting as many as 14-100% of all patients receiving the therapy (33). Beyond apoptosis induced through its DNA binding, cisplatin in PT epithelial cells can be transformed through interaction with brush border enzymes and CYP enzymes (34). Doxorubicin is another chemotherapeutic agent commonly clinically used to treat soft tissue sarcomas, carcinomas, and hematological malignancies, affecting proliferating cells (e.g., cancer cells) through DNA intercalation and interaction with topoisomerase II enzyme, effectively inhibiting DNA replication. Doxorubicin exhibits multiple-organ adverse effects, including nephrotoxicity. The exact mechanism of doxorubicin-induced nephrotoxicity is unknown, but is suggested to involve oxidative stress, lipid peroxidation, and protein oxidation as contributors to kidney pathology associated with this drug (35). PAP is paracetamol's (e.g., acetaminophen) metabolite found to induce PT-specific toxicity (36). Similar to cisplatin, PAP is thought to exert toxicity through biotransformation via  $\gamma$ -glutamyl-transferase and targeting of mitochondria (36). Colchicine is an anti-inflammatory drug approved to treat gout and familial Mediterranean fever. As a classical microtubule inhibitor drug, colchicine induces apoptosis in rapidly dividing cell by microtubule polymerization and mitosis inhibition (37). Colchicine's therapeutic use for other pathologies, like cancer, although explored in the literature, is limited by its toxicity *in vivo*.

Colchicine is a suspected proximal tubule-disrupting drug, since microtubule disruption was previously linked to disruption of endocytosis, membrane recycling, and polarized distribution of aquaporin-1 and gp330. Given these drugs, cisplatin would be considered the most potent proximal tubule nephrotoxicant, followed by doxorubicin and PAP, while colchicine can be classified as an alleged kidney toxicity agent.

Toxicity biomarkers for these studies focused on assays commonly performed for *in vivo* drug studies rather than *in vitro* assays. This design was proposed to distinguish current approaches in 2-D cell-based *in vitro* toxicology testing and performance distinctions for new 3-D organoid culture methods, both relative to documented *in vivo* toxicities for each drug. As a first step,  $EC_{50}$  values for drugs in confluent monolayer cell cultures of HEK 293, LLC-PK1, and primary PT epithelial cell in 3-D hydrogel cultures were established (Table 5.1). Data in Table 5.1 serve two main purposes: 1) to compare a common toxicity indicator currently used in the literature, and 2) to establish a reference point for these cell models for further experiments. Significant differences in cell viability were found between immortalized kidney cell lines grown in 2-D versus those in primary organoid 3-D models. Primary cells proved to be 1.6-164-fold more sensitive to drugs compared to transformed cell lines (Table 5.1). Colchicine produced the greatest  $EC_{50}$  difference and doxorubicin exhibited the least significant alteration in cell viability. Because all tested agents belonged to distinct drug families, it is difficult to speculate on the nature of such significant variations in drug  $EC_{50}$  values between cell models, but it is worth noting that colchicine produced the greatest differences among the immortalized cell lines. HEK 293, the transformed cell line least resembling *in vivo* epithelial kidney cells in this study, had the highest  $EC_{50}$  values for all

drugs. Hence, lack of drug-induced cell death could be due to the oversimplified nature of the kidney cell lines.

Kidney toxicity is a common side effect of clinical pharmacology interventions for numerous pathologies. Several biomarkers have been explored with varying degrees of sensitivity, epithelial cell specificity, and expediency of up-regulation in response to drug-induced injury. Several of these *in-vivo*-relevant biomarkers were selected for monitoring in the 3-D organoid PT cell culture. Specifically, this included the induction of soluble proteins linked to kidney injury including NAG,  $\gamma$ -glutamyl-transferase, and Kim-1; TNF $\alpha$  cytokine up-regulation in inflammation concomitant to epithelial damage; down-regulation of drug-specific cytochrome P450 enzymes; and stimulation of nephrotoxicity-associated genes.

#### NAG and $\gamma$ -glutamyl-transferase

Epithelial cell damage *in vivo* is commonly correlated to increases in NAG and  $\gamma$ -glutamyl-transferase in the urine of patients or animals (13-15). NAG is a high molecular weight lysosomal enzyme highly active in kidney PT cells (38). NAG appearance in tubular fluid is commonly associated with PT necrosis *in vivo* due to a variety of kidney diseases and inflammatory processes (38). Although NAG measurement in urine is still not a part of a standard hospital kidney damage panel, many clinical studies have shown that its changes are a useful indicator of ongoing tubular injury (38). Gamma-glutamyl-transferase is another active PT enzyme. Located on the brush border of the PT cells,  $\gamma$ -glutamyl-transferase is an important part of the  $\gamma$ -glutamyl metabolic cycle, and provides a key recycling pathway for glutathione and a

detoxification pathway for reactive species (39). Elevation of  $\gamma$ -glutamyl-transferase levels is a known indicator of cell damage and is currently a standard assay of liver problems. The increase of  $\gamma$ -glutamyl-transferase maybe a useful marker of PT damage by barbiturates, chemotherapeutics, aminoglycoside antibiotics, nonsteroidal anti-inflammatory drugs, chronic kidney damage and inflammation (26). Drug exposures to all cell lines at their  $EC_{50}$  values produced measurable amounts of NAG and  $\gamma$ -glutamyl-transferase but there were noteworthy differences in their up-regulation among the cell models. Specifically, similar to *in vivo* data, 3-D organoid culture had significant induction of NAG and  $\gamma$ -glutamyl-transferase enzymes in the media for all drugs tested (Figure 5.1). In primary cells, NAG stimulation exhibited less variation between experiments and appeared more sensitive as a toxicity marker than  $\gamma$ -glutamyl-transferase. Overall, no NAG up-regulation was associated with cell damage and only a few less toxic drugs produced  $\gamma$ -glutamyl-transferase induction in the immortalized cells. In contrast, primary cells responded to drug-induced cell damage with *in vivo*-relevant trends (14, 15).

#### Inflammatory protein production

Previous studies indicate that PT epithelium may be involved pro-inflammatory events linked to drug-induced toxicity, leading to the acute kidney injury (AKI) (18, 25). Initial injury is thought to initiate a sequence of events resulting in cell phenotypic changes and cytokine/chemokine induction that attracts immune system cells to the injury site. In the drug-induced AKI model, pro-inflammatory cytokine,  $TNF\alpha$ , is an important mediator of tissue damage that regulates

production of monocyte chemotactic protein-1 (MCP-1), macrophage inflammatory protein 1 $\alpha$  (MIP-1 $\alpha$ ), and regulated upon activation normal T-cell expressed and secreted (RANTES) chemokines, contributing to tissue injury and inflammatory kidney disease (25). Additionally, TNF $\alpha$  is central to kidney structural damage and renal dysfunction in cisplatin-induced AKI (18). Inhibition of TNF $\alpha$  production *in vivo* resulted in down-regulation of transforming growth factor  $\beta$  (TGF- $\beta$ ), RANTES, MIP-2, MCP-1, and interleukin 1 $\beta$  (IL-1 $\beta$ ) cytokines, while TNF $\alpha$ -deficient mice were resistant to drug's nephrotoxicity, suggesting the cytokine's key relevance to cisplatin-induced pathogenesis (18). The PT 3-D organoid culture demonstrated significant up-regulation of TNF $\alpha$  in cells treated with cisplatin, PAP, and doxorubicin, similar to that reported for these drugs *in vivo* (Figure 5.2) (18, 40, 41). Furthermore, the 3-D PT culture lacked statistically significant TNF $\alpha$  induction upon exposure to colchicine, similar to reports in animal studies, reflecting colchicine's ability to decrease TNF $\alpha$  protein expression on cell surfaces as a result of impaired cytoskeletal organization (Figure 5.2). Unlike primary cells, immortalized cells showed no statistically significant changes or sporadic up-regulation in TNF $\alpha$  (see Figure 5.2, Supplemental Figures). These data point to significant similarities in pro-inflammatory cytokine production between *in vivo* and 3-D organoid cultures, and limited expression of inflammatory mediators produced by traditional 2-D kidney cell line cultures.

#### CYP enzymatic response

The PT epithelium consists of metabolically active cells. Central to this function, the cytochrome P450 family of metabolic enzymes performs phase I oxidative metabolism to detoxify



xenobiotic environmental agents (42). CYP2B1/2 and CYP2E1 are some of the most common, highly produced P450 isoforms that are crucial for biotransformation of toxic compounds in rodents (16). Furthermore, given the significant distribution of kidney-active CYPs in different species, both CYP2B1 and CYP2E1 have been previously shown in porcine LLC-PK1 cells as capable of processing chemotherapeutic drugs cisplatin and ifosfamide (43). Humans are not known to express either enzyme in the healthy kidney tissue, but there is no information about their possible up-regulation in response to toxicants (16). CYP2B1 and CYP2E1 induction was measured in all three cell cultures assayed here, with both enzymes producing staining in all samples measured (see Figures 5.3, 5.4 and Supplemental Figures). CYP2B1 expression in HEK 293 cells was very low, almost 8-fold less than in LLC-PK1 cells (see Supplemental Figures). CYP2E1 expression was similar between the two immortalized cell lines (see Supplemental Figures). *In vivo*, kidney exposure to cisplatin down-regulates CYP2E1 content in the PT epithelium, generating reactive oxygen species, hydrogen peroxide, and catalytic iron, resulting in cisplatin-induced apoptosis. Doxorubicin, colchicine, and PAP are not known to be substrates for either CYP2B1 or CYP2E1. Comparing *in vitro* to current *in vivo* data on drug cytochrome induction, it is clear that the immortalized cells produced no information consistent with clinical data. On the other hand, 3-D organoid culture correctly predicted cisplatin down-regulation of CYP2E1. Stimulation of cytochrome P450 enzymes in drug-induced models suggests that 3-D PT organoid culture has greater predictive potential for *in vivo* drug-CYP interactions than immortalized cell lines, which not only poorly reflect animal data but have produced many false-positive indicators.

### Kim-1 induction

Nephrotoxicity biomarkers commonly lack sensitivity in predicting early events associated with kidney injury. Kim-1 (also called Tim-1) is a type I cell membrane glycoprotein with mucin-like and immunoglobulin-like extracellular domains that induce phagocytic properties in PT epithelial cells. Kim-1 specifically recognizes molecular apoptosis epitope, phosphatidylserine, and oxidized lipoproteins on the surfaces of damaged epithelial cells, and directs them to lysosomes for degradation (17, 27). Up-regulation of Kim-1 in PTs leads to removal of apoptotic cells in a timely fashion, presumably avoiding secondary necrosis and aiding in tissue remodeling and restoration of PT function (17). Kim-1 is shown to significantly up-regulate in response to drug-, ischemia-, and environmental agent-specific injury in a dose-responsive manner (17, 27, 44). It has been shown to outperform other biomarkers of kidney damage in humans, and is even thought to be predictive of post-surgical complications within hours of the medical procedure. Given the central role of Kim-1 in kidney damage, its endogenous production was evaluated in secondary cell lines and 3-D primary cells. The three-day time point was chosen due to original discovery of elevated Kim-1 mRNA induction during the first 48 hours after the initial injury (44). No protein staining by murine Kim-1 antibody in the immortalized cells was observed (data not shown). This was attributed most likely to lack of protein production in these cells since HEK 293 had poor endogenous production of kidney proteins and LLC-PK1 cells have been used as an expression cell line for Kim-1 expression constructs (27). Unlike immortalized cells, 3-D PT organoid cultures showed induction of Kim-1 in response to all drugs (Figure 5.5). Cisplatin and doxorubicin seemed to induce the strongest effect on protein production (Figure 5.5B,D) with drug-specific protein

distribution. Specifically, cisplatin produced more diffuse cytoplasmic distribution as previously observed *in vivo* (45), but doxorubicin had more nucleus-associated Kim-1 localization. Since only one time point was observed, variances in cellular localization could be due to differences in protein induction kinetics by the different drugs (cytoplasmic for cisplatin, PAP, and colchicine and punctate for doxorubicin). Data on Kim-1 up-regulation, similar to other information collected in this study, point to dissimilarities between differentially stable primary cells and immortalized cell lines in production of clinically important biomarkers of toxicity in response to environmental assaults.

#### Induction of nephrotoxicity-associated genes

Several gene products have been identified as predictive of early PT epithelial drug-induced damage. In this work, several of the most prominent biomarkers -- NGAL, VIM, CLU, HO-1, Spp1 -- were tested in immortalized and primary tissue replacement 3-D culture upon exposure to nephrotoxic drugs. NGAL is a cytosolic (or secreted) protein that belongs to the lipocalin superfamily (20). NGAL was first discovered in activated neutrophils, but was subsequently found to be inducible by many different cells in response to injury. NGAL in PT epithelial cells was shown to be induced *in vivo* in response to AKI and chronic kidney disease (CKD), but most researchers found NGAL protein to be elevated within hours of acute kidney injury (46).

VIM is a class III intermediate filament of cytoskeleton. VIM is expressed in normal tissues of mesenchymal origin and the rapidly proliferating epithelial lining commonly associated with cancers and tissue injury. Expression of VIM in proximal tubule cells is allied with pathological changes in PTs, and is thought to be a marker of cell de-differentiation (19). VIM kidney induction

*in vivo* was previously found in ischemia-induced injury and nephrotoxic tubular necrosis (47).

CLU is heterodynamic glycoprotein ubiquitously produced throughout the body (21). Up-regulation of CLU in adult tissues has been linked to various disease states but exact biological significance of the protein is still unknown (21). CLU was implicated in membrane recycling, apoptosis, and even suggested to be a type of stress-induced heat shock protein (21). The body of evidence from protein knockout mice (*CLU*<sup>-/-</sup>) suggests that CLU can interact with different signaling molecules in affected tissues, promoting or inhibiting cellular death (48). *In vivo* in the proximal tubule epithelial cells, CLU up-regulation has been associated with both ischemia- and drug-induced kidney damage (49).

HO-1 is a microsomal enzyme that catalyzes conversion of heme to biliverdin, producing iron and carbon monoxide (22). In injured tissues up-regulation of HO-1 is associated with protective response against oxidizing agents (22). *In vivo*, induction of HO-1 has been previously reported in the case of cisplatin, hydrogen peroxide, nitric oxide, endotoxin, cytokines, ultraviolet A irradiation, shear stress, hyperoxia, and oxidized low-density lipoproteins (LDL) (22).

Spp1 is a structural glycoprotein highly preserved among different species. Spp1 is a multi-potent agent whose role in kidney damage is two-fold: Spp1 acts as chemoattractant for inflammatory cells and may play an anti-apoptotic cellular role. *In vivo*, Spp1 was found to be significantly elevated in nephrotoxic and ischemic forms of AKI and together with CLU and NGAL, Spp1 is considered to be a most potent early predictor of kidney tissue injury (23).

In this study, all gene biomarkers were assessed using qPCR at their corresponding EC<sub>50</sub> values after 3 days of culture/incubation with the selected drugs in immortalized and primary 3-D

organoid cultures. HEK 293 cell line showed no induction of nephrotoxicity-associated genes except for VIM in the case of doxorubicin. LLC-PK1 cells had greater but still rather limited induction of biomarkers: up-regulated NGAL, VIM, and HO-1 after treatment with PAP; NGAL, VIM, Spp1, and HO-1 after exposure to cisplatin; and VIM when exposed to doxorubicin. Unlike immortalized cell lines, primary PT cells induced all tested gene biomarkers for all tested drugs. Furthermore, except for NGAL, transcriptional stimulation in the 3-D PT cell culture, unlike immortalized cell lines, resulted in mostly statistically significant up-regulation, reflecting greater reproducibility of mRNA increase in this model vs. traditional 2-D culture. Lack of significant NGAL stimulation was most likely due to the fact that NGAL is induced only after significant degree of tissue damage (46). Here mRNA was collected after 3 days and might have been extracted from cells under recovery. Overall, data closely followed other immortalized cell studies that showed inability of such cells to replicate animal data, and *in vivo* rodent and human studies used to elucidate and validate gene biomarkers (50).

### Conclusions

This study focused on assessing the ability of primary 3-D organoid cell cultures of proximal tubules and immortalized kidney cell lines grown using traditional 2-D culture methods to respond to nephrotoxic drugs with known *in vivo*-relevant toxicity biomarkers. Significant differences were found between the drug responses of 2-D and 3-D kidney cell culture models. Immortalized cell lines responded to nephrotoxic agents with no or limited induction of NAG and  $\gamma$ -glutamyl-transferase cellular enzymes, TNF $\alpha$  and Kim-1 inflammatory proteins, VIM, CLU, Spp1,

NGAL, and HO-1 genes , and produced no *in vivo*-relevant CYP down-regulation. By contrast, 3-D hydrogel-based PT tissue culture allowed relatively unhindered drug and media diffusion and responded to drugs with biomarkers similar to animal and clinical published data. Furthermore, 3-D organoid PT model cultures were more sensitive to toxic insult compared to immortalized cell lines. Overall, current work indicates that stabilization of cellular differentiation status via preservation of *in vivo* tissue architecture in 3-D culture induces clinically relevant toxicity biomarkers. This study provides further validation for the use of semi-synthetic extracellular matrices based on HA to evaluate drug toxicity in an *in vitro* setting that better mimics *in vivo* nephrotoxicity outcomes.

#### Acknowledgements

We thank Dr. J.V. Bonventre, Brigham and Women's Hospital/Harvard Medical School, and Dr. R. Hitchcock, University of Utah, for generous donation of R9 Kim-1 and secondary Alexa-488 antibodies, respectively. We are grateful to G. Stoddard, University of Utah Statistical Core, for helpful discussion of statistical analysis, Dr. C. Rodesch, University of Utah Imaging Facility, for assistance with 3-D imaging, and Dr. J. Yockman, University of Utah, for help with qPCR. Partial financial support was provided by SEED and Micro grants from the University of Utah. The University of Utah Study Design and Biostatistics Center, is supported by UL1-RR025764 and C06-RR11234 grants from the National Center for Research Resources.

### References

1. Pampaloni F., Reynaud E.G., and Stelzer E.H. The third dimension bridges the gap between cell culture and live tissue. *Nat Rev.* 2007;8(10):839-45.
2. Prestwich G.D. Evaluating drug efficacy and toxicology in three dimensions: using synthetic extracellular matrices in drug discovery. *Acc Chem Res.* 2008;41(1):139-48.
3. Prestwich G.D. Hyaluronic acid-based clinical biomaterials derived for cell and molecule delivery in regenerative medicine. *J Control Release.* 2011;155(2):193-9.
4. US Department of Human and Health Services. US Food and Drug Administration (FDA). Innovation or stagnation: challenge and opportunity on the critical path to new medical products. 2004.
5. Schuster D., Laggner C., and Langer T. Why drugs fail--a study on side effects in new chemical entities. *Curr Pharm Des.* 2005;11(27):3545-59.
6. Olson S. RS. and Giffin R., editor. Accelerating the development of biomarkers for drug safety: workshop summary. Forum on drug discovery, development, and translation: National Academy of Science: Institute of Medicine; 2009; Washington, DC.
7. Pabla N. and Dong Z. Cisplatin nephrotoxicity: mechanisms and renoprotective strategies. *Kidney Int.* 2008;73(9):994-1007.
8. Hanigan M.H. and Devarajan P. Cisplatin nephrotoxicity: molecular mechanisms. *Cancer Ther.* 2003;1:47-61.
9. McLarnon S., Holden D., Ward D., Jones M., Elliott A., and Riccardi D. Aminoglycoside antibiotics induce pH-sensitive activation of the calcium-sensing receptor. *Biochem Biophys Res Commun.* 2002;297(1):71-7.
10. Godek M.L., Michel R., Chamberlain L.M., Castner D.G., and Grainger D.W. Adsorbed serum albumin is permissive to macrophage attachment to perfluorocarbon polymer surfaces in culture. *J Biomed Mat Res.* 2009;88(2):503-19.
11. Terryn S., Jouret F., Vandenabeele F., Smolders I., Moreels M., and Devuyt O., et al. A primary culture of mouse proximal tubular cells, established on collagen-coated membranes. *Am J Physiol Renal Physiol.* 2007;293(2):F476-85.
12. Miller R.L., Zhang P., Chen T., Rohrwasser A., and Nelson R.D. Automated method for the isolation of collecting ducts. *Am J Physiol Renal Physiol.* 2006;291(1):F236-45.

13. Nishimura K., Kawada M., Suehiro T., Yamano T., and Hashimoto K. [Urinary N-acetyl-beta-D-glucosaminidase and gamma-glutamyl-transpeptidase activities for evaluation of renal disturbance in patients with multiple myeloma]. *Nippon Jinzo Gakkai shi*. 1992;34(10):1087-94.
14. Davis J.W. and Kramer J.A. Genomic-based biomarkers of drug-induced nephrotoxicity. *Expert Opin Drug Metab Toxicol*. 2006;2(1):95-101.
15. Sieber M., Hoffmann D., Adler M., Vaidya V.S., Clement M., and Bonventre J.V., et al. Comparative analysis of novel noninvasive renal biomarkers and metabonomic changes in a rat model of gentamicin nephrotoxicity. *Toxicol Sci*. 2009;109(2):336-49.
16. Martignoni M., Groothuis G.M., and de Kanter R. Species differences between mouse, rat, dog, monkey and human CYP-mediated drug metabolism, inhibition and induction. *Expert Opin Drug Metab Toxicol*. 2006;2(6):875-94.
17. Huo W., Zhang K., Nie Z., Li Q., and Jin F. Kidney injury molecule-1 (KIM-1): a novel kidney-specific injury molecule playing potential double-edged functions in kidney injury. *Transplant Rev*. 2010;24(3):143-6.
18. Ramesh G. and Reeves W.B. TNF-alpha mediates chemokine and cytokine expression and renal injury in cisplatin nephrotoxicity. *J Clin Invest*. 2002;110(6):835-42.
19. Bonventre J.V. Dedifferentiation and proliferation of surviving epithelial cells in acute renal failure. *J Am Soc Nephrol*. 2003;14 Suppl 1:S55-61.
20. Flower D.R., North A.C., and Sansom C.E. The lipocalin protein family: structural and sequence overview. *Biochim Biophys Acta*. 2000;1482(1-2):9-24.
21. Jones S.E. and Jomary C. Clusterin. *Int J Biochem Cell Biol*. 2002;34(5):427-31.
22. Platt J.L. and Nath K.A. Heme oxygenase: protective gene or trojan horse. *Nat Med*. 1998 ;4(12):1364-5.
23. Bonventre J.V., Vaidya V.S., Schmouder R., Feig P., and Dieterle F. Next-generation biomarkers for detecting kidney toxicity. *Nat Biotech*. 2010;28(5):436-40.
24. Livak K.J. and Schmittgen T.D. Analysis of relative gene expression data using real-time quantitative PCR and the 2(-Delta Delta C(T)) Method. *Methods*. 2001;25(4):402-8.
25. Akcay A., Nguyen Q., and Edelstein C.L. Mediators of inflammation in acute kidney injury. *Mediators Inflamm*.;2009:137072.
26. Teppala S., Shankar A., Li J., Wong T.Y., and Ducatman A. Association between serum



gamma-glutamyltransferase and chronic kidney disease among US adults. *Kidney Blood Press Res.* ;33(1):1-6.

27. Ichimura T., Asseldonk E.J., Humphreys B.D., Gunaratnam L., Duffield J.S., and Bonventre J.V. Kidney injury molecule-1 is a phosphatidylserine receptor that confers a phagocytic phenotype on epithelial cells. *J Clin Invest.* 1998;118(5):1657-68.

28. Rebelo L., Carmo-Fonseca M., and Moura T.F. Redistribution of microvilli and membrane enzymes in isolated rat proximal tubule cells. *Biol Cell*;74(2):203-9.

29. Hartmann F. and Bissell D.M. Metabolism of heme and bilirubin in rat and human small intestinal mucosa. *J Clin Invest.* 1982;70(1):23-9.

30. Simmons N.L. A cultured human renal epithelioid cell line responsive to vasoactive intestinal peptide. *Exp Physiol.* 1990;75(3):309-19.

31. Larsson M., Hjalml G., Sakwe A.M., Engstrom A., Hoglund A.S., and Larsson E., et al. Selective interaction of megalin with postsynaptic density-95 (PSD-95)-like membrane-associated guanylate kinase (MAGUK) proteins. *Biochem J.* 2003;373(Pt 2):381-91.

32. Lenz W., Herten M., Gerzer R., and Drummer C. Regulation of natriuretic peptide (urodilatin) release in a human kidney cell line. *Kidney Int.* 1999;55(1):91-9.

33. Miller R.P., Ramesh G., and Reeves W.B. Mechanisms of cisplatin nephrotoxicity. *Toxins.* 2010;2:2490-518.

34. Daley-Yates P.T. and McBrien D.C. Cisplatin metabolites in plasma, a study of their pharmacokinetics and importance in the nephrotoxic and antitumour activity of cisplatin. *Biochem Pharmacol.* 1984;33(19):3063-70.

35. Mohan M., Kamble S., Gadhi P., and Kasture S. Protective effect of solanum torvum on doxorubicin-induced nephrotoxicity in rats. *Food Chem Toxicol.* 2010;48(1):436-40.

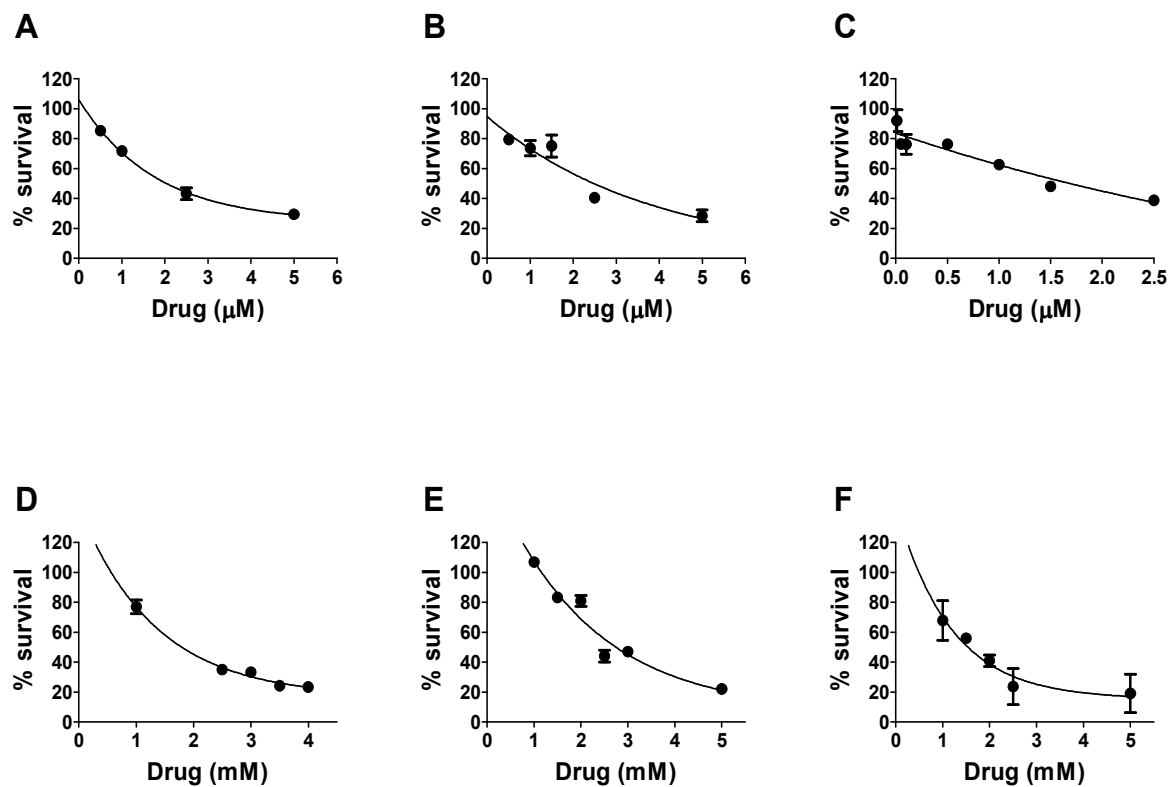
36. Lock E.A., Cross T.J., and Schnellmann R.G. Studies on the mechanism of 4-aminophenol-induced toxicity to renal proximal tubules. *Hum Exp Toxicol.* 1993;12(5):383-8.

37. Zieve G.W., Turnbull D., Mullins J.M., and McIntosh J.R. Production of large numbers of mitotic mammalian cells by use of the reversible microtubule inhibitor nocodazole. Nocodazole accumulated mitotic cells. *Exp Cell Res.* 1980;126(2):397-405.

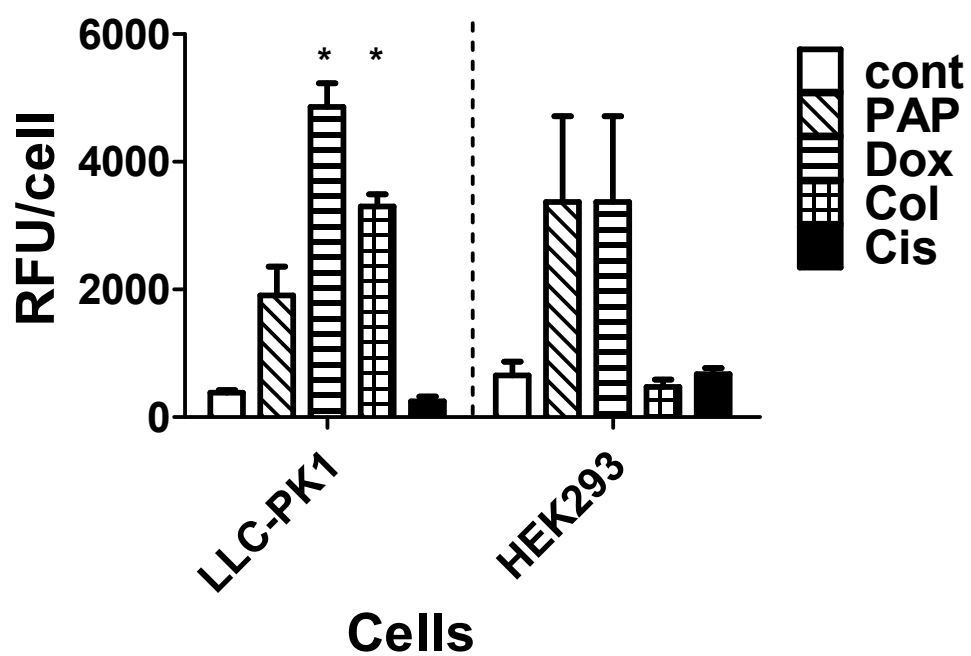
38. Kunin C.M., Chesney R.W., Craig W.A., England A.C., and DeAngelis C. Enzymuria as a marker of renal injury and disease: studies of N-acetyl-beta-glucosaminidase in the general population and in patients with renal disease. *Pediatrics.* 1978;62(5):751-60.

39. Tate S.S. and Meister A. Identity of maleate-stimulated glutaminase with gamma-glutamyl transpeptidase in rat kidney. *J Biol Chem.* 1975;250(12):4619-27.
40. Ghosh J., Das J., Manna P., and Sil P.C. Acetaminophen induced renal injury via oxidative stress and TNF-alpha production: therapeutic potential of arjunolic acid. *Toxicology.* 2010;268(1-2):8-18.
41. Niiya M., Niiya K., Kiguchi T., Shibakura M., Asaumi N., and Shinagawa K., et al. Induction of TNF-alpha, uPA, IL-8 and MCP-1 by doxorubicin in human lung carcinoma cells. *Cancer Chemother Pharmacol.* 2003;52(5):391-8.
42. Hook J.B. Toxic responses of the kidney. In J. Doull, C.D. Klaassen, and M.O. Amdur (eds.), *Casarett and Doull's toxicology: the basic science of poisons*, Macmillan, New York, 1980.
43. Liu H., Baliga M., and Baliga R. Effect of cytochrome P450 2E1 inhibitors on cisplatin-induced cytotoxicity to renal proximal tubular epithelial cells. *Anticancer Res.* 2002;22(2A):863-8.
44. Ichimura T., Bonventre J.V., Bailly V., Wei H., Hession C.A., and Cate R.L., et al. Kidney injury molecule-1 (KIM-1), a putative epithelial cell adhesion molecule containing a novel immunoglobulin domain, is up-regulated in renal cells after injury. *J Biol Chem.* 1998;273(7):4135-42.
45. Ichimura T., Hung C.C., Yang S.A., Stevens J.L., and Bonventre J.V. Kidney injury molecule-1: a tissue and urinary biomarker for nephrotoxicant-induced renal injury. *Am J Physiol Renal Physiol.* 2004;286(3):F552-63.
46. Supavekin S., Zhang W., Kucherlapati R., Kaskel F.J., Moore L.C., and Devarajan P. Differential gene expression following early renal ischemia/reperfusion. *Kidney Int.* 2003;63(5):1714-24.
47. Dierick A.M., Praet M., Roels H., Verbeeck P., Robyns C., and Oosterlinck W. Vimentin expression of renal cell carcinoma in relation to DNA content and histological grading: a combined light microscopic, immunocytochemical and cytophotometrical analysis. *Histopathology.* 1991;18(4):315-22.
48. Han B.H., DeMattos R.B., Dugan L.L., Kim-Han J.S., Brendza R.P., and Fryer J.D., et al. Clusterin contributes to caspase-3-independent brain injury following neonatal hypoxia-ischemia. *Nat Med.* 2001;7(3):338-43.
49. Ishii A., Sakai Y., and Nakamura A. Molecular pathological evaluation of clusterin in a rat model of unilateral ureteral obstruction as a possible biomarker of nephrotoxicity. *Toxicol Pathol.* 2007;35(3):376-82.
50. Yang A., Trajkovic D., Illanes O., and Ramiro-Ibanez F. Clinicopathological and tissue

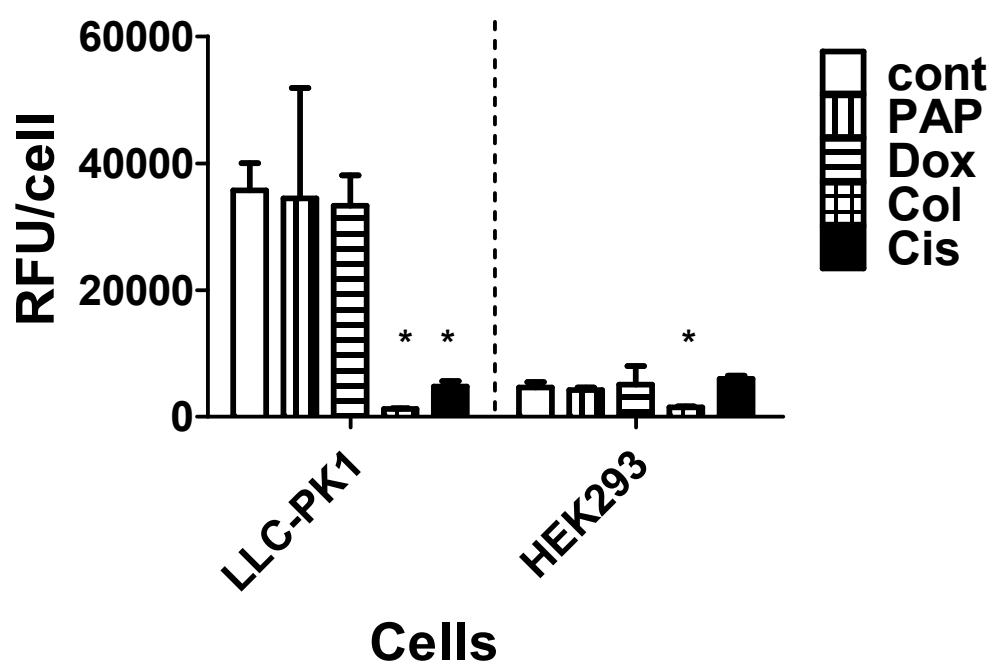
indicators of para-aminophenol nephrotoxicity in sprague-dawley rats. *Toxicol Pathol.* 2007;35(4):521-32.



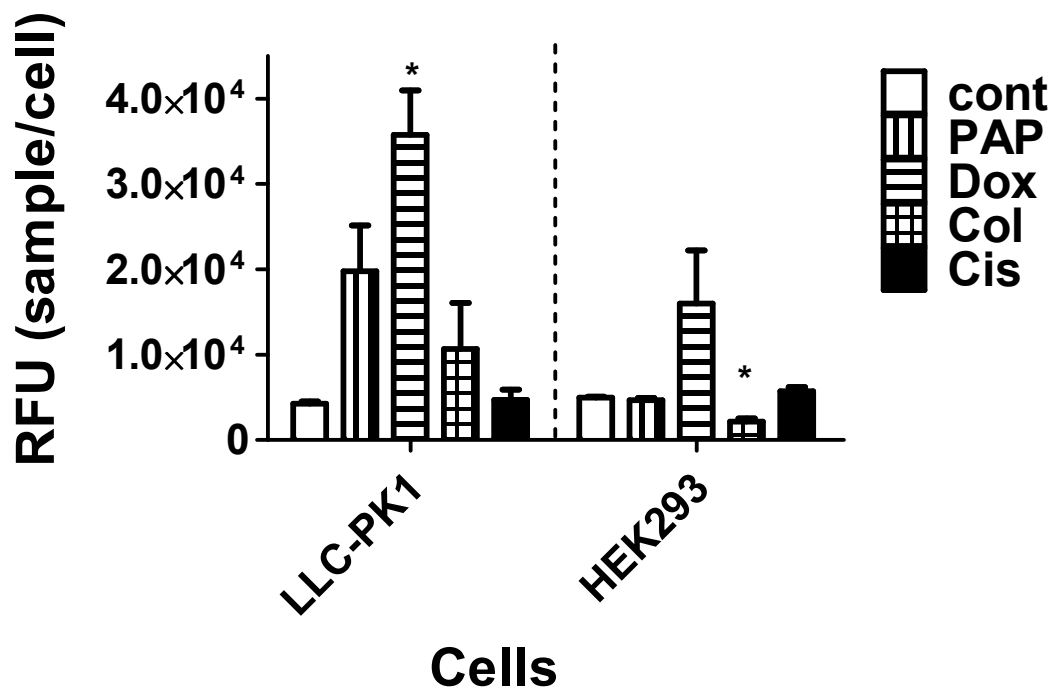
**Supplemental Figure 5.1.** Dose-response curves for doxorubicin (A-C) and cisplatin (D-F) in three cell culture models: LLC-PK1 (A,D), HEK293 (B,E), and 3-D HA gel PT organoid model (C,F).



**Supplemental Figure 5.2.** TNF- $\alpha$  expression on cultured cell surfaces at drugs' EC<sub>50</sub> values in different kidney cell cultures normalized to cell number (LLC-PK1 and HEK293 are 2-D monolayers on plastic; RFU=relative fluorescence units).



**Supplemental Figure 5.3.** CYP2B1 intracellular expression at drugs' EC<sub>50</sub> values in different kidney cell lines normalized to cell number (LLC-PK1 and HEK293 are 2-D monolayers on plastic; RFU=relative fluorescence units).



**Supplemental Figure 5.4.** CYP2E1 intracellular expression at drugs' EC<sub>50</sub> values in different kidney cell cultures normalized to cell number (LLC-PK1 and HEK293 are 2-D monolayers on plastic; RFU=relative fluorescence units).

## CHAPTER 6

### SUMMARY AND FUTURE WORK

#### Summary

Kidney toxicity or nephrotoxicity is a pathological condition that commonly occurs as a result of drug or environmental exposure (1). Proximal tubule (PT) epithelial cells that line proximal tubules (Figure 2.3H) are the most frequently affected part of the kidney, due to the large surface area and reabsorption function of these cells (1). Although kidney toxicity is a major medical problem, there are no *in vitro* models that can reproducibly and reliably reflect pathological cellular mechanisms of the condition. Current (Chapter 5) and previous literature indicate that current *in vitro* models that primarily rely on immortalized cell lines cultured on two-dimensional plastic supports (1), are incapable or highly limited in their ability to reproduce typically measured *in vivo* indicators of nephrotoxicity -- induction of CYP enzymes (CYP2B1 and CYP2E1, Chapter 3,5), drug metabolism (Chapter 3), inflammatory mediators (Kim-1, IL-6, TNF, MCP-1, IL-1 $\beta$ , MIP-1 $\alpha$ , RANTES, Chapter 3) and genes of toxicity up-regulation (CLU, VIM, NGAL, Spp1, HO, Chapter 5) (2), and enzyme shedding ( $\gamma$ -glutamyl-transferase brush border and N-acetyl- $\beta$ -D-glucosaminidase intracellular enzymes, Chapter 5). Furthermore, commonly practiced differences in culturing conditions can result in extreme variability within the produced data as well as *in vivo*-irrelevant toxicological data (Chapter 4). Nevertheless, the differences



between clinically obtained results and *in vitro* data most likely reflect limited structural similarities between the kidney tissue *in vivo* and transformed cell lines. Specifically, immortalized kidney cells were shown to lack or have minimal expression of drug transporters and cell ligands (3) that are involved in drug up-take (4-11), intracellular drug targets (12), drug metabolizing CYP enzymes (Chapter 5) and enzymes that may be involved in drug biotransformation (13). Hence, these cellular models are intrinsically limited in their ability to facilitate *in vivo*-like cellular damage processes (Chapter 4). This work presents a new model of proximal tubule-centered nephrotoxicity that unlike other models published in the literature overcomes the above mentioned problems and can respond to environmental assaults with clinically-relevant biomarkers such as proteins Kim-1 and TNF- $\alpha$ ; N-acetyl- $\beta$ -D-glucosaminidase and  $\gamma$ -glutamyl-transferase enzymes enzyme shedding; HO, Spp1, CLU, VIM toxicity gene up-regulation; MCP-1, RANTES, MIP-1 $\alpha$ , IL-1 $\beta$ , IL-6 cytokine release; cytochrome CYP2E2 and CYP2B1 induction; and metabolite production (Chapter 3). The model was created by encapsulating whole fragments of the proximal tubules that contain proximal tubule epithelial cells in a hyaluronic acid (HA) gel. The design retained cell-cell, cell-matrix, and tissue architecture that were hypothesized to promote cellular differentiation and functional stability *in vitro*. Biomarker production was assessed in response to nephrotoxic molecules -- cisplatin, colchicine, PAP, and doxorubicin. The obtained results indicated significant similarities in production of toxicity indicators between *in vivo* and 3-D organoid cultures of proximal tubules (Chapter 3), suggesting that preservation of *in vitro* cellular phenotype through recapitulation of the cells' native microenvironment is critical to making *in vitro* models that can respond to toxicity with clinically-relevant cellular damage. Observations of 3-D

cultured PTs established fundamental rules that must be considered when developing *in vitro* models with clinical importance and proving that appropriate *in vitro* culture systems can respond to toxic agents with a wide variety of *in vivo* biomarkers.

### Future Work

The results described in the body of this work demonstrated the powerful influence the native microenvironment has on primary cell differentiation and functional potential. *In vitro preservation* of cell-cell, cell-native matrix, and 3-D architecture are crucial for retaining *in vivo*-like cell characteristics as well as their ability to function as a tissue unit in response to toxic exposure. Using this information as the stepping stone, several avenues for future research can be suggested to improve the model's long-term culturing, physiological relevance, and high throughput (HTS) capability.

### Improvements to HTS potential of the model

The biggest obstacle in using the proposed 3-D organoid PT model is proximal tubule isolation. The current isolation method 1) takes over 2 hours to process the PTs from a mouse to encapsulation in the 3-D HA culture, 2) is labor intensive, and 3) has a relatively small yield. Several alternative methods have been discussed in the literature, including gradient methods (Percoll size and density purification) (14), mechanical isolation (iron oxide perfusion, purification by sieving, and magnetic removal of glomeruli) (14), surgical microdissection (15), and flow cytometric isolation (16). Gradient methods are similar in principle to the method used in this work and therefore have similar issues. Use of larger animals, such as rabbits (15), may allow for

surgical isolation of proximal tubules; however, the protocols are equally labor intensive, expensive, and not applicable to HTS studies. Miller et al. published a method for automated isolation of the collective ducts using flow cytometry on kidney digests from transgenic mice expressing green fluorescent protein (GFP) in that part of the nephron (16). Unfortunately, the protocol involved genetically altered species, had small yield, and required exclusive use of non-sterile worm sorters as the regular flow cytometry equipment cannot handle the size of the organoid fractions (16). A more HTS applicable model may involve use of thin kidney slices that are encapsulated in the gel. There are several advantages to such a model. Automated methods for organ slicing that can reduce the thickness of tissue slices as well as minimize human labor associated with their preparation have been published (17). Additionally, this method has a much greater yield of nephron sections, which would improve the 'signal' levels in the collected data. Although this isolation and culture method may initially seem superior, it cannot be underestimated that minimization of tissue thickness is an important variable in increasing oxygen and nutrient diffusion to the cells in a 3-D culture that lacks blood vessels. Nevertheless, introduction of the automated method would reduce tissue handling times, improving the reproducibility of the procedure and increasing the number of tissue fragments that can be created per kidney and per unit of time. All of these improvements would be of significant value to HTS methods. It is important to note that the downside of using kidney (or any tissue) slices vs. isolated organoid structures is that each slice would contain many different cell types, increasing the 'noise level' in the acquired data. For example, kidneys contain ~20 different cell types (18) and are likely to severely increase the signal-to-noise ratio in measurements. Hence, empirical evaluation would be

required to evaluate the value and relevance of the data collected from these models as compared to *in vivo* measurements.

#### Improvements to histological/ TEM avaluation of the model

One of the difficulties with using the 3-D HA model is its incompatibility with common tissue techniques such as histology or TEM. Both of these techniques are of significant value to 3-D toxicological assessment due to significant knowledge associated with morphological changes during nephrotoxicity (19). The gel (1.5% CMHA, 7.5% PEGDA) is too soft for easy slicing that is done during both procedures. Hence, use of the gel that is easy to degrade, such as HA with cleavable bonds might be of significant value. The remaining tissue (PTs or slices) can be embedded into materials more suitable for TEM and histological assessment. An example of such gel can be CMHA with disulfide-containing crosslinkers, PEG(SS)DA, PEG(SS)<sub>2</sub>DA, PEG(SS)<sub>3</sub>DA (20). These gels can be broken down using mild reducing and cell-comparable agents such as *N*-acetyl-cysteine or glutathione (20). Furthermore, other techniques, such as RNA isolation for RT-PCR and qPCR, might also benefit from using easily degradable HA, because it is almost impossible to remove all the gel from RNA preparation using TRIzol® solubilization method.

#### Improvements to cell viability

One of the major downsides of the presented 3-D organoid model was limited cell viability in 3-D culture. The data indicated that this was most likely due to the inadequate oxygen delivery to the deep layers of the gel. Having a perfused system instead of the static system would greatly improve the oxygenation of the 3-D constructs. This could be achieved by converting the culture

system to either a plate design (Figure 6.1) with an integrated perfusion system with or without Transwell® inserts (Figure 6.1B) or to a bioreactor.

Figure 6.1 shows a possible design for the perfusion plate that could be used in combination with existing Transwell® technology. The design is focused on creation of a novel multitasking tissue culture plate that would enable simplified cell surveillance. The primary advantages of the design are improvements in 3-D culture perfusion as well as the possibility of simultaneous types of environmental exposure. The proposed prototype plate is a modification of a 12-well tissue culture plate, but the suggested alterations can be applied to any size plate already on the market. The primary features of the prototype are small pipes under valve control that can connect wells within the tissue culture plate or similarly can be joined with a dynamic perfusion system (Fig 6.1A). The system of valves within the plate will allow for as many as 12 different parameters to be assessed simultaneously, where both the timing and length of the exposure can be modulated by the researcher (Fig 6.1C and D). The experimental setup can be further customized by addition of a perfusion system or a pump to explore conditions of shear stress and flow (Fig 6.1A). All wells would be protected by a 0.22µm filter inserted at the joint with the pipe to prevent cross-contamination and sterility of the plate. The design can be applied to 12-well plates with inserts (as shown in Figure 6.1) or to 96-well plates. Table 6.1 summarizes advantages of the perfused plate design over the traditional static Transwell® system.

Use of bioreactor with a perfusion system is another option. Many different prototypes can be found in the literature or purchased from commercial vendors. 3D Biotech™ bioreactor is a good example of commercially available perfusion system, due to its simplicity and compatibility with

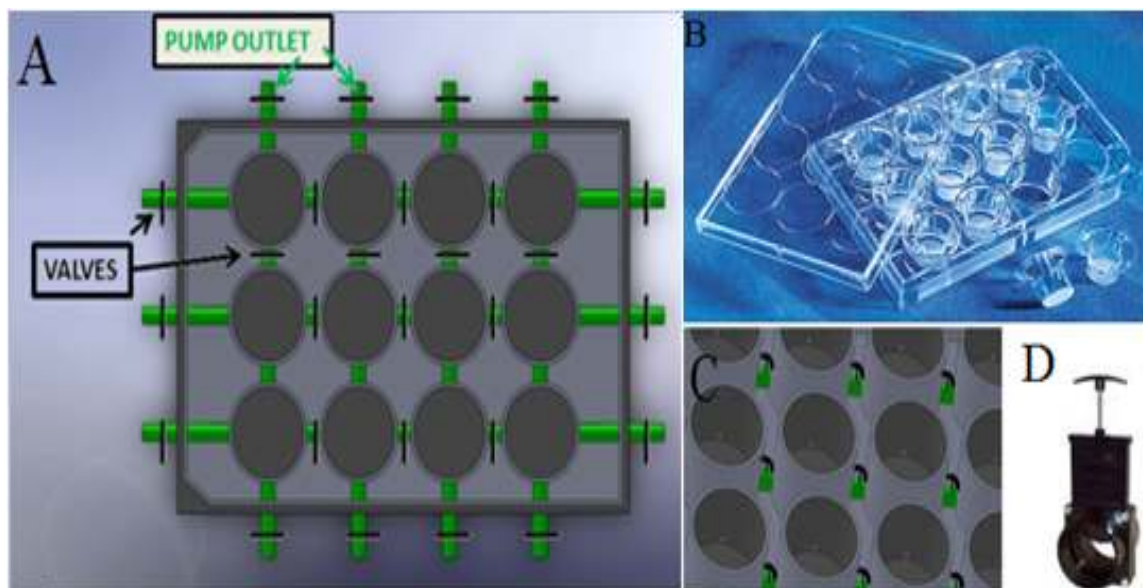


Figure 6.1. Possible perfusion plate layout. A) Transwell® prototype-plate layout, B) Corning transwell, C) Transwell® prototype-section that shows the placement of gate micro valves, D) Slide gate micro valve

Table 6.1 Comparison of profused plate to the Transwell® 12-well Corning® plate

| <b>Point of comparison</b>                           | <b>Corning® Traswell® Plate</b>   | <b>Prototype</b>   |
|--|---|--|
| <b>Basic Design</b>                                  | Each well has an insert with a filter that can support cell growth. Different cells are cultured on the tissue culture polystyrene (bottom) and polycarbonate or polyester membrane of the insert (top) | Cells are expanded on the tissue culture polystyrene at the bottom of the wells. Different cells can be plated in different wells and communication can be established by opening a valve in the connecting pipe |
| <b>Effect on culture O<sub>2</sub> supply</b>        | Cells grown on the filter and the bottom of the well will see different O <sub>2</sub> concentrations, which dictate cell viability   | None   |
| <b>Flow and shear stress studies</b>                 | No  | Yes  |
| <b>Requires different models for different cells</b> | Yes   | No   |

the 3-D organoid or 3-D tissue slice design. Alternatively, the 3D Profusion Bioreactor® (3D Biotech™, USA) is small enough to fit into a cell culture incubator and can hold up to 120 constructs at the same time. The entire unit, with the exception of the pump, can be pressure and steam sterilized and can be used with a wide size range of 3-D scaffolds.

#### Future data analysis

The most exciting finding of the 3D organoid model was discovery that for the first time a wide range of *in vivo*-relevant biomarkers can be assessed from an *in vitro* culture system. This allows the direct comparisons between animal and *in vitro* cultures using libraries of drugs with known nephrotoxic properties (e.g., cisplatin, nomifensine, methoxyflurane, PAP, colchicine, doxorubicin, ifosfomide, gefitinib, cyclophosphamide, mithramycin, azacitidine, methotrexate, imatinib, pentostatin, bisphosphonates(19)) and established biomarkers (e.g., cytokines -- Kim-1, NGAL, MCP-1, TNF $\alpha$ , RANTES, MIP-1 $\alpha$ , IL-1 $\beta$ , IL-6, IL-18, enzymes -- N-acetyl- $\beta$ -D-glucosaminidase and  $\gamma$ -glutamyl-transferase, cytochromes -- CYP2E2 and CYP2B1, and genes of toxicity -- HO, Spp1, Kim-1, NGAL, CLU, VIM, RBP, AA819244 EST, IGF-BP3, Sgp2,  $\beta$ -alanine-pyruvate amino transferase, vitamin D binding protein, class I beta-tubulin, UDPGT, EGF, nerve growth factor, P4502D18, AA957270 EST, syaptonygrin 2, BHMT, AA925142 EST (20)). Although there is no expectation that 3-D cultures would be able to respond with every biomarker to every drug, the direct comparison of several molecules would allow the establishment of a rubric outlining the impact of individual 'positive' biomarker assays as well as the statistically relevant change in biomarker levels required for the overall determination of predictive *in vitro* toxicity (Chapter 1).



Although no *in vitro* culture system will ever perfectly mimic the exact sensitivity or tissue response of an *in vivo* system, empirical evaluation of the most dependable, sensitive, and reproducible assays are needed for *in vitro-in vivo* comparisons. The 3-D organoid culture model described herein presents a significant step toward this lofty goal.

### References

1. M.A. Dorato and L.A. Buckley. Toxicology testing in drug discovery and development. Current Protocols in Toxicology, John Wiley & Sons, Inc., 2001.
2. T. Ichimura, E.J. Asselton, B.D. Humphreys, L. Gunaratnam, J.S. Duffield, and J.V. Bonventre. Kidney injury molecule-1 is a phosphatidylserine receptor that confers a phagocytic phenotype on epithelial cells. The Journal of Clinical Investigation. 118:1657-1668 (2008).
3. M. Larsson, G. Hjalmarsson, A.M. Sakwe, A. Engstrom, A.S. Hoglund, E. Larsson, R.C. Robinson, C. Sundberg, and L. Rask. Selective interaction of megalin with postsynaptic density-95 (PSD-95)-like membrane-associated guanylate kinase (MAGUK) proteins. Biochem J. 373:381-391 (2003).
4. Y. Chen, S. Li, C. Brown, S. Cheatham, R.A. Castro, M.K. Leabman, T.J. Urban, L. Chen, S.W. Yee, J.H. Choi, Y. Huang, C.M. Brett, E.G. Burchard, and K.M. Giacomini. Effect of genetic variation in the organic cation transporter 2 on the renal elimination of metformin. Pharmacogenet Genomics. 19:497-504 (2009).
5. Y. Hagos, W. Krick, T. Braulke, C. Muhlhausen, G. Burckhardt, and B.C. Burckhardt. Organic anion transporters OAT1 and OAT4 mediate the high affinity transport of glutarate derivatives accumulating in patients with glutaric acidurias. Pflugers Arch. 457:223-231 (2008).
6. M. Sato, H. Mamada, N. Anzai, Y. Shirasaka, T. Nakanishi, and I. Tamai. Renal secretion of uric acid by organic anion transporter 2 (OAT2/SLC22A7) in human. Biol Pharm Bull. 33:498-503 (2010).
7. A.R. Erdman, L.M. Mangravite, T.J. Urban, L.L. Lagpacan, R.A. Castro, M. de la Cruz, W. Chan, C.C. Huang, S.J. Johns, M. Kawamoto, D. Stryke, T.R. Taylor, E.J. Carlson, T.E. Ferrin, C.M. Brett, E.G. Burchard, and K.M. Giacomini. The human organic anion transporter 3 (OAT3; SLC22A8): genetic variation and functional genomics. Am J Physiol

- Renal Physiol. 290:F905-912 (2006).
8. P. Anderle, C.U. Nielsen, J. Pinsonneault, P.L. Krog, B. Brodin, and W. Sadee. Genetic variants of the human dipeptide transporter PEPT1. *J Pharmacol Exp Ther.* 316:636-646 (2006).
  9. R. Noshiro, N. Anzai, T. Sakata, H. Miyazaki, T. Terada, H.J. Shin, X. He, D. Miura, K. Inui, Y. Kanai, and H. Endou. The PDZ domain protein PDZK1 interacts with human peptide transporter PEPT2 and enhances its transport activity. *Kidney Int.* 70:275-282 (2006).
  10. D. Grundemann, J. Babin-Ebell, F. Martel, N. Ording, A. Schmidt, and E. Schomig. Primary structure and functional expression of the apical organic cation transporter from kidney epithelial LLC-PK1 cells. *The Journal of Biological Chemistry.* 272:10408-10413 (1997).
  11. F.H. Leibachand and V. Ganapathy. Peptide transporters in the intestine and the kidney. *Annu Rev Nutr.* 16:99-119 (1996).
  12. B. Gowda, M. Sar, X. Mu, J. Cidlowski, and T. Welbourne. Coordinate modulation of glucocorticoid receptor and glutaminase gene expression in LLC-PK1-F+ cells. *The American Journal of Physiology.* 270:C825-831 (1996).
  13. A. Benesic, G. Schwerdt, S. Mildenerger, R. Freudinger, N. Gordjani, and M. Gekle. Disturbed Ca<sup>2+</sup>-signaling by chloroacetaldehyde: a possible cause for chronic ifosfamide nephrotoxicity. *Kidney International.* 68:2029-2041 (2005).
  14. D.P. Rodeheaver, M.D. Aleo, and R.G. Schnellmann. Differences in enzymatic and mechanical isolated rabbit renal proximal tubules: comparison in long-term incubation. *In Vitro Cell Dev Biol.* 26:898-904 (1990).
  15. L. Chuman, L.G. Fine, A.H. Cohen, and M.H. Saier, Jr. Continuous growth of proximal tubular kidney epithelial cells in hormone-supplemented serum-free medium. *The Journal of Cell Biology.* 94:506-510 (1982).
  16. R.L. Miller, P. Zhang, T. Chen, A. Rohrwasser, and R.D. Nelson. Automated method for the isolation of collecting ducts. *Am J Physiol Renal Physiol.* 291:F236-245 (2006).
  17. J.M. Catania, A.M. Pershing, and A.J. Gandolfi. Precision-cut tissue chips as an in vitro toxicology system. *Toxicol In Vitro.* 21:956-961 (2007).
  18. L.E. O'Brien, M.M. Zegers, and K.E. Mostov. Opinion: Building epithelial architecture: insights from three-dimensional culture models. *Nature Reviews.* 3:531-537 (2002).
  19. R.P. Amin, A.E. Vickers, F. Sistare, K.L. Thompson, R.J. Roman, M. Lawton, J. Kramer,

- H.K. Hamadeh, J. Collins, S. Grissom, L. Bennett, C.J. Tucker, S. Wild, C. Kind, V. Oreffo, J.W. Davis, 2nd, S. Curtiss, J.M. Naciff, M. Cunningham, R. Tennant, J. Stevens, B. Car, T.A. Bertram, and C.A. Afshari. Identification of putative gene based markers of renal toxicity. *Environmental Health Perspectives*. 112:465-479 (2004).
20. J. Zhang, A. Skardal, and G.D. Prestwich. Engineered extracellular matrices with cleavable crosslinkers for cell expansion and easy cell recovery. *Biomaterials*. 29:4521-4531 (2008).
21. Z. Qi, I. Whitt, A. Mehta, J. Jin, M. Zhao, R.C. Harris, A.B. Fogo, and M.D. Breyer. Serial determination of glomerular filtration rate in conscious mice using FITC-inulin clearance. *Am J Physiol Renal Physiol*. 286:F590-596 (2004).
22. V. Sahni, D. Choudhury, and Z. Ahmed. Chemotherapy-associated renal dysfunction. *Nat Rev Nephrol*. 5:450-462 (2009).

## APPENDIX

### STANDARD OPERATION PROTOCOLS (SOPs)

## GRAINGER LAB

Protocol: PT media

Date Originated: 12/2/11

Revision Date

Reviser Name:

Original Author: Astashkina A

Reference(s): Terryn et.al. "A primary culture of mouse proximal tubular cells, established on collagen-coated membranes" *Am J Physiol Renal Physiol* 293: F476–F485, 2007;

**Required Equipment:** BSL 2 hood, 50 sterile ml t.t.

### Materials Needed:

- FCS
- Anti-anti
- Sodium pyruvate
- Insulin/transferrin/selenium
- DMEM:F12 (no phenol red)
- Non-essential am.ac
- Hydrocortisone

**Estimated Time:** 10 min

**Before you Begin:** FCS and anti-anti is -20° fridge across my bench in the cell-media components shelf. Hydrocortisone is stored at -20° in the corner fridge by -80° freezer in my box . All other items are in 4° fridge next to my bench.

### Procedure:

For 50mL:

FCS-500µL

Sodium pyruvate -275 µL

Non-essential am.ac.-500 µL

Insulin/transferrin/selenium- 500 µL

Hydrocortisone - 18 µL

Anti-anti-500 µL

DMEM:F12 (no phenol red)-47.707mL

Store in 50ml sterile t.t at -20°C fridge.

**Notes:** I do not filter because all items are cell-culture grade (sterile).

## GRAINGER LAB

Protocol: PT isolation and making of 3D constructs

Date Originated: 12/2/11

Revision Date

Reviser Name:

Original Author: Astashkina A

Reference(s): Terryn et.al. "A primary culture of mouse proximal tubular cells, established on collagen-coated membranes" *Am J Physiol Renal Physiol* 293: F476–F485, 2007;

**Required Equipment:** BSL 2 hood, 50 mL and 1.5 mL sterile t.t, sterile surgical tools, and autoclaved 250µm sieve, sterile 70 µm filters, UVed razor blade, non-tissue culture treated sterile large plates (bacterial).

### Materials Needed:

- Ice-cold KREBS
- Warm PT media
- Resuspended HA and PEGDA
- Sterile enzyme solution

**Estimated Time:** 2-5 hours

### Before you Begin

Before starting PT isolation, you need to have sterile KREBS, enzyme digestion solution, polymers, sterile surgical tools, and sterile large 250µm filter ready. Enzyme solutions and polymers are made right before each experiment. You need to plan starting making your enzyme and polymer solutions about 2 hours before the start of the experiment, because HA takes almost 1 hour to resuspend. I do not autoclave razor blades (for mechanical kidney disruption) because they get dull. Spray razor blade with 70% ethanol and UV it in the hood for 20 min before starting PT isolation.

Before getting mice, your hood should have the following items: sterile tools, UVed razor blade, sterile enzyme solution, sterile non-tissue culture round plates, cold KREBS, and 70% ethanol-sprayed paper towel (for animal surgery).

### Solutions and chemicals:

1. **KREBS:** 145 mM NaCl, 10mM HEPES, 5 mM KCl, 1mM NaH<sub>2</sub>PO<sub>4</sub>, 2.5 mM CaCl<sub>2</sub>, 1.8 mM MgSO<sub>4</sub>, 5 mM glucose, pH 7.3)

To make 1L of KREBS:

|                                    |        |
|------------------------------------|--------|
| NaCl-                              | 8.48g  |
| HEPES-                             | 2.38g  |
| KCl-                               | 0.373g |
| NaH <sub>2</sub> PO <sub>4</sub> - | 0.12 g |
| CaCl <sub>2</sub> -                | 0.277g |
| MgSO <sub>4</sub> -                | 0.217g |
| D-glucose-                         | 0.9g   |

Resuspend all chemicals in 1L of dH<sub>2</sub>O, pH to 7.3 with KOH, sterile filter using 0.22µm cell culture filtration system. Store in 4° fridge.

2. Enzyme solution: 10ml KREBS+2mg/ml hyaluronidase +3mg/ml collagenase IV + 0.1mg/ml DNase I

You need to make 5mL of it for each mouse. For 5mL enzyme solution:

Collagenase IV (Worthington, cat# LS004188) - 15mg

DNase I (Sigma, cat #DN25-100mg) - a tiny speckle

Hyaluronidase (Worthington, cat# LS002592) - 10mg

Combine all chemicals in 50 mL t.t., sterile filter into another 50 ml t.t. using 0.22  $\mu$ m filter in the hood. Store in 4° fridge before experiment.

3. Polymers: Take out (from -80° freezer) and defrost HA for 30 min before weighing (because it is so hygroscopic). I use 1.5% HA (15mg/1000mL) and 7.5% PEGDA (75mg/1000mL) to make my gels. I resuspend dry chemicals in sterile (cell culture grade) PBS<sup>++</sup> in the hood, but PBS<sup>--</sup> or full media should also be fine (just stay consistent). It takes almost 1 hour at RT on the shaker for HA to go into solution. Once PEGDA and HA are resuspended, sterile filter them with 0.22  $\mu$ m filter in the hood. Store at RT before the experiment. Do not freeze, UV, or reuse unused HA/PEG. I make about 1.3mL of HA and 500 $\mu$ L per mouse.

For each well you will use 40  $\mu$ L of HA and 10  $\mu$ L of PEG (4:1 HA:PEG). When PEG and HA are mixed with cells, each well in a 96 well plate should get about 52  $\mu$ L (to account for cell volume).

#### **Procedure:**

1. Black C57 mice should be killed in the animal facility using CO<sub>2</sub> and brought back to the lab as soon as possible.
2. Spray all mice with 70% ethanol prior to bringing them in the hood.
3. Open mouse abdomen and remove kidneys (they are large, bean shaped organs on the posterior side) and place them in ICE COLD KREBS in a non-tissue culture plate.
4. Remove blood vessels, ureter, and thin film that surrounds the organ. Place cleaned kidneys in ICE COLD KREBS for storage (if you are doing more than 1 mouse).
5. Take out kidneys from KREBS and finely mince them using sterile razor blade.
6. Put minced kidney into enzyme solution and digest for 30 min SHAKING at 37°C (in the water bath).
7. Add 10-15 ml of cold KREBS to the digested kidney, pipet up and down, filter through 70  $\mu$ m filter (sterile small filters). DISCARD the flow through.
8. Kidney pieces that were greater than 70  $\mu$ m (what was left in the filter) should be filtered again through 250  $\mu$ m filter (large metal filter) using 20mL of KREBS. KEEP the flow through (20mL total volume).
9. Take out 300  $\mu$ L of the PT suspension from step 8 and put it into 1.5mL t.t. (for counting).
10. Spin 20mL of PTs in KREBS (from step 8) in the large centrifuge at 12,000 rpm for 12 min. Simultaneously spin 300  $\mu$ L in the smaller centrifuge for 5 min at max speed.
11. When 300  $\mu$ L (for counting) t.t. is done spinning, remove all solution and resuspend PTs in 30  $\mu$ L (concentrating sample 10 times). Count PTs using hemocytometer, calculate concentration (remember to multiply by 0.1 dilution factor). Calculate how much PEG and HA needs to be added to get 5000 PTs/well
12. When 20mL t.t. is done, remove all solution and add calculated amount of PEGDA and HA. Vortex to get a homogeneous solution of PEG/HA/PTs

13. Put 52uL of step 12 mixture into Teflon-coated 96 well plates. You will have to use you tip to spread the drop in the well.
14. Let the gel crosslink for 30 min in the incubator. After 30 min the gel should be almost set (you can tilt the wells to see if the gel is running). Add 100-150  $\mu$ L of warm PT media to each well. Do not directly pipette on the top of the gel because it is usually too soft and may change shape. I add media to the wall of the well, and let the drop slide onto the gel.
15. Let cells recover overnight before doing anything

**Notes:** I buy all enzymes from Worthington. The company has a layaway program where they store 3g of each enzyme lot for future purchase. Since each lot varies in activity, use of the same lot is highly suggested. If you enzyme strength changes, you will most likely have to adjust the incubation time with the enzyme or the concentrations of enzymes in the enzyme solution.



## GRAINGER LAB

Protocol: making TeflonAF® plates

Date Originated: 12/2/11

Revision Date

Reviser Name:

Original Author: Astashkina A

Reference(s):

**Required Equipment:** Hood with UV lamp

**Materials Needed:**

- Resuspended TeflonAF
- 96 well non-tissue culture plates

**Estimated Time:** 3-4 hours

**Before you Begin:** Teflon is located in the Chemical lab in the 'rare polymers' shelving section

**Procedure:**

1. Make sure you use NON tissue culture 96 well plates
2. Only coat 2-3 rows/plate because Teflon is very expensive and you will not be using more than 3 rows for any experiments
3. Add 150uL of Teflon AF to each well
4. Put for 2 h in the dry oven at 57C (mark #3) to evaporate organic solvent
5. UV is the hood for 20-30 min
6. Parafilm and store at RT

**Notes:** Never use the oven unless you were properly trained

## GRAINGER LAB

Protocol: Immunohistochemistry for 3D PT constructs

Date Originated: 12/2/11

Revision Date

Reviser Name:

Original Author: Astashkina A

Reference(s):

**Required Equipment:** tips, foil

**Materials Needed:**

- Ab
- PBS with NaAzide (1% or 0.08%)
- 4% paraformaldehyde
- Triton X
- iT signal enhancer

**Estimated Time:** 1-7 day procedure

**Before you Begin:** Ab is usually located in the Ab box in the 4°C fridge or at -20°C fridge

**Procedure:**

1. Remove all the media and add 4% paraformaldehyde. Incubate overnight in a 4°C fridge
2. Wash with PBS (with NaAzide) 2X times
3. If you are staining for markers on the cell surface, skip to item #4. If staining for intracellular markers, then add 0.1% Triton X (in PBS with NaAzide) for 20 min. Wash 2X times
4. Add iT signal enhancer (Invitrogen)- about 1-2 drops per culture-for 30min. Incubate at room temperature (RT)
5. Wash with PBS (with NaAzide) 2X times
6. Add primary antibody. The final concentration and time of incubation might have to be optimized for each antibody. I used anywhere from 1:500 (for Kim-1) to 1:2000 (for OAT-1). Most primary antibodies worked well at 1:1000. Usually 100uL/well of final concentration is enough. Majority of antibodies stained well after 3 days in a 4°C fridge (but I also had to reduce time to 2h at RT for OAT-1 and increase to 7 days for AQP-1)
7. Wash with PBS (with NaAzide) 2X times
8. Add secondary antibody for 1.5-2h at RT (cover with foil during incubation). If you need to do nuclear stain, use PI (I tried many other stains, and they do not look good, or look diffused on confocal image). PI needs 10-20 min to stain the 3-D culture (long incubation can result in the entire PTs turning red). 2uL/well tends to be enough.

**Notes:** every Ab is different; you may need to adjust Ab concentration and incubation time

## GRAINGER LAB

Protocol: RNA extraction using TRIzol Reagent for 3D PT constructs

Date Originated: 12/2/11

Revision Date

Reviser Name:

Original Author: Astashkina A

Reference(s):

**Required Equipment:** RNase-free tips and 1.5 mL t.t., working area cleaned with RNase spray, hand-held tissue terror wiped with RNase-free wipe

### Materials Needed:

- 75% ethanol
- Trizol
- glycogen

**Estimated Time:** 2 day procedure

**Before you Begin:** Mix 75% ethanol: 7.5 ml 200proof ethanol + 2.5 ml DEPC treated water  
Turn on dry bath to 56°C.

Clean a crucible with pestle with RNase away. Cool to -80°C if you will be using it in step 2.

Note: keep the RNA on the ice unless otherwise stated.

rcf=g

### Procedure:

1. Take off media. Add Trizol 200uL directly to constructs. Pipette up and down to dissolve as much as possible. Transfer to the crucible.
2. Add 590 ul of Trizol+10uLof glycogen to crucible. Mechanically break down undissolved chunks with pestle. **NOTE:** you do not need to mechanically break constructs when you think you will get plenty of RNA. You can just add 590 ul of Trizol+10uLof glycogen to 1.5mL RNase-free t.t.
3. Move 800uL of dissolved 3D constructs in TRIzol/glycogen from crucible into one 1.5 ml microcentrifuge tubes (RNase-free). If you did not mechanically break down 3D constructs, move 200uL of supernatant with dissolved 3D construct to 1.5 ml microcentrifuge tube that already had 590 ul of Trizol+10uLof glycogen to crucible (making total volume 800uL). Use hand-held tissue terror to further mince tissues.
4. Centrifuge at 12,000 g for 15 min at 4°C
5. Collect the supernatant (RNA will be in supernatant) and transfer it into a new RNase-free tubes. Discard the pellet that has gel and cell membranes.
6. Add 160ul of chloroform to eppendorf ( 0.2 ml chloroform per 1ml TRIzol®)
7. Shake tube vigorously by hand for 15 seconds.
8. Centrifuge the samples at 12,000 g for 20 minutes at 4°C.
9. Following centrifugation, the mixture separates into a lower red, phenol-chloroform phase, an interphase, and a colorless upper aqueous phase (see pictures). RNA remains exclusively in the aqueous phase. The volume of the aqueous phase is about 60% of the volume of TRIzol® Reagent used for homogenization.
10. Transfer the aqueous phase to one RNase-free 1.5ml fresh tube. Precipitate the RNA from the aqueous phase by mixing with isopropyl alcohol. Use 400 ul of ice-cold isopropyl alcohol per eppendorf . Incubate samples at -20°C for 1h or overnight.

11. Centrifuge at 20,000 g for 15 minutes at RT. The RNA precipitate, often invisible before centrifugation, forms a gel-like pellet on the side and bottom of the tube.
12. Discard the supernatant. Wash the RNA pellet once with 75% ethanol, adding 200ul to eppendorf.
13. Mix the sample by vortexing and centrifuge at 20,000 g **for 10 minutes at 4C**.
14. Discard the wash and air- dry the RNA pellet for 5-10 minutes. **It is important not to let the RNA pellet dry completely as this will greatly decrease its solubility.** Dissolve RNA in 30uL RNase-free water and incubate for 10 minutes at 55 to 60°C in the drybath.
15. Add 1uL of DNase I and incubate for 30 min at 37°C.

**Notes:** TRIzol is usually located in the door of the 4°C media fridge. Glycogen is in my box at -20°C fridge.

## GRAINGER LAB

Protocol: CyQuant NF for 3D PT constructs

Date Originated: 12/2/11

Revision Date

Reviser Name:

Original Author: Astashkina A

Reference(s): see Invitrogen manual for CyQuantNF

**Required Equipment:** spectrophotometer

**Materials Needed:**

- CyQuant solution (CQ)
- PBS
- peroxide

**Estimated Time:** 1.5-3.5 h procedure

**Before you Begin:** Make CyQuantNF according to manufacturer's instruction (do not use solution C)

**Procedure:**

1. Take off media. Wash 1X with sterile PBS. Wash more if you were using phenol-containing media
2. If you are comparing to gel with no cells, you need to incubate all constructs for 1 hour 0.01mM H<sub>2</sub>O<sub>2</sub>. Wash 1X again. If you are comparing to gel with cells (no treatment control), you can skip step#2
3. Add 100uL of CQ solution, incubate for 1h in the incubator
4. Remove CQ solution (pipette up and down, try to not get bubbles) and plate it in a new 96 well plate. Read fluorescence at 485 nm excitation and 530 nm emission

**Notes:** There should be a CyQuant NF program ready to go on Synergy 2

## GRAINGER LAB

Protocol: qPCR for 3D PT constructs

Date Originated: 12/2/11

Revision Date

Reviser Name:

Original Author: Astashkina A

Reference(s): Livak KJ, Schmittgen TD. Analysis of relative gene expression data using real-time quantitative PCR and the 2<sup>(-Delta Delta C(T))</sup> Method. Methods. 2001 Dec;25(4):402-8.

**Required Equipment:** RNase-free tips and 1.5 mL t.t., working area cleaned with RNase spr, Step One Plus qPCR cycler (Kim's lab)

**Materials Needed:**

- RNA-C<sub>T</sub> Taqman Kit (Applied Biosystems, USA)

**Estimated Time:** 2-3 hours

**Before you Begin:** You will need to get RNA from your samples (see SOP for RNA extraction).

**Procedure:**

1. Measure RNA concentration using Nanodrop (In Lim's or Kim's Lab). Dilute your samples to 100 ng/μL (good RNA quality) or 300ng/μL (poor RNA quality). I used 300ng/μL
2. Use RNA-C<sub>T</sub> Taqman Kit (Applied Biosystems, USA) because it is more sensitive to poor RNA quality material
3. Follow manufactures instructions for kit dilution
4. Run 2-3 technical replicas per sample
5. Use GAPDH as internal control. Always run GAPDH on the same plate as samples and for every condition
6. I analyzed QPCR data using the 2<sup>-ΔΔC<sub>T</sub></sup> method. It measures only by how much gene expression increased or decreased, not the actual number of RNA copies in the cell. Samples that did not express genes after 40 cycles were assigned 41-cycle expression for calculations

qPCR I performed used commercial TaqMan® Gene expression Assays (Applied Biosystems, USA): Mm9999915\_g1 for GAPDH, Mm01324470\_m1 for Lcn2 (NGAL), Mm004427773\_m1 for CLU, Mm00516005\_m1 for HO, Mm01333430\_m1 for VIM, Mm00436767\_m1 for Spp1

**Notes:** RNA-C<sub>T</sub> Taqman Kit is usually located in the door of the 4°C media fridge. TaqMan® Gene expression Assays are in the door of the -20°C fridge. If you are using Kim's lab machine, ask them for their plate's manufacturer. The regular Applied Biosystems plates DO NOT FIT Step One.

## GRAINGER LAB

Protocol: NAG measurement

Date Originated: 12/2/11

Revision Date

Reviser Name:

Original Author: Astashkina A

Reference(s): Barcelos LS, Talvani A, Teixeira AS, Vieira LQ, Cassali GD, Andrade SP, et al. Impaired inflammatory angiogenesis, but not leukocyte influx, in mice lacking TNFR1. Journal of leukocyte biology. 2005 Aug;78(2):352-8.

### Required Equipment:

#### Materials Needed:

- *p*-nitrophenyl-*N*-acetyl- $\beta$ -D-glucosaminide (Sigma Aldrich, USA) solution
- 1 mM 4-nitrophenol standard

Citrate/phosphate buffer: 0.1 M citric acid, 0.1 M Na<sub>2</sub>HPO<sub>4</sub>, pH 4.5

*p*-nitrophenyl-*N*-acetyl- $\beta$ -D-glucosaminide solution: 2.24mM in citrate/phosphate buffer

**Estimated Time:** 20 min

**Before you Begin:**

### Procedure:

1. Collect the media (no phenol red) with NAG
2. Incubate 100  $\mu$ L of media for 10 min at room temperature with 100  $\mu$ L of 2.24mM *p*-nitrophenyl-*N*-acetyl- $\beta$ -D-glucosaminide solution.
3. Read absorbance at 405 nm on the microplate reader and referenced against a 1 mM 4-nitrophenol standard

**Notes:** NAG can be measured only in solution, inside cells there is too much interference with intrinsic cellular absorbance. It is strongly suggested for you to keep your media+ drug and measure its absorbance at 405 nm. You can subtract the dug+media background from your samples.